

DESIGN AND SYNTHESIS OF NOVEL SMALL-MOLECULE ANTIMICROBIALS

DESIGN AND SYNTHESIS OF NOVEL SMALL-MOLECULE ANTIMICROBIALS

By CARLA E. BROWN, B. Art. Sc., M. Sc.

A Thesis Submitted to the School of Graduate Studies in Partial Fulfilment of the
Requirements for the Degree Doctor of Philosophy

McMaster University © Copyright by Carla E. Brown, June 2017

Ph.D. Thesis – C. Brown; McMaster University – Chemistry and Chemical Biology

McMaster University DOCTOR OF PHILOSOPHY (2017) Hamilton, Ontario (Chemical
Biology)

TITLE: Design and Synthesis of Novel Small-molecule Antimicrobials AUTHOR: Carla
E. Brown, BArtSc. (McMaster University), M.Sc. (University of Toronto)

SUPERVISOR: Professor James McNulty NUMBER OF PAGES: xiii, 281

There is a need to discover new antimicrobial drugs to combat drug-resistant infections. We are trying to find new molecules that can prevent the growth of parasites and viruses by developing and using novel chemical reactions, as well as by isolating new products from plants and fungi. This text describes a new way to make quinolines, a type of molecule found in many drugs. A molecule prepared by this method inhibited the parasite *T. gondii* at low concentrations. We have also identified quinazolinones, molecules that can be rapidly assembled by combining three components, which inhibit parasites and viruses. The thesis also includes a faster way to make derivatives of an antiviral molecule from daffodils, which can help determine which parts of the molecule are important for antiviral activity. We have also identified new molecules from the fungus *Xylaria polymorpha* and an antiviral compound from the *Ficus benjamina* tree.

Antimicrobial resistance is a significant threat to global health, and it is necessary to identify new drugs and drug targets for pathogenic bacteria, parasites, viruses, and fungi. Novel small molecules with antimicrobial activity may be discovered in the lab through chemical synthesis or from nature as secondary metabolites. This thesis describes our efforts to synthesize and identify antiparasitic and antiviral small molecules. The preparation of 3-diarylether quinolines with 5 μM activity against the parasite *T. gondii*, through a novel TFA-catalysed Povarov reaction using enol ethers as carbonyl surrogates is described. Libraries of quinazolinone and dihydroquinazolinone derivatives have been prepared through a multicomponent synthetic route. Structure activity relationship analysis allowed for differentiation of the antiparasitic pharmacophore from the antiviral pharmacophore, as well as the identification of compounds with single digit micromolar activity against both *T. gondii* and Herpes Simplex Virus 1. This work also details the design and synthesis of B-ring aza-analogs of bioactive Amaryllidaceae alkaloids in just 5 steps from chiral pool reagents. Aza-substitution of the B-ring eliminated antiviral activity, and this modification may also affect anticancer activity. Analysis of several natural product sources has also identified novel small molecules. Isolation of metabolites from *Xylaria polymorpha* identified three novel polyketide derivatives with unknown biological activity. The alkaloid candicine was found to be the primary polar metabolite from *Ficus benjamina* latex, as well as a potent inhibitor of murine cytomegalovirus. By identifying the mechanisms of action of these bioactive small molecules, we may identify targets for further drug development.

Firstly, I would like to sincerely thank my supervisor, Dr. Jim McNulty, for his thoughtful guidance, criticism, and encouragement. Jim: thank you for giving me so many opportunities to learn inside and outside the lab, for pushing me to be a better chemist, and for always finding time to talk to through an idea on the board. To my committee members, Dr. Nathan Magarvey and Dr. John Valliant, thank you for your helpful feedback and suggestions. I also want to thank our research collaborators at Johns Hopkins University (Dr. Lori Jones-Brando, Claudia Bordon, Dr. Bob Yolken) and the University of Pittsburgh (Dr. Dino D’Aiuto, Dr. Vish Nimgaonkar, Matt Demers, and Dr. Lora McClain) who performed all biological testing.

I would also like to thank all of my colleagues in the McNulty lab: Dave McLeod, Janice Calzvara, Alex Nielsen, Carlos Zepeda, Kunal Keskar, Sean van den Berg, Chanti Dokuburra, Arkesh Narayanapappa, Omkar Revu, Dave Hurem, and Suresh Borra. I am especially grateful to Alex Nielsen and Dave McLeod for their encouragement and commiseration during long days in the lab and Friday nights at the Phoenix. I also want to thank Tiffany Kong, our fantastic undergraduate student who helped me prepare our quinazolinone library.

I’m extremely grateful to my family and friends that have supported me throughout graduate school. To my parents, Grace and Peter: thank you for your endless love and support. To my sister, Anita: thank you for always cheering me up when my chemistry went wrong. Finally, I want to thank my husband Kenwick. Kenwick, thank you for sharing every day of this process with me. You have made the difficult times bearable and the good times wonderful.

Table of Contents

1	Introduction to antimicrobial chemotherapy	xi
1.1	The origins of antimicrobial drug discovery.....	1
1.2	Parasitic diseases have a global impact	3
1.3	Antiparasitics target different functions in the apicomplexan lifestyle	7
1.4	Human viruses with neurological implications	10
1.5	Herpesviridae and Flaviviridae are viruses with neurological outcomes.....	12
1.6	Antiviral therapy: reviewing the approved treatments and mechanisms of action of antiviral drugs	13
1.7	A strategy for identifying novel small molecules with activity against parasites and viruses.....	20
1.8	References.....	21
2	Synthesis of antiparasitic quinolines.....	32
2.1	Classical quinoline synthesis	32
2.2	Quinolines with activity against <i>T. gondii</i>	33
2.3	Enol ethers as carbonyl surrogates in a modification of the Povarov synthesis of 3-arylquinolines and their anti- <i>Toxoplasma</i> activity	34
2.4	Conclusion and future work.....	48
2.5	Experimental.....	49
2.6	References.....	60
3	Design and synthesis of bioactive quinazolinones	64
3.1	Introduction to quinazolinone heterocycles.....	64
3.2	Synthesis of substituted quinazolinones in the literature.....	66
3.3	Preparation of the initial quinazolinone library	68
3.4	Quinazolinones with activity against <i>T. gondii</i>	71
3.5	Quinazolinones with activity against HSV-1.....	76
3.6	Design and synthesis of second generation quinazolinones	80
3.7	Second generation quinazolinones – <i>T. gondii</i> SAR	84
3.8	Second generation quinazolinones – HSV-1 SAR	88
3.9	Conclusions and future work	92
3.10	Experimental.....	93
3.11	References	114
4	Design and synthesis of quinazolinone alkaloids	120
4.1	Amaryllidaceae alkaloids have potent bioactivity.....	120
4.2	Phenanthridone quinazolinone hybrids.....	122
4.3	Synthetic route from D-ribose:	124
4.4	Synthetic route from L-arabinose:	126
4.5	Biological activity of quinazolinone alkaloids	132
4.6	Conclusion and future work.....	135
4.7	Experimental.....	136
4.8	References.....	146

5	Isolation of natural products from <i>Xylaria polymorpha</i>....	150
5.1	Natural products are a rich source of antimicrobial drug leads	150
5.2	Isolation of novel natural products from <i>Xylaria polymorpha</i>	152
5.3	<i>X. polymorpha</i> collection and extraction	153
5.4	Isolation of ergosterol-5,8-endoperoxide.....	154
5.5	Isolation of di(2-ethylhexyl) adipate and structural reassignment of microdiplactone.....	156
5.6	Isolation of New Xylarals and Xylactams	159
5.6.1	Xylaral B	160
5.6.2	Xylactam C	161
5.6.3	Xylactam D.....	162
5.7	Conclusion and future work.....	163
5.8	Experimental.....	164
5.9	References.....	167
6	Natural products from <i>Ficus benjamina</i> latex	173
6.1	Natural products for plant defense.....	173
6.2	Isolation of candicine from <i>F. benjamina</i>	174
6.2.1	Discovery of candicine as the major induced latex constituent in <i>Ficus benjamina</i> (Moraceae) and its potent, selective antiviral activity	175
6.3	Experimental.....	183
6.4	References.....	184
7	Conclusion and future directions	186

List of figures, tables, and schemes

Figure 1.1: Life cycle of apicomplexan parasites.....	5
Figure 1.2: Structures of known antiparasitics.....	9
Figure 1.3: The cytochrome bc ₁ complex, an essential component of parasitic mitochondrial respiration.....	10
Figure 1.4: Inhibitors of viral DNA synthesis. Compounds in red act as uridine analogs, while compounds in blue are guanosine analogs.....	16
Figure 1.5: Drugs and drug candidates active against herpesviridae that inhibit viral entry, helicase-primase, DNA maturation, and DNA nuclear egress.....	18
Figure 1.6: Small molecules with activity against flaviviruses	20
Figure 2.1: Synthesis and activity of our published 4-arylquinoline-2-carboxylate compounds against <i>T. gondii</i>	33
Figure 2.2: Structures of select antiparasitic agents: the 4-quinolones endochin and ELQ316 ^{6a} , the quinolines chloroquine and mefloquine and novel hybrid 3-aryl quinoline derivatives prepared in this work.....	35
Figure 2.3: Retrosynthetic analysis of the proposed 3-aryl quinolines as products of a three component coupling of substituted aniline and phenylacetaldehyde derivatives with ethyl glyoxylate.....	37
Figure 2.4: Substrate scope of the multicomponent reaction. Unless otherwise stated, reaction conditions: 1 (1.2 eq), 2, (1.2 eq), 3a-1 (1.0 eq), TFA (1.05 eq), DCM, 0°C, 5 min. ^b TFA (2.05 eq), ^c 15 minutes ^d 1 hour.....	41
Figure 2.5: Quantification of <i>T. gondii</i> invasion inhibition by quinolines.....	45
Figure 2.6: Proposed structure of a 3-diarylether quinoline analog. A 4-halogenated quinoline may have improved anti- <i>Toxoplasma</i> activity if a halogen group can mimic the hydrogen bonding interaction of the quinolone core.....	49
Figure 3.1: Quinazolinone and dihydroquinazolinone cores	64
Figure 3.2: Natural products and pharmaceuticals with a quinazolinone core	65
Figure 3.3: Literature methods for synthesis of quinazolinones.....	67
Figure 3.4: Invasion of tachyzoites into a host cell after treatment with first generation quinazolinones	75
Figure 3.5: Replication of <i>T. gondii</i> tachyzoites in a vacuole after treatment with first generation quinazolinones.....	76
Figure 3.6: Percentage of neurons expressing EGFP after infection with an HSV-1 strain, normalized to untreated cells.....	78
Figure 3.7: Toxicity of ACV, 3-15, and 3-21 to Vero cells, neural stem cells, and neurons compared to vehicle.....	80
Figure 3.8: Second generation quinazolinones containing varying N3 substituents	82
Figure 3.9: Second generation quinolines containing varying C2 substituents	84
Figure 3.10: Invasion of tachyzoites into a host cell after treatment with second-generation quinazolinones.....	87
Figure 3.11: Replication of <i>T. gondii</i> tachyzoites in a vacuole after treatment with second-generation quinazolinones.....	88

Figure 3.12: Percentage of neurons expressing EGFP after infection with an HSV-1 strain, normalized to untreated cells	89
Figure 3.13: Toxicity of 3-40 and 3-42 to Vero cells, neural stem cells, and neurons compared to vehicle.	90
Figure 3.14: ChIP assay to determine H3K27Me3 enrichment in acutely infected cells, and cells treated with either R430 or 3-21.	91
Figure 3.15: Pharmacophores of antiparasitic and antiviral quinazolinones.	93
Figure 4.1: Common structure of phenanthrindone-type Amaryllidaceae alkaloids.	120
Figure 4.2: Structure of antiviral Amaryllidaceae alkaloids synthesized by the McNulty group	123
Figure 4.3: Structure of antiviral alkaloid trans-dihydrolycoricidine and a general quinazolinone, with similar core structures highlighted	124
Figure 4.4: Retrosynthetic analysis of target molecule, showing both the pentose sugar and anthranillamide fragments.	124
Figure 4.5: Synthesis of quinazolinone alkaloid 4-6 from D-ribose.	126
Figure 4.6: Proposed conversion of 4-5 to target molecule through selective deprotection and inversion at C2.	126
Figure 4.7: Attempts to cyclize aldehyde 4-10, obtained from L-arabinose over 3 steps, with anthranilamide were unsuccessful.	127
Figure 4.8: L-arabinose and anthranillamide undergo a reductive amination to give 4-11, which was then completely protected with TES-Cl. Swern oxidation to directly remove the primary TBS and oxidize gave an undesired product.	128
Figure 4.9: Selective deprotection of the primary TES group could not be accomplished either through a direct oxidation or a two-step hydrolysis and oxidation procedure.	129
Figure 4.10: L-arabinose is protected at the C5 alcohol with TBS-Cl, then coupled to anthranilamide in a reductive amination. The resulting product is protected as a triacetate to give 4-16 in 64% yield over 3 steps.	130
Figure 4.11: Deprotection, oxidation, and ring closure to form quinazolinone core	131
Figure 4.12: Synthesis of 4-26 and 4-27 from L-arabinose and 3,4-methylenedioxyanthranilamide	132
Figure 4.13: Anti-HSV-1 activity of quinazolinone alkaloids in neurons.	133
Figure 4.14: Anti-HSV-1 activity of quinazolinone alkaloid analogs in Vero cells.	134
Figure 5.1: Isolation tree-diagram from <i>Xylaria polymorpha</i> fruiting bodies	154
Figure 5.3: Proposed structure of microdiplactone. We propose the revised structure, di(2-ethylhexyl) adipate.	157
Figure 5.4: Structures of <i>Xylaria</i> polyketide natural products, xylaral, xylactam, and xylactam B.	159
Figure 5.5: Proposed structure of 5-3, xylactam B.	161
Figure 5.6: Proposed structure of 5-4, xylactam C	162
Figure 5.7: Structure of 5-5, xylactam D.	163
Figure 6.1: Natural products involved in plant defence.	174
Figure 6.2: A selection of known alkaloids identified from <i>Ficus benjamina</i>	176
Figure 6.3: Latex obtained from <i>F. benjamina</i> leaf (l) and leaf node (r).	177

Figure 6.4: Structure of candicine and related phenethylamine tyramine	178
Table 2.1: Optimized conditions for the multicomponent reaction	39
Table 2.2: Synthesis of 3-diaryl ether quinoline derivatives	42
Table 2.3: Anti-Toxoplasmosis activity of 4-arylquinolines	43
Table 3.1: Anti- <i>Toxoplasma</i> activity of quinazolinone-based library	72
Table 3.2: Anti- <i>Toxoplasma</i> activity of second generation quinazolinone-based library	85
Scheme 2.1: General synthesis of phenylacetaldehyde derivatives; Three-component coupling using 4-hydroxyphenylacetaldehyde, <i>p</i> -anisidine and ethyl glyoxylate to yield the quinoline.....	38
Scheme 2.2: Possible stepwise (Path A) or concerted (Path B) reaction pathways available for the new enol ether-mediated cycloaddition process.....	41
Scheme 3.1: Synthesis of 2- and 3-substituted quinazolinone analogs using CSA and DMSO in 27-83% yield	69
Scheme 3.2: First generation quinazolinone library	70
Scheme 3.3: Synthesis of diaryl ether, benzyloxybenzyl ether, and diaryl amine quinazolinones	83
Scheme 6.1: Isolation tree-diagram from the air-dried latex of <i>Ficus benjamina</i>	178
Scheme 6.2: Synthesis of candicine iodide from tyramine using iodomethane with 2,6-lutidine in DMF.....	179

List of abbreviations and symbols

HIV	Human Immunodeficiency Virus
L-DOPA	L-Dopamine
DNA	Deoxyribonucleic acid
RNA	Ribonucleic acid
QH ₂	Quinol
Q	Quinone
ELQ	Endochin-like quinolone
mRNA	Messenger Ribonucleic acid
HSV	Herpes Simplex virus
VZV	Varicella Zoster virus
CMV	Cytomegalovirus
AIDS	Acquired Immune Deficiency Syndrome
ZIKV	Zika virus
dATP	Deoxyadenosine triphosphate
dGTP	Deoxyguanosine triphosphate
TK	Thymidine kinase
ACV	Aciclovir
GTP	Guanosine triphosphate
HCV	Hepatitis C virus
NMR	Nuclear Magnetic Resonance
DCM	Dichloromethane
TFA	Trifluoroacetic acid
TLC	Thin Layer Chromatography
CSA	Camphorsulfonic acid
PTSA	p-Toluenesulfonic acid
HFF	Human Foreskin Fibroblasts
IC ₅₀	Median Inhibitory Concentration
TD ₅₀	Median Cytotoxic Dose
TI	Therapeutic Index
CPD	Compound
DMSO	Dimethylsulfoxide
VHL	Vehicle
LiHMDS	Lithium bis(trimethylsilyl)amide
EtOAc	Ethyl acetate
TRPA1	Transient receptor potential cation channel, subfamily A, member 1
EtOH	Ethanol
MeOH	Methanol
CRGP	Chlorophenol Red-β-D-galactopyranoside
SAR	Structure Activity Relationship
iPSC	Induced Pluripotent Stem Cell
EGFP	Enhanced Green Fluorescent Protein
RFP	Red Fluorescent Protein

Cyp450	Cytochrome P450
DMF	N,N-dimethylformamide
SARS	Severe acute respiratory syndrome
TBS	tert-Butyldimethylsilyl
TBAF	Tetrabutylammonium fluoride
DMT	Dimethoxytrityl
TES	Triethylsilyl
PCC	Pyridinium chlorochromate
PPTS	Pyridinium p-toluenesulfonate
DMP	Dess–Martin Periodinane
PAMPA	Parallel Artificial Membrane Permeability Assay
DIPEA	Diisopropylethylamine
HRMS	High Resolution Mass Spectrometry
DEHA	Di(2-ethylhexyl) Adipate
DEPT	Distortionless Enhancement by Polarization Transfer
COSY	Homonuclear Correlation Spectroscopy
HSQC	Heteronuclear Single Quantum Coherence Spectroscopy
HMBC	Heteronuclear Multiple Bond Correlation
DEHP	Di(2-ethylhexyl) Pthalate

Declaration of academic achievement

All chemistry outlined in this thesis was done by myself and T. Kong. I performed all reactions and isolations described in Chapter 2, 4, 5, and 6. I prepared the first generation quinazolinone library described in section 3.3, 3.4, and 3.5, as well as the antiviral targeted quinazolinones described in 3.8. Tiffany Kong, an undergraduate student working in the McNulty group, prepared the 2nd generation collection of quinazolinones described section 3.7.

All biological assays were carried out at Johns Hopkins University (antiparasitic) and the University of Pittsburgh (antiviral). These assays were performed by Claudia Bordon and Dr. Lorraine Jones-Brando (JHU) and Leonardo D' Aiuto, Matt Demers, and Lora McClain (UPitt).

1 Introduction to antimicrobial chemotherapy

1.1 The origins of antimicrobial drug discovery

The development of antimicrobial drugs for the treatment of bacterial, parasitic, viral, and fungal diseases is one of the biggest contributions science has made to human health in the past century and a half. Since the discovery that microorganisms cause infectious diseases by Pasteur and Koch in the mid-19th century,¹ designing molecules to treat these diseases has been a priority for chemical research. The concept of a ‘magic bullet’, a molecule that can selectively kill disease-causing microorganisms without damaging the host, was first proposed by Paul Ehrlich.² Ehrlich discovered the first synthetic antibiotic, arsphenamine, which was first used in the treatment of syphilis in 1910. This discovery sparked further research to identify more ‘magic bullets’ for the treatment of other infectious diseases, culminating in the production of prontosil, the first sulfonamide antibiotic.³ Sulfonamide drugs revolutionized the treatment of bacterial infections, and are still used to treat bacterial, parasitic, and fungal diseases. The discovery of arsphenamine and prontosil through the first large-scale screening programs provided the template for further antimicrobial drug discovery in the pharmaceutical industry.

Concurrent with the development of synthetic antimicrobials, scientists were realizing the potential of natural products in medicine.⁴ Cinchona bark, containing the alkaloid quinine, has been used for centuries for the treatment of malaria.⁵ Quinine was first isolated and identified as the active component of cinchona bark in 1820. The purified alkaloid and related drugs are still used in modern medicine as antiparasitics. Another

major discovery in the development of antimicrobials was made in 1929, when Fleming first isolated penicillin from *Penicillium* fungus and determined its antibacterial properties.⁶ Natural products chemistry continued to be a fruitful source of new anti-infective drugs from the 1950s-1970s.⁷ This period is considered to be a ‘golden age’ of antimicrobial drug development as the majority of new compound classes, both natural product derived and synthetic, were discovered during this time.

Given the widespread global use of pharmaceuticals to treat infectious diseases, there has also been a rise in the microorganisms resistant to our current drugs. The World Health Organization has identified antimicrobial-drug resistance as a major threat to global public health, particularly drug-resistant tuberculosis, malaria, and HIV.⁸ There is therefore a need to develop new molecules that inhibit bacterial, parasitic, and viral infections, and to identify novel mechanisms of action that can be further targeted for drug development. This review will focus particularly on the development of novel small-molecule anti-parasitic and antiviral agents.

Natural products and synthetic small molecules are both valuable tools for modulating biological interactions.⁹ Natural products are often finely tuned for biologically active through evolutionary pressure, making natural product libraries a rich source of lead compounds.¹⁰ However, such secondary metabolites do not typically interact with less druggable targets, such as transcription factors and other protein-protein interactions, that are a new priority for medicinal chemistry research.¹¹ Synthetic small molecules can access chemical space not usually explored by nature and may represent a useful way to drug these targets. Commercial synthetic libraries, however, are typically

lacking in chirality and structurally diverse scaffolds.¹² Diversity oriented synthesis is one way to approach this problem; in diversity-oriented synthesis, simple starting materials are rapidly assembled into more complex libraries with different carbon skeletons.¹³ A number of techniques for creating scaffold diversity have been reported.^{14,15} A complementary approach to drug discovery involves preparing smaller, focused libraries of compounds based on an initial compound lead, which may be predicted based on the literature or identified from a primary screen. In the course of this work, we have used several different strategies to identify antiparasitic and antiviral small molecules. Based on hits we have identified, as well as a close review of the literature for related compounds, we designed and prepared focused libraries of compounds that we hypothesized would be bioactive. We also isolated several novel natural products produced by plants and fungi under stress conditions, when we hypothesized these species may be more likely to produce defensive small molecules. We hypothesized that a combination of these two strategies would allow us to efficiently identify novel small-molecule antimicrobials.

1.2 Parasitic diseases have a global impact

Parasitic diseases have a massive public health impact in developed and developing nations.^{16,17} Malaria and toxoplasmosis are prevalent diseases caused by infection with apicomplexan, intracellular parasites *Plasmodium falciparum* and *Toxoplasma gondii*, respectively.^{18,19} There are more than 200 million clinical cases of malaria and as many as 1.2 million deaths each year from malaria.²⁰ Toxoplasmosis is a less severe disease than malaria in immunocompetent individuals, but can be life-

threatening to immunocompromised individuals and developing fetuses.^{21,22} *T. gondii* infection is common in North America, with 10-20% of adults showing evidence of exposure in their blood serum.²³ Most of these infections are latent, with no acute symptoms present. Recently, latent *T. gondii* infection has been associated with neurological diseases, particularly schizophrenia, generating new interest in anti-*Toxoplasma* research.²⁴⁻²⁶

Apicomplexan parasites are named for the apical complex; this unique structural feature of the parasite contains secretory organelles, called micronemes and rhoptries, that produce proteins involved in attachment to and invasion of a host cell.¹⁸ The invasion process begins when the parasite apical region makes contact with the host cell membrane.²⁷ The contents of the secretory organelles are excreted as the parasite invades in an endocytotic manner. The parasite occupies a parasitophorous vacuole inside the host, and a parasitophorous vacuole membrane is constructed to shield against the host's defenses. The dense granules are secreted once the parasite has entered the host cell and may be involved in host manipulation.²⁸

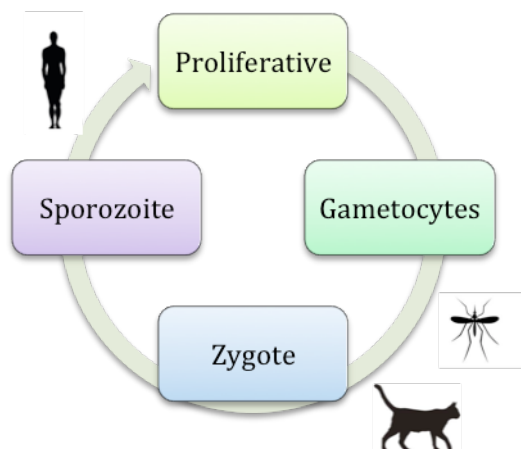


Figure 1.1: Life cycle of apicomplexan parasites. Apicomplexans undergo reproduction in non-human hosts. Sporozoites then infect secondary hosts and replicate, becoming proliferative tachyzoites/bradyzoites (*T. gondii*) or merozoites (*P. falciparum*).

Humans are secondary hosts for *P. falciparum* and *T. gondii*, but the apicomplexan lifecycle is completed through sexual reproduction in the primary hosts, which are mosquitos and cats, respectively (Figure 1.1).²⁹ After fertilization, parasite sporozoites find a secondary host and begin to replicate. When sporozoites burst, the proliferative forms of the parasite invade new host cells and continue to reproduce, spreading infection. In humans, the proliferative form of *P. falciparum* is merozoites and *T. gondii* is tachyzoites.

The life cycle of *T. gondii* within a human host has two stages: actively reproducing tachyzoites, and latent bradyzoites.²⁹ Tachyzoites replicate inside a host cell until it dies and ruptures, when they invade new host cells. In order to avoid detection and destruction by the host immune system, tachyzoites can go into a dormant state and form cysts, or clusters of bradyzoites, inside brain and muscle tissue. Cysts can later be reactivated. During reactivation, the cyst wall is lysed to release infectious tachyzoites which further colonize the host. Chronic *T. gondii* infections are very common, with

public health organizations estimating 10-20% of North Americans may be infected.²³ In immunocompetent people, latent infections do not induce the flu-like symptoms of active infections, but in immunocompromised populations, reactivation of latent *T. gondii* can be extremely dangerous.²²

Recent research has suggested that chronic *T. gondii* infections may also have neurological complications in otherwise healthy people, as evidence suggests *T. gondii* can manipulate brain function. Mice with cerebral *T. gondii* cysts show decreased predator aversion; healthy mice are repelled by the scent of cat urine, but *T. gondii* positive mice are attracted to the smell.³⁰ This makes parasite-infected mice more likely to be consumed by cats, and thus allowing the parasite to complete its life cycle through sexual reproduction in cats. This behavioural manipulation is hypothesized to be an evolutionary device for increasing parasite transmission. The mechanism is not known, but may be related to altered metabolism of the neurotransmitter dopamine.³¹ *T. gondii* bradyzoites have recently been found to express a unique aromatic amino acid hydroxylase that produces L-DOPA, which is the rate-limiting step in human dopamine production.³² Infected neural cells have been shown to release higher amounts of dopamine.³¹ Chronic *T. gondii* infection has also been associated with neurological disorders in humans, primarily schizophrenia, which may be caused in part to dysregulation of dopamine metabolism.³³ Seropositivity corresponds to a greater risk of developing schizophrenia than other genetic and environmental factors.²⁶ Additionally, haloperidol, a dopamine antagonist used to treat schizophrenia, has been shown to mitigate the behavioural changes in mice with chronic *T. gondii* infections.³⁴ Based on

this evidence, there is great interest in how treatment of chronic toxoplasmosis in humans can affect schizophrenia. Small molecules capable of clearing latent *T. gondii* infections could be used to study the effect of bradyzoite cysts in human neurology.

1.3 Antiparasitics target different functions in the apicomplexan lifestyle

Although there are a number of antiparasitic agents with different targets used to treat malaria and toxoplasmosis, parasite resistance to clinically available treatments is a major threat to global health.³⁵ The first antiparasitic agent was quinine, derived from the bark of the cinchona tree (Figure 1.2).³⁶ Other 4-aminoquinolines have since been developed that are easier to prepare, less toxic to the host, and more clinically effective. Aminoquinolines form complexes with heme generated from metabolism of host hemoglobin for nutrients.³⁷ These toxic complexes disrupt cell membranes. Chloroquine, an inhibitor of the aminoquinoline class, was used for prevention and treatment of malaria for decades, however resistance to chloroquine is now prevalent in all areas where *P. falciparum* malaria is common (Figure 1.2).³⁸ Resistance is believed to result from mutations in the Chloroquine Resistance Transporter, a membrane protein that effluxes chloroquine from its site of action in the malaria digestive vacuole.³⁸ Resistant strains rapidly transport chloroquine, rendering it ineffective.

Anti-folate drugs are also commonly used in treating both bacterial and parasitic infections, particularly toxoplasmosis.^{39,40} Sulfadiazene is an inhibitor of dihydropteroate synthase, while pyrimethamine and trimethoprim inhibit dihydrofolate reductase (Figure 1.2). When co-administered, these drugs prevent the synthesis of tetrahydrofolic acid,

thus inhibiting parasitic DNA and RNA synthesis.⁴¹ Widespread resistance to anti-folate compounds is the result of point mutations to the dihydropteroate synthase and dihydrofolate reductase that prevent inhibitor binding.³⁹

The current standard treatment for malaria is artemisinin, a sesquiterpene lactone isolated from sweet wormwood, and semi-synthetic artemisinin derivatives (Figure 1.2).³⁵ Artemisinin derivatives with activity against *T. gondii* have also been reported.⁴² Labelling studies of artemisinin suggests the peroxide functionality is activated by heme in the parasite, which causes rapid and unselective covalent bonding with a large number of parasite proteins.⁴³ Since artemisinins have multiple targets, resistance to this class of molecules has developed more slowly than other antiparasitics. Since artemisinates are a last-line therapy for malaria, wide-spread resistance could be disastrous. To mitigate this risk, artemisinins are usually administered as combination therapies to prevent the development of resistance.³⁵ Resistance to artemisinins has been recently reported in several isolated areas, and the mechanism of this resistance is unknown.

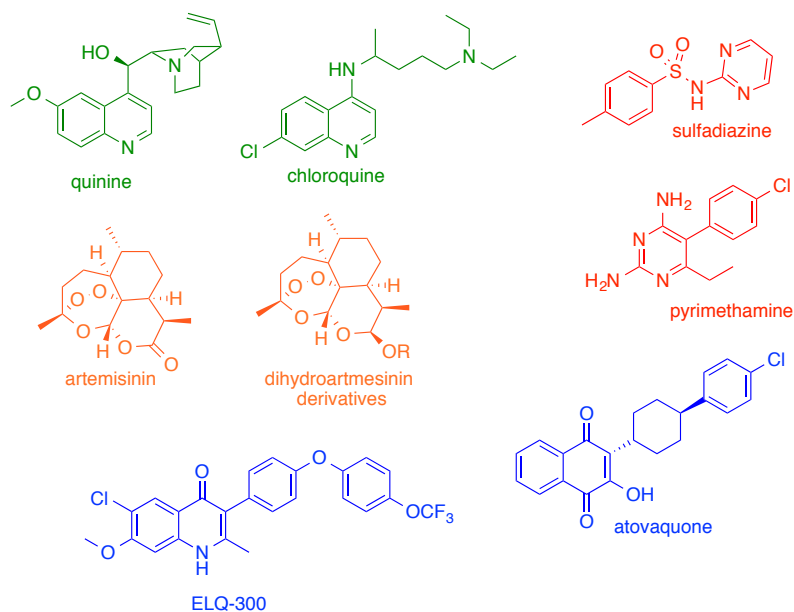


Figure 1.2: Structures of known antiparasitics. Aminoquinolines, which bind heme to form toxic complexes, are shown in green. Inhibitors of folic acid synthesis are shown in red. Artemisinin and derivatives are shown in orange. Inhibitors of the metabolic respiration are shown in blue. Resistance to compounds from each class has been reported.

Another important target of antiparasitic drugs is the cytochrome bc_1 complex (Figure 1.3), which maintains the membrane potential of mitochondria and is thus essential in mitochondrial respiration,^{44,45} This complex oxidizes quinol (QH₂) to quinone (Q), generating four protons and two electrons, to maintain membrane potential. Atovaquone, a commercial antiparasitic, targets the quinol oxidation site (Q_o), but atovaquone-resistant parasites have developed point mutations to this site that prevent atovaquone binding (Figure 1.2). One class of novel inhibitors of bc_1 are the endochin-like quinone (ELQ) compounds (Figure 1.2)^{46,47}, which target the quinone reduction site and are therefore active against atovaquone resistant strains.

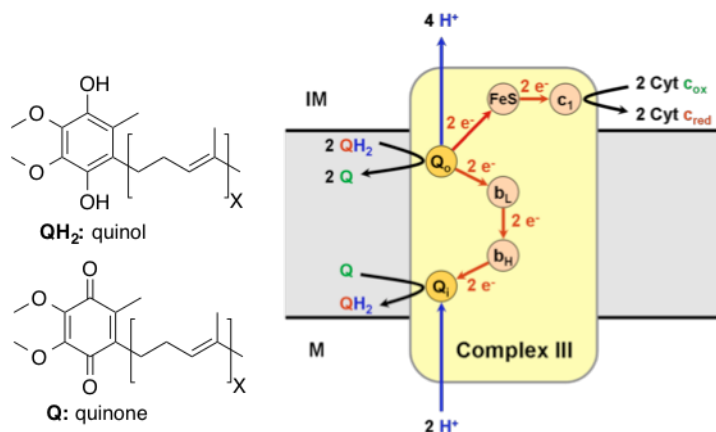


Figure 1.3: The cytochrome bc_1 complex, an essential component of parasitic mitochondrial respiration. Quinol (QH_2) is oxidized to quinone (Q) which generates four protons and two electrons in order to maintain membrane potential. Atovaquone targets the quinol oxidation site (Q_o), while ELQs target the quinone reduction site (Q_i). Image adapted from https://commons.wikimedia.org/wiki/File:Complex_III.png.

One major challenge in studying and treating chronic toxoplasmosis is that most commercially available antiparasitics are only active against acute infections.²³ This may be because the inhibition of the targets of commercial anti-*Toxoplasma* agents are not as toxic to slow-growing bradyzoites and the rapidly dividing tachyzoites. However, inhibition of cytochrome bc_1 with ELQ-316 has been shown to affect *T. gondii* bradyzoites.^{9,48} The solubility and bioavailability of ELQ-316 may limit the use of these compounds in the clinic, as infected mice treated with ELQ compounds display a non-dose dependent response. This validates respiratory metabolism as a valid target for inhibiting bradyzoites, and thus represents an exciting target for new bioactive small molecules.

1.4 Human viruses with neurological implications

Diseases caused by viruses can also have neurological complications. Viral diseases are spread through virions, or infectious viral particles, that contain three components.⁴⁹ The first is the viral genome, which may be comprised of DNA or RNA, may be single or double stranded, and in the case of single stranded nucleic acids, either sense or antisense. The genetic material is contained in a capsid, a viral protein coat with a defined geometric shape that can be used to classify viruses. Finally, in some viral families, the capsid is coated in a lipid envelope derived from the host cell membrane. This membrane is studded with proteins of both host and viral origin that are involved in mediating endocytotic viral entry into the host cell.

Viral invasion of a host cell begins with recognition between the viral protein in the lipid envelope and the host cell surface proteins.⁵⁰ The virion then penetrates the host cell, typically through endocytosis or membrane fusion. The viral genetic material enters the cell and is uncoated by disaggregation of the capsid. In the case of DNA viruses, the genetic material is then localized to the nucleus. The process of viral replication can then begin. RNA viruses are replicated in the cytoplasm, and can be immediately translated into a polypeptide that is cleaved into replication and structural proteins.⁵¹ Following maturation and packaging of the virion in the Golgi, infectious particles egress from the host cell.

In the replication process of DNA viruses, the first genes to be expressed are the immediate early genes, which are involved in product of viral mRNA and RNA synthase, as well as disabling the recognition of host transcriptional factors.⁵² This is followed by the production of viral proteins and reproduction of the viral genome. Late gene

expression, which controls the synthesis of structural and virion proteins, is then followed by assembly of virions. Finally, cell lysis occurs as virions bud from the initial host cell and seeking new hosts. This process is known as the lytic process. Some viruses, such as Herpesviridae, can also exist as latent infections.⁵³ In its latent form, viral genes are not actively expressed but the viral genome remains dormant in host cells. Viral gene expression can be reactivated, causing the virus to reenter the lytic cycle and become infectious once more.⁵⁴

1.5 Herpesviridae and Flaviviridae are viruses with neurological outcomes

This review will focus on viruses in the Herpesviridae and Flaviviridae families, which are not only responsible for several human diseases but also linked to neurological complications and cognitive deficits. Herpes viruses are double stranded DNA viruses with icosahedral capsids that are passed between humans with no other hosts or vectors.⁵⁵ Some well-known members of the Herpesviridae family include Herpes Simplex Virus (HSV) 1 and 2, Varicella Zoster Virus (VZV), and Cytomegalovirus (CMV). HSV is the most common of these viruses, and as many as 90% of the global population is seropositive for HSV-1 or -2.⁵⁶ HSV-1 typically infects oral epithelial mucosa cells, while HSV-2 is more commonly found in genital epithelial cells. Acute symptomatic herpes infections are lytic, but the virus is also capable of existing indefinitely in a latent form which causes no symptoms in its host.⁵² During latency, the latency-associated transcript is expressed, which suppresses transcription of lytic viral genes.⁵³ Reactivation of latent HSV can be triggered by stress or a weakened immune system in a process

tightly is controlled by epigenetic regulation. In cell culture, histone deacetylase inhibitors induce reactivation of latent infections.⁵⁷

Recurring HSV and CMV infections are a particular health hazard for immunocompromised individuals, particularly HIV-AIDS patients.⁵⁸ Immunosuppressed patients are prone to developing complications like encephalitis and ocular lesions, and often require long-term treatment with antiviral therapy. Resistance to current antiviral treatments is an ongoing problem⁵⁹, necessitating the development of new antiviral drugs and the identification of novel antiviral drug targets. Additionally, latent HSV-1 infections have been linked to cognitive deficits in older adults and individuals with mental illness, driving research into new drugs that are active against latent HSV.^{60,61}

Flaviviridae, which are single stranded, positive sense RNA viruses transmitted through insect vectors, have also been associated with neurological complications. Within flaviviridae, species are subdivided into several genera, including flaviviruses and hepaciviruses.⁶² The most common hepacivirus is Hepatitis C. Common flaviviruses that affect humans are Dengue fever, Zika virus (ZIKV), West Nile virus, and chikungunya. Zika virus is of particular interest to the medical community because of its association with neurological complications like Guillain-Barre syndrome and fetal microencephaly.^{63,64} The process by which ZIKV induces neurological changes is not well understood. There are few drugs used clinically to treat flavivirus infections, and no compounds approved for ZIKV.

1.6 Antiviral therapy: reviewing the approved treatments and mechanisms of action of antiviral drugs

Since the approval of idoxuridine in 1963, there have been 90 drugs approved for the treatment of viral infections, most of which are specifically used for the treatment of HIV.⁶⁵ A smaller number of drugs have been developed for the treatment of herpesviruses and flaviviruses. Idoxuridine, the first approved antiviral agent for the topical treatment of ocular herpes infections, was initially developed as an anti-tumour agent, and serendipitously found to have antiviral activity (Figure 1.4).^{66 67} Idoxuridine, as well as the later developed trifluridine, is a 5-substituted 2-deoxyuridine analog⁶⁸ that is phosphorylated in vivo to produce triphosphorylated idoxuridine. The phosphorylated acts a mimic of uridine, and thus inhibits viral DNA polymerase.⁶⁹ These 5-substituted 2-deoxyuridine analogs also inhibit cellular DNA polymerase, and are thus toxic and typically restricted to topical anti-HSV use.

The next development in antiviral nucleoside analogs came from the isolation of vidarabine from the sea sponge, *Tethya crypta*⁷⁰. Originally identified for its anti-cancer activity, vidarabine was found to be a potent inhibitor of viral DNA replication in HSV and VZV. Like idoxuridine-type nucleoside analogs, vidarabine is phosphorylated in vivo and inhibits DNA polymerase by mimicking dATP. Vidarabine was the first nucleoside analog used clinically against herpesviruses infections⁷¹, and although it is no longer in use in the clinic due to poor solubility and rapid deamination in vivo, its discovery has prompted the development of improved nucleoside analogs, like aciclovir. Aciclovir is an acyclic guanosine mimic, which is selectively phosphorylated by viral thymidine kinases to its active form (Figure 1.4)^{72,73}. It is particularly active against HSV-1 and HSV-2, and is still the most common drug clinically used in the treatment of both infections.⁵⁹

Ganciclovir, a closely related drug, is more commonly used to treat CMV infections, while penciclovir is most effective against VZV.⁷⁴ A number of related dGTP analogs that are prodrugs of acyclovir, ganicyclovir, and penciclovir have also been developed, including valaciclovir and valganciclovir, the valine-ester analogs of acyclovir and ganicyclovir respectively, and famicyclovir, the acylated analog of penciclovir (Figure 1.4). Because dGTP analogs require activation by thymidine kinase (TK), this class of inhibitors is not active against virus mutants that do not express thymidine kinases; this is the mechanism of resistance that develops to acyclovir in immunocompromised patients that receive long-term treatment.⁷⁵

Nucleoside analog-resistant herpesvirus infections can be treated with pyrophosphate analogs. Forscarnet, the only approved pyrophosphate inhibitor, does not require phosphorylation to directly bind viral DNA polymerases (Figure 1.4).⁷⁶ Forcarnet is a clinically used in the treatment of TK-deficient HSV and CMV.^{74,77} Cidofovir and other acyclic nucleoside phosphonate analogs are another possible treatment for TK-deficient herpesvirus infections.⁷⁸ Cidofovir contains a phosphonate group that can mimic a monophosphorylated nucleoside, and can be phosphorylated in vivo twice by host cell kinases. Once incorporated into viral DNA, the more stable phosphonate linkage cannot be cleaved by DNA polymerases, and thus acts as a chain termination inhibitor.

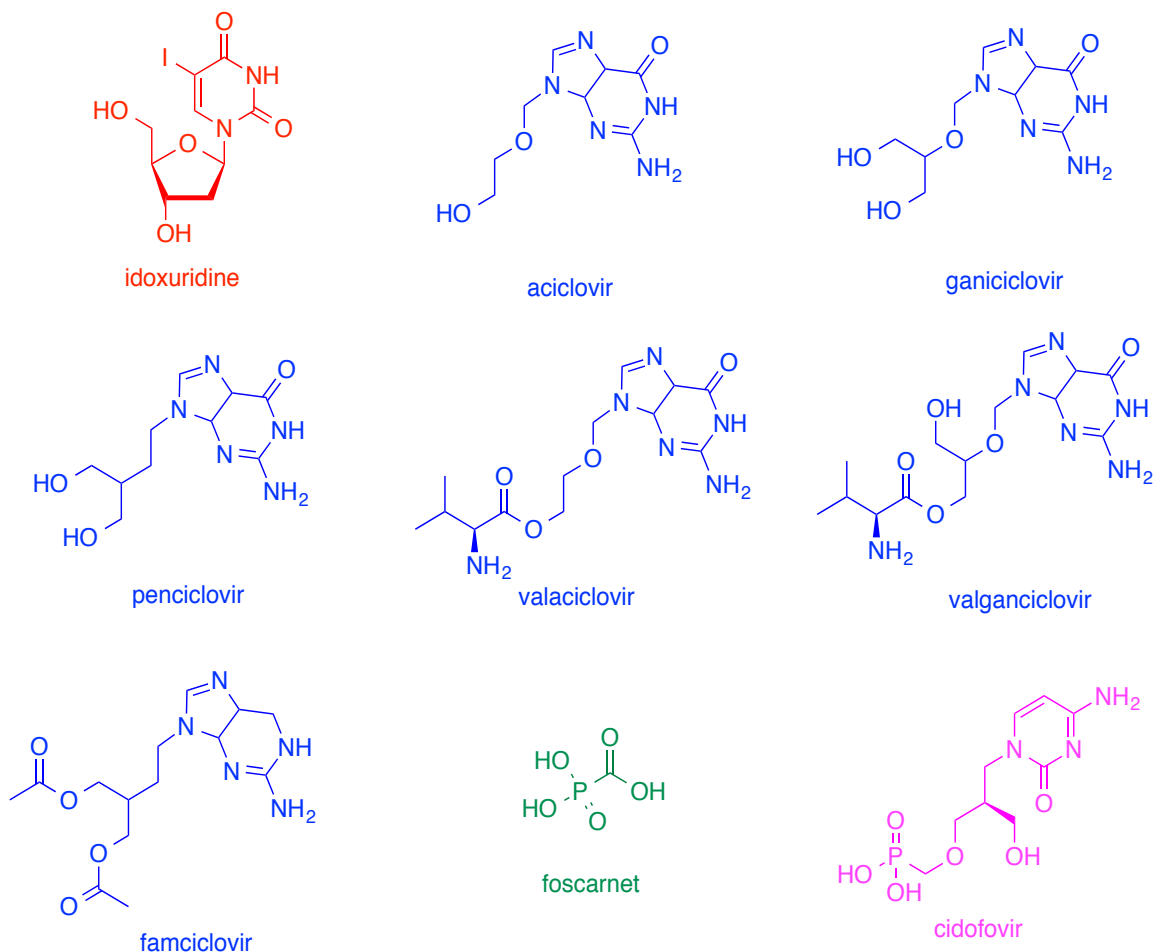


Figure 1.4: Inhibitors of viral DNA synthesis. Compounds in red act as uridine analogs, while compounds in blue are guanosine analogs. Each requires phosphorylation by viral kinases to be activated. Shown in green and purple are inhibitors of pyrophosphate and phosphonate analogs.

In addition to inhibition of viral DNA polymerase, there are a number of other targets for antiviral chemotherapy that are under exploration. Docosanol, an over-the-counter anti-HSV agent used for the treatment of cold sores, has a different mechanism of action than other antiviral drugs (Figure 1.5).⁷⁹ Docosanol is an inhibitor of viral entry, and may act by disrupting the binding of viral entry protein in the lipid envelope with host cell surface receptors⁸⁰. Although this mechanism is not well characterized, and

docosanol is only effective externally, the development of further inhibitors of viral entry may be an effective method of treating herpesviruses.

There are also a number of drugs in preclinical and clinical development that have novel mechanisms of action against herpesviruses. For the treatment of HSV, inhibitors of helicase primase, like pritelivir, may have utility.⁸¹ The helicase-primase complex unwinds viral DNA and generates primers to allow for replication by DNA polymerase.⁸² Inhibitors of this process may increase the affinity of helicase-primase for viral DNA, thus preventing DNA synthesis. Pritelivir has had some success in the clinic, as it reduced viral shedding and genital lesions in patients with HSV-2 in a recent phase II trial.⁸³ Clinical trials with pritelivir and other helicase-primase inhibitors are ongoing.

Inhibition of the later stages of viral replication, particularly DNA maturation, packaging, and capsid nuclear egress, is a promising strategy for the development of new antiviral chemotherapeutics, particularly for CMV.⁸⁴ Letemovir, a novel drug candidate completing phase 3 trials for the treatment of CMV, is an inhibitor of CMV terminase complex (Figure 1.5). The terminase complex is involved in DNA maturation, specifically cleavage of large viral DNA segments into the viral genome, as well as packaging the viral genome into capsids.⁸⁵ Inhibition of this process leads to the accumulation of high-molecular weight DNA fragments and capsids, and prevents viral transmission. Maribavir, which is also in development as an anti-CMV drug, inhibits viral nuclear egress (Figure 1.5).⁸⁶ Maribavir specifically targets the UL97 kinase, which is involved in the release of packaged viral capsids from the nucleus. The clinical results for both letemovir and maribavir demonstrate that drugs targeting viral DNA maturation,

packaging, and nuclear egress represent promising treatment options for both drug-resistant HSV and CMV.

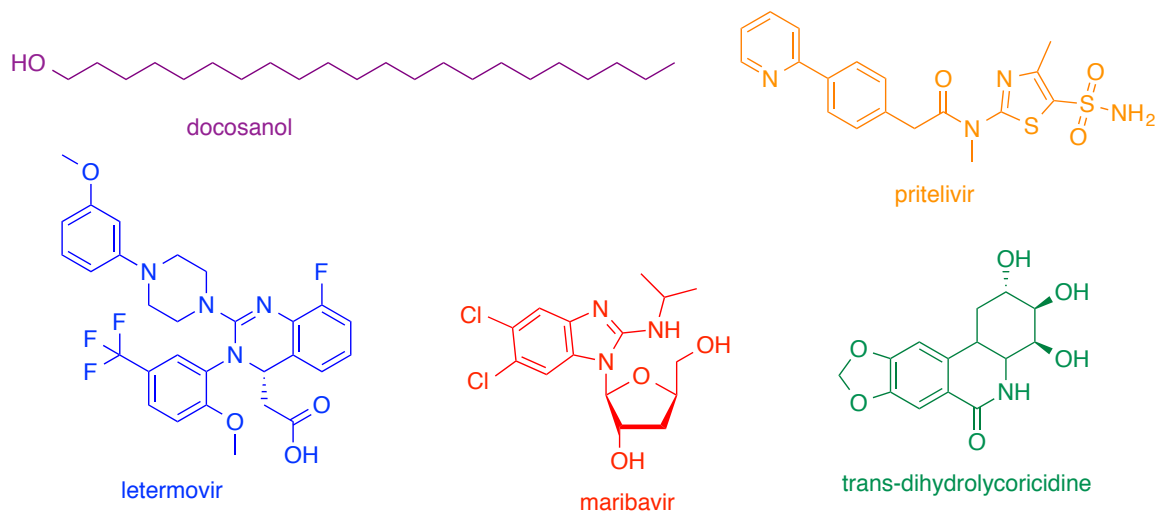


Figure 1.5: Drugs and drug candidates active against herpesviridae that inhibit viral entry, helicase-primase, DNA maturation, and DNA nuclear egress.

Despite the significant achievements made in the treatment of herpesviruses, there are no drugs that can eliminate or prevent reactivation of latent infections. This means that patients require many courses of treatment as their infections recur, and makes it likely that resistance to our current arsenal of antivirals will develop.⁵⁹ Additionally, further study of the relationship between latent HSV-1 infection and cognitive deficits is limited by the lack of drugs that can suppress latent HSV-1 infection. There is therefore a need to identify small molecules that are active against herpesvirus through novel mechanisms, particularly mechanisms involved in regulating latency. Our group has recently reported the potent anti-HSV activity of the Amaryllidaceae alkaloid trans-dihydrolicoricidine, which inhibits both acute and latent forms of HSV (Figure 1.5).⁸⁷

The mechanism of action of this molecule has not yet been identified, but may represent a valuable target for further drug development efforts.

Despite the significant advances made in the treatment of herpesviruses, there are very few clinical options for the treatment of flaviviruses. There is an urgent need for clinical candidates to treat flaviviruses in light of the 2016 ZIKV outbreak. Repurposing other antiviral drugs to find treatment for flaviviruses has led to the identification of several candidates. Ribavirin is a broad spectrum inhibitor of RNA synthesis in several types of viruses, and has moderate antiviral activity against Flaviridae (Figure 1.6).^{88,89} Ribavirin inhibits inosine-5'-monophosphate dehydrogenase, a key enzyme involved in the synthesis of GTP, thus reducing viral RNA replication.⁹⁰ Ribavirin is used in the treatment of HCV, influenza, and other viruses.⁹¹ Despite some efficacy in vitro, no Flaviviruses have been successfully treated in the clinic with ribavirin.⁸⁹ Other nucleoside analog drug candidates, such as BCX-4430⁹² and MK-608,⁹³ were developed for the treatment of other viruses, but have shown activity against flaviviruses like Dengue⁹³ and Zika.^{94,95} Recent reports indicate that sofosbuvir, a drug approved for the treatment of related hepacivirus Hepatitis C (HCV), can also inhibit replication of the flavivirus ZIKV (Figure 1.6).⁹⁶ Sofosbuvir acts as uridine nucleotide analog to inhibit the viral RNA polymerase (NS5B), whose structure may be conserved among Flaviridae.⁹⁷ In addition to the reported activity of other antiviral drugs, considerable efforts have been made to identify FDA-approved drugs with previously unreported antiviral activity. Bromocriptine, an ergoline analog clinically approved to treat type-II diabetes and Parkinson's disease, has recently been shown to be a potent inhibitor of ZIKV in vitro.⁹⁸

Though the target has not been conclusively identified, molecular docking suggests interaction between bromocriptine and the ZIKV-NS2B-NS3 protease. The activity of the compounds has not yet been demonstrated in an animal model.

Natural products may also be a valuable source of novel activity against ZIKV and other flaviviruses. Recently, the alkaloid trans-dihydronarciclasine was found to inhibit ZIKV replication with an IC_{50} of 100 nM, representing one of the most potent anti-ZIKV compounds reported in the literature (Figure 6).⁹⁹ The target of trans-dihydronarciclasine is not yet known. If trans-dihydronarciclasine has a novel antiviral mechanism, this may represent a promising area for further antiviral drug discovery.

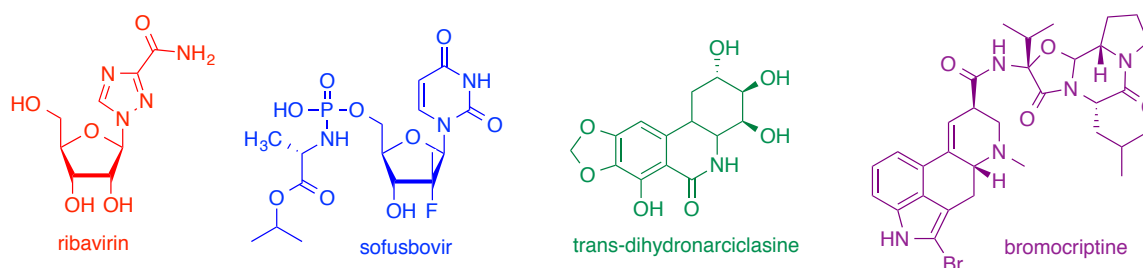


Figure 1.6: Small molecules with activity against flaviviruses

1.7 A strategy for identifying novel small molecules with activity against parasites and viruses

Based on the rapid spread of resistance to current anti-infective drugs, as well as the lack of available pharmaceuticals for treating latent parasitic and viral infections, there is a need to identify new classes of small molecules with activity against microorganisms. This work details our efforts to use novel heterocyclic chemistry and natural product isolation to identify molecules with activity against apicomplexan

parasites and herpesviruses. A new synthetic method for producing 2,3-disubstituted quinolines using aryl enol ethers in a Povarov cyclization, as well as the anti-*Toxoplasma* activity of those quinolines, is detailed in Chapter 2. Chapter 3 will discuss a facile synthesis of dihydroquinazolinones and quinazolinones, as well as our attempts to differentiate the anti-*Toxoplasma* and anti-HSV pharmacophores of these molecules. Chapter 4 will detail the design and synthesis of novel quinazolinone-based analogs of the Amaryllidacea alkaloid, trans-dihydrolycoricidine, and the biological activities of these compounds. Chapter 5 is a report of the isolation of candicine, an abundant defensive alkaloid, from *F. benjamina* latex and the isolation of three novel polyketides from *X. polymorpha*. Chapter 6 will conclude with a summary of the progress contained in this thesis and a view of the further experiments needed to elucidate the biological activity of the synthetic heterocycles and natural products in this work.

1.8 References

- (1) Gaynes, R. P. (2011) Germ theory: medical pioneers in infectious diseases. ASM Press.
- (2) Williams, K. J. (2009) The introduction of “chemotherapy” using arsphenamine - the first magic bullet. *J. R. Soc. Med.* 102, 343–348.
- (3) Aminov, R. I. (2010) A brief history of the antibiotic era: lessons learned and challenges for the future. *Front. Microbiol.* 1, 134.
- (4) Wright, G. D. (2017) Opportunities for natural products in 21st century antibiotic discovery. *Nat. Prod. Rep.* 34, 694-701.
- (5) Staines, H. M., and Krishna, S. (2012) Treatment and prevention of malaria: Antimalarial drug chemistry, action and use. Springer Basel.
- (6) Fleming, A. (2001) On the antibacterial action of cultures of a penicillium, with

special reference to their use in the isolation of *B. influenzae*. 1929. *Bulletin of the World Health Organization* 79, 780–790.

(7) Shen, B. (2015) A new golden age of natural products drug discovery. *Cell* 163, 1297–1300.

(8) World Health Organization. Antimicrobial resistance: Global report on surveillance. Geneva: WHO; 2014.

(9) Schreiber, S. L. (2005) Small molecules: the missing link in the central dogma. *Nat. Chem. Biol.* 1, 64–66.

(10) Harvey, A. L., Edrada-Ebel, R., and Quinn, R. J. (2015) The re-emergence of natural products for drug discovery in the genomics era. *Nat. Rev. Drug. Discov.* 14, 111–129.

(11) Schreiber, S. L. (2009) Organic chemistry: Molecular diversity by design. *Nature* 457, 153–154.

(12) Galloway, W. R. J. D., Isidro-Llobet, A., and Spring, D. R. (2010) Diversity-oriented synthesis as a tool for the discovery of novel biologically active small molecules. *Nat Commun* 1, 80–13.

(13) Burke, M. D., and Schreiber, S. L. (2004) A planning strategy for diversity-oriented synthesis. *Angew. Chem. Int. Ed.* 43, 46–58.

(14) Firth, J. D., Craven, P. G. E., Lilburn, M., Pahl, A., Marsden, S. P., and Nelson, A. (2016) A biosynthesis-inspired approach to over twenty diverse natural product-like scaffolds. *Chem. Commun.* 52, 9837–9840.

(15) Morton, D., Leach, S., Cordier, C., Warriner, S., and Nelson, A. (2008) Synthesis of natural-product-like molecules with over eighty distinct scaffolds. *Angew. Chem. Int. Ed* 48, 104–109.

(16) Montoya, J. G., and Liesenfeld, O. (2004) Toxoplasmosis. *Lancet* 363, 1965–1976.

(17) Sachs, J., and Malaney, P. (2002) The economic and social burden of malaria. *Nature* 415, 680–685.

(18) Kim, K., and Weiss, L. M. (2004) *Toxoplasma gondii*: the model apicomplexan. *Int. J. Parasitol.* 34, 423–432.

(19) Hay, S. I., Guerra, C. A., Gething, P. W., Patil, A. P., Tatem, A. J., Noor, A. M.,

- Kabaria, C. W., Manh, B. H., Elyazar, I. R. F., Brooker, S., Smith, D. L., Moyeed, R. A., and Snow, R. W. (2009) A world malaria map: *Plasmodium falciparum* endemicity in 2007. *PLoS Med* 6, e1000048.
- (20) Murray, C. J., Rosenfeld, L. C., Lim, S. S., Andrews, K. G., Foreman, K. J., Haring, D., Fullman, N., Naghavi, M., Lozano, R., and Lopez, A. D. (2012) Global malaria mortality between 1980 and 2010: a systematic analysis. *Lancet* 379, 413–431.
- (21) Contini, C. (2008) Clinical and diagnostic management of toxoplasmosis in the immunocompromised patient. *Parassitologia* 50, 45–50.
- (22) Ambroise-Thomas, P., and Pelloux, H. (1993) Toxoplasmosis - congenital and in immunocompromised patients: a parallel. *Parasitol. Today* 9, 61–63.
- (23) Hencken, C. P., Jones-Brando, L., Bordón, C., Stohler, R., Mott, B. T., Yolken, R., Posner, G. H., and Woodard, L. E. (2010) Thiazole, oxadiazole, and carboxamide derivatives of artemisinin are highly selective and potent inhibitors of *Toxoplasma gondii*. *J. Med. Chem.* 53, 3594–3601.
- (24) Torrey, E. F., Bartko, J. J., Lun, Z.-R., and Yolken, R. H. (2007) Antibodies to *Toxoplasma gondii* in patients with schizophrenia: a meta-analysis. *Schizophr. Bull.* 33, 729–736.
- (25) Wang, T., Tang, Z.-H., Li, J.-F., Li, X.-N., Wang, X., and Zhao, Z.-J. (2013) A potential association between *Toxoplasma gondii* infection and schizophrenia in mouse models. *Exp. Parasitol.* 135, 497–502.
- (26) Torrey, E. F., Bartko, J. J., and Yolken, R. H. (2012) *Toxoplasma gondii* and other risk factors for schizophrenia: an update. *Schizophr. Bull.* 38, 642–647.
- (27) Baum, J., Gilberger, T. W., Frischknecht, F., and Meissner, M. (2008) Host-cell invasion by malaria parasites: insights from *Plasmodium* and *Toxoplasma*. *Trends Parasitol.* 24, 557–563.
- (28) Laliberté, J., and Carruthers, V. B. (2008) Host cell manipulation by the human pathogen *Toxoplasma gondii*. *Cell. Mol. Life Sci.* 65, 1900–1915.
- (29) Nappi, A. J., and Vass, E. (2002) Parasites of medical importance. CRC Press.
- (30) Ingram, W. M., Goodrich, L. M., Robey, E. A., and Eisen, M. B. (2013) Mice

infected with low-virulence strains of *Toxoplasma gondii* lose their innate aversion to cat urine, even after extensive parasite clearance. *PLoS ONE* 8, e75246.

(31) Prandovszky, E., Gaskell, E., Martin, H., Dubey, J. P., Webster, J. P., and McConkey, G. A. (2011) The neurotropic parasite *Toxoplasma gondii* increases dopamine metabolism. *PLoS ONE* 6, e23866.

(32) Gaskell, E. A., Smith, J. E., Pinney, J. W., Westhead, D. R., and McConkey, G. A. (2009) A unique dual activity amino acid hydroxylase in *Toxoplasma gondii*. *PLoS ONE* 4, e4801.

(33) Howes, O. D., Kambeitz, J., Kim, E., Stahl, D., Slifstein, M., Abi-Dargham, A., and Kapur, S. (2012) The nature of dopamine dysfunction in schizophrenia and what this means for treatment. *Arch. Gen. Psychiatry* 69, 776–786.

(34) Webster, J. P. (2007) The effect of *Toxoplasma gondii* on animal behavior: playing cat and mouse. *Schizophr. Bull.* 33, 752–756.

(35) World Health Organization. (2011) Global plan for artemisinin resistance containment (GPARC). WHO Press.

(36) Achan, J., Talisuna, A. O., Erhart, A., Yeka, A., Tibenderana, J. K., Baliraine, F. N., Rosenthal, P. J., and D'Alessandro, U. (2011) Quinine, an old anti-malarial drug in a modern world: role in the treatment of malaria. *Malar. J.* 10, 144.

(37) Sullivan, D. J., Gluzman, I. Y., Russell, D. G., and Goldberg, D. E. (1996) On the molecular mechanism of chloroquine's antimalarial action. *Proc. Natl. Acad. Sci.* 93, 11865–11870.

(38) Martin, R. E., Marchetti, R. V., Cowan, A. I., Howitt, S. M., Bröer, S., and Kirk, K. (2009) Chloroquine transport via the malaria parasite's chloroquine resistance transporter. *Science* 325, 1680–1682.

(39) Gregson, A., and Plowe, C. V. (2005) Mechanisms of resistance of malaria parasites to antifolates. *Pharmacol. Rev.* 57, 117–145.

(40) Kaye, A. (2011) Toxoplasmosis: diagnosis, treatment, and prevention in congenitally exposed infants. *J. Pediatr. Health Care* 25, 355–364.

(41) Bertino, J. R. (1963) The mechanism of action of the folate antagonists in man.

Cancer Res. 23, 1286–1306.

(42) Jones-Brando, L., D'Angelo, J., Posner, G. H., and Yolken, R. (2006) In vitro inhibition of *Toxoplasma gondii* by four new derivatives of artemisinin. *Antimicrob. Agents Chemother.* 50, 4206–4208.

(43) Wang, J., Zhang, C.-J., Chia, W. N., Loh, C. C. Y., Li, Z., Lee, Y. M., He, Y., Yuan, L.-X., Lim, T. K., Liu, M., Liew, C. X., Lee, Y. Q., Zhang, J., Lu, N., Lim, C. T., Hua, Z.-C., Bin Liu, Shen, H.-M., Tan, K. S. W., and Lin, Q. (2015) Haem-activated promiscuous targeting of artemisinin in *Plasmodium falciparum*. *Nat. Commun.* 6, 10111.

(44) Barton, V., Fisher, N., Biagini, G. A., Ward, S. A., and O'Neill, P. M. (2010) Inhibiting *Plasmodium* cytochrome bc₁: a complex issue. *Curr. Opin. Chem. Biol.* 14, 440–446.

(45) Crofts, A. R. (2004) The cytochrome bc₁ complex: function in the context of structure. *Annu. Rev. Physiol.* 66, 689–733.

(46) Nilsen, A., LaCrue, A. N., White, K. L., Forquer, I. P., Cross, R. M., Marfurt, J., Mather, M. W., Delves, M. J., Shackleford, D. M., Saenz, F. E., Morrissey, J. M., Steuten, J., Mutka, T., Li, Y., Wirjanata, G., Ryan, E., Duffy, S., Kelly, J. X., Sebayang, B. F., Zeeman, A.-M., Noviyanti, R., Sinden, R. E., Kocken, C. H. M., Price, R. N., Avery, V. M., Angulo-Barturen, I., Jiménez-Díaz, M. B., Ferrer, S., Herreros, E., Sanz, L. M., Gamo, F.-J., Bathurst, I., Burrows, J. N., Siegl, P., Guy, R. K., Winter, R. W., Vaidya, A. B., Charman, S. A., Kyle, D. E., Manetsch, R., and Riscoe, M. K. (2013) Quinolone-3-diarylethers: a new class of antimalarial drug. *Sci. Transl. Med.* 5, 177ra37.

(47) Winter, R., Kelly, J. X., Smilkstein, M. J., Hinrichs, D., Koop, D. R., and Riscoe, M. K. (2011) Optimization of endochin-like quinolones for antimalarial activity. *Exp. Parasitol.* 127, 545–551.

(48) Doggett, J. S., Nilsen, A., Forquer, I., Wegmann, K. W., Jones-Brando, L., Yolken, R. H., Bordón, C., Charman, S. A., Katneni, K., Schultz, T., Burrows, J. N., Hinrichs, D. J., Meunier, B., Carruthers, V. B., and Riscoe, M. K. (2012) Endochin-like quinolones are highly efficacious against acute and latent experimental toxoplasmosis. *Proc. Natl. Acad. Sci.* 109, 15936–15941.

- (49) Gelderblom, H. R. (1996) Structure and classification of viruses, in *Medical Microbiology* (Baron, S., Ed.) 4 ed. University of Texas Medical Branch at Galveston, Galveston.
- (50) Roizman, B. (1996) Multiplication, in *Medical Microbiology* (Brachman, P. S., Ed.) 4 ed. University of Texas Medical Branch at Galveston, Galveston.
- (51) Fernandez-Garcia, M.-D., Mazzon, M., Jacobs, M., and Amara, A. (2009) Pathogenesis of flavivirus infections: Using and abusing the host cell. *Cell Host Microbe* 5, 318–328.
- (52) Knipe, D. M., and Cliffe, A. (2008) Chromatin control of herpes simplex virus lytic and latent infection. *Nat. Rev. Microbiol.* 6, 211–221.
- (53) Nicoll, M. P., Hann, W., Shivkumar, M., Harman, L. E. R., Connor, V., Coleman, H. M., Proença, J. T., and Efstathiou, S. (2016) The HSV-1 Latency-Associated Transcript functions to repress latent phase lytic gene expression and suppress virus reactivation from latently infected neurons. *PLoS Pathog.* 12, e1005539.
- (54) Grinde, B. (2013) Herpesviruses: latency and reactivation - viral strategies and host response. *J. Oral. Microbiol.* 5, 283.
- (55) Brachman, P. S. (1996) Epidemiology, in *Medical Microbiology* (Baron, S., Ed.) 4 ed. University of Texas Medical Branch at Galveston, Galveston.
- (56) Wald, A., and Corey, L. (2007) Persistence in the population: epidemiology, transmission, in *Human herpesviruses Biology, therapy, and immunoprophylaxis* (Arvin A., Ed). Cambridge University Press, Cambridge.
- (57) Bloom, D. C., Giordani, N. V., and Kwiatkowski, D. L. (2010) Epigenetic regulation of latent HSV-1 gene expression. *Biochim. Biophys. Acta* 1799, 246–256.
- (58) Gilden, D. H., Mahalingam, R., Cohrs, R. J., and Tyler, K. L. (2007) Herpesvirus infections of the nervous system. *Nat. Clin. Pract. Neuro.* 3, 82–94.
- (59) Frobert, E., Burrel, S., Ducastelle-Lepretre, S., Billaud, G., Ader, F., Casalegno, J.-S., Nave, V., Boutolleau, D., Michallet, M., Lina, B., and Morfin, F. (2014) Resistance of herpes simplex viruses to acyclovir: an update from a ten-year survey in France. *Antiviral Res.* 111, 36–41.

- (60) Nimgaonkar, V. L., and Yolken, R. H. (2012) Neurotropic infectious agents and cognitive impairment in schizophrenia. *Schizophr. Bull.* 38, 1135–1136.
- (61) Dickerson, F. B., Boronow, J. J., Stallings, C., Origoni, A. E., Cole, S., Krivogorsky, B., and Yolken, R. H. (2004) Infection with herpes simplex virus type 1 is associated with cognitive deficits in bipolar disorder. *Biol. Psychiatry* 55, 588–593.
- (62) Schmaljohn, A. L., and McClain, D. (1996) Alphaviruses (togaviridae) and flaviviruses (flaviviridae), in *Medical Microbiology* (Baron, S., Ed.) 4 ed. University of Texas Medical Branch at Galveston, Galveston.
- (63) Singh, M. V., Weber, E. A., Singh, V. B., Stirpe, N. E., and Maggirwar, S. B. (2017) Preventive and therapeutic challenges in combating Zika virus infection: are we getting any closer? *J. Neurovirol.* 23, 347–357.
- (64) Chevalier, M. S., Biggerstaff, B. J., Basavaraju, S. V., Ocfemia, M. C. B., Alsina, J. O., Climent-Peris, C., Moseley, R. R., Chung, K.-W., Rivera-García, B., Bello-Pagán, M., Pate, L. L., Galel, S. A., Williamson, P., and Kuehnert, M. J. (2017) Use of blood donor screening data to estimate Zika virus incidence, Puerto Rico, April-August 2016. *Emerging Infect. Dis.* 23, 790–795.
- (65) De Clercq, E., and Li, G. (2016) Approved antiviral drugs over the past 50 years. *Clin. Microbiol. Rev.* 29, 695–747.
- (66) Prusoff, W. H. (1959) Synthesis and biological activities of iododeoxyuridine, an analog of thymidine. *Biochim. Biophys. Acta* 32, 295–296.
- (67) Kaufman, H. E. (1962) Clinical cure of herpes simplex keratitis by 5-iodo-2'-deoxyuridine. *Exp. Biol. Med.* 109, 251–252.
- (68) Kaufman, H. E., and Heidelberger, C. (1964) Therapeutic antiviral action of 5-trifluoromethyl-2'-deoxyuridine in Herpes simplex keratitis. *Science* 145, 585–586.
- (69) Delamore, I. W., and Prusoff, W. H. (1962) Effect of 5-iodo-2'-deoxyuridine on the biosynthesis of phosphorylated derivatives of thymidine. *Biochem. Pharmacol.* 11, 101–112.
- (70) Privatdegarilhe, M., and De Rudder, J. (1964) Effect of 2-arabinose nucleosides on the multiplication of Herpes virus and vaccine in cell culture. *C. R. Hebd. Seances. Acad.*

Sci. 259, 2725–2728.

(71) Whitley, R., Alford, C., Hess, F., and Buchanan, R. (1980) Vidarabine: A preliminary review of its pharmacological properties and therapeutic use. *Drugs* 20, 267–282.

(72) Elion, G. B., Furman, P. A., Fyfe, J. A., Miranda, P. D., Beauchamp, L., and Schaeffer, H. J. (1977) Selectivity of action of an antiherpetic agent, 9-(2-hydroxyethoxymethyl)guanine. *Proc. Natl. Acad. Sci.* 74, 5716–5720.

(73) Field, H. J., Bell, S. E., Elion, G. B., Nash, A. A., and Wildy, P. (1979) Effect of acycloguanosine treatment of acute and latent herpes simplex infections in mice. *Antimicrob. Agents Chemother.* 15, 554–561.

(74) De Clercq, E. (2004) Antiviral drugs in current clinical use. *J. Clin. Virol.* 30, 115–133.

(75) Bacon, T. H., Levin, M. J., Leary, J. J., Sarisky, R. T., and Sutton, D. (2003) Herpes simplex virus resistance to acyclovir and penciclovir after two decades of antiviral therapy. *Clin. Microbiol. Rev.* 16, 114–128.

(76) Helgstrand, E., Eriksson, B., Johansson, N., Lannero, B., Larsson, A., Misiorny, A., Noren, J., Sjoberg, B., Stenberg, K., Stening, G., Stridh, S., and Oberg, B. (1978) Trisodium phosphonoformate, a new antiviral compound. *Science* 201, 819–821.

(77) Chrisp, P., and Clissold, S. P. (1991) Foscarnet: A review of its antiviral activity, pharmacokinetic properties and therapeutic use in immunocompromised patients with cytomegalovirus retinitis. *Drugs* 41, 104–129.

(78) De Clercq, E. (2003) Clinical potential of the acyclic nucleoside phosphonates cidofovir, adefovir, and tenofovir in treatment of dna virus and retrovirus infections. *Clin. Microbiol. Rev.* 16, 569–596.

(79) Sacks, S. L., Thisted, R. A., Jones, T. M., Barbarash, R. A., Mikolich, D. J., Ruoff, G. E., Jorizzo, J. L., Gunnilla, L. B., Katz, D. H., Khalil, M. H., Morrow, P. R., Yakatan, G. J., Pope, L. E., and Berga, J. E. (2001) Clinical efficacy of topical docosanol 10% cream for herpes simplex labialis: A multicenter, randomized, placebo-controlled trial. *J. Am. Acad. Dermatol.* 45, 222–230.

- (80) Pope, L. E., Marcelletti, J. F., Katz, L. R., Lin, J. Y., Katz, D. H., Parish, M. L., and Spear, P. G. (1998) The anti-herpes simplex virus activity of n-docosanol includes inhibition of the viral entry process. *Antiviral Res.* *40*, 85–94.
- (81) Wald, A., Corey, L., Timmler, B., Magaret, A., Warren, T., Tyring, S., Johnston, C., Kriesel, J., Fife, K., Galitz, L., Stoelben, S., Huang, M.-L., Selke, S., Stobernack, H.-P., Ruebsamen-Schaeff, H., and Birkmann, A. (2014) Helicase–primase inhibitor pritelivir for HSV-2 infection. *N. Engl. J. Med.* *370*, 201–210.
- (82) Slanina, H., Weger, S., Stow, N. D., Kuhrs, A., and Heilbronn, R. (2006) Role of the Herpes Simplex Virus helicase-primase complex during adeno-associated virus DNA replication. *J. Virol.* *80*, 5241–5250.
- (83) Wald, A., Timmler, B., Magaret, A., Warren, T., Tyring, S., Johnston, C., Fife, K., Selke, S., Huang, M.-L., Stobernack, H.-P., Zimmermann, H., Corey, L., Birkmann, A., and Ruebsamen-Schaeff, H. (2016) Effect of pritelivir compared With calacyclovir on genital HSV-2 shedding in patients with frequent recurrences. *JAMA* *316*, 2495–2503.
- (84) Rubin, R. H. (2007) The pathogenesis and clinical management of cytomegalovirus infection in the organ transplant recipient: the end of the silo hypothesis? *Curr. Opin. Infect. Dis.* *20*, 399–407.
- (85) Goldner, T., Hewlett, G., Ettischer, N., Ruebsamen-Schaeff, H., Zimmermann, H., and Lischka, P. (2011) The novel anticytomegalovirus compound AIC246 (Letermovir) inhibits human cytomegalovirus replication through a specific antiviral mechanism that involves the viral terminase. *J. Virol.* *85*, 10884–10893.
- (86) Bright, P. D., Gompels, M., Donati, M., and Johnston, S. (2017) Successful oral treatment of Ganciclovir resistant cytomegalovirus with Maribavir in the context of primary immunodeficiency: First case report and review. *J. Clin. Virol.* *87*, 12–16.
- (87) McNulty, J., D'Aiuto, L., Zhi, Y., McClain, L., Zepeda-Velázquez, C., Ler, S., Jenkins, H. A., Yee, M. B., Piazza, P., Yolken, R. H., Kinchington, P. R., and Nimgaonkar, V. L. (2016) iPSC neuronal assay identifies Amaryllidaceae pharmacophore with multiple effects against herpesvirus infections. *ACS Med Chem Lett* *7*, 46–50.
- (88) Canonico, P. G., Kende, M., Luscri, B. J., and Huggins, J. W. (1984) In-vivo activity

- of antivirals against exotic RNA viral infections. *J. Antimicrob. Chemother.* *14*, 27–41.
- (89) García, L. L., Padilla, L., and Castaño, J. C. (2017) Inhibitors compounds of the flavivirus replication process. *Virology* *14*, 67.
- (90) Wray, S. K., Gilbert, B. E., Noall, M. W., and Knight, V. (1985) Mode of action of ribavirin: Effect of nucleotide pool alterations on influenza virus ribonucleoprotein synthesis. *Antiviral Res* *5*, 29–37.
- (91) Thomas, E., Ghany, M. G., and Liang, T. J. (2012) The application and mechanism of action of ribavirin in therapy of hepatitis C. *Antivir. Chem. Chemother.* *23*, 1–12.
- (92) Warren, T. K., Wells, J., Panchal, R. G., Stuthman, K. S., Garza, N. L., Van Tongeren, S. A., Dong, L., Retterer, C. J., Eaton, B. P., Pegoraro, G., Honnold, S., Bantia, S., Kotian, P., Chen, X., Taubenheim, B. R., Welch, L. S., Minning, D. M., Babu, Y. S., Sheridan, W. P., and Bavari, S. (2014) Protection against filovirus diseases by a novel broad-spectrum nucleoside analogue BCX4430. *Nature* *508*, 402–405.
- (93) Schul, W., Liu, W., Xu, H. Y., Flamand, M., and Vasudevan, S. G. (2007) A Dengue fever viremia model in mice shows reduction in viral replication and suppression of the inflammatory response after treatment with antiviral drugs. *J. Infect. Dis.* *195*, 665–674.
- (94) Julander, J. G., Siddharthan, V., Evans, J., Taylor, R., Tolbert, K., Apuli, C., Stewart, J., Collins, P., Gebre, M., Neilson, S., Van Wettre, A., Lee, Y.-M., Sheridan, W. P., Morrey, J. D., and Babu, Y. S. (2017) Efficacy of the broad-spectrum antiviral compound BCX4430 against Zika virus in cell culture and in a mouse model. *Antiviral Res.* *137*, 14–22.
- (95) Zmurko, J., Marques, R. E., Schols, D., Verbeken, E., Kaptein, S. J. F., and Neyts, J. (2016) The viral polymerase inhibitor 7-deaza-2'-c-methyladenosine is a potent inhibitor of in vitro Zika virus replication and delays disease progression in a robust mouse infection model. *PLOS Negl. Trop. Dis.* *10*, e0004695.
- (96) Sacramento, C. Q., De Melo, G. R., and De Freitas, C. S. (2017) The clinically approved antiviral drug sofosbuvir inhibits Zika virus replication. *Sci. Rep.* *7*, 40920.
- (97) Götte, M., and Feld, J. J. (2016) Direct-acting antiviral agents for hepatitis C: structural and mechanistic insights. *Nat. Rev. Gastroenterol. & Hepatol.* *13*, 338–351.

- (98) Chan, J. F.-W., Chik, K. K.-H., Yuan, S., Yip, C. C.-Y., Zhu, Z., Tee, K.-M., Tsang, J. O.-L., Chan, C. C.-S., Poon, V. K.-M., Lu, G., Zhang, A. J., Lai, K.-K., Chan, K.-H., Kao, R. Y.-T., and Yuen, K.-Y. (2017) Novel antiviral activity and mechanism of bromocriptine as a Zika virus NS2B-NS3 protease inhibitor. *Antiviral Res.* *141*, 29–37.
- (99) Revu, O., Zepeda-Velázquez, C., Nielsen, A. J., McNulty, J., Yolken, R. H., and Jones-Brando, L. (2016) Total synthesis of the natural product (+)-trans-dihydronarciclasine via an asymmetric organocatalytic [3+3]-cycloaddition and discovery of its potent anti-Zika virus (ZIKV) activity. *ChemistrySelect* *1*, 5895–5899.

2 Synthesis of antiparasitic quinolines

2.1 Classical quinoline synthesis

Quinolines have been used in medicine and manufacturing for centuries, so there are a number of name reactions that have been used to prepare quinolines since the 1880s. The Friedlander reaction can be used to prepare 2,3,4-substituted quinolines from carbonyls with a α -methylene group and *o*-amino aryl aldehydes or ketones.^{1,2} This process is often Lewis or Bronsted acid-catalysed^{3, 4,5}, and there are recent reports of organocatalytic Friedlander reactions.⁶ Variations on the Friedlander synthesis employing *o*-amino benzoic acids, as in the Niementowski reaction,⁷ or isatins, as in the Pfitzinger reaction,⁸ give products with hydroxyl or carboxy substituents at C4 respectively. The Skraup-Doebner-VonMiller reaction is commonly used for the preparation of 2,4-disubstituted quinolines from anilines and α,β -unsaturated carbonyls. Though initially requiring harsh conditions and affording quinolines in low yields,⁹ Skraup-Doebner-vonMiller chemistry has now been reported using milder Lewis and Bronsted acids.^{4,10} 2,4-quinolines can also be prepared using β -diketones and anilines in an acid-catalysed process known as the Combes reaction.¹¹ Povarov, or aza-Diels-Alder, chemistry has also been well established as a method for quinoline synthesis.^{12,13} This three-component cyclization between anilines, aldehydes, and alkenes or alkynes afford 2,4-disubstituted quinolines using transition metal or acid catalysis.^{14,15,16,17}

2.2 Quinolines with activity against *T. gondii*

Our work on anti- *T. gondii* compounds started with the synthesis of a library of 4-arylquinoline-2-carboxylates through a Povarov cyclization. A previous member of our group developed a one-step multicomponent reaction catalyzed by AgOTf to construct these quinolines from anilines, ethyl glyoxalate, and phenylacetylenes (Figure 1.1).¹⁷ Screening of the preliminary library indicated that the compounds had moderate activity in the μM range. These compounds were also found to inhibit parasite penetration but not attachment to a host cell. This unusual activity prompted us to explore the structure activity relationships of these compounds in order to improve potency.

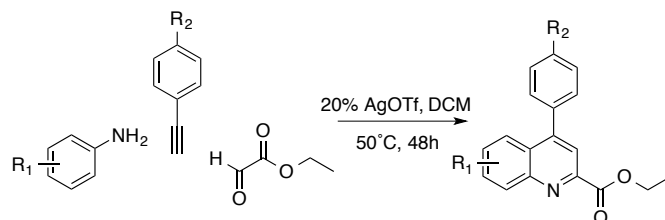


Figure 2.1: Synthesis and activity of our published 4-arylquinoline-2-carboxylate compounds against *T. gondii*. The quinolines were prepared through a AgOTf catalyzed multi-component reaction. The most active compound has an IC₅₀ of 34.0 μM .

A review of the literature identified a number of quinolines and similar heterocycles with anti-*Toxoplasma* activity (Figure 2.2). Endochin, a quinolone natural product, was first reported to have antiparasitic activity in 1948.¹⁸ The poor metabolic properties of endochin led to the development of a series of pyridone¹⁹ and endochin-like quinolone (ELQ)^{20,21} analogs with improved potency and metabolic profiles. These ELQ compounds inhibit parasite cytochrome bc₁, and ELQ-316 (Figure 2.2) is active against both acute and latent *T. gondii* in animal models.²¹ Although their inhibition of

bradyzoites and potency makes ELQ derivatives promising drug candidates, these compounds show poor solubility due to strong intermolecular hydrogen bonding that promotes crystallization.²² We hypothesized that we could improve the potency of our quinolines and the solubility of the ELQ analogs by making hybrid compounds that contain a quinoline core with the substituents of ELQ-316.

In order to make a series of 3-arylquinoline-2-carboxylates, including the 3-arylether derivatives we hypothesized to be active, a novel method using aryl enol ethers as carbonyl surrogates was developed. This work was published in *Org. Biomol. Chem.*, 2016, 14, 5951-5955 and is reproduced below without modifications with permission. C. E. Brown performed all synthetic transformations described in the text, C. Bordon and L. Brando performed assays to determine the activity of diaryl ether compounds. C.E. Brown and J. McNulty prepared the manuscript.

2.3 Enol ethers as carbonyl surrogates in a modification of the Povarov synthesis of 3-arylquinolines and their anti-*Toxoplasma* activity

The development of multicomponent reaction cascade sequences has proven to be of great value for the rapid and efficient construction of heterocyclic compound classes, particularly those with interesting biological activity. Such advances enable synthetic access to collections of analogues in a compound class, permitting the investigation of structure-activity relationships. Substituted quinolines and 4-quinolones have proven to be particularly active against a variety of biological targets,²³⁻²⁵ especially as anti-parasitic agents, where members have shown potent anti-malarial and anti-toxoplasmosis activities (Fig. 2.2).

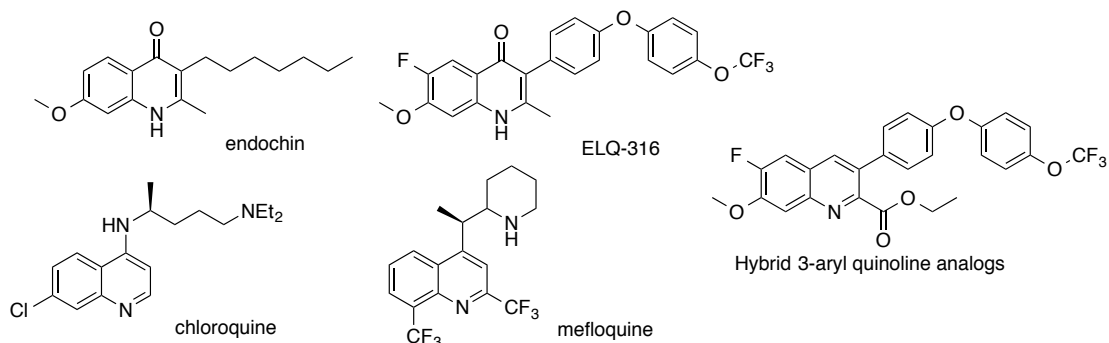


Figure 2.2: Structures of select antiparasitic agents: the 4-quinolones endochin and ELQ316^{6a}, the quinolines chloroquine and mefloquine and novel hybrid 3-aryl quinoline derivatives prepared in this work.

The syntheses of both quinolone and quinoline derivatives has been achieved through multicomponent reaction sequences.^{4,5a} We recently described a one-pot, three-component cascade leading to the synthesis of 4-aryl quinoline derivatives, members of which exhibited modest activity against *Toxoplasma gondii* (*T. gondii*), the parasite responsible for toxoplasmosis.^{5a} As an extension of this work,⁵ we wished to investigate the development of a one-pot, multicomponent sequence for the synthesis of 3-aryl, 2,3-disubstituted quinolines. Quinolones, particularly the natural product endochin and synthetic derivative ELQ-316 (Fig. 2.2), are known to be very potent inhibitors of parasite metabolic respiration^{6a} in *T. gondii*, targeting the cytochrome bc₁ complex. Unfortunately, these derivatives have shown limited bioavailability due to strong intermolecular hydrogen bonding and poor solubility.^{6b,6c} In consideration of the structure of these quinolones, in conjunction with anti-parasitic quinolines such as chloroquine and mefloquine (Fig. 2.2), we hypothesized that hybrid 2,3-substituted quinolines having an electron-withdrawing substituent at C2 and an aryl substituent at C3 could serve as useful analogues of the quinolone/quinoline pharmacophores. Additionally, simple salt forms

(HX salts) or zwitterionic forms of these quinolines could be prepared to mitigate solubility issues. Our initial work on Povarov-type approach to quinolines using phenylacetylenes gave 4-arylquinolines with high regioselectivity.^{5a} In order to access 3-arylquinolines, a process offering reversed regioselectivity would be required, for example employing a phenylacetaldehyde as an umpoled synthetic equivalent of a phenylacetylene. The inverse-electron-demand Povarov cyclization (IEDP) appeared to be an ideal multicomponent reaction cascade for this purpose.⁷

The IEDP reaction is a Lewis acid^{7a,7b,7c} or Bronsted acid^{7d,7e} catalysed process. The reaction typically involves the cyclization (concerted or stepwise) of an imine, derived from an aniline and aldehyde, with an electron rich dienophile, such as ethylvinyl ether^{7a,7d} or a cyclic enol ether,^{7b,7d,7e} leading to tetrahydro-quinolines. Alternatively, enols generated from enolisable aldehyde can be used as dienophile equivalents, affording 3-substituted quinolines.⁸

Retrosynthetic analysis (Fig. 2.3) along these lines reveals that application of the IEDP cascade to this core would require the incorporation of a reactive phenylacetaldehyde derivative in order to access the 3-aryl quinolines. Unfortunately, successful application of phenylacetaldehyde derivatives has been extremely limited in this reaction with only a few moderately yielding examples being reported,^{8d,8e} and others reporting “dirty” reactions providing only traces of the desired products detectable by NMR.^{8c} In this communication we present our initial results that confirm these findings and introduce a novel modification of the Povarov cascade using enol-ether derivatives of phenylacetaldehydes as synthetic equivalents. The development of an efficient one-pot

reaction cascade leading to the desired 3-aryl quinolines and preliminary results on the screening of a selection of derivatives against *T. gondii* is also reported.

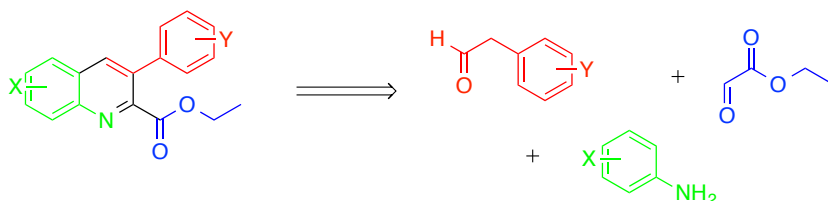
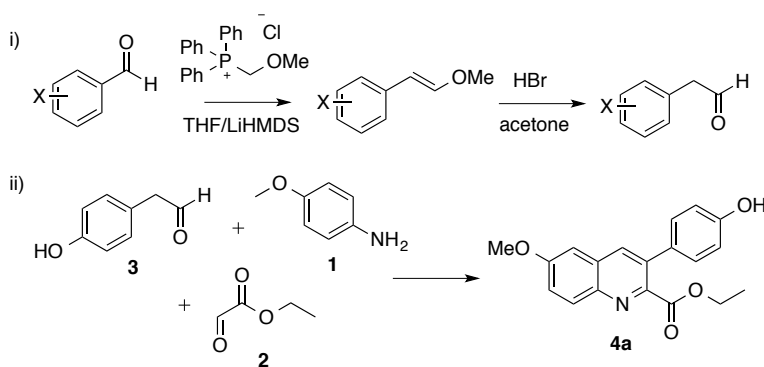


Figure 2.3: Retrosynthetic analysis of the proposed 3-aryl quinolines as products of a three component coupling of substituted aniline and phenylacetaldehyde derivatives with ethyl glyoxylate.

Despite the anticipated difficulty of preparing 3-aryl derivatives, the possibility of achieving the one-pot, three-component cascade as shown in Figure 2.3, encouraged us to investigate the process under mild conditions with phenylacetaldehyde derivatives. The required phenylacetaldehyde derivatives were prepared from available benzaldehydes using the standard methoxymethyl-triphenyl-phosphonium salt, Scheme 1, i).⁹ The intermediate enol-ethers were obtained in high yield and hydrolysed using 1.1 eq HBr in acetone to produce the phenylacetaldehyde derivatives. As a point of entry, we investigated the three component coupling of 4-hydroxyphenylacetaldehyde **3** with ethyl glyoxylate **2** and 4-methoxyaniline **1** (*p*-anisidine), Scheme 2.1, ii). Under a variety of conditions investigated, the desired quinoline **4a** was obtained in a maximum yield of 21% over two steps from the enol ether, still containing impurities by NMR that co-eluted and could not be removed. While these negative results forced us to abandon the direct phenylacetaldehyde route, the intermediacy of the vinyl ether (Scheme 2.1, i) prompted us to consider its direct incorporation as the unpoled phenylacetylene, a route that would

also eliminate the hydrolysis step and prevent unwanted side-reactions of the free phenylacetaldehyde. To our delight, this process met with immediate success.

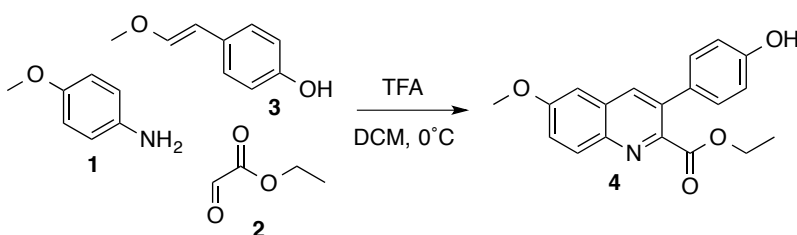


Scheme 2.1: i) General synthesis of phenylacetaldehyde derivatives through hydrolysis of the vinyl ether **3**, prepared from the Wittig reagent⁸ derived from methoxymethyltriphenylphosphonium chloride. ii) Three-component coupling using 4-hydroxyphenylacetaldehyde, *p*-anisidine and ethyl glyoxylate to yield the quinoline **4a**.

A number of conditions were explored to effect this multicomponent coupling (Table 2.1). Dichloromethane (DCM) was found to be a suitable solvent for this reaction. Trifluoroacetic acid (TFA) was the most effective acid reagent although other protic and Lewis acids also afforded the desired product in lower yields. Additionally, we found that imine formation *in situ* gave higher yields than use of pre-formed imines. The multicomponent reaction is completed *very rapidly* in just 5 minutes at 0 °C. Longer reaction times and warmer temperatures lead to lower yields; the appearance of several new spots on TLC after several hours indicates that degradation of the product occurs under the reaction conditions. These conditions are mild in comparison to previous procedures for the preparation of 3-substituted quinolines.⁸ Overall, the method allowed

for the preparation of a wide range of 3-arylquinolines quickly and efficiently as summarized in Fig. 2.4.

Table 2.1: Optimized conditions for the multicomponent reaction



Acid	Solvent	Imine formation	Temp. (°C)	Reaction Time	Yield (%)
TFA	DCM	In situ	0	5 min	82
TFA	Toluene	In situ	0	5 min	70
CSA	DCM	In situ	0	5 min	43
PTSA	DCM	In situ	0	5 min	N.R.
AlCl ₃	DCM	In situ	0	5 min	59
Yb(OTf) ₃	DCM	In situ	0	5 min	N.R.
TFA	DCM	Isolated	0	5 min	50
TFA	DCM	In situ	0	16 hours	trace
TFA	DCM	In situ	RT	5 min	44
None	DCM	Isolated	0	5 min	N.R.

Generally, the reaction proved highly effective using electron-rich enol ethers. Enol ethers with electron withdrawing aryl substituents gave slightly lower yields that were not improved by longer reaction times. This reaction proceeds with *ortho*, *meta*, or *para* substituents on the enol ether fragment, with lactonisation being observed with the 2-hydroxy derivative yielding the tetracycle **4c**. The new method is particularly effective for the direct preparation of phenolic quinolines, as no protecting groups are required. The electronic effects observed in the reaction and the requirement of proton catalysis and led

us to postulate the following mechanism (Scheme 2.2). Condensation of the aniline with ethyl glyoxylate gives the imine, protonation of which leads to intermediate (i). Two possible pathways can be considered for the reaction, a stepwise (Path A) Mannich-aldol type process proceeding through intermediate (ii) to give intermediate (iii) or a concerted inverse-electron-demand Diels-Alder process (Path B) leading directly to intermediate (iii). Loss of a proton to rearomatise followed by loss of methanol and spontaneous oxidation leads to the desired product. No observable intermediates have been detected during the reaction, and the autoxidation step is spontaneous, despite the reaction occurring rapidly in an inert atmosphere.

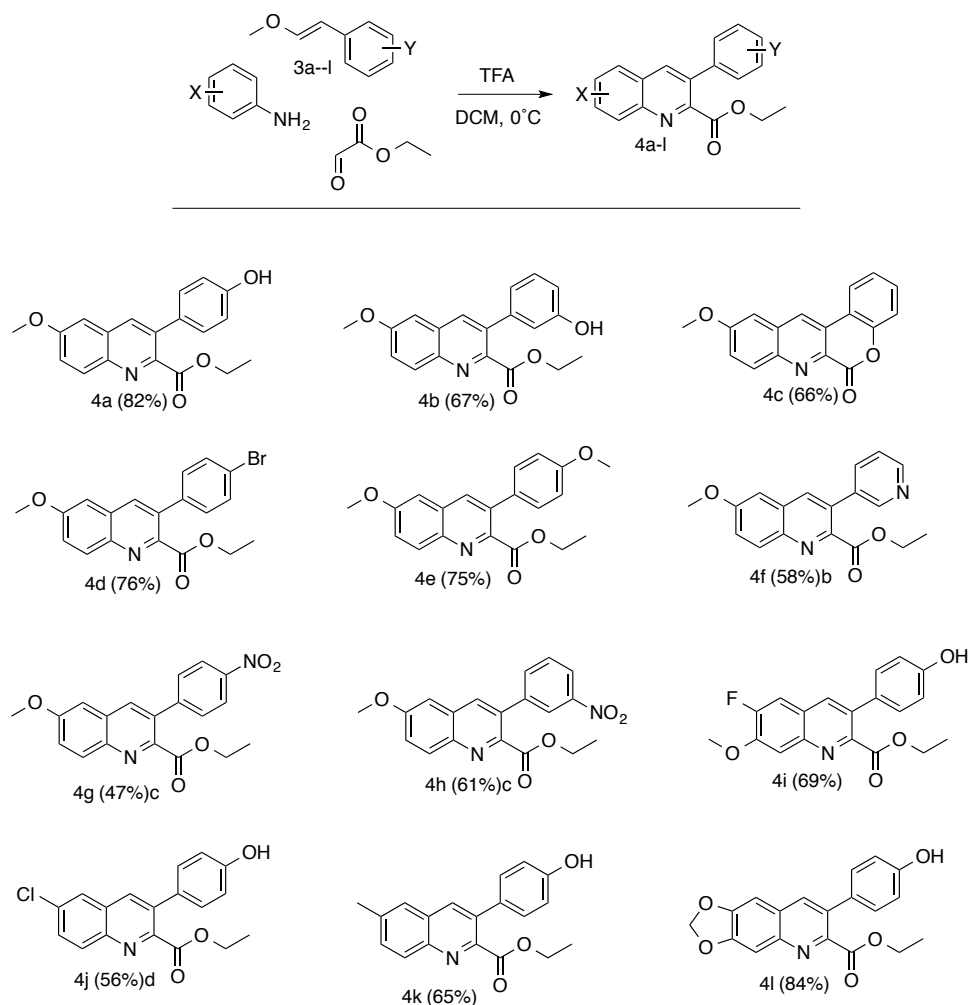
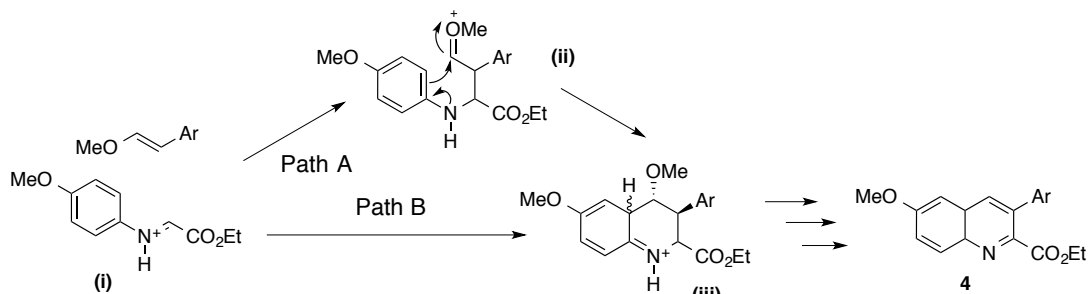


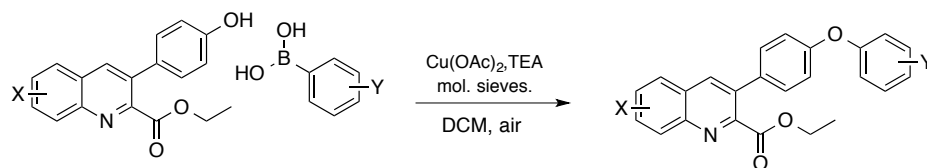
Figure 2.4: Substrate scope of the multicomponent reaction. Unless otherwise stated, reaction conditions: **1** (1.2 eq), **2**, (1.2 eq), **3a-l** (1.0 eq), TFA (1.05 eq), DCM, 0°C, 5 min. ^b TFA (2.05 eq), ^c 15 minutes ^d 1 hour



Scheme 2.2: Possible stepwise (Path A) or concerted (Path B) reaction pathways available for the new enol ether-mediated cycloaddition process

We next investigated *O*-arylation on a selection of these quinolines containing the C3-substituted phenols in order to access quinoline-analogues of the known anti-toxoplasmosis quinolones, such as ELQ-316 (Fig. 2.2). Fortunately, the phenolic quinoline **4i**, readily underwent Chan-Lam coupling¹⁰ with 4-trifluoromethoxyphenylboronic acid permitting installation of the diaryl ether functionality. The product of this reaction, **5a**, contains identical diaryl ether and 3-methoxy-4-fluoro aryl ring-A substituents as found in ELQ-316 (Table 2.2). To explore the effects of fluorination on the diaryl ether and quinoline core, we also prepared two other diaryl ether analogs **5b** and **5c** from phenols **4i** and **4a** using the Cham-Lam conditions.¹⁰ We next proceeded to investigate the biological activity of three compounds against *T. gondii*.

Table 2.2: Synthesis of 3-diaryl ether quinoline derivatives



X	Y	Product	Yield (%)
6-F, 7-OMe	OCF ₃	5a	80
6-F, 7-OMe	OCH ₃	5b	70
6-OMe	OCF ₃	5c	53

A well-established colourimetric assay was used to screen the compounds for inhibition of *T. gondii* growth.¹¹ In short, human foreskin fibroblast (HFF; ATCC) host cells were first exposed to a concentration range (320 – 0.32μM) of test compounds or

assay positive control trimethoprim. Directly following this, tachyzoites of *T. gondii* RH-2F (ATCC), a strain that constitutively expresses β -galactosidase, were added to the cells. Equivalent compound-exposed cells were left uninfected for determination of compound cytotoxicity. Infected and uninfected cells were incubated for four days, and then the β -galactosidase substrate chlorophenol red- β -D-galactopyranoside (CPRG) was added. In the presence of live *T. gondii* expressing β -galactosidase, this substrate is hydrolysed to chlorophenol red, which can be detected by measuring absorbance at 570 nm. Viability of uninfected, compound-exposed cells is ascertained by the amount of bio-reduction of a cell viability reagent (CellTiter 96® Aqueous One Solution; Promega, WI), as determined colourimetrically by measurement of absorbance at 490 nm. Absorbance data were used to calculate the median inhibitory concentration (IC_{50}) and the median cytotoxic dose (TD_{50}) for each compound using CalcuSyn software (Biosoft, Cambridge, U.K.). The therapeutic index (TI), an indicator of the specific activity against the tachyzoites, was calculated using the formula $TI = TD_{50} / IC_{50}$ (Table 2.3).

Table 2.3: Anti-toxoplasmosis activity of 4-arylquinolines

Compound	IC_{50} (μ M)	TD_{50} (μ M)	TI
5a	5	≥ 320	64
5b	21	≥ 320	15
5c	26	≥ 320	12
Trimethoprim	12	≥ 320	27

Compounds **5a-5c** were further evaluated for the ability to inhibit the invasion of host cells by tachyzoites using an established red/green invasion assay.¹¹ For this assay, purified extracellular tachyzoites are incubated with test compounds and then added to

actively growing HFF host cells. Fluorescent staining is used to distinguish tachyzoites that have penetrated the host cell (Figure 2.5, green bars) from tachyzoites that have attached to the host cell but were unable to penetrate (Figure 2.5, red bars) as well as from tachyzoites that began but were unable to complete host cell invasion (Figure 2.5, yellow bars). A decrease in the number of penetrated (green) tachyzoites relative to vehicle [DMSO (VHL)] indicates inhibition of invasion. Further, a difference in the total number of tachyzoites (Figure 4, green + yellow + red) relative to the same for VHL, indicates an effect on tachyzoite attachment to host cells.¹¹ As shown in Figure 2.5, all three quinolines significantly inhibit tachyzoite invasion; quinoline **5a** additionally inhibits tachyzoite attachment.

All three compounds displayed modest to potent ability to inhibit tachyzoite growth and invasion while remaining non-cytotoxic ($TD_{50} \geq 320 \mu\text{M}$). Compound **5a**, the most direct analogue of ELQ-316, was especially effective against *T. gondii* growth ($IC_{50} = 5 \mu\text{M}$) and inhibited both attachment and invasion. Thus, removal of fluorinated substituents on the diaryl ether (**5b**) or benzenoid ring (**5c**) appeared to decrease the overall efficacy of this compound. This finding presents an opportunity to interrogate structure-activity relationship of this pharmacophore. The three quinolines prepared show moderate activity, however, they are 1000-fold less active than related quinolones.^{6a} This difference in potency may be due to reduced hydrogen bonding ability of the quinoline core when compared to quinolones.¹² Nonetheless, the good activity shown in conjunction with no apparent host cell cytotoxicity for all three compounds **5a-5c**

demonstrates the new 3-aryl quinoline scaffold to be a promising lead towards the development of selective anti-toxoplasmosis agents.

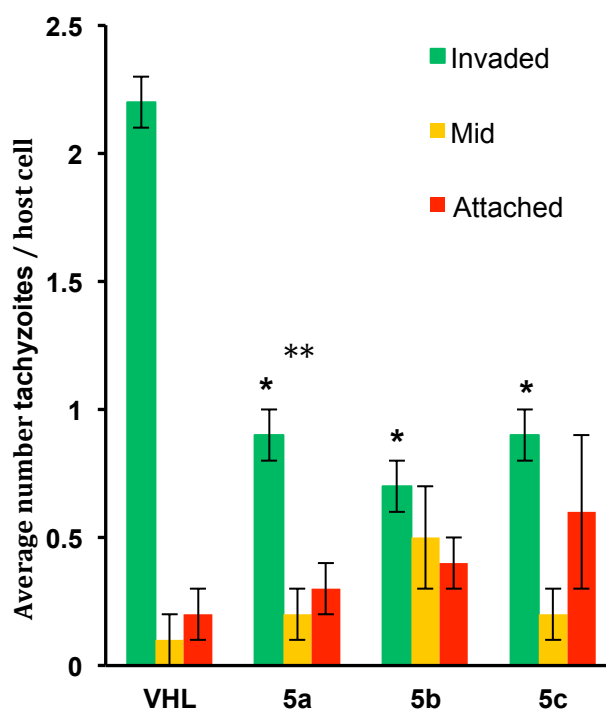


Figure 2.5: Quantification of *T. gondii* invasion inhibition by quinolines. Compounds were tested at 10 μ M on extracellular tachyzoites using an established method. Green bars represent invaded parasites, while red bars represent tachyzoites attached to the surface of the host cell. Yellow bars represent tachyzoites in the process of invasion. *Tachyzoite invasion was significantly decreased ($P \leq 0.05$, two-tailed Student's *t*-test) relative to VHL. **Tachyzoite attachment to host cell was significantly decreased ($P \leq 0.05$, two-tailed Student's *t*-test) relative to VHL.

In conclusion, we report a novel, highly effective method for the preparation of 3-aryl, 2,3-disubstituted quinolines using enol ethers as surrogates of arylacetaldehydes. The reaction occurs rapidly under mild conditions giving quinolines in good to high yields. The reaction proceeds through either a stepwise Mannich-aldol sequence or a concerted Povarov-type process. The use of aryl enol ethers also allows access to products having

reversed regioselectivity in comparison to standard Povarov products.^{5a} The chemistry was utilised to prepare a wide range of 3-aryl quinolines and a narrower selection of vaulted diaryl ether analogues. These were shown to possess growth inhibitory activity to *T. gondii* and proved non-cytotoxic to the host cells. The preparation of a wider selection of functionalized 3-aryl quinolines and analysis of their anti-parasitic activities is under current investigation in our laboratories.

Notes and References:

- 1 O. Di Pietro, E. Vicente-García, M. C. Taylor, D. Berenguer, E. Viayna, A. Lanzoni, I. Sola, H. Sayago, C. Riera, R. Fisa, M. V. Clos, B. Pérez, J. M. Kelly, R. Lavilla and D. Muñoz-Torrero, *Eur. J. Med. Chem.*, 2015, **105**, 120–137.
- 2 A. M. Gilbert, M. G. Bursavich, S. Lombardi, K. E. Georgiadis, E. Reifenberg, C. R. Flannery and E. A. Morris, *Bioorg. Med. Chem. Lett.*, 2008, **18**, 6454–6457.
- 3 A. Mai, D. Rotili, D. Tarantino, A. Nebbioso, S. Castellano, G. Sbardella, M. Tini and L. Altucci, *Bioorg. Med. Chem. Lett.*, 2009, **19**, 1132–1135.
- 4 (a) E. Vicente-García, R. Ramón, S. Preciado and R. Lavilla, *Beilstein J. Org. Chem.*, 2011, **7**, 980–987. (b) S. Majumder, K. R. Gipson and A. L. Odom, *Org. Lett.*, 2009, **11**, 4720–4723. (c) B.-B. Feng, J. Xu, M.-M. Zhang, X.-S. Wang, *Synthesis*, 2016, **48**, 65-72.
- 5 (a) J. McNulty, R. Vemula, C. Bordón, R. Yolken and L. Jones-Brando, *Org. Biomol. Chem.*, 2014, **12**, 255–260. (b) J. McNulty, K. Keskar, C. Bordón, R. Yolken and L. Jones-Brando, *Chem. Comm.*, 2014, **50**, 8904-8907. (c) McNulty, K. Keskar, H. A. Jenkins, N. H. Werstiuk, C. Bordón, R. Yolken and L. Jones-Brando, *Org. Biomol. Chem.*, 2015, **13**, 10015-10024.
- 6 (a) J. S. Doggett, A. Nilsen, I. Forquer, K. W. Wegmann, L. Jones-Brando, R. H. Yolken, C. Bordón, S. A. Charman, K. Katneni, T. Schultz, J. N. Burrows, D. J. Hinrichs, B. Meunier, V. B. Carruthers and M. K. Riscoe, *Proc. Nat. Acad. Sci.*,

- 2012, **109**, 15936–15941. (b) G. P. Miley, S. Pou, R. Winter, A. Nilsen, Y. Li, J. X. Kelly, A. M. Stickles, M. W. Mather, I. P. Forquer, A. M. Pershing, K. White, D. Shackleford, J. Saunders, G. Chen, L.-M. Ting, K. Kim, L. N. Zakharov, C. Donini, J. N. Burrows, A. B. Vaidya, S. A. Charman and M. K. Riscoe, *Antimicrob. Agents Chemother.*, 2015, **59**, 5555–5560. (c) A. Nilsen, G. P. Miley, I. P. Forquer, M. W. Mather, K. Katneni, Y. Li, S. Pou, A. M. Pershing, A. M. Stickles, E. Ryan, J. X. Kelly, J. S. Doggett, K. L. White, D. J. Hinrichs, R. W. Winter, S. A. Charman, L. N. Zakharov, I. Bathurst, J. N. Burrows, A. B. Vaidya and M. K. Riscoe, *J. Med. Chem.*, 2014, **57**, 3818–3834.
- 7 (a) Povarov, L.S. *Russ. Chem. Rev.* 1967, **36**, 656-670. (b) Batey, R.A., Powell, D.A., Acton, A. Lough, A.J. 2001, *Tetrahedron Lett.* **42**, 7935-7939. (c) Zhou, Z., Xu, F., Han, Z., Zhou, J., Shen, Q. *Eur. J. Org. Chem.* 2007, **31**, 5265-5269. (d) Akiyama, T., Morita, H., Fuchibe, K. *J. Am. Chem. Soc.* 2006, **128**, 13070-13071. (e) Galvin, A. Calleja, J., Gonazalez-Perez, A.B., Alvarez, R., de Lera, A, Fananas, F.J., Roriguez, F. *Chem. Eur. J.* 2015, **21**, 16769–16774.
- 8 (a) M. H. So, Y. Liu, C. M. Ho, K. Y. Lam and C. M. Che, *ChemCatChem*, 2011, **3**, 386-393. (b) L. He, J.-Q. Wang, Y. Gong, Y.-M. Liu, Y. Cao, H.-Y. He and K.-N. Fan, *Angew. Chem. Int. Ed. Engl.*, 2011, **50**, 10216–10220. (c) X. Jia, F. Peng, C. Qing, C. Huo, Y. Wang and X. Wang, *Tetrahedron Lett.*, 2013, **54**, 4950-4952. (d) T. Igarashi, T. Inada, T. Sekioka, T. Nakajima and I. Shimizu, *Chem. Lett.*, 2005, **34**, 106-107.. (e) R. I. Khusnutdinov, A. R. Baygusina and R. I. Aminov, *Russ. J. Org. Chem*, 2012, **48**, 690-693.. (f) Lin, X.-F., Cui, S.-L., Wang, Y.-G. *Tetrahedron Lett.*, 2006, **47**, 3127-3130. (g) S.-Y. Tanaka, M. Yasuda and A. Baba, *J. Org. Chem.*, 2006, **71**, 800–803. (h) Q. Guo, W. Wang, W. Teng, L. Chen and Y. Wang, *Synth. Comm.*, 2012, **42**, 2574-2584.
- 9 (a) Levine, S. G. *J. Am. Chem. Soc.* 1958, **80**, 6150–6151. (b) Wittig, G., Boll, W., Kruck, K. H. *Chem. Ber.* 1962, **95**, 2514–2525. (c) Schlude, H. *Tetrahedron* 1975, **31**, 89–92. (d) Kruse, C. G., Poels, E. K., van der Gen, A. *J. Org. Chem.* 1979, **44**,

- 2911–2915. (e) Coulson, D. R. *Tetrahedron Lett.* 1964, **5**, 3323–3326. (f) Das, P., McNulty, J. *Eur. J. Org. Chem.*, 2010, **2010**, 3587-3591.
- 10 (a) D.A. Evans, J.L. Katz, T.R. West, *Tetrahedron Lett.*, 1998, **39**, 2937-2940. (b) P.Y.S. Lam, C.G. Clark, S. Saubern, J. Adams, M.P. Winters, D.M.T. Chan, A. Combs, *Tetrahedron Lett.*, 1998, **39**, 2941-2944. (c) D.M.T. Chan, K.L. Monaco, R. Wang, M.P. Winters, *Tetrahedron Lett.*, 1998, **39**, 2933-2936.
- 11 L. Jones-Brando, E. F. Torrey and R. Yolken, *Schizophr. Res.*, 2003, **62**, 237–244.
- 12 C. P. Hencken, L. Jones-Brando, C. Bordón, R. Stohler, B. T. Mott, R. Yolken, G. H. Posner and L. E. Woodard, *J. Med. Chem.*, 2010, **53**, 3594–3601.
- 13 M.J. Capper et al, *Proc. Natl. Acad. Sci.*, 2015, **112**, 755-760.

2.4 Conclusion and future work

We sought to develop a new method of preparing 3-arylquinolines that would minimize the difficulties in handling phenylacetaldehydes and improve yield. We found that the intermediate enol ethers generated in our initial route could cyclize with imines to afford the desired 3-arylquinolines in superior yields in a process promoted by TFA. This reaction proceeds to completion in just 5 minutes and is tolerant of different aldehydes and anilines. It is a particularly effective way to prepare phenolic quinoline compounds without protecting groups. This method allowed us to quickly prepare 3-diarylether analogs with and without the fluorinated groups employed in the pyridone¹⁹ and ELQ series.²¹

These 3-diarylether quinolines were more potent than the initial 4-arylquinoline-2-carboxylates, with the most potent derivative **2-5a** inhibiting *T. gondii* with an IC₅₀ of 5 μM. **5a** also inhibited the attachment and invasion abilities of the parasite. Additionally, our quinoline derivatives displayed none of the solubility issues or non-linear dose

response curves observed in the ELQ series.²¹ However, this compound is significantly less active than comparable analogs in the ELQ series. This suggests that the hydrogen bonding interactions between the quinolone carbonyl and the cytochrome bc₁ target are crucial for activity. Our most potent analog, **5a**, lacks any group that may act as a hydrogen bond acceptor at position 4. Future work on these compounds could involve the preparation of 3-arylquinolines with a ketone bioisostere, such as a halogen, at the 4-position.²⁶

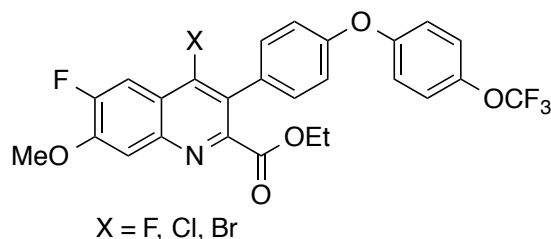


Figure 2.6: Proposed structure of a 3-diarylether quinoline analog. A 4-halogenated quinoline may have improved anti-*Toxoplasma* activity if a halogen group can mimic the hydrogen bonding interaction of the quinolone core.

In addition to the exciting biological activity of the quinolines prepared, this novel method for the preparation of 2,3-disubstituted quinolines merits further exploration. The aryl enol ether synthon used as a carbonyl surrogate in this reaction may have interesting reactivity in other cycloadditions. [2+2] and [2+3] cycloaddition with these enol ethers would allow for access to a variety of interesting 4- and 5-membered ring systems.

2.5 Experimental

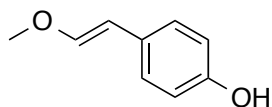
General Information:

All reagents were obtained from Sigma-Aldrich and used as received. Solvents were freshly distilled (DCM was distilled over CaH₂, toluene was distilled over sodium/benzophenone). All reactions were performed with oven-dried glassware under

dry N₂ atmosphere. Thin layer chromatography (TLC) was performed using aluminium sheets precoated with silica gel 60F₂₅₄ (Macherey-Nagel) and visualized using 254 nm UV light. ¹H and ¹³C NMR spectra were recorded on a Bruker AV 600 spectrometer using CDCl₃ or methanol-d₄ as solvents. Chemical shifts (δ) are reported in ppm and coupling constants (J) are expressed in Hertz (Hz).

General procedure for preparation of enol ethers:

Methoxymethyltriphenylphosphine chloride (1.2 eq) was dissolved in THF under N₂ (1 mM) and cooled to 0°C in an ice bath. LiHMDS (1.3 eq, 1M solution in THF) was added dropwise. The reaction was allowed to stir for 20 minutes at 0°C to allow for imine formation. The benzaldehyde (1.0 eq) was dissolved in THF (1 mM) and added dropwise to the ylide solution. The reaction was allowed to warm to room temperature over 2 hours, then quenched by the addition of a saturated NH₄Cl solution. The reaction mixture was extracted with DCM, and the organic layers were combined and concentrated under reduced pressure. The crude product was purified by silica gel chromatography using a hexane:EtOAc (9:1) gradient elution to afford the desired product.



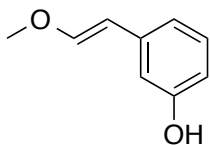
4-(2-methoxyethenyl)-phenol (3a): colourless oil (>95%)

Major isomer (2:1)

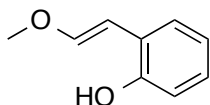
¹H NMR (600 MHz, CDCl₃): δ 3.75 (3H, s), 5.16 (1H, d, J = 7.0 Hz), 6.05 (1H, d, J = 7.0 Hz), 6.75 (2H, d, J = 8.7 Hz), 7.46 (2H, d, J = 8.7 Hz)

Minor Isomer

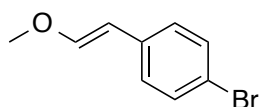
¹H NMR (600 MHz, CDCl₃): δ 3.66 (3H, s), 5.77 (1H, d, J = 13.0 Hz), 6.74 (1H, d, J = 8.6 Hz), 6.92 (2H, d, J = 13.0 Hz), 7.11 (2H, d, J = 8.5 Hz)



3-(2-methoxyethenyl)-phenol (3b): colourless oil (74%); filtered through a silica plug and used without further purification.



2-(2-methoxyethenyl)-phenol (3c): colourless oil (33%); ^1H NMR (600 MHz, CDCl_3): δ 3.84 (3H, s), 5.39 (1H, d, $J = 7.1$ Hz), 6.06 (1H, d, $J = 7.2$ Hz), 6.84 (1H, td, $J = 1.2, 7.5$ Hz), 6.91 (1H, dd, $J = 1.2, 8.1$ Hz), 7.09 (1H, dd, $J = 1.6, 7.7$ Hz), 7.15 (1H, ddd, $J = 1.7, 7.2, 8.1$ Hz), 7.60 (1H, broad s); ^{13}C NMR (150 MHz, CDCl_3): δ 60.8, 105.4, 117.9, 120.2, 121.6, 128.9, 131.1, 143.5, 153.8.



1-bromo-4-(2-methoxyethenyl)-benzene (3d): colourless oil (>95%)

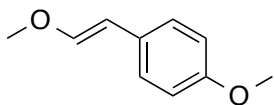
Major isomer (7:2)

^1H NMR (600 MHz, CDCl_3): δ 3.68 (3H, s), 5.74 (1H, d, $J = 13.0$ Hz), 7.04 (1H, d, $J = 13.0$ Hz), 7.09 (2H, d, $J = 8.4$ Hz), 7.37 (2H, d, $J = 8.5$ Hz); ^{13}C NMR (150 MHz, CDCl_3): δ 56.7, 104.2, 119.3, 126.7, 131.7, 135.5

Minor Isomer

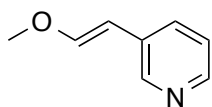
^1H NMR (600 MHz, CDCl_3): δ 3.79 (3H, s), 5.16 (1H, d, $J = 7.0$ Hz), 6.16 (1H, d, $J = 7.0$ Hz), 7.39 (2H, d, $J = 8.7$ Hz), 7.44 (2H, d, $J = 8.6$ Hz); ^{13}C NMR (150 MHz, CDCl_3): δ 60.9, 104.7, 119.1, 129.8, 131.3, 135.0

High resolution MS: m/z calc. for $\text{C}_9\text{H}_{10}\text{BrO}^+$: 211.9837, found 211.9826.



1-methoxy-4-(2-methoxyethenyl)benzene (3e): colourless oil (70%); filtered through a silica plug and used without further purification.

High resolution MS: m/z calc. for $C_{10}H_{12}O_2^+$: 164.0837, found 164.0828.



3-(2-methoxyethenyl)pyridine (3f): colourless oil (92%)

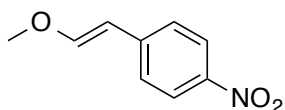
Major Isomer

1H NMR (600 MHz, $CDCl_3$): δ 3.71 (3H, s), 5.75 (1H, d, $J = 13.1$ Hz), 7.07 (1H, s, $J = 13.1$ Hz), 7.17 (1H, dd, $J = 0.5, 4.8, 7.9$ Hz), 7.52-7.53 (1H, m), 8.36 (1H, dd, $J = 1.6, 4.8$ Hz), 8.47 (1H, d, $J = 2.2$ Hz); ^{13}C NMR (150 MHz, $CDCl_3$): δ 56.8, 77.2, 101.5, 123.6, 131.7, 132.4, 146.9, 147.1, 150.3

Minor Isomer

1H NMR (600 MHz, $CDCl_3$): δ 3.81 (3H, s), 5.20 (1H, d, $J = 6.9$ Hz), 6.26 (1H, d, $J = 6.9$ Hz), 7.19-7.21 (1H, m), 7.98 (1H, d, $J = 8.0$ Hz), 8.35-8.35 (1H, m), 8.67 (1H, s); ^{13}C NMR (150 MHz, $CDCl_3$): δ 60.8, 101.9, 123.1, 131.9, 134.9, 146.3, 149.1, 149.8

High resolution MS: m/z calc. for $C_8H_{10}NO^+$: 135.0684, found 135.0672.



1-(2-methoxyethenyl)-4-nitrobenzene (3g): yellow oil (28%)

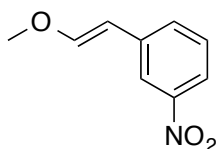
Major isomer

1H NMR (600 MHz, $CDCl_3$): δ 3.87 (3H, s), 5.29 (1H, d, $J = 7.0$ Hz), 6.34 (1H, d, $J = 7.0$ Hz), 7.67 (2H, d, $J = 7.9$ Hz), 8.10-8.13 (2H, m); ^{13}C NMR (150 MHz, $CDCl_3$): δ 57.1, 104.1, 125.1, 128.5, 143.0, 145.5, 152.6

Minor Isomer

^1H NMR (600 MHz, CDCl_3): δ 3.75 (3H, s), 5.84 (1H, d, $J = 13.0$ Hz), 7.23 (1H, d, $J = 13.0$ Hz), 7.32 (2H, d, $J = 8.8$ Hz), 8.10-8.13 (2H, m); ^{13}C NMR (150 MHz, CDCl_3): δ 61.5, 103.8, 123.8, 124.3, 143.9, 145.2, 151.7

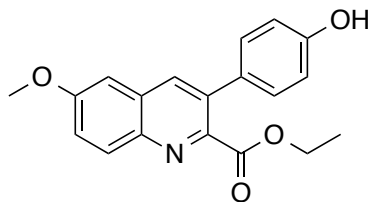
High resolution MS: m/z calc. for $\text{C}_9\text{H}_{10}\text{NO}_3^+$: 179.0582, found 179.0572.



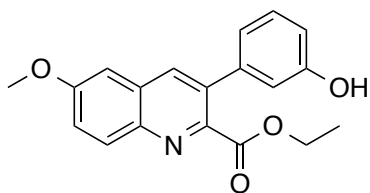
1-(2-methoxyethenyl)-3-nitrobenzene (3h): yellow oil (43%); filtered through a silica plug and used without further purification.

High resolution MS: m/z calc. for $\text{C}_9\text{H}_{10}\text{NO}_3^+$: 179.0582, found 179.0567.

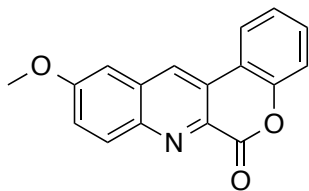
General procedure for the preparation of quinolines: Aniline (1.2 eq) and ethyl glyoxalate (1.2 eq) were dissolved in DCM (0.5 mM) under N_2 and allowed to stir for 20 minutes to allow for imine formation. Enol ether (1.0 eq) was dissolved in DCM (0.5 mM) and added to the reaction mixture. The reaction was cooled to 0°C in an ice bath, then TFA (1.05 eq) was added dropwise. The reaction was monitored by TLC. Upon completion (generally 5-15 minutes from addition of TFA), the reaction was quenched by the addition of a saturated NaHCO_3 solution. The product was then extracted using DCM and concentrated under reduced pressure. The crude product was purified using silica gel chromatography with a hexane/EtOAc (9:1 – 1:1) solvent gradient to afford the desired product.



Ethyl-3-(4-hydroxyphenyl)-6-methoxyquinoline-2-carboxylate (4a): pale yellow oil (82%); ^1H NMR (600 MHz, CDCl_3): δ 1.17 (3H, t, $J = 7.2$ Hz), 3.95 (3H, s), 4.27 (2H, q, $J = 7.2$ Hz), 6.91 (2H, dt, $J = 3.0, 8.4$ Hz), 7.09 (1H, d, $J = 2.8$ Hz), 7.30 (2H, dt, $J = 3.0$ Hz, 8.4 Hz), 7.39 (1H, dd, $J = 2.8, 9.2$ Hz), 8.05 (1H, s), 8.12 (1H, d, $J = 9.3$ Hz); ^{13}C NMR (150 MHz, CDCl_3): δ 14.0, 55.7, 62.0, 104.7, 115.7, 123.4, 129.9, 130.0, 130.7, 131.0, 134.0, 136.1, 142.2, 148.0, 156.2, 159.2, 167.6; High resolution MS: m/z calc. for $\text{C}_{19}\text{H}_{18}\text{NO}_4^+$: 324.1236, found 324.1236.



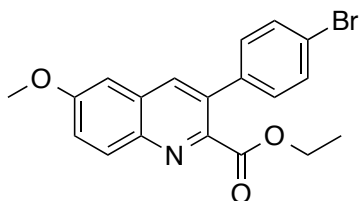
Ethyl-3-(3-hydroxyphenyl)-6-methoxyquinoline-2-carboxylate (4b): pale yellow oil (67%); ^1H NMR (600 MHz, CDCl_3): δ 1.13 (3H, t, $J = 7.1$ Hz), 3.96 (3H, s), 4.26 (2H, q, $J = 7.2$ Hz), 6.89 (1H, ddd, $J = 0.9, 2.5, 8.1$ Hz), 6.94 (1H, t, $J = 2.0$ Hz), 6.98 (1H, ddd, $J = 0.9, 1.56, 7.6$ Hz), 7.10 (1H, d, $J = 2.8$ Hz), 7.3 (1H, t, $J = 7.9$ Hz), 7.43 (1H, dd, $J = 2.9, 9.3$ Hz), 8.09 (1H, s), 8.18 (1H, d, $J = 9.3$ Hz); ^{13}C NMR (150 MHz, CDCl_3): δ 13.9, 55.8, 62.0, 104.8, 115.1, 115.7, 121.1, 123.5, 129.7, 129.9, 131.4, 134.0, 136.1, 140.4, 142.6, 156.0, 159.3, 167.5; High resolution MS: m/z calc. for $\text{C}_{19}\text{H}_{18}\text{NO}_4^+$: 324.1236, found 324.1234.



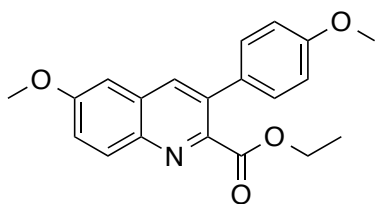
Ethyl-3-(2-hydroxyphenyl)-6-methoxyquinoline-2-carboxylate (4c): white solid (66%); ^1H NMR (600 MHz, CDCl_3): δ 4.02 (3H, s), 7.22 (1H, d, $J = 2.8$ Hz), 7.40-7.43 (2H, m), 7.50 (1H, dd, $J = 2.8, 9.3$ Hz), 7.54 (1H, ddd, $J = 1.4, 7.1, 8.4$ Hz), 8.17 (1H, dd, $J = 1.5, 7.9$ Hz), 8.78 (1H, s); ^{13}C NMR (150 MHz, CDCl_3): δ 56.0, 104.1, 107.2, 107.6,

110.0, 118.2, 123.1, 125.0, 125.5, 127.7, 131.1, 131.9, 132.8, 132.9, 136.4, 145.6, 150.8;

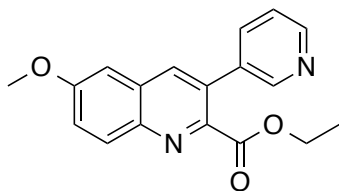
High resolution MS: m/z calc. for $C_{17}H_{12}NO_3^+$: 278.0817, found 278.0805.



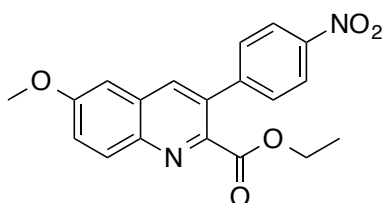
Ethyl-3-(4-bromophenyl)-6-methoxyquinoline-2-carboxylate (4d): pale yellow oil (76%); 1H NMR (600 MHz, $CDCl_3$): δ 1.16 (3H, t, $J = 7.1$ Hz), 3.96 (3H, s), 4.27 (2H, q, $J = 7.1$ Hz), 7.31 (2H, dt, $J = 2.4, 9.0$ Hz), 7.43 (1H, dd, $J = 2.8, 9.2$ Hz), 7.58 (2H, dt, $J = 2.3, 9.0$ Hz), 8.04 (1H, s), 8.14 (1H, d, $J = 9.2$ Hz); ^{13}C NMR (150 MHz, $CDCl_3$): δ 14.0, 55.9, 62.2, 104.8, 122.5, 124.0, 129.8, 130.3, 131.3, 131.8, 133.3, 136.5, 137.8, 142.3, 147.1, 159.6, 166.7; High resolution MS: m/z calc. for $C_{19}H_{17}BrNO_3^+$: 386.0392, found 386.0397.



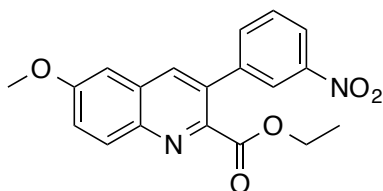
Ethyl-3-(4-methoxyphenyl)-6-methoxyquinoline-2-carboxylate (4e): pale yellow oil (75%); 1H NMR (600 MHz, $CDCl_3$): δ 1.16 (3H, t, $J = 7.1$ Hz), 3.87 (3H, s), 3.95 (3H, s), 4.28 (2H, q, $J = 7.1$ Hz), 6.99 (2H, dt, $J = 2.4, 9.0$ Hz), 7.09 (1H, d, $J = 2.8$ Hz), 7.37 (2H, dt, $J = 2.4, 8.4$ Hz), 7.40 (1H, dd, $J = 2.8, 9.2$ Hz), 8.06 (1H, s), 8.14 (1H, d, $J = 9.3$ Hz); ^{13}C NMR (150 MHz, $CDCl_3$): δ 14.0, 55.5, 55.8, 61.9, 104.7, 114.1, 123.2, 126.8, 131.2, 131.4, 133.9, 135.9, 142.2, 148.2, 159.2, 159.6, 167.6; High resolution MS: m/z calc. for $C_{20}H_{20}NO_4^+$: 338.1392, found 338.1379.



Ethyl-3-(3-pyridinyl)-6-methoxyquinoline-2-carboxylate (4f): white solid (58%); ^1H NMR (600 MHz, CDCl_3): δ 1.17 (3H, t, $J = 7.1$ Hz), 3.97 (3H, s), 4.29 (2H, q, $J = 7.1$ Hz), 7.13 (1H, d, $J = 2.8$ Hz), 7.41 (1H, dd, $J = 4.9, 7.8$ Hz), 7.46 (1H, dd, $J = 2.8, 9.3$ Hz), 7.78 (1H, dt, $J = 2.0, 7.8$ Hz), 8.07 (1H, s), 8.17 (1H, d, $J = 9.2$ Hz), 8.68 (1H, dd, $J = 1.6, 4.9$ Hz), 8.70 (1H, d, $J = 2.3$ Hz); ^{13}C NMR (150 MHz, CDCl_3): δ 14.0, 55.9, 62.1, 104.7, 123.3, 124.1, 129.7, 131.0, 135.3, 136.4, 136.8, 143.1, 146.8, 148.7, 148.9, 166.6; High resolution MS: m/z calc. for $\text{C}_{18}\text{H}_{17}\text{N}_2\text{O}_3^+$: 309.1239, found 309.1231.

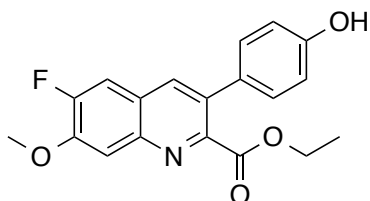


Ethyl-3-(4-nitrophenyl)-6-methoxyquinoline-2-carboxylate (4g): pale yellow oil (47%); ^1H NMR (600 MHz, CDCl_3): δ 1.19 (3H, t, $J = 7.1$ Hz), 3.97 (3H, s), 4.29 (2H, q, $J = 7.1$ Hz), 7.13 (1H, d, $J = 2.8$ Hz), 7.481 (1H, dd, $J = 2.8$ Hz, 9.3 Hz), 7.60 (2H, dt, $J = 2.4, 9.0$ Hz), 8.08 (1H, s), 8.18 (1H, d, $J = 9.3$ Hz), 8.33 (2H, dt, $J = 2.4, 9.6$ Hz); ^{13}C NMR (150 MHz, CDCl_3): δ 14.1, 55.9, 62.2, 104.8, 114.8, 123.7, 124.4, 129.6, 129.6, 131.7, 132.7, 136.5, 146.3, 147.6, 159.9, 166.5; High resolution MS: m/z calc. for $\text{C}_{19}\text{H}_{17}\text{N}_2\text{O}_5^+$: 353.1137, found 353.1146.

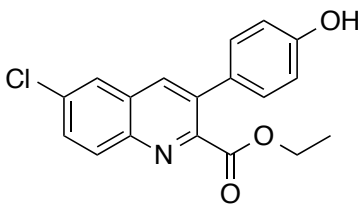


Ethyl-3-(3-nitrophenyl)-6-methoxyquinoline-2-carboxylate (4h): pale yellow oil (61%); ^1H NMR (600 MHz, CDCl_3): δ 1.20 (3H, t, $J = 7.1$ Hz), 3.97 (3H, s), 4.30 (2H, q,

$J = 7.1$ Hz), 7.13 (1H, d, $J = 2.7$ Hz), 7.47 (1H, dd, $J = 2.8, 9.3$ Hz), 7.63 (1H, t, $J = 7.9$ Hz), 7.75 (1H, ddd, $J = 1.0, 1.7, 7.6$ Hz), 8.10 (1H, s), 8.17 (1H, d, $J = 9.3$ Hz), 8.29 (1H, ddd, $J = 1.0, 2.2, 8.2$ Hz), 8.33 (1H, t, $J = 1.9$ Hz); ^{13}C NMR (150 MHz, CDCl_3): δ 14.1, 55.9, 62.2, 104.8, 122.8, 123.7, 124.2, 129.4, 129.7, 131.7, 132.4, 134.8, 136.7, 140.9, 143.1, 146.5, 148.4, 159.8, 166.5; High resolution MS: m/z calc. for $\text{C}_{19}\text{H}_{17}\text{N}_2\text{O}_5^+$: 353.1137, found 353.1137.

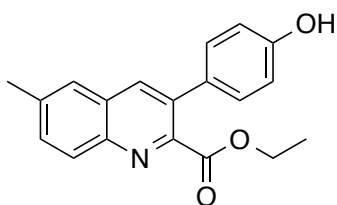


Ethyl-3-(4-hydroxyphenyl)-6-fluoro-7-methoxyquinoline-2-carboxylate (4i): pale yellow oil (69%); ^1H NMR (600 MHz, CDCl_3): δ 1.17 (3H, t, $J = 7.1$ Hz), 4.03 (3H, s), 4.28 (2H, q, $J = 7.1$ Hz), 6.91 (2H, d, $J = 8.6$ Hz), 7.30 (2H, d, $J = 8.6$ Hz), 7.46 (1H, d, $J = 10.9$ Hz), 7.64 (1H, d, $J = 8.1$ Hz), 8.04 (1H, s); ^{13}C NMR (150 MHz, CDCl_3): δ 14.0, 56.5, 62.1, 110.0, 111.1, 111.2, 115.7, 123.7, 130.0, 130.7, 132.2, 136.5, 144.3, 150.0, 152.8, 155.9, 167.4; High resolution MS: m/z calc. for $\text{C}_{19}\text{H}_{17}\text{FNO}_4^+$: 342.1142, found 342.1128.

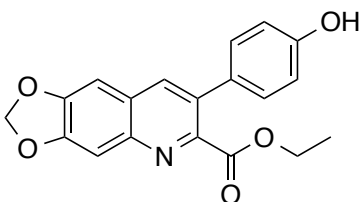


Ethyl-3-(4-hydroxyphenyl)-6-chloroquinoline-2-carboxylate (4j): pale yellow oil (56%); ^1H NMR (600 MHz, CDCl_3): δ 1.17 (3H, t, $J = 7.2$ Hz), 4.29 (2H, q, $J = 7.2$ Hz), 6.93 (2H, d, $J = 8.6$ Hz), 7.32 (2H, d, $J = 8.6$ Hz), 7.69 (1H, dd, $J = 2.3, 9.0$ Hz), 7.85 (1H, d, $J = 2.3$ Hz), 8.09 (1H, s), 8.18 (1H, d, $J = 9.0$ Hz); ^{13}C NMR (150 MHz, CDCl_3): δ 14.0, 62.3, 115.8, 126.3, 129.1, 130.0, 130.2, 131.3, 134.3, 134.4, 136.4, 144.3, 151.0,

156.2, 167.1; High resolution MS: m/z calc. for $C_{18}H_{14}ClNO_3^+$: 328.0740, found 328.0747.



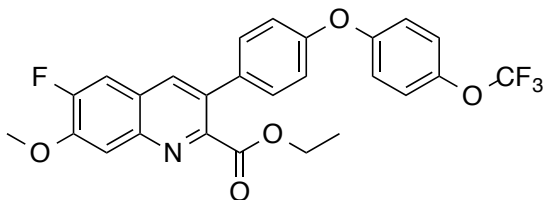
Ethyl-3-(4-hydroxyphenyl)-6-methylquinoline-2-carboxylate (4k): pale yellow oil (65%); 1H NMR (600 MHz, $CDCl_3$): δ 1.17 (3H, t, $J = 7.2$ Hz), 2.57 (3H, s), 4.28 (2H, q, $J = 7.2$ Hz), 6.91 (2H, d, $J = 8.6$ Hz), 7.12 (2H, d, $J = 8.6$ Hz), 7.59 (1H, dd, $J = 1.8, 8.7$ Hz), 7.62 (1H, s), 8.09 (1H, s), 8.14 (1H, d, $J = 8.7$ Hz); ^{13}C NMR (150 MHz, $CDCl_3$): δ 14.0, 21.9, 62.2, 115.8, 126.5, 128.7, 129.1, 130.0, 131.4, 132.8, 133.5, 137.0, 138.7, 149.6, 156.3, 167.5; High resolution MS: m/z calc. for $C_{19}H_{18}NO_3^+$: 338.1287, found 338.1277.



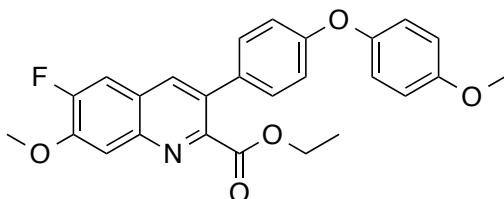
Ethyl-3-(4-hydroxyphenyl)-[1,3]dioxolo-6,7-quinoline-2-carboxylate (4k): pale yellow oil (84%); 1H NMR (600 MHz, $CDCl_3$): δ 1.16 (3H, t, $J = 7.1$ Hz), 4.27 (2H, q, $J = 7.1$ Hz), 6.15 (2H, s), 6.90 (2H, d, $J = 8.6$ Hz), 7.08 (1H, s), 7.27 (2H, d, $J = 8.6$ Hz), 7.57 (1H, s), 8.0 (1H, s); ^{13}C NMR (150 MHz, $CDCl_3$): δ 14.0, 62.2, 102.4, 102.5, 105.3, 110.0, 115.7, 126.4, 130.0, 130.4, 132.3, 137.0, 137.0, 137.0, 149.7, 151.9, 156.1; High resolution MS: m/z calc. for $C_{19}H_{16}NO_5^+$: 338.1028, found 338.1024.

General procedure for Chan-Lam coupling: Aryl quinoline **4a** or **4i** (1 eq) was dissolved in dry DCM (0.1 mM) to which was added crushed molecular sieves (4A),

CuOAc₂ (1 eq), TEA (5 eq), and an aryl boronic acid (3 eq). The reaction was stirred under air at room temperature for two days. The crude reaction mixture was then concentrated and purified by silica gel chromatography using a Hexane:EtOAc 3:1 gradient for elution. This afforded the pure product as a colourless oil.

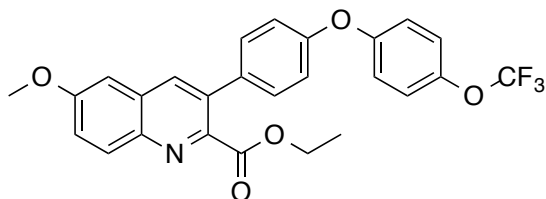


Ethyl-6-Fluoro-7-methoxy-3-(4-(4-(trifluoromethoxy)phenoxy)phenyl)quinoline-2-carboxylate (5a): colourless oil (80%); ¹H NMR (600 MHz, CDCl₃): δ 1.22 (3H, t, J = 7.1 Hz), 4.08 (3H, s), 4.34 (2H, q, J = 7.1 Hz), 7.10 (2H, d, J = 9.1 Hz), 7.12 (2H, d, J = 8.7 Hz), 7.25 (2H, dd, J = 0.7, 9.0 Hz), 7.44 (2H, d, J = 8.7 Hz), 7.51 (1H, d, J = 10.8 Hz), 7.71 (1H, d, J = 8.0 Hz), 8.11 (1H, s); ¹³C NMR (150 MHz, CDCl₃): δ 14.1, 56.6, 62.2, 110.0, 111.2 (d, J = 19 Hz), 119.0, 120.1, 120.7 (q, J = 255 Hz), 122.9, 123.6 (d, J = 9 Hz), 130.3, 131.9, 133.7, 136.7 (d, J = 6 Hz), 144.7 (d, J = 73 Hz), 149.7, 151.8, 152.9, 154.6, 155.5, 157.1, 167.0; High resolution MS: m/z calc. for C₂₆H₂₀F₄NO₅⁺: 502.1278, found 502.1287.



Ethyl-6-Fluoro-7-methoxy-3-(4-(4-(methoxy)phenoxy)phenyl)quinoline-2-carboxylate (5b): yellow oil (70%); ¹H NMR (600 MHz, CDCl₃): δ 1.20 (3H, t, J = 7.1 Hz), 3.83 (3H, s), 4.05 (3H, s), 4.31 (2H, q, J = 7.1 Hz), 6.92 (2H, d, J = 9.1 Hz), 7.01 (2H, d, J = 8.8 Hz), 7.03 (2H, d, J = 9.1 Hz), 7.35 (2H, d, J = 8.8 Hz), 7.48 (1H, d, J = 10.6 Hz), 7.73 (1H, d, J = 8.05), 8.09 (1H, s); ¹³C NMR (150 MHz, CDCl₃): δ 14.0, 55.8, 56.6, 62.2, 109.7, 111.2 (d, J = 20 Hz), 115.1, 117.5, 121.3, 123.7 (d, J = 9 Hz), 130.0,

132.1 (d, J = 4 Hz), 136.9, 144.0, 149.5, 149.7, 151.8 (d, J = 14 Hz), 152.9, 154.6, 156.4, 159.0, 166.9; High resolution MS: m/z calc. for C₂₆H₂₃FNO₅⁺: 448.1560, found 448.1562.



Ethyl-6-Methoxy-3-(4-(4-(trifluoromethoxy)phenoxy)phenyl)quinoline-2-carboxylate

(5c): yellow oil (53%); ¹H NMR (600 MHz, CDCl₃): δ 1.21 (3H, t, J = 7.1 Hz), 3.97 (3H, s), 4.31 (2H, q, J = 7.1 Hz), 7.07-7.12 (5H, m), 7.22 (2H, dd, J = 0.7, 9.0 Hz), 7.42-7.45 (3H, m), 8.10 (1H, s), 8.20 (1H, d, J = 9.2 Hz); ¹³C NMR (150 MHz, CDCl₃): δ 14.1, 55.8, 62.1, 104.8, 118.9, 120.2, 120.7 (q, J = 255 Hz), 122.8, 123.8, 129.9, 130.3 (d, J = 4 Hz) 131.1, 133.6, 134.0, 136.6, 142.1, 144.9, 147.5, 155.5, 157.1, 159.5, 166.9; High resolution MS: m/z calc. for C₂₆H₂₁F₃NO₅⁺: 484.1372, found 484.1384.

2.6 References

- (1) Friedlaender, P. (1882) Ueber o-Amidobenzaldehyd. *Chem Ber* 15, 2572–2575.
- (2) Cheng, C. C., and Yan, S. J. (1982) The Friedländer synthesis of quinolines in *Org. React.* 28, 37-201.
- (3) Zolfigol, M. A., Salehi, P., Ghaderi, A., and Shiri, M. (2007) A catalytic and green procedure for Friedlander quinoline synthesis in aqueous media. *Catal. Commun.* 8, 1214–1218.
- (4) Wu, J., Xia, H. G., and Gao, K. (2006) Molecular iodine: a highly efficient catalyst in the synthesis of quinolines via Friedländer annulation. *Org. Biomol. Chem.* 4, 126-129.
- (5) Jia, C.-S., Zhang, Z., Tu, S.-J., and Wang, G.-W. (2006) Rapid and efficient synthesis of poly-substituted quinolines assisted by p-toluene sulphonic acid under solvent -free conditions: comparative study of microwave irradiation versus conventional heating. *Org. Biomol. Chem.* 4, 104–110.

- (6) Bañón-Caballero, A., Guillena, G., and Nájera, C. (2013) Solvent-free enantioselective Friedländer condensation with wet 1,1'-binaphthalene-2,2'-diamine-derived prolinamides as organocatalysts. *J. Org. Chem.* *78*, 5349–5356.
- (7) Manske, R. H. (1942) The Chemistry of Quinolines. *Chem. Rev.* *30*, 113–144.
- (8) Knight, J. A., Porter, H. K., and Calaway, P. K. (1944) The synthesis of quinolines by the Pfitzinger reaction. *J. Am. Chem. Soc.* *66*, 1893-1894.
- (9) Doebner, O., and Miller, von, W. (1881) Ueber eine dem chinolin homologe base. *Chem. Ber.* *14*, 2812–2817.
- (10) Denmark, S. E., and Venkatraman, S. (2006) On the mechanism of the Skraup-Doebner-Von Miller quinoline synthesis. *J. Org. Chem.* *71*, 1668–1676.
- (11) Roberts, E., and Turner, E. E. (1927) The factors controlling the formation of some derivatives of quinoline, and a new aspect of the problem of substitution in the quinoline series. *J. Chem. Soc.* *0*, 1832–1857.
- (12) Povarov, L. S. (1967) $\alpha\beta$ -Unsaturated ethers and their analogues in reactions of diene synthesis. *Russ. Chem. Rev.* *36*, 656–670.
- (13) Yao, C., Qin, B., Zhang, H., Lu, J., Wang, D., and Tu, S. (2012) One-pot solvent-free synthesis of quinolines by C–H activation /C–C Bond formation catalyzed by recyclable iron(iii) triflate. *RSC Adv.* *2*, 3759–3764.
- (14) Xiao, F., Chen, Y., Liu, Y., and Wang, J. (2008) Sequential catalytic process: synthesis of quinoline derivatives by AuCl₃/CuBr-catalyzed three-component reaction of aldehydes, amines, and alkynes. *Tetrahedron* *64*, 2755–2761.
- (15) Cao, K., Zhang, F. M., Tu, Y. Q., Zhuo, X. T., and Fan, C. A. (2009) Iron(iii)-catalyzed and air-mediated tandem reaction of aldehydes, alkynes and amines: An efficient approach to substituted quinolines. *Chem. Eur. J.* *15*, 6332–6334.
- (16) Zhang, X., Liu, B., Shu, X., Gao, Y., Lv, H., and Zhu, J. (2012) Silver-mediated C-H activation: oxidative coupling/cyclization of N-arylimines and alkynes for the synthesis of quinolines. *J. Org. Chem.* *77*, 501–510.
- (17) McNulty, J., Vemula, R., Bordón, C., Yolken, R., and Jones-Brando, L. (2014) Synthesis and anti-toxoplasmosis activity of 4-arylquinoline-2-carboxylate derivatives.

Org. Biomol. Chem. 12, 255–260.

- (18) Salzer, W., Timmler, H., and Andersag, H. (1948) A new type of compounds active against avian malaria. *Eur. J. Inorg. Chem.* 81, 12–19.
- (19) Bueno, J. M., Herreros, E., Angulo-Barturen, I., Ferrer, S., Fiandor, J. M., Gamo, F. J., Gargallo-Viola, D., and Derimanov, G. (2012) Exploration of 4(1H)-pyridones as a novel family of potent antimalarial inhibitors of the plasmodial cytochrome bc₁. *Future Med. Chem.* 4, 2311–2323.
- (20) Nilsen, A., Miley, G. P., Forquer, I. P., Mather, M. W., Katneni, K., Li, Y., Pou, S., Pershing, A. M., Stickles, A. M., Ryan, E., Kelly, J. X., Doggett, J. S., White, K. L., Hinrichs, D. J., Winter, R. W., Charman, S. A., Zakharov, L. N., Bathurst, I., Burrows, J. N., Vaidya, A. B., and Riscoe, M. K. (2014) Discovery, synthesis, and optimization of antimalarial 4(1H)-quinolone-3-diarylethers. *J. Med. Chem.* 57, 3818–3834.
- (21) Doggett, J. S., Nilsen, A., Forquer, I., Wegmann, K. W., Jones-Brando, L., Yolken, R. H., Bordón, C., Charman, S. A., Katneni, K., Schultz, T., Burrows, J. N., Hinrichs, D. J., Meunier, B., Carruthers, V. B., and Riscoe, M. K. (2012) Endochin-like quinolones are highly efficacious against acute and latent experimental toxoplasmosis. *Proct. Natl. Acad. Sci.* 109, 15936–15941.
- (22) Miley, G. P., Pou, S., Winter, R., Nilsen, A., Li, Y., Kelly, J. X., Stickles, A. M., Mather, M. W., Forquer, I. P., Pershing, A. M., White, K., Shackleford, D., Saunders, J., Chen, G., Ting, L.-M., Kim, K., Zakharov, L. N., Donini, C., Burrows, J. N., Vaidya, A. B., Charman, S. A., and Riscoe, M. K. (2015) ELQ-300 prodrugs for enhanced delivery and single-dose cure of malaria. *Antimicrob. Agents Chemother.* 59, 5555–5560.
- (23) Di Pietro, O., Vicente-García, E., Taylor, M. C., Berenguer, D., Viayna, E., Lanzoni, A., Sola, I., Sayago, H., Riera, C., Fisa, R., Clos, M. V., Pérez, B., Kelly, J. M., Lavilla, R., and Muñoz-Torrero, D. (2015) Multicomponent reaction-based synthesis and biological evaluation of tricyclic heterofused quinolines with multi-trypanosomatid activity. *Eur. J. Med. Chem.* 105, 120–137.
- (24) Gilbert, A. M., Bursavich, M. G., Lombardi, S., Georgiadis, K. E., Reifenberg, E., Flannery, C. R., and Morris, E. A. (2008) N-((8-hydroxy-5-substituted-quinolin-7-

yl)(phenyl)methyl)-2-phenyloxy/amino-acetamide inhibitors of ADAMTS-5

(Aggrecanase-2). *Bioorg. Med. Chem. Lett.* 18, 6454–6457.

(25) Mai, A., Rotili, D., Tarantino, D., Nebbioso, A., Castellano, S., Sbardella, G., Tini, M., and Altucci, L. (2009) Identification of 4-hydroxyquinolines inhibitors of p300/CBP histone acetyltransferases. *Bioorg. Med. Chem. Lett.* 19, 1132–1135.

(26) McNulty, J., Nielsen, A. J., Brown, C. E., Difrancesco, B. R., Vurgun, N., Nair, J. J., Crankshaw, D. J., and Holloway, A. C. (2013) Investigation of aryl halides as ketone bioisosteres: Refinement of potent and selective inhibitors of human cytochrome P450 19A1 (aromatase). *Bioorg. Med. Chem. Lett.* 23, 6060–6063.

3 Design and synthesis of bioactive quinazolinones

3.1 Introduction to quinazolinone heterocycles

Quinazolinones are a common heterocyclic core found in both natural products and pharmaceuticals (Figure 3.1). Due to their frequent appearance in nature and pharmaceuticals, as well as their diverse biological activity, quinazolinones may represent a privileged scaffold.^{1,2,3,4,5,6} There are a number of known alkaloids of varying complexities that contain a quinazolinone or dihydroquinazolinone core and have potent biological activity (Figure 3.2). Luotonin A, a pentacyclic quinazolinone alkaloid isolated from *Peganum nigellastrum*, is a topoisomerase I inhibitor that is cytotoxic to several cancer cell lines.⁷ Febrifugine was first isolated from the Chinese herb *Dichroa febrifuga*, which was used to treat malaria in traditional Chinese medicine.⁸ Febrifugine is indeed an antiparasmodial agent that inhibits protein synthesis, and derivatives of febrifugine have also been used in veterinary medicine as a general antiparasitic.⁹ Tryptanthrin, which bears little structural similarity to febrifugine outside of their common quinoline core, also has antiparasitic activity.¹⁰ Norquinadoline A, a more complex quinazolinone alkaloid containing an indole derived moiety, shows inhibitory activity against the influenza virus H1N1.¹¹

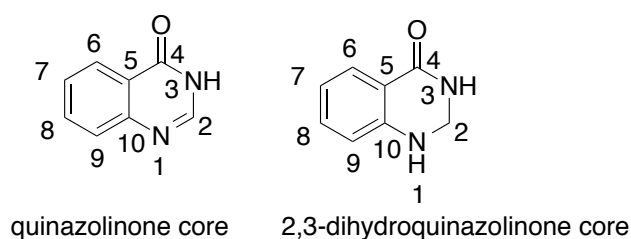


Figure 3.1: Quinazolinone and dihydroquinazolinone cores

In addition to the broad selection of quinazolinone alkaloid with biological activity, there are synthetic quinazolinones used as approved pharmaceuticals in a variety of disease areas. For example, albaconazole is an antifungal drug containing a quinazolinone fragment¹². Ispinesib, a kinesin spindle protein inhibitor with a quinazolinone core, is undergoing clinical trials as an anticancer agent¹³. Recently, Amgen reported novel quinazolinone antagonists of transient receptor potential A1 (TRPA1) that may have use in treating chronic pain.¹⁴ Given the wide variety of targets quinazolinone containing molecules are able to interact with, this privileged scaffold may represent an interesting core for the development of new antimicrobials with novel mechanisms of action. Based on the known antiparasitic activity of febrifugine and tryptanthrin, as well as the structural similarity between antiparasitic quinolones, quinolines, and the quinazolinone scaffold, we hypothesized that a library of 2,3-disubstituted quinazolinones and 2,3-dihydroquinazolinones may reveal novel compounds with activity against *T. gondii*.

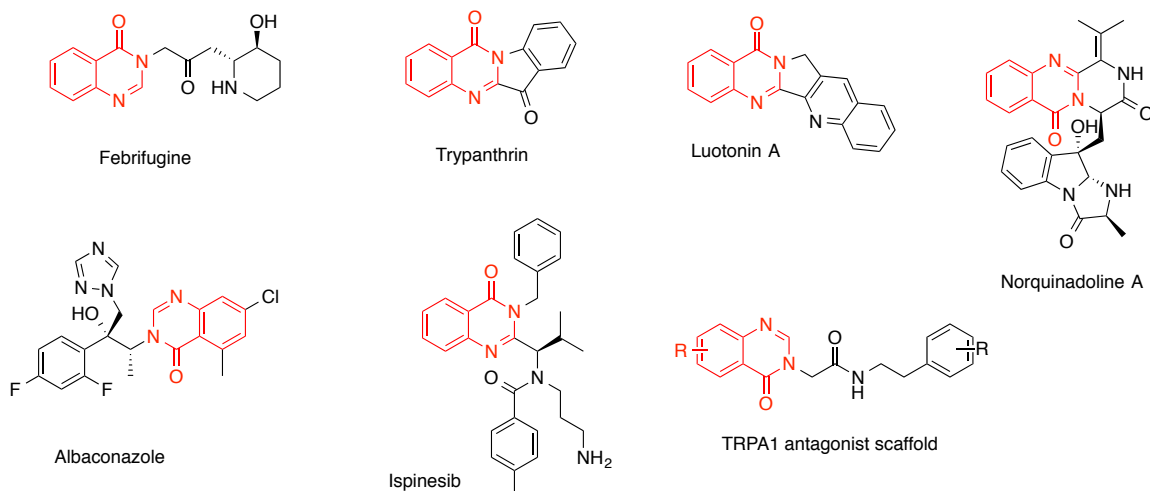


Figure 3.2: Natural products and pharmaceuticals with a quinazolinone core

3.2 Synthesis of substituted quinazolinones in the literature

There is considerable literature describing the synthesis of quinazolinones (Figure 3.3). Classically, quinazolinones are prepared through condensation reactions with anthranilic acid-type derivatives and carbonyls. The Niematowski synthesis, for example, employs an *o*-amino benzoic acid and amides under conventional or microwave heating to prepare quinazolinones^{15,16}. Condensation of *o*-amino benzamides with carbonyls produces quinazolinones in a process catalyzed by protic acids,^{17,18} Lewis acids,¹⁹ and other catalysts.^{20,21} Aldehydes and ketones are common substrates for this chemistry, but diketones²² and β -ketoesters¹⁷ can also be used. Aldehydes can also be generated in situ from benzyl alcohols under hydrogen transfer conditions.²³ To generate quinazolinones from dihydroquinazolinone intermediates, additional oxidants are sometimes employed.^{24,25}

One-pot, multicomponent methodology has also been explored to eliminate prior preparation of benzamides.²⁶ Quinazolinones and dihydroquinazolinones have been prepared in one-pot from isatoic anhydride, primary amines, and aldehydes using catalytic I₂.¹⁹ Khosropour et al have also reported the cyclization of *o*-amino benzoic acid, orthoesters, and amines using 5 mol % of Bi(TFA)₃ immobilized on ionic liquid *n*-butylpyridinium tetrachloroferrate.²⁷

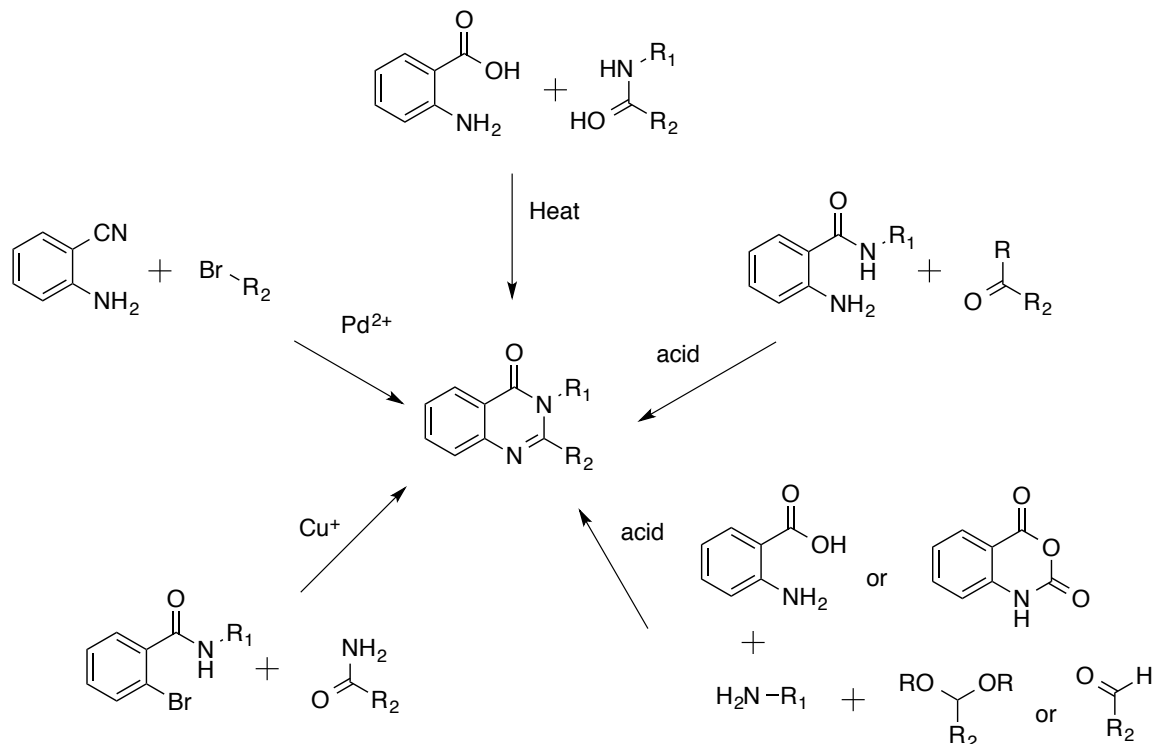


Figure 3.3: Literature methods for synthesis of quinazolinones

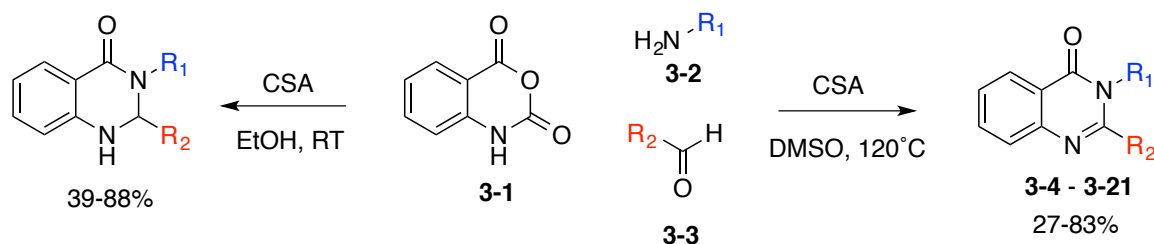
In addition to these condensation processes, several transition metal catalyzed route to quinazolinones have been reported. N-Substituted o-bromo benzamides can be coupled with substituted amides in a CuI catalyzed process, resulting in 2,3-disubstituted quinazolinones.²⁸ Pd²⁺ has also been employed in catalytic carbonylation chemistry for the synthesis of quinazolinones. Beller reported the preparation of 2-aryl quinazolinones in a Pd(OAc)₂ mediated cascade from o-amino benzamides and aryl bromides, and later extended this methodology to include o-aminobenzonitriles.²⁹ The Alper group has extended the scope of this methodology by using imidoyl chlorides and o-iodoanilines to prepare 2,3-disubstituted quinazolinones.³⁰ A number of recent publications have

improved on this carbonylative cyclization using milder conditions and broader substrate scope.³¹

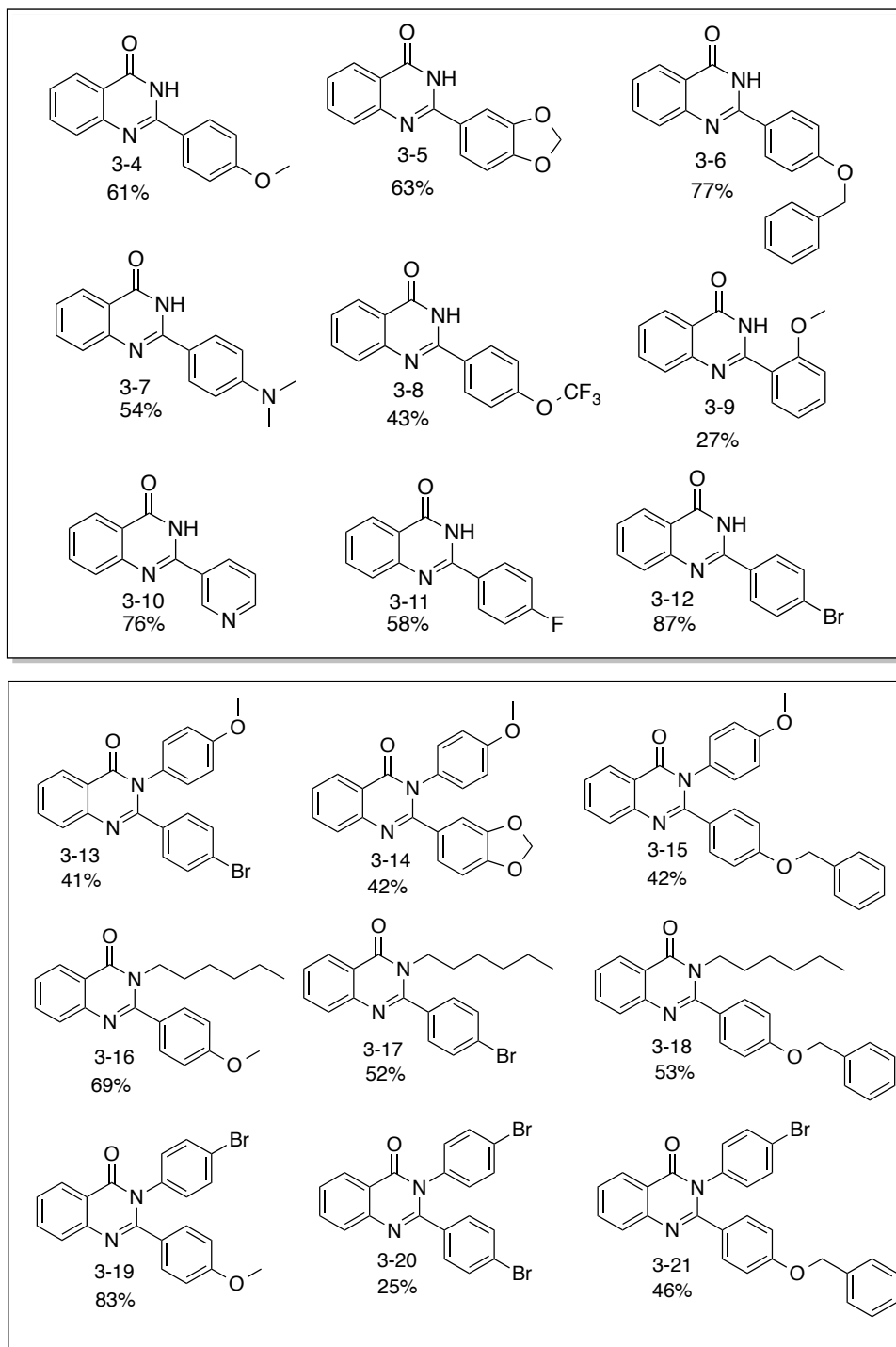
3.3 Preparation of the initial quinazolinone library

To prepare a small library of 2,3-disubstituted quinazolinones, we opted for a condensation-based approach, as this would allow us to use commercially available starting materials, with a broad substrate scope and fairly mild conditions. We initially attempted to prepare quinazolinones from isatoic anhydride, amines, and aldehydes or ketones in an I₂ catalyzed multicomponent reaction.¹⁹ However, we found that incomplete oxidation in this reaction sometimes afforded a mixture of quinazolinone and dihydroquinazolinone products. We found dihydroquinazolinones and quinazolinones could be prepared in one-pot from commercially available isatoic anhydride, amines, and carbonyls using camphor sulfonic acid (CSA), a mild acid catalyst (Scheme 3.1). This route can be used to generate either the aromatic or reduced product through solvent selection. Protic solvents, such as EtOH, at room temperature produce the dihydroquinazolinone product in 39-88% yield. In all cases, the product precipitated from the reaction mixture and could be purified by washing with ethanol. To obtain quinazolinones **3-4** to **3-21**, we can instead perform the same reaction in DMSO at 110°C to afford quinazolinones in 27-83% yield. 2-Substituted quinazolinones precipitated as described previously. 2,3-Disubstituted quinazolinones were obtained as oils and thus required silica gel chromatography for purification. This methodology allows us to perform the aminolysis of isatoic anhydride, imine formation, a Mannich-type cyclization, and an oxidation in one pot to afford products much more complex than the

commercially available reagents. Additionally, this chemistry allows us to control the oxidation state of the products through solvent selection, incorporate diverse substrates, and easily isolate the desired products. For these reasons, we thought the chemistry was amenable for use in preparing a collection of quinazolinones. Thus, this is a suitable synthetic method for preparing small libraries of 2,3-dihydroquinazolinones and quinazolinones for biological testing (Scheme 3.2). Our initial quinazolinone compound collection was screened for activity against *T. gondii* and HSV-1.



Scheme 3.1: Synthesis of 2- and 3-substituted quinazolinone analogs using CSA and DMSO in 27-83% yield. 2-substituted quinazolinones precipitated the reaction mixture and purified by washing with EtOH. 2,3-disubstituted quinazolinones were isolated with silica gel chromatography.



Scheme 3.2: First generation quinazolinone library

3.4 Quinazolinones with activity against *T. gondii*

Three assays were used to screen compounds **3-4** to **3-21** for their activity against *T. gondii*. In the 5-day growth assay, host cells are pre-treated with compounds before a 5-day incubation period with *T. gondii* tachyzoites. This assay determines a compound's ability to slow *T. gondii* growth in a new infection. An invasion assay was also performed to determine how test compounds affected the attachment and penetration of tachyzoites through a host cell membrane. Finally, the ability of each compound to inhibit replication of intracellular tachyzoites inside a parasitophorous vacuole was assessed in a replication assay. These assays were performed by L. Jones-Brando and C. Bordon in the Yolken Lab at Johns Hopkins University according to previously published protocols.

A published colourmetric assay protocol was employed for the 5-day growth assay.³² Briefly, human foreskin fibroblasts (HFF) were treated with varying concentrations of the test compounds. Cells were then infected with a strain of *T. gondii* modified to constitutively express β -galactosidase. Uninfected cells were also treated with our test compounds to determine cell toxicity. Infected and uninfected cells were incubated for four days, then treated with chlorophenol red- β -D-galactopyranoside (CRGP). In the presence of live *T. gondii* expressing β -galactosidase, this substrate is hydrolyzed to chlorophenol, which can be detected by monitoring absorbance at 570-650 nM. Uninfected cells are treated with a cell viability reagent, and bioreduction of this reagent by viable cells can be detected by absorbance at 490-650 nM. This information allows us to determine the IC₅₀ and TD₅₀ for each compound (Table 1.1).

In this assay, we found that none of the dihydroquinazolinone analogs prepared to show any activity (data not shown). Oxidized quinazolinones were generally more active, and further SAR analysis could be used to determine which substituents contributed to this activity.

Table 3.1: Anti-*Toxoplasma* activity of quinazolinone-based library

CPD	IC ₅₀ (μM)	IC ₉₀ (μM)	TD ₅₀ (μM)	TI
3-4	20	121	125	6
3-5	50	443	≥320	6
3-6	153	4989	≥320	2
3-7	14	281	≥320	23
3-8	27	447	≥320	12
3-9	56	266	305	5
3-10	94	225	≥320	3
3-11	29	260	≥320	11
3-12	92	414	≥320	3
3-13	32	81	≥320	10
3-14	40	91	≥320	8
3-15	4	14	4	1
3-16	10	48	42	4
3-17	60	193	88	1
3-18	10	45	178	18
3-19	31	83	196	6
3-20	44	126	≥320	7
3-21	3	12	5	2
ATV	0.2	0.6	21	111

SAR analysis of this data demonstrates that the substituent at N3 was important for activity. Derivatives with a hexyl group at N3 (**3-16**, **3-17**, **3-18**) were generally more active than the derivatives that were unsubstituted at N3 (**3-4**, **3-6**, **3-12**) with identical C2 substituents. Quinazolinones with either electron-rich or electron-deficient aryl groups at N3 were similarly active to N3-alkyl analogs but also significantly more toxic.

Electron-rich aryl substituents at C2 also seem to be crucial for anti-*Toxoplasma* activity. The most potent compounds have 4-methoxy, 4-dimethylamino, or 4-benzyloxy aryl groups at this position. Two quinazolinones (**3-15**, **3-21**) from this group are similarly potent to artemisinin, but toxic to human foreskin fibroblasts. These compounds contain a benzyloxybenzyl substituent at C2, and an aryl substituent at N3. This toxicity is not observed with other electron-aryl groups at C2 or with alkyl functionality at N3. The most promising C2 substituent is the 4-dimethylamino aryl ring, as derivative **3-7** containing the functionality displays low μM activity with minimal toxicity. The most potent compounds in the 5-day growth assay are **3-7**, **3-15**, **3-18**, and **3-21** with IC_{50} values below 15 μM .

The activity of these quinazolinones to inhibit invasion and replication of *T. gondii* was also studied. In the invasion assay, extracellular tachyzoites are incubated with test compounds (10 μM) then allowed to infect host HFF host cells³³. Fluorescent staining is used to differentiate and quantify tachyzoites that have penetrated the host cell (Figure 3.4, green bars), tachyzoites that have attached to the host cell but were unable to penetrate (Figure 3.4, red bars), and tachyzoites that began but were unable to complete host cell invasion (Figure 3.4, yellow bars). A decrease in the number of penetrated (green) tachyzoites indicates inhibition of invasion, while a decrease in the total number of tachyzoites associated with the cell (green, red, and yellow) indicates inhibition of attachment. The most active compounds identified in the 5-day growth assay (**3-7**, **3-15**, **3-18**, **3-21**) inhibit invasion. **3-7**, **3-15**, and **3-18** also inhibit attachment of tachyzoites to the host (Figure 3.4).

A previously published replication assay was also performed to assess the ability of each compound to inhibit replication of an intracellular parasite in an established infection.³⁴ In this assay, purified tachyzoites are allowed to invade a host cell (HFF) and establish infection for 2h, at which time potential inhibitors are added and the parasites are allowed to replicate. After 24h, the number of tachyzoites in each parasitophorous vacuole is counted and compared to the untreated control. Vacuoles containing 8, 4, 2, and 1 tachyzoites indicate that 3, 2, 1, and 0 cycles of replication have taken place respectively. Compounds are considered to inhibit replication if the proportion of tachyzoites undergoing 3 cycles of replication is smaller than the proportion of tachyzoites that did not replicate (Figure 3.5). In this assay, three compounds showed inhibition of replication at 10 μ M: **3-12**, **3-16**, and **3-21**. Of these compounds, only **3-21** also showed activity in the 5-day growth inhibition and invasion assays. Unfortunately, **3-21** is significantly toxic to the host HFF at low μ M concentrations. **3-7** and **3-18**, which show good potency and minimal toxicity in the 5-day growth inhibition assay, are not able to inhibit an established *T. gondii* infection.

We wanted to prepare a second-generation library of compounds to minimize the toxicity of our compounds while improving their potency against new and established infection. We hypothesized that the toxicity of **3-21** may be related to the benzyloxybenzyl group at C2, as the only compounds that showed toxicity had this functionality. This toxic effect did seem to be mitigated by the N3 substituent: N-aryl substituents contributed toward toxicity, while the N-alkyl substituted derivative was not cytotoxic. Based on this information, as well as our initial SAR analysis indicating the

benefits of electron-rich aryl substituents at C2, we decided to prepare a second-generation of quinazolinones targeting *T. gondii* with electron-rich C2 moieties and varying alkyl substituents at N3.

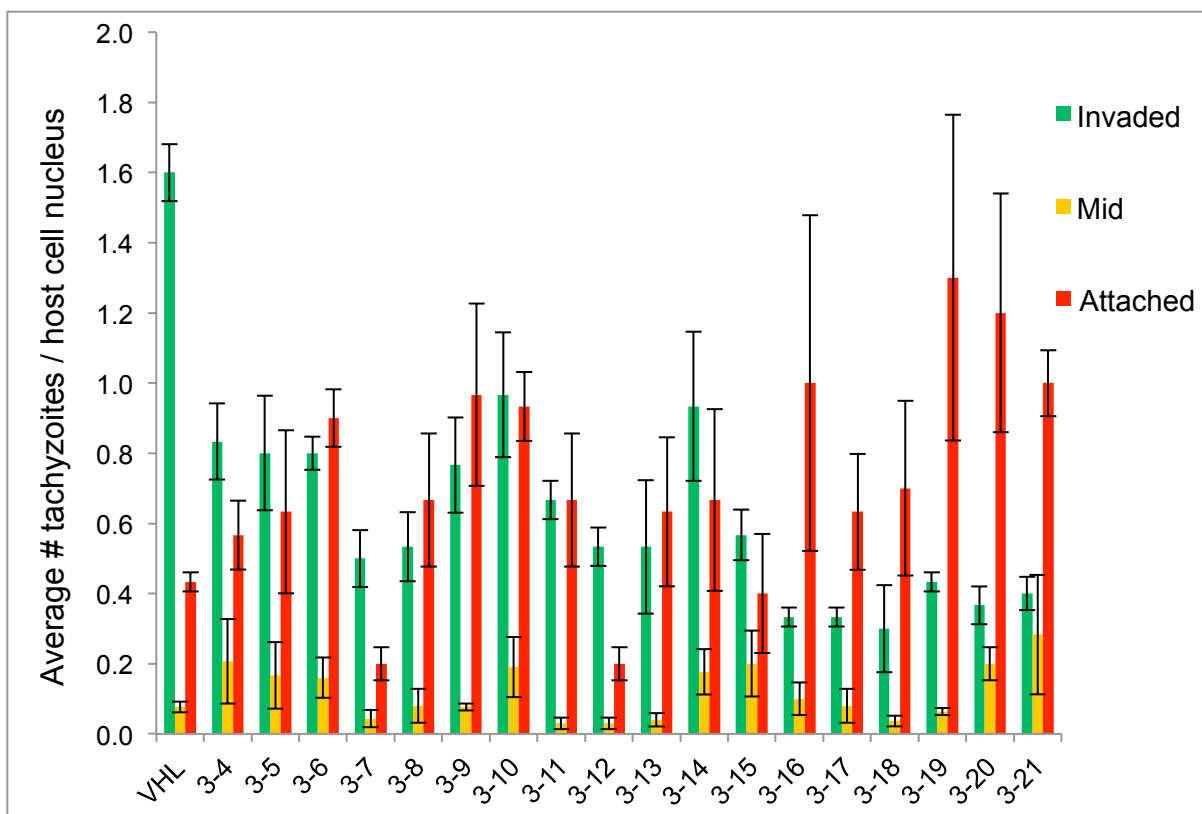


Figure 3.4: Invasion of tachyzoites into a host cell after treatment with first generation quinazolinones. Tachyzoites attached to the host are shown in red, tachyzoites that have penetrated are shown in green, and tachyzoites midway through the invasion process are shown in yellow. The most active compounds identified in the 5-day growth assay (3-7, 3-15, 3-18, 3-21) inhibit invasion. 3-7, 3-15, and 3-18 appear to also inhibit attachment of the tachyzoite to the host.

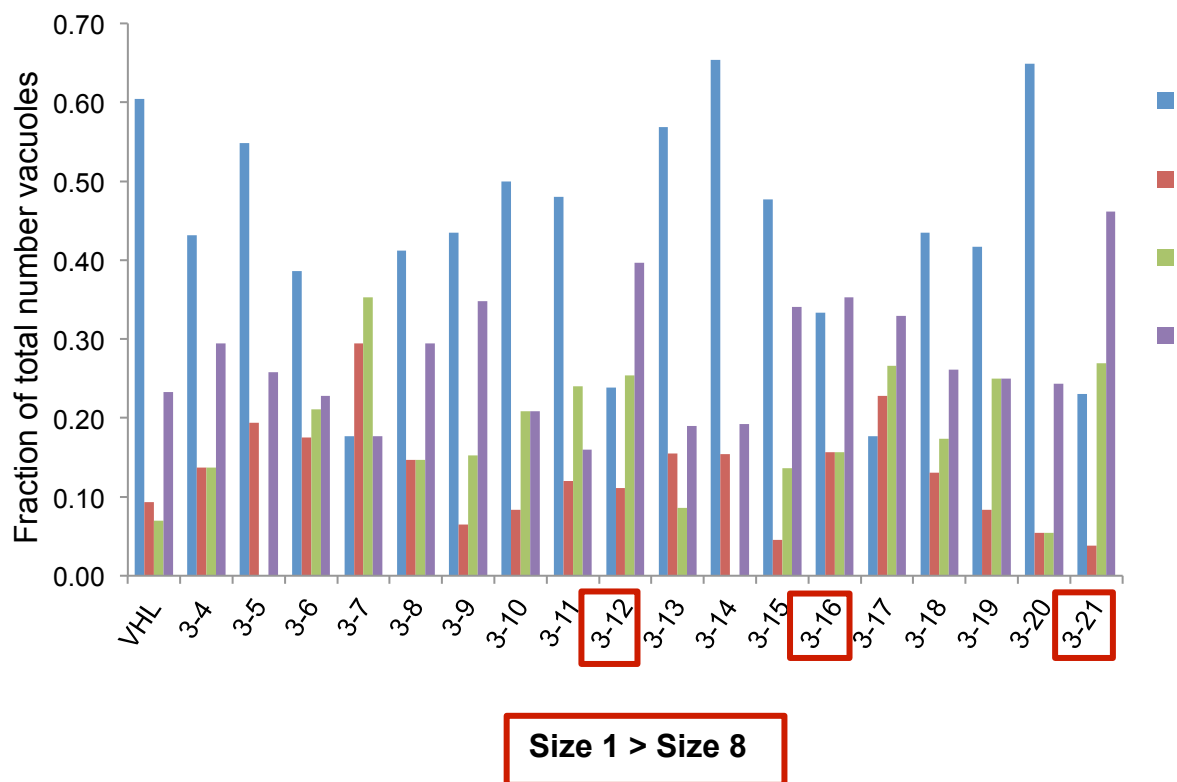


Figure 3.5: Replication of *T. gondii* tachyzoites in a vacuole after treatment with first generation quinazolinones. Vacuoles containing 8, 4, 2, and 1 indicate that 3, 2, 1, and 0 cycles of replication have taken place, and are shown in blue, red, green, and purple respectively. Compounds 3-12, 3-16, and 3-21 reduced replication of tachyzoites (more vacuoles contain one tachyzoites than vacuoles that contain 8 tachyzoites). 3-7 also showed moderate inhibition of replication.

3.5 Quinazolinones with activity against HSV-1

In addition to their promising anti-Toxoplasmosis activity, we hypothesized that these quinazolinones may have biological activity against HSV-1, particularly latent HSV-1. Several known antivirals have a similar core, including norquinadoline A and letermovir, an experimental drug for treating cytomegalovirus. Additionally,

quinazolinone derivatives are known modulators of epigenetic regulations³⁵. During HSV-1 latency, viral gene repression is controlled by host-cell epigenetic regulation, specifically by binding of deacetylated viral DNA to histones, and reactivation of latent infections involves acetylation of lytic genes.^{36,37} Reactivation of latent infections can be induced by treatment of histone deacetylase inhibitors,^{38,39} which suggests that small molecules that disrupt in epigenetic regulation may be an effective method of preventing HSV-1 recurrence. Given this evidence, we thought it prudent to evaluate the antiviral activity of our quinazolinone compound collection.

The anti-HSV screening was performed by Dr. Nimgaonkar and colleagues at the University of Pittsburgh according to a previously described protocol.^{40,41} Vero cells were infected with an HSV-1 strain engineered to contain enhanced green fluorescent protein (EGFP) and red fluorescent protein (RFP) as reporter genes for expression of viral promoters ICP0 and glycoprotein C respectively. Vero cells infected with HSV-1 were cultured at 2 h postinfection in media containing the test compounds or acyclovir (50 μ M). Flow cytometry analysis was then used to determine the percentage of cells expressing EGFP and RFP, indicating viral gene replication, which was normalized to the untreated control.

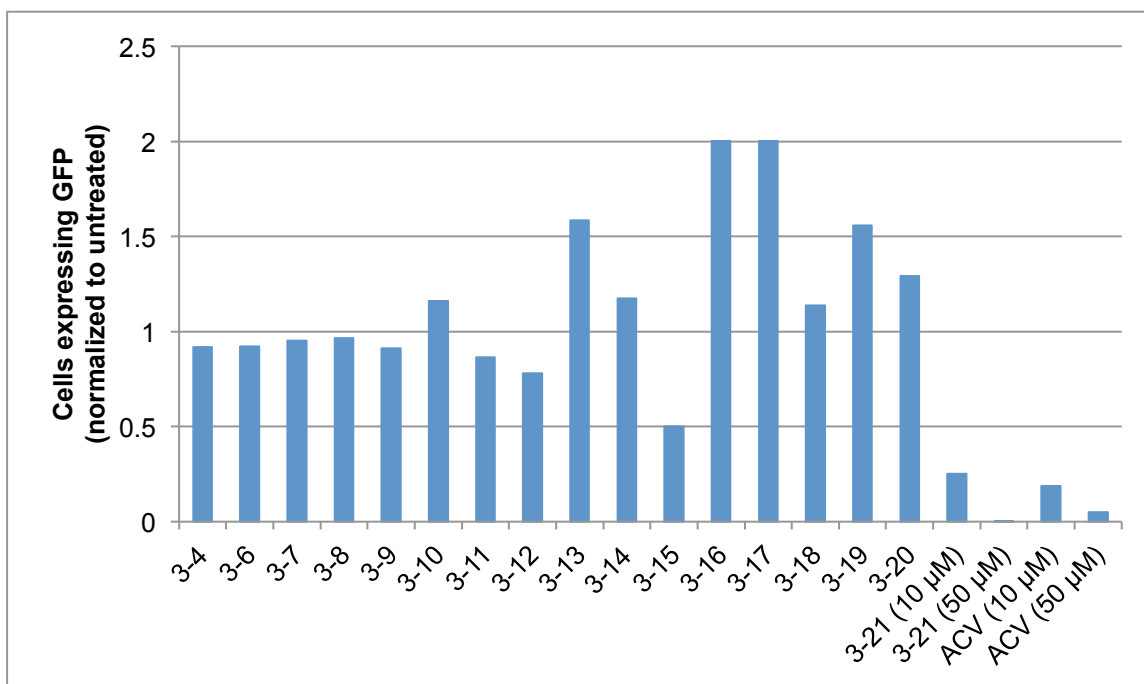


Figure 3.6: Percentage of neurons expressing EGFP after infection with an HSV-1 strain, normalized to untreated cells. At 50 μM , **6c** and **6i** show significant reduction in fluorescence, indicating inhibition of viral replication. At 10 μM , only **6i** shows inhibition of HSV-1.

At 50 μM , **3-15** and **3-21** decreased the percentage of cells expressing GFP by at least 50% compared to untreated controls (Figure 3.6). This indicates reduced expression of ICP0, and thus inhibition of viral replication. **3-21** showed stronger inhibition of viral replication than ACV and was also active at 10 μM . The active compounds have common structural features: an aryl substituent at N3 and a benzyloxybenzyl substituent at C2. Analogous derivatives instead containing an alkyl substituent or no substituent at N3 are inactive, indicating that the aryl substituent at N3 is important for activity. Compound **3-21**, containing a 4-bromophenyl substituent at N3 is more active than **3-15**, which

contains a more electron rich 4-methoxyphenyl moiety at the same position. We also observed that the substituent at C2 is important for antiviral activity. Incorporation of any aryl at C2 other than a benzyloxybenzyl group resulted in a complete loss of activity. Thus a specific pharmacophore can be identified for anti-HSV-1 quinazolinones.

Compounds that showed activity in our initial screen were further tested for toxicity against host neurons using a LIVE/DEAD Fixable Aqua dead cell stain kit according to previously published protocols.³³ Although **3-15** and **3-21** had little effect on cell viability (Figure 3.7), some morphological changes in neurons were observed after they had been treated with **3-15** and **3-21** for 48-72 hours. As this toxicity was not immediately observed, we hypothesized that these molecules could be unstable under the assay conditions, and thus decomposing or being metabolized to more toxic species. We identified the benzyloxybenzyl group as a particularly labile site. The functional group is crucial for anti-HSV activity, but we hypothesized that analogs with similar large, hydrophobic groups at C2 might retain antiviral activity while minimizing toxicity to the host. We thus envisioned a second generation of quinazolinones targeted towards HSV-1 activity with substituted benzyl ethers, diaryl ethers, and diaryl amines that might fit these criteria.

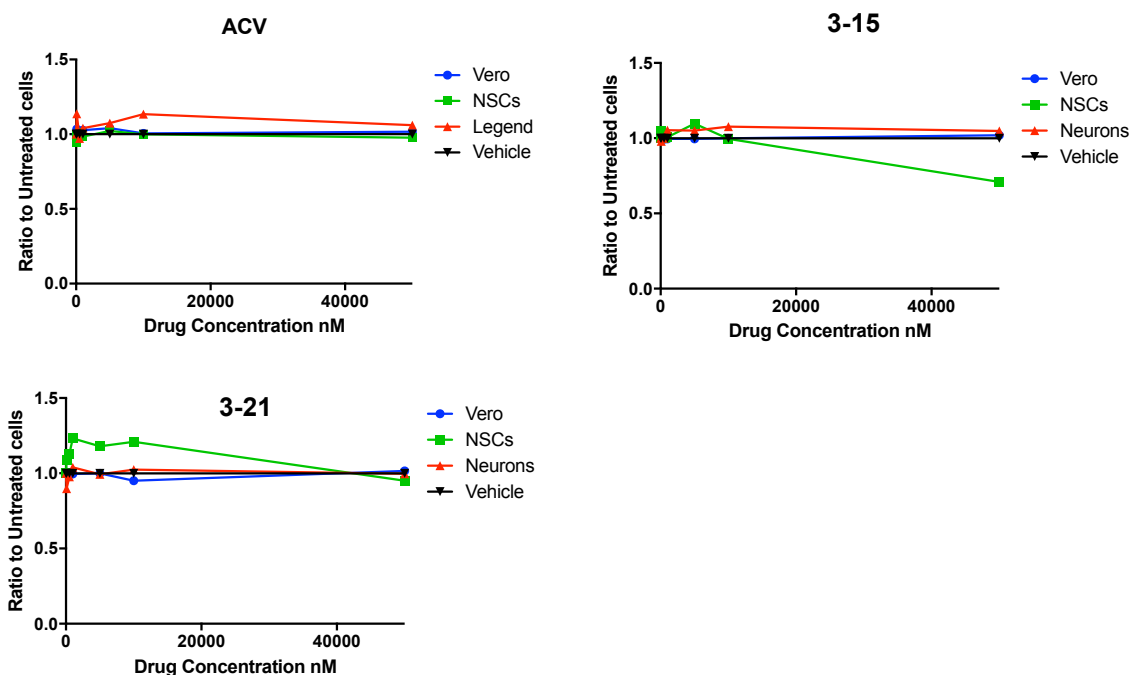


Figure 3.7: Toxicity of ACV, 3-15, and 3-21 to Vero cells, neural stem cells, and neurons compared to vehicle. Minimal affect on cell viability is observed.

3.6 Design and synthesis of second generation quinazolinones

Given the interesting biological activity toward both *T. gondii* and HSV-1, we wanted to prepare a 2nd generation quinazolinone library both to optimize potency and to differentiate the pharmacophore responsible for the antiparasitic activity from that responsible for the antiviral activity.

Based on this preliminary SAR for anti-*T. gondii* activity, we prepared a second generation of compounds with 4-dimethyl amino or 4-benzyloxybenzyl substituents at C2 and a selection of primarily alkyl substituents at N3 (Figure 3.8). This library was prepared by T. Kong, an undergraduate student under the supervision of C. Brown. These compounds were prepared as previously described for the 1st generation quinazolinone

library using 4-dimethylaminobenzaldehyde or 4-benzyloxybenzaldehyde and a variety of alkyl amines.

In order to probe the SAR for anti-HSV activity, we sought to prepare a collection of compounds with different large hydrophobic groups at C2. Our initial results suggested that the benzyloxybenzyl group was crucial for activity, but these compounds also seemed to induce changes in cell morphology that could be related to the reactivity of this benzyloxybenzyl group. We hypothesized that diaryl ether and diaryl amine analogs may retain this potency but also be more metabolically stable. We also prepared several quinazolinones substituted on the benzyl ring to explore substituent effects at this site.

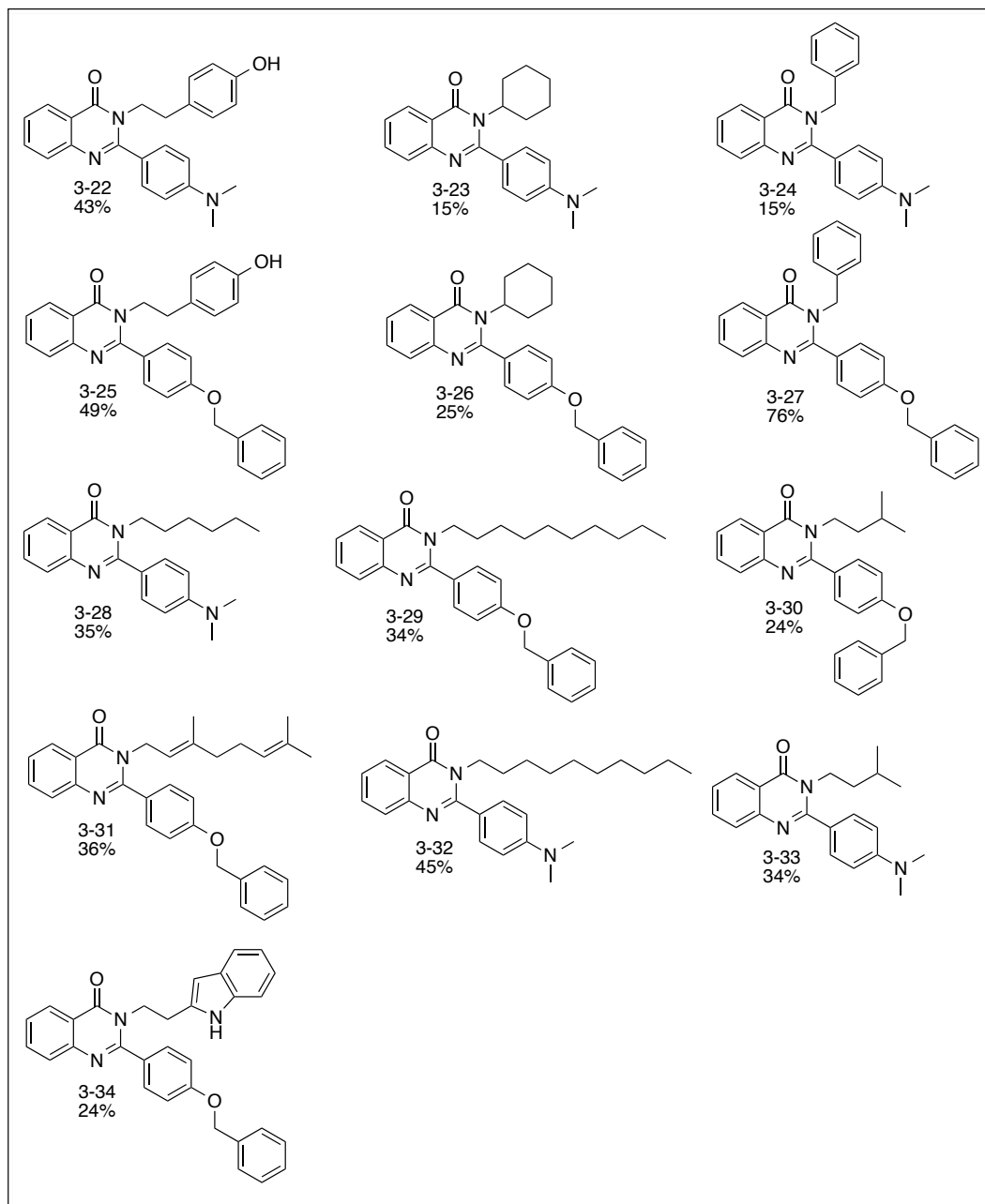
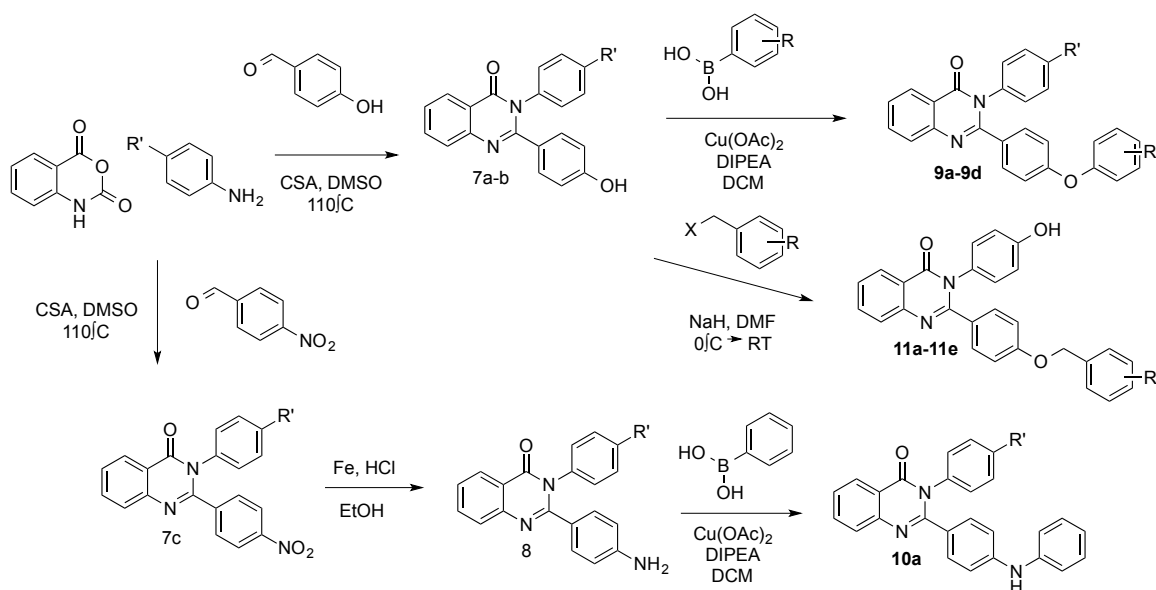


Figure 3.8: Second generation quinazolinones containing varying N3 substituents

To prepare the C2 substituted quinazolinones, common synthetic intermediates from the cyclization of isatoic anhydride, p-anisidine or 4-bromoaniline, and 4-

hydroxybenzaldehyde were prepared (Scheme 3.3). These phenols could then be coupled to boronic acids under Chan-Lam conditions to afford diaryl ethers, or alkylated using benzyl halides to produce benzyloxybenzyl ethers. A number of diaryl ethers and benzyloxybenzyl ethers with different substituents on the terminal aryl ring were prepared (Figure 3.7). Additionally, a diaryl amine analog was prepared from by the cyclization of isatoic anhydride, p-anisidine, and 4-nitrobenzaldehyde, followed by the reduction of the nitro group and Chan-Lam coupling (Scheme 3.3).



Scheme 3.3: Synthesis of diaryl ether, benzyloxybenzyl ether, and diaryl amine quinazolinones

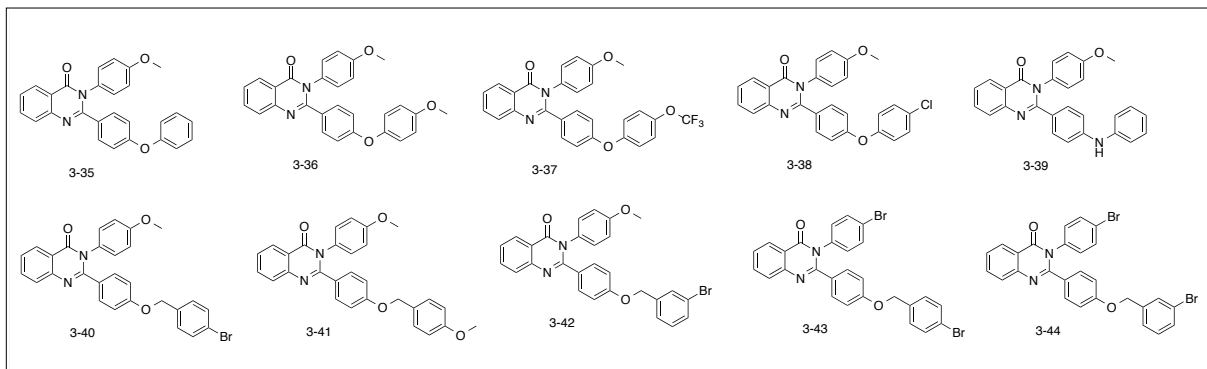


Figure 3.9: Second generation quinolines containing varying C2 substituents

3.7 Second generation quinazolinones – *T. gondii* SAR

Our 2nd generation quinazolinones, including both the collections of compounds targeting towards *T. gondii* and HSV-1, were screened for activity against *T. gondii* as described previously. Generally, a 4-benzyloxybenzyl substituent at C2 improved the anti-*T. gondii* activity of a compound compared to 4-(N,N-dimethylamino) derivative (Table 3.2). This improvement in potency was not specific to the benzyloxybenzyl group; several diaryl ether derivatives prepared for other applications also showed activity, indicating that the size of the C2 derivative may be more significant than the electron-rich nature of the ring. Additionally, we observed that bulky aliphatic groups at N3 contributed to potency, with the most active derivatives bearing a cyclohexyl- or geranyl- group at this position. Compounds with aryl substituents at N3 showed good potency, but were also very toxic to the host HFF cells. Based on this SAR, we have selected two compounds for further testing: **3-26** and **3-31**, with an IC₅₀ of 6 μM and 8 μM, and TI of 50 and 38 respectively.

Table 3.2: *Anti-Toxoplasma* activity of second generation quinazolinone-based library

CPD	IC ₅₀ (μM)	IC ₉₀ (μM)	TD ₅₀ (μM)	TI
3-22	112	353	196	2
3-23	15	67	112	7
3-24	12	60	133	11
3-25	17	52	229	13
3-26	6	46	≥320	53
3-27	13	71	≥320	25
3-28	18	52	50	3
3-29	45	175	≥320	7
3-30	12	55	118	10
3-31	7	58	≥320	46
3-32	49	170	≥320	7
3-33	35	116	85	2
3-33	25	119	≥320	13
3-34	154	724	≥320	2
3-35	24	63	≥320	13
3-36	29	56	≥320	11
3-37	22	59	≥320	15
3-38	18	53	≥320	18
3-39	37	116	≥320	9
3-40	3	18	4	1
3-41	6	41	27	5
3-42	5	20	6	1
ART	2	19	≥320	160

The activity of these second-generation quinazolinones to inhibit invasion and replication of an established parasitic infection was determined. Many of the second-generation quinazolinones significantly inhibited replication of intracellular tachyzoites at 10 μM (Figure 3.11). All derivatives with an N-alkyl substituent and an electron-rich aryl group at C2, slowed replication of the parasite such the number of tachyzoites that had not replicated was larger than those that had undergone three replication cycles. The most active compounds in this assay, **3-26**, **3-27**, and **3-40**, completely inhibited replication in

greater than 50% of tachyzoites, and reduced the fraction of tachyzoites undergoing three cycles of replication to less than 10%. Each of these compounds contains a benzyloxybenzyl group at C2, indicating this group contributes towards the potency of this class of molecules. These results are consistent with those of our 5-day growth assay, which showed compounds **3-26** and **3-27** to be among the most potent and selective compounds.

When tested in a previously described invasion assay, **3-26**, **3-27**, and **3-31** did not show inhibition of *T. gondii* attachment to or penetration of the host cell (Figure 3.10). This suggests that the target of these compounds is not involved in the invasion process. Few other N-alkyl quinazolinones prepared inhibited tachyzoites invasion, in contrast to the N-aryl substituted quinazolinones in the first- and second-generation. This difference in activity, combined with the toxicity of the N-aryl derivatives, suggests that these two classes compounds may not be acting on the same target; however, the target of these compounds remains to be elucidated. Since the quinazolinone core is synthetically accessible, tagged quinazolinones containing an azide or alkyne could be prepared. These derivatives could be linked to fluorescent or affinity probes to identify the target of quinazolinones in *T. gondii*.

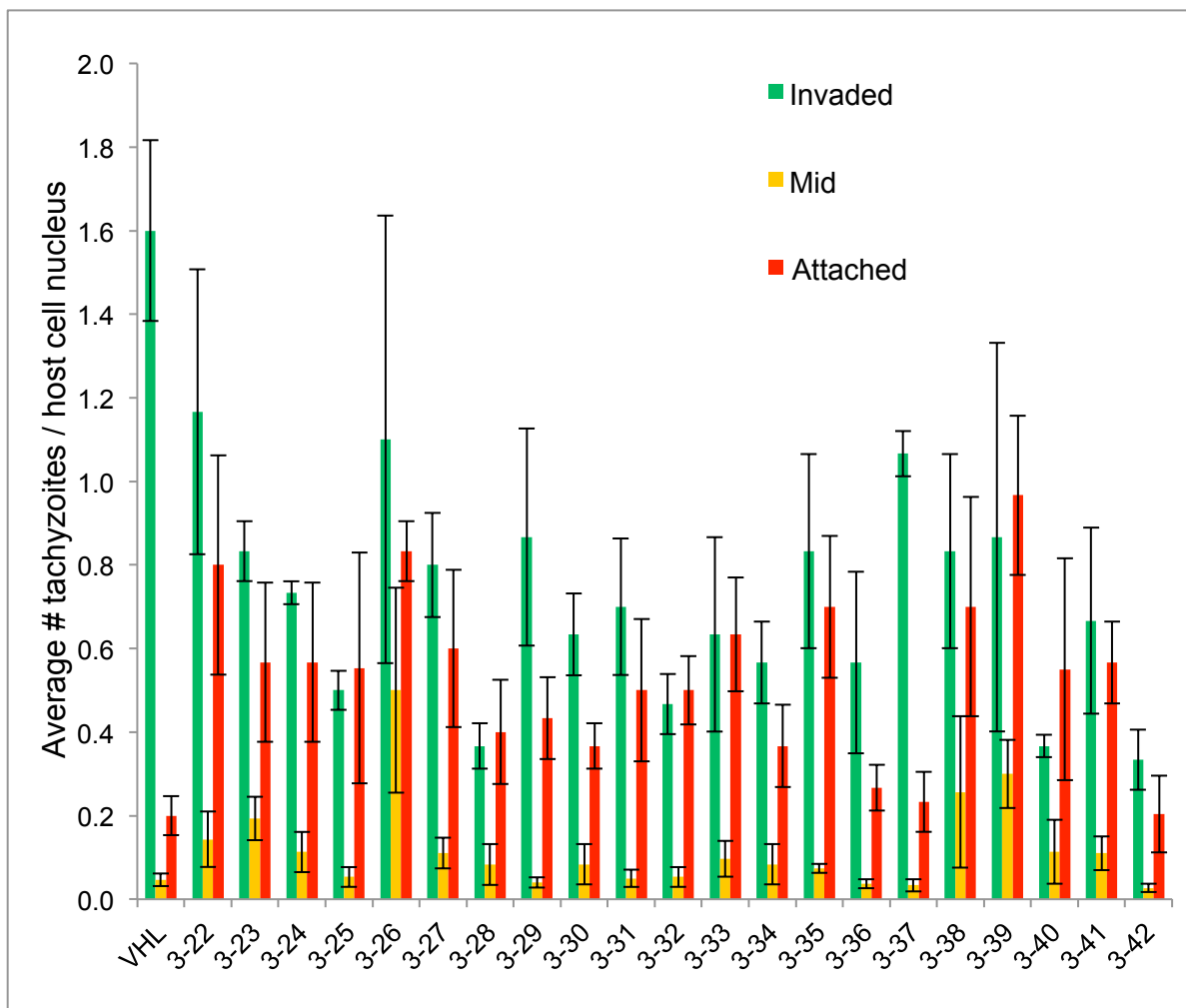


Figure 3.10: Invasion of tachyzoites into a host cell after treatment with second-generation quinazolinones.

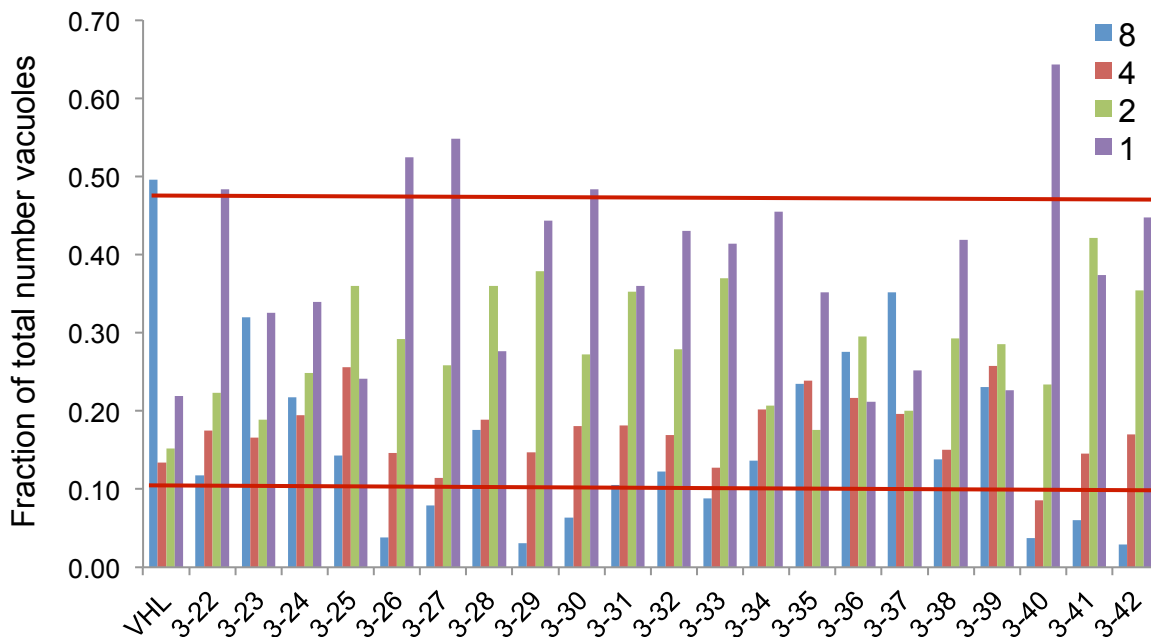


Figure 3.11: Replication of *T. gondii* tachyzoites in a vacuole after treatment with second-generation quinazolinones. The majority of quinazolinones tested inhibit replication. 3-27, 3-28, and 3-40 are particularly potent.

3.8 Second generation quinazolinones – HSV-1 SAR

Our second-generation quinazolinones were again tested for activity against HSV-1 (Figure 3.12)). To our surprise, replacement of the benzyloxybenzyl substituent with a diaryl ether completely eliminated activity. The diaryl ethers and diaryl amine demonstrated no activity against HSV-1. This large difference in activity suggests the terminal ring in the C2 substituent is very important for activity. The benzyl methylene may be required for this ring to reach its binding site, either as a spacer or by providing additional flexibility to the chain. Some of the substituted benzyloxybenzyl ethers (**3-40**, **3-41**, **3-42**) did retain activity against HSV-1. The derivatives containing a 3- or 4-bromobenzyloxybenzyl moiety were more active than the corresponding electron rich 4-

methoxybenzyloxybenzyl analog. This may be due to the changes induced in the electronegativity of the benzyl ring. Although both **3-40** and **3-42** were slightly less active than **3-21**, we were pleased to find that they were also less toxic than **3-15** and **3-21** (Figure 3.13), This suggests substitution of the benzyl ring may prevent oxidation of this compound by Cyp450 enzymes and thus minimize the formation of toxic byproducts.

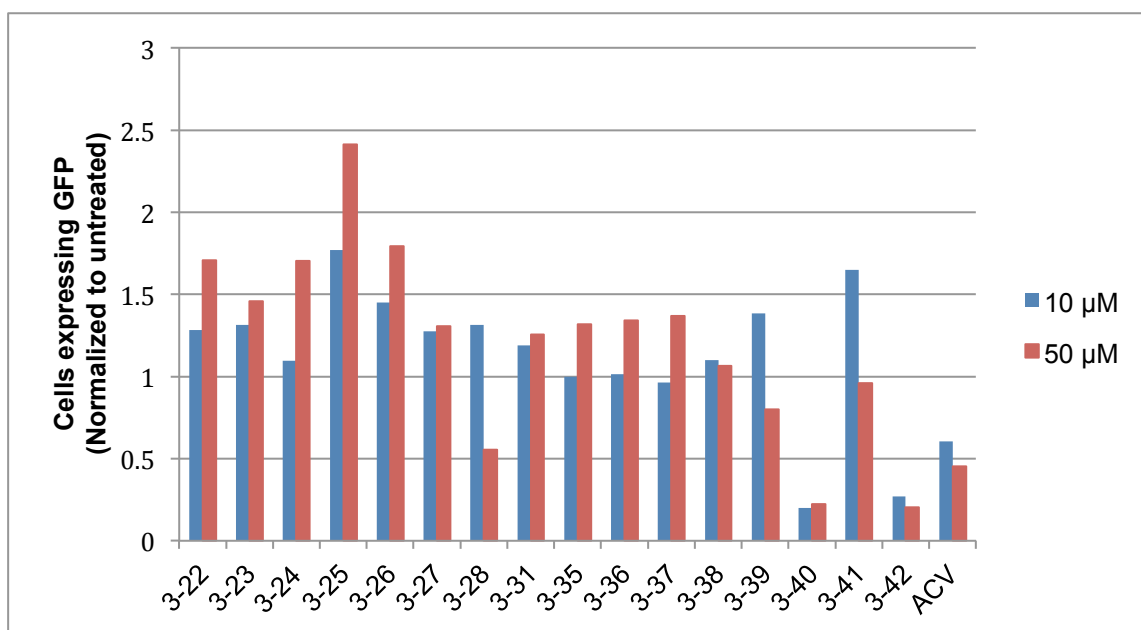


Figure 3.12: Percentage of neurons expressing EGFP after infection with an HSV-1 strain, normalized to untreated cells. At 10 and 50 μM, 13-40 and 3-42 show significant reduction in fluorescence, indicating inhibition of viral replication.

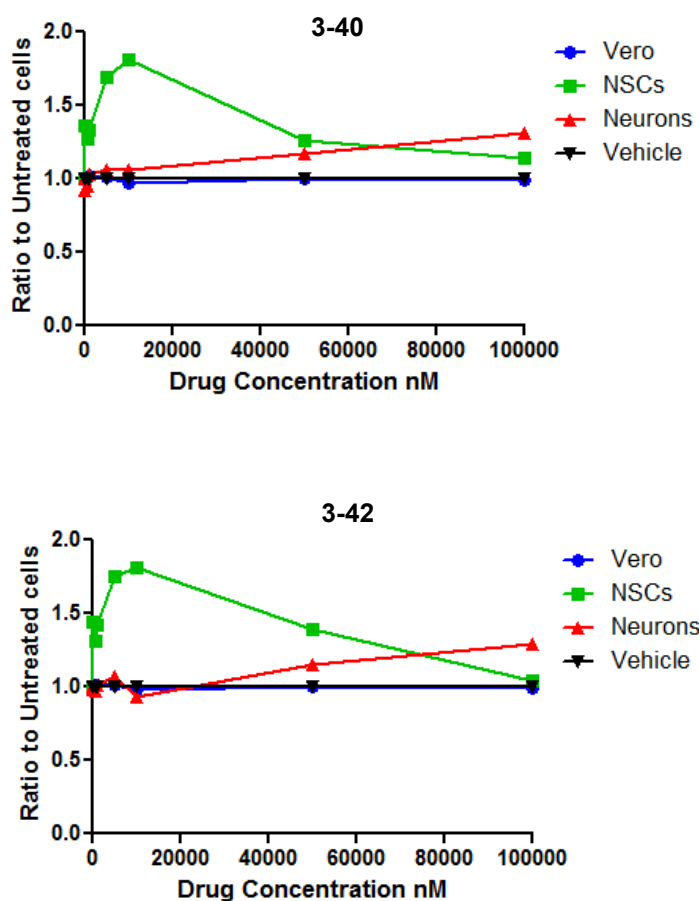


Figure 3.13: Toxicity of 3-40 and 3-42 to Vero cells, neural stem cells, and neurons compared to vehicle. No decrease in cell viability is observed at high concentrations, and at low concentrations a small increase in cell viability is apparent.

3-40 and **3-42** were found to be the most promising compounds in the 2nd generation library. These compounds show good potency, comparable or better to ACV in preliminary assays against active HSV-1, as well as little toxicity to Vero cells and neuronal stem cells. However, neither compound was quite as potent as **3-21**. Given that these compounds are potent inhibitors of acute HSV-1, we next wanted to determine if these compounds are able to inhibit reactivation of latent HSV-1.

To study the effect of **3-21** on heterochromatin dimerization, a chromatin immunoprecipitation (ChIP) assay was performed by collaborators at University of Pittsburgh (Dr. Leonardo D’Aiuto). In this assay, cells were infected with HSV-1 and treated with the compound of interest. This was followed by harvesting, fragmentation of chromatin, and analysis of the enrichment of H3K27Me3 at the viral ICP4 promoter. The data was then normalized to rhodopsin (RHO). Compared to acutely infected cells, cells treated with **3-21** showed no enrichment of H3K27Me3, indicating that the compound does not induce heterochromatinization (Figure 3.14). This indicates that **3-21** is active only against acute HSV-1 infections.

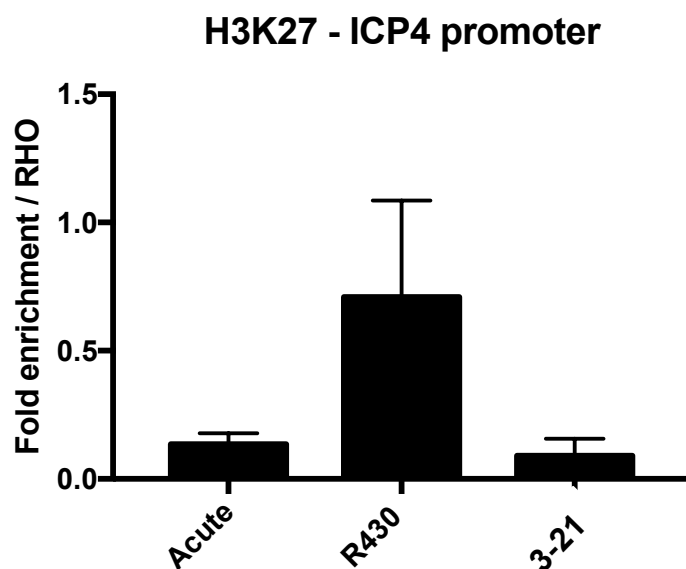


Figure 3.14: ChIP assay to determine H3K27Me3 enrichment in acutely infected cells, and cells treated with either R430 or 3-21. Unlike R430, 3-21 does not induce heterochromatinization.

3.9 Conclusions and future work

In conclusion, our quinazolinone library led to the identification of both anti-parasitic and anti-viral lead compounds. Through diversification and SAR at the N3 and C2 positions, we were able to identify different active pharmacophores for anti-*T. gondii* and anti-HSV-1 activity (Figure 3.15). Our most promising anti-*T. gondii* derivatives, **3-26** and **3-31**, contain an a bulky alkyl group at N3 with a large, lipophilic C2 substituent, such as a benzyloxybenzyl or diaryl ether group. Both compounds are active in the single-digit micromolar range, and show little toxicity to the human host cell. We have thus identified these two compounds as good candidates for further testing. We intend to test the cytotoxicity of these compounds to bradyzoites, the latent form of the *T. gondii* life cycle, to see whether they may have utility against chronic toxoplasmosis.

In contrast, the most potent compounds we have identified against HSV-1 contain an aryl substituent at N3 and a benzyloxybenzyl moiety at C2. This pharmacophore appears to be quite specific, and modifying either C2 or N3 substituents eliminates activity. The most potent quinazolinone was studied to see if it induced heterochromatinization in an HSV-1 infected host. No heterochromatinization was observed, indicating that these compounds are not active against latent HSV-1 infections. We had hypothesized that quinazolinones might effect their antiviral activity by interfering with epigenetic regulation; as this is not the target of **3-21**, the mechanism of action of these compounds is yet unknown. RNAseq or a pull-down assay could be used to determine the target of these compounds.

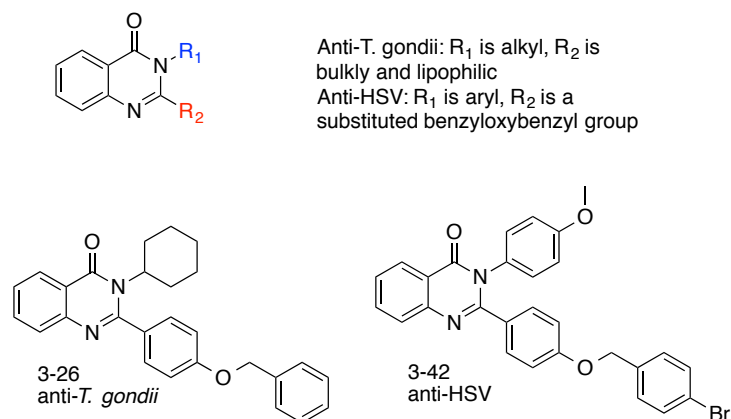


Figure 3.15: Pharmacophores of antiparasitic and antiviral quinazolinones.

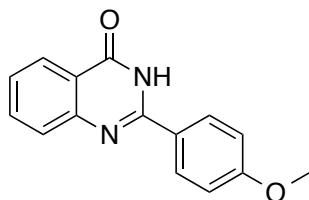
3.10 Experimental

General Information:

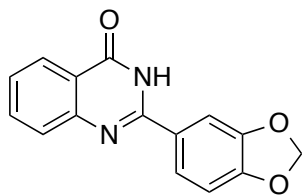
All reagents were obtained from Sigma-Aldrich and used as received. Reagent grade ethanol, dimethylsulfoxide, and dimethylformamide were used without further purification. Dichloromethane was distilled over CaH₂. All reactions were performed under dry N₂ atmosphere unless otherwise stated. Thin layer chromatography (TLC) was performed using aluminium sheets precoated with silica gel 60F₂₅₄ (Macherey-Nagel) and visualized using 254 nm UV light. ¹H and ¹³C NMR spectra were recorded on a Bruker AV 600 spectrometer using CDCl₃ or DMSO-d₆ as solvents. Chemical shifts (δ) are reported in ppm and coupling constants (J) are expressed in Hertz (Hz).

General procedure A for the preparation of 2-substituted quinazolinones:

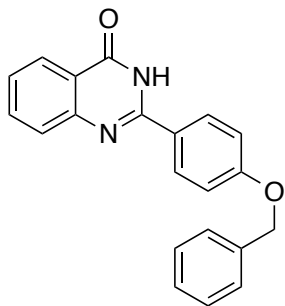
Isatoic anhydride (1.0 eq), ammonium acetate (1.1 eq), and aldehyde (1.2 eq) were dissolved in reagent grade DMSO (1 mL/mmol isatoic anhydride). Camphor sulfonic acid (0.1 eq) was added and the mixture was heated to 120 °C for 48h under air atmosphere. After 48h, ethanol was added to precipitate product from the reaction mixture. The resulting solid was washed with ethanol and dried to yield the desired product without further purification.



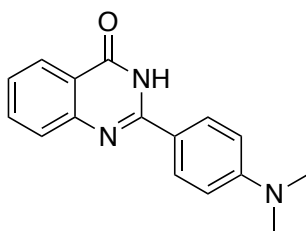
2-(4-methoxyphenyl)quinazolin-4(3H)-one (3-4): pale yellow amorphous solid (61%); ^1H NMR (600 MHz, $\text{DMSO-}d_6$) δ 12.41 (s, 1H), 8.19 (d, $J = 8.5$ Hz, 2H), 8.13 (dd, $J = 7.9, 1.6$ Hz, 1H), 7.84 – 7.80 (m, 1H), 7.71 (d, $J = 8.2$ Hz, 1H), 7.49 (t, $J = 7.5$ Hz, 1H), 7.13 – 7.08 (m, 2H), 3.85 (s, 3H); ^{13}C NMR (150 MHz, $\text{DMSO-}d_6$): δ 162.3, 161.9, 134.6, 129.5, 127.0, 126.2, 125.8, 125.7, 124.6, 120.6, 114.0, 109.4, 55.5; ESI MS: m/z calc. for $\text{C}_{15}\text{H}_{12}\text{N}_2\text{O}_2^+$: 253.0972, found 253.0969.



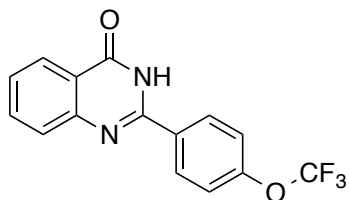
2-(benzo[d][1,3]dioxol-5-yl)quinazolin-4(3H)-one (3-5): white amorphous solid (63%); ^1H NMR (600 MHz, $\text{DMSO-}d_6$) δ 12.38 (s, 1H), 8.13 (dd, $J = 7.9, 1.5$ Hz, 1H), 7.82 (td, $J = 7.8, 1.7$ Hz, 2H), 7.75 (d, $J = 1.8$ Hz, 1H), 7.70 (dd, $J = 8.3, 1.0$ Hz, 1H), 7.51 – 7.47 (m, 1H), 7.08 (d, $J = 8.2$ Hz, 1H), 6.14 (s, 2H); ^{13}C NMR (151 MHz, DMSO) δ 162.22, 151.59, 150.06, 148.74, 147.68, 134.58, 127.33, 126.48, 126.28, 125.82, 122.83, 120.72, 108.28, 107.55, 101.88; ESI MS: m/z calc. for $\text{C}_{15}\text{H}_{10}\text{N}_2\text{O}_2^+$: 267.0764, found 267.0758.



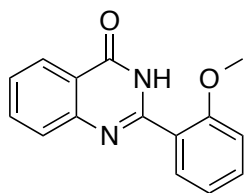
2-(4-(benzyloxy)phenyl)quinazolin-4(3H)-one (3-6): white amorphous solid (77%); ^1H NMR (600 MHz, $\text{DMSO-}d_6$) δ 8.20 – 8.17 (m, 2H), 8.13 (dd, $J = 7.9, 1.5$ Hz, 1H), 7.83 – 7.81 (m, 1H), 7.71 (d, $J = 8.2$ Hz, 1H), 7.49 (t, $J = 7.6$ Hz, 3H), 7.42 (t, $J = 7.5$ Hz, 2H), 7.36 (d, $J = 7.3$ Hz, 1H), 7.19 – 7.16 (m, 2H), 5.22 (s, 2H); ^{13}C NMR (151 MHz, CDCl_3) δ 162.29, 160.97, 151.97, 136.63, 134.57, 129.50, 128.48, 127.97, 127.78, 127.07, 126.19, 125.84, 124.88, 120.64, 114.82, 69.44; ESI MS: m/z calc. for $\text{C}_{21}\text{H}_{16}\text{N}_2\text{O}_2^+$: 329.1285, found 329.1272.



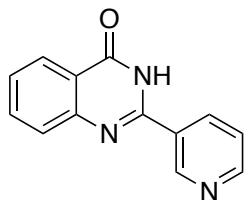
2-(4-(dimethylamino)phenyl)quinazolin-4(3H)-one (3-7): brown amorphous solid (54%); ^1H NMR (600 MHz, $\text{DMSO-}d_6$) δ 12.65 (s, 1H), 8.35 – 8.26 (m, 2H), 8.16 (dd, $J = 7.9, 1.5$ Hz, 1H), 7.85 (ddd, $J = 8.5, 7.1, 1.6$ Hz, 1H), 7.75 (dd, $J = 8.2, 1.1$ Hz, 1H), 7.62 – 7.48 (m, 3H); ^{13}C NMR (151 MHz, DMSO) δ 162.4, 152.3, 134.5, 129.2, 128.9, 126.7, 126.6, 125.8, 125.5, 120.3, 118.4, 111.2, 40.0; ESI MS: m/z calc. for $\text{C}_{16}\text{H}_{15}\text{N}_3\text{O}^+$: 266.1288, found 266.1283.



2-(4-(trifluoromethoxy)phenyl)quinazolin-4(3H)-one (3-8): pale yellow crystalline solid (43%); ^1H NMR (600 MHz, CDCl_3): δ 12.7 (1H, s), 8.31 (2H, d, $J = 8.8$ Hz), 8.17 (1H, dd, $J = 1.2, 7.9$ Hz), 7.84-7.87 (1H, m), 7.75-7.76 (1H, d, $J = 8.1$ Hz), 7.54-7.56 (3H, m); ^{13}C NMR (150 MHz, CDCl_3): δ 162.2, 151.2, 150.4, 148.5, 134.7, 131.9, 130.1, 127.5, 126.8, 125.8, 121.0, 120.3 (q, $J = 170$ Hz), 120.6; ESI MS: m/z calc. for $\text{C}_{15}\text{H}_9\text{F}_3\text{N}_2\text{O}_2^+$: 307.0689, found 307.0683.

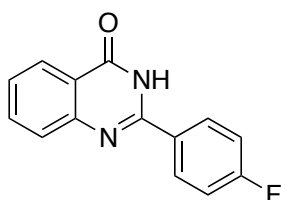


2-(2-methoxyphenyl)quinazolin-4(3H)-one (3-9): white crystalline solid (27%); ^1H NMR (600 MHz, CDCl_3): δ 12.10 (1H, s), 8.15 (1H, dd, $J = 1.3, 7.9$ Hz), 7.81-7.84 (1H, m), 7.69-7.72 (2H, m), 7.52-7.55 (2H, m), 7.20 (1H, d, $J = 8.3$ Hz), 7.10 (1H, t, $J = 7.5$ Hz), 3.86 (3H, s); ^{13}C NMR (151 MHz, DMSO) δ 161.3, 157.1, 134.4, 132.2, 131.3, 130.4, 129.3, 127.4, 126.5, 125.8, 122.7, 120.4, 117.4, 111.9, 55.8.

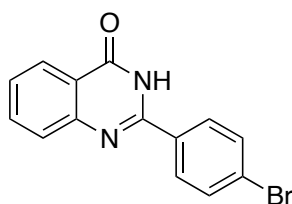


2-(pyridin-3-yl)quinazolin-4(3H)-one (3-10): yellow amorphous solid (76%); ^1H NMR (600 MHz, CDCl_3): δ 12.75 (1H, s), 9.30 (1H, d, $J = 1.9$ Hz), 8.76 (1H, dd, $J = 1.5, 4.8$ Hz), 8.51 (1H, ddd, $J = 1.7, 2.3, 8.0$ Hz), 8.17 (1H, dd, $J = 1.1, 7.9$ Hz), 7.86 (1H, ddd, $J = 1.4, 7.0, 8.3$ Hz), 7.77 (1H, dd, $J = 0.5, 8.1$ Hz), 7.60 (1H, ddd, $J = 0.7, 4.8, 8.0$ Hz), 7.56

(1H, td, J = 1.0, 7.5 Hz); ^{13}C NMR (150 MHz, CDCl_3): δ 169.6, 162.1, 151.7, 150.7, 148.6, 135.5, 134.7, 128.8, 127.5, 127.0, 125.9, 123.6, 121.1; ESI MS: m/z calc. for $\text{C}_{13}\text{H}_9\text{N}_3\text{O}^+$: 233.0746, found 233.0819.



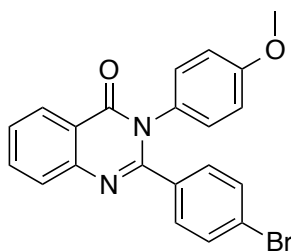
2-(4-fluorophenyl)quinazolin-4(3H)-one (3-11): white crystalline solid (58%); ^1H NMR (600 MHz, $\text{DMSO}-d_6$): δ 12.59 (1H, s), 8.25 (2H, dd, J = 5.4, 8.9 Hz), 8.15 (1H, dd, J = 1.1, 7.9 Hz), 7.84 (1H, ddd, J = 1.4, 7.0, 8.3 Hz), 7.74 (1H, d, J = 8.2 Hz), 7.53 (1H, td, J = 0.9, 7.5 Hz), 7.40 (2H, t, J = 8.9 Hz); ^{13}C NMR (151 MHz, DMSO) δ 163.2, 148.5, 134.6, 130.4, 130.4, 129.2 (d, J = 6 Hz), 127.4, 126.6, 126.2, 125.9, 120.9, 115.7, 115.6; ESI MS: m/z calc. for $\text{C}_{14}\text{H}_9\text{FN}_2\text{O}^+$: 241.0772, found 241.0771.



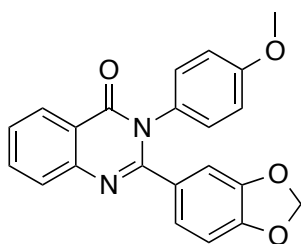
2-(4-bromophenyl)quinazolin-4(3H)-one (3-12): yellow amorphous solid (87%); ^1H NMR (600 MHz, CDCl_3): δ 8.16 (1H, dd, J = 1.1, 7.9 Hz), 8.13 (2H, d, J = 8.6 Hz), 7.84-7.86 (1H, m), 7.77 (2H, d, J = 8.6 Hz), 7.75 (1H, d, J = 8.2 Hz), 7.53-7.55 (1H, m); ^{13}C NMR (151 MHz, DMSO) δ 162.2, 151.5, 148.5, 134.7, 131.9, 131.6, 129.8, 127.4, 126.8, 125.9, 125.2, 121.0; ESI MS: m/z calc. for $\text{C}_{14}\text{H}_9\text{BrN}_2\text{O}_2^+$: 300.9971, found 300.9960.

General synthetic procedure B for the preparation of 2,3-disubstituted quinazolinones:

Isatoic anhydride (1.0 eq), ammonium acetate (1.1 eq), and aldehyde (1.2 eq) were dissolved in reagent grade DMSO (1 mL/mmol isatoic anhydride). Camphor sulfonic acid (0.1 eq) was added and the mixture was heated to 120 °C for 48h under air atmosphere. After 48h, the reaction mixture was partitioned between water (7 mL) and dichloromethane (7 mL). and the aqueous was extracted three times with dichloromethane (3 x 7 mL). The combined organic fractions were dried over sodium sulphate and evaporated to dryness. The crude product was further purified using silica gel chromatography (100:0 Hexane:EtOAc → 60:40 Hexane:EtOAc) to afford the product as a clear, colourless oil.

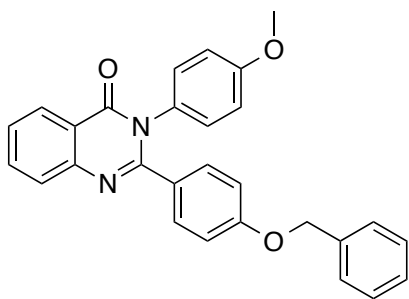


2-(4-bromophenyl)-3-(4-methoxyphenyl)quinazolin-4(3H)-one (3-13): clear, colourless oil (41%); ^1H NMR (600 MHz, CDCl_3): δ 8.34 (1H, d, $J = 8.1$ Hz), 7.81 (2H, m), 7.54 (1H, ddd, $J = 2.2, 5.9, 8.0$ Hz), 7.38 (2H, d, $J = 8.5$ Hz), 7.23 (2H, sd, $J = 8.5$ Hz), 7.04 (2H, d, $J = 8.9$ Hz), 6.85 (2H, d, $J = 8.9$ Hz), 3.80 (3H, s); ^{13}C NMR (150 MHz, CDCl_3): δ 162.5, 159.5, 154.6, 147.4, 134.6, 131.4, 130.8, 130.1, 127.8, 127.6, 127.4, 124.0, 121.1, 114.7, 114.6, 55.6; ESI MS: m/z calc. for $\text{C}_{21}\text{H}_{15}\text{BrN}_2\text{O}_2^+$: 407.0390, found 407.0388.

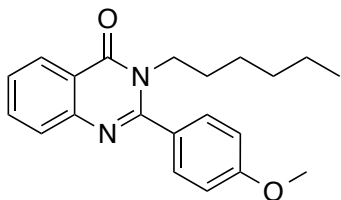


2-(benzo[d][1,3]dioxol-5-yl)-3-(4-methoxyphenyl)quinazolin-4(3H)-one (3-14): clear, colourless oil (42%); ^1H NMR (600 MHz, CDCl_3): δ 8.33 (1H, d, $J = 7.7$ Hz), 7.78-7.82

(2H, m), 7.51 (1H, ddd, $J = 1.6, 6.6, 8.0$ Hz), 7.07 (2H, d, $J = 9.0$ Hz), 6.83-6.87 (4H, m), 6.65 (1H, d, $J = 8.1$ Hz), 5.93 (2H, s), 3.80 (3H, s); ^{13}C NMR (150 MHz, CDCl_3): δ 162.7, 159.3, 155.2, 148.6, 147.5, 134.9, 130.5, 130.0, 127.9, 127.6, 127.3, 124.1, 121.0, 114.5, 109.7, 108.1, 101.6, 60.5, 55.6; ESI MS: m/z calc. for $\text{C}_{22}\text{H}_{16}\text{N}_2\text{O}_2^+$: 373.1183, found 373.1184.

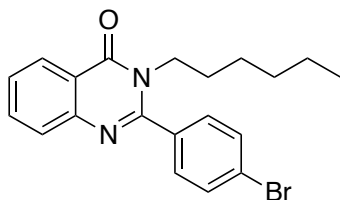


2-(4-(benzyloxy)phenyl)-3-(4-methoxyphenyl)quinazolin-4(3H)-one (3-15): clear, colourless oil (42%); ^1H NMR (600 MHz, CDCl_3): δ 8.34 (1H, d, $J = 7.8$ Hz), 7.78-7.84 (2H, m), 7.50-7.52 (1H, m), 7.37-7.37 (4H, m), 7.31 (2H, d, $J = 8.8$ Hz), 7.06 (2H, d, $J = 8.1$ Hz), 6.85 (2H, d, $J = 8.9$ Hz), 6.82 (2H, d, $J = 8.8$ Hz), 5.03 (2H, s), 3.80 (3H, s); ^{13}C NMR (150 MHz, CDCl_3): δ 162.7, 159.6, 159.3, 155.5, 136.5, 134.8, 131.0, 130.6, 130.1, 128.7, 128.2, 128.1, 127.6, 127.4, 127.2, 120.9, 115.4, 114.8, 114.5, 114.5, 70.1, 55.6; ESI MS: m/z calc. for $\text{C}_{28}\text{H}_{22}\text{N}_2\text{O}_3^+$: 435.1703, found 435.1708.

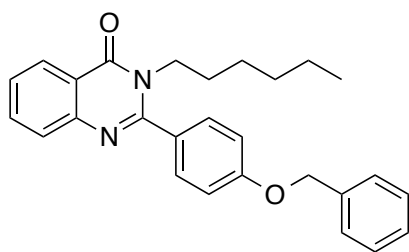


3-hexyl-2-(4-methoxyphenyl)quinazolin-4(3H)-one (3-16): clear, colourless oil (69%); ^1H NMR (600 MHz, CDCl_3): δ 0.80 (3H, t, $J = 7.2$ Hz), 1.12-1.20 (6H, m), 1.59 (2H, dt, $J = 7.5, 15.2$ Hz), 4.00 (2H, m), 7.01 (2H, d, $J = 8.8$ Hz), 7.46-7.48 (3H, m), 7.70-7.74 (2H, m), 8.30 (1H, d, $J = 7.8$ Hz); ^{13}C NMR (150 MHz, CDCl_3): δ 162.4, 160.7, 156.3,

147.3, 134.3, 129.5, 128.1, 127.4, 126.9, 126.8, 120.9, 114.2, 55.5, 46.1, 31.2, 28.7, 26.4, 22.5, 14.0; ESI MS: m/z calc. for $C_{21}H_{24}N_2O_2^+$: 337.1911, found 337.1904.

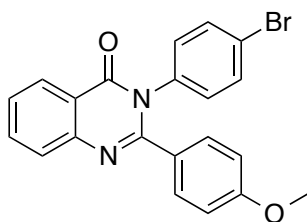


2-(4-bromophenyl)-3-hexylquinazolin-4(3H)-one (3-17): clear, colourless oil (52%); 1H NMR (600 MHz, $CDCl_3$) δ 8.32 (dd, $J = 8.1, 1.4$ Hz, 1H), 7.78 – 7.71 (m, 2H), 7.69 – 7.66 (m, 2H), 7.51 (ddd, $J = 8.1, 6.9, 1.3$ Hz, 1H), 7.44 – 7.40 (m, 2H), 3.99 – 3.93 (m, 2H), 1.59 (p, $J = 7.2$ Hz, 2H), 1.21 – 1.12 (m, 6H), 0.82 (t, $J = 7.2$ Hz, 3H); ^{13}C NMR (151 MHz, $CDCl_3$) δ 162.08, 155.4, 147.0, 134.6, 134.4, 132.2, 129.7, 127.5, 127.4, 127.0, 124.5, 121.0, 46.1, 31.2, 28.8, 26.4, 22.5, 14.1; ESI MS: m/z calc. for $C_{20}H_{21}BrN_2O_2^+$: 385.0910, found 385.0896.

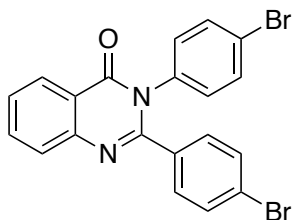


2-(4-(benzyloxy)phenyl)-3-hexylquinazolin-4(3H)-one (3-18): clear, colourless oil (53%); 1H NMR (600 MHz, $CDCl_3$) δ 8.32 (dt, $J = 8.0, 1.1$ Hz, 1H), 7.76 – 7.71 (m, 2H), 7.51 – 7.44 (m, 5H), 7.41 (t, $J = 7.6$ Hz, 2H), 7.37 – 7.33 (m, 1H), 7.12 – 7.07 (m, 2H), 5.15 (s, 2H), 4.03 – 3.97 (m, 2H), 1.60 (t, $J = 7.8$ Hz, 2H), 1.22 – 1.13 (m, 6H), 0.82 (t, $J = 7.2$ Hz, 3H); ^{13}C NMR (151 MHz, $CDCl_3$) δ 162.4, 160.0, 156.3, 136.6, 134.4, 129.6,

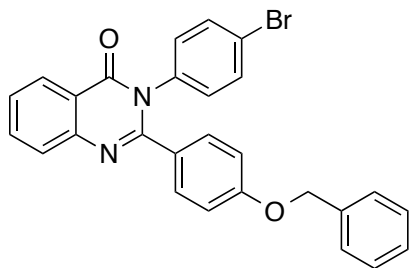
128.8, 128.3, 127.6, 127.4, 127.0, 126.9, 120.9, 115.2, 70.3, 46.2, 31.2, 28.7, 26.5, 22.5, 14.1; ESI MS: m/z calc. for $C_{27}H_{28}BrN_2O_2^+$: 413.2224, found 413.2229.



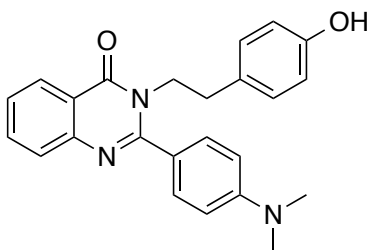
3-(4-bromophenyl)-2-(4-methoxyphenyl)quinazolin-4(3H)-one (3-19): clear, colourless oil (83%); 1H NMR (600 MHz, $CDCl_3$) δ 8.25 (dd, $J = 8.0, 1.4$ Hz, 1H), 7.79 (d, $J = 8.2$ Hz, 1H), 7.74 (ddd, $J = 8.3, 7.0, 1.6$ Hz, 1H), 7.62 (d, $J = 8.6$ Hz, 0H), 7.47 – 7.44 (m, 1H), 7.42 – 7.39 (m, 2H), 7.24 – 7.20 (m, 2H), 6.99 – 6.95 (m, 2H), 6.72 – 6.68 (m, 2H), 3.71 (s, 3H); ^{13}C NMR (151 MHz, $CDCl_3$) δ 160.4, 145.4, 135.7, 134.8, 134.7, 132.8, 132.2, 130.7, 130.7, 129.8, 128.6, 127.8, 127.6, 127.6, 127.1, 113.6, 55.2. ; ESI MS: m/z calc. for $C_{21}H_{15}BrN_2O_2^+$: 407.039, found 407.0373.



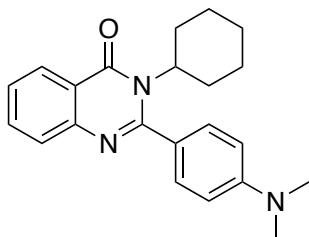
2,3-bis(4-bromophenyl)quinazolin-4(3H)-one (3-20): clear, colourless oil (25%); 1H NMR (600 MHz, $CDCl_3$) δ 8.33 (dd, $J = 8.0, 1.3$ Hz, 1H), 7.85 – 7.79 (m, 2H), 7.55 (ddd, $J = 8.1, 6.7, 1.6$ Hz, 1H), 7.50 – 7.47 (m, 2H), 7.42 – 7.39 (m, 2H), 7.23 – 7.20 (m, 2H), 7.05 – 7.01 (m, 2H); ^{13}C NMR (151 MHz, $CDCl_3$) δ 162.1, 153.7, 147.4, 136.6, 135.2, 134.1, 132.6, 132.1, 131.6, 130.8, 128.0, 127.8, 127.4, 124.4, 122.9, 120.8, 116.9, 31.1; ESI MS: m/z calc. for $C_{20}H_{12}Br_2N_2O^+$: 453.9316, found 454.9379.



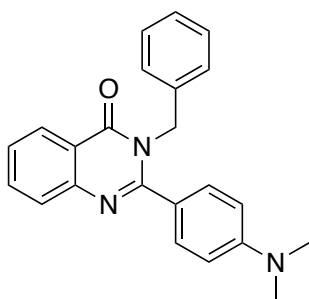
2-(4-(benzyloxy)phenyl)-3-(4-bromophenyl)quinazolin-4(3H)-one (3-21): clear, colourless oil (46%); ^1H NMR (600 MHz, CDCl_3) δ 8.32 (dd, $J = 8.1, 1.4$ Hz, 1H), 7.85 (d, $J = 8.3$ Hz, 1H), 7.83 – 7.79 (m, 1H), 7.55 – 7.51 (m, 1H), 7.49 – 7.46 (m, 2H), 7.39 – 7.36 (m, 4H), 7.33 (dq, $J = 7.5, 2.7$ Hz, 1H), 7.30 – 7.27 (m, 2H), 7.06 – 7.01 (m, 2H), 6.86 – 6.81 (m, 2H), 5.04 (d, $J = 1.2$ Hz, 2H); ^{13}C NMR (151 MHz, CDCl_3) δ 162.3, 159.8, 154.7, 147.3, 137.0, 136.4, 135.1, 132.4, 131.0, 130.8, 128.7, 128.3, 127.6, 127.6, 127.4, 127.4, 122.6, 120.6, 114.7, 70.1; ESI MS: m/z calc. for $\text{C}_{27}\text{H}_{19}\text{BrN}_2\text{O}_2^+$: 483.0703, found 483.0704.



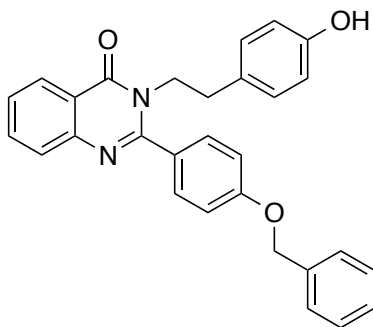
2-(4-(dimethylamino)phenyl)-3-(4-hydroxyphenethyl)quinazolin-4(3H)-one (3-22): off white amorphous solid (43%); ^1H NMR (600 MHz, $\text{DMSO}-d_6$) δ 8.17 (dd, $J = 8.0, 1.5$ Hz, 1H), 7.81 (ddd, $J = 8.4, 7.1, 1.6$ Hz, 1H), 7.64 – 7.61 (m, 1H), 7.52 (ddd, $J = 8.2, 7.1, 1.1$ Hz, 1H), 7.41 – 7.36 (m, 2H), 6.83 – 6.77 (m, 2H), 6.69 – 6.67 (m, 2H), 6.58 (d, $J = 8.4$ Hz, 2H), 4.17 – 4.09 (m, 2H), 3.00 (s, 6H), 2.74 – 2.69 (m, 2H); ^{13}C NMR (151 MHz, DMSO) δ 161.55, 156.59, 155.84, 150.90, 147.09, 134.32, 129.30, 129.21, 127.99, 127.03, 126.45, 126.12, 122.48, 120.10, 115.18, 111.11, 47.15, 39.87, 32.97; ESI HRMS: m/z calc. for $\text{C}_{24}\text{H}_{22}\text{N}_3\text{O}_2^+$: 384.1712, found 384.1696.



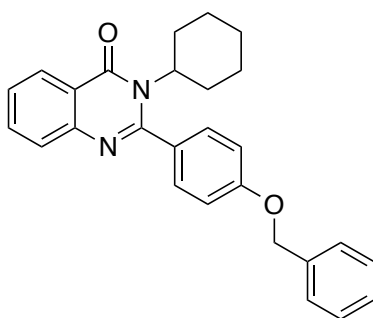
3-cyclohexyl-2-(4-(dimethylamino)phenyl)quinazolin-4(3H)-one (3-23): white amorphous solid (15%); ^1H NMR (600 MHz, Chloroform-*d*) δ 8.26 (dt, $J = 7.9, 1.0$ Hz, 1H), 7.78 – 7.68 (m, 2H), 7.46 – 7.40 (m, 3H), 6.80 – 6.76 (m, 2H), 4.12 (tt, $J = 11.9, 3.7$ Hz, 1H), 3.04 (s, 6H), 2.79 – 2.72 (m, 2H), 1.79 (d, $J = 13.3$ Hz, 2H), 1.73 (dd, $J = 12.2, 3.4$ Hz, 2H), 1.57 (d, $J = 13.5$ Hz, 1H), 1.30 – 1.21 (m, 1H), 1.07 (dtd, $J = 13.2, 9.6, 4.8$ Hz, 2H); ^{13}C NMR (151 MHz, CDCl_3) δ 163.38, 157.84, 151.34, 147.30, 134.01, 128.75, 127.22, 126.53, 126.39, 124.00, 122.07, 111.98, 62.72, 40.44, 29.24, 26.43, 25.23; ESI MS: m/z calc. for $\text{C}_{22}\text{H}_{26}\text{N}_3\text{O}^+$: 348.2076, found 348.2068.



3-benzyl-2-(4-(dimethylamino)phenyl)quinazolin-4(3H)-one (3-24): yellow amorphous solid (15%); ^1H NMR (600 MHz, Chloroform-*d*) δ 8.35 (dd, $J = 8.0, 1.1$ Hz, 1H), 7.80 – 7.76 (m, 2H), 7.50 (d, $J = 4.0$ Hz, 1H), 7.35 – 7.31 (m, 2H), 7.29 – 7.22 (m, 3H), 7.09 – 7.04 (m, 2H), 6.72 – 6.68 (m, 2H), 5.39 (s, 2H), 3.03 (s, 6H); ^{13}C NMR (151 MHz, CDCl_3) δ 163.04, 157.28, 151.53, 147.76, 137.22, 134.47, 132.09, 129.56, 128.64, 127.57, 127.36, 127.12, 126.99, 126.67, 122.82, 120.71, 111.73, 110.83, 77.37, 77.16, 76.95, 49.44, 40.40; ESI MS: m/z calc. for $\text{C}_{23}\text{H}_{22}\text{N}_3\text{O}^+$: 356.1763, found 356.1755.

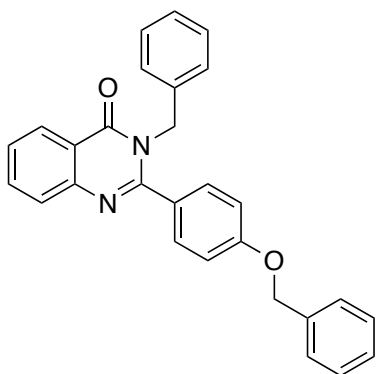


2-(4-(benzyloxy)phenyl)-3-(4-hydroxyphenethyl)quinazolin-4(3H)-one (3-25): white crystalline solid (49%); ^1H NMR (600 MHz, Chloroform-*d*) δ 8.36 (dd, $J = 7.9, 1.3$ Hz, 1H), 7.77 – 7.71 (m, 2H), 7.54 – 7.48 (m, 1H), 7.45 – 7.40 (m, 2H), 7.42 – 7.36 (m, 3H), 7.34 (d, $J = 7.2$ Hz, 1H), 7.27 – 7.22 (m, 2H), 5.11 (s, 2H), 4.24 – 4.17 (m, 2H), 2.82 (t, $J = 7.6$ Hz, 2H); ^{13}C NMR (151 MHz, CDCl_3) δ 162.54, 159.86, 156.52, 155.23, 146.99, 136.48, 134.74, 130.00, 129.48, 129.23, 128.78, 128.28, 127.68, 127.54, 127.25, 126.89, 120.78, 115.63, 115.11, 70.21, 48.03, 33.87, 29.82; ESI MS: m/z calc. for $\text{C}_{29}\text{H}_{25}\text{N}_2\text{O}_3^+$: 449.1865, found 449.1851.

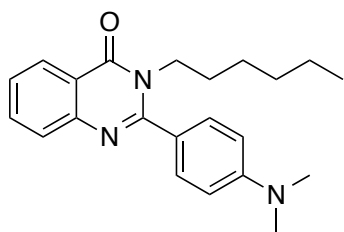


2-(4-(benzyloxy)phenyl)-3-cyclohexylquinazolin-4(3H)-one (3-26): pale, yellow solid (25%); ^1H NMR (600 MHz, Chloroform-*d*) δ 8.28 (dd, $J = 8.0, 1.4$ Hz, 1H), 7.74 – 7.66 (m, 2H), 7.49 – 7.44 (m, 5H), 7.41 (t, $J = 7.6$ Hz, 2H), 7.37 – 7.34 (m, 1H), 7.11 – 7.07 (m, 2H), 5.16 (s, 2H), 3.95 (ddt, $J = 11.9, 7.4, 3.7$ Hz, 1H), 2.75 (qd, $J = 12.7, 3.7$ Hz, 2H), 1.79 (d, $J = 13.7$ Hz, 2H), 1.70 (d, $J = 11.2$ Hz, 2H), 1.57 (d, $J = 13.0$ Hz, 1H), 1.28

– 1.21 (m, 1H), 1.02 (dddd, $J = 16.9, 13.2, 8.3, 3.6$ Hz, 2H); ^{13}C NMR (151 MHz, CDCl_3) δ 162.98, 159.85, 156.93, 146.98, 136.57, 134.17, 129.27, 128.94, 128.79, 128.28, 127.59, 127.27, 126.82, 126.60, 122.24, 115.34, 62.76, 29.11, 26.39, 25.13; ESI MS: m/z calc. for $\text{C}_{27}\text{H}_{27}\text{N}_2\text{O}_2^+$: 411.2073, found 411.2063.

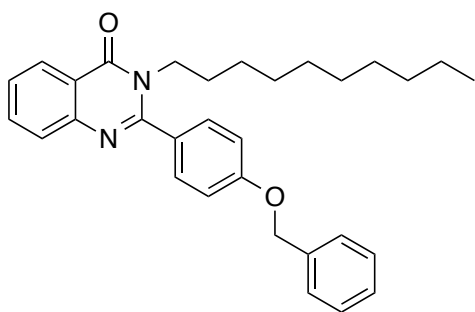


3-benzyl-2-(4-(benzyloxy)phenyl)quinazolin-4(3H)-one (3-27): white crystalline solid (76%); ^1H NMR (600 MHz, Chloroform- d) δ 8.36 (dt, $J = 7.9, 1.1$ Hz, 1H), 7.79 – 7.74 (m, 2H), 7.53 – 7.50 (m, 1H), 7.45 – 7.42 (m, 2H), 7.40 (t, $J = 7.5$ Hz, 2H), 7.36 – 7.33 (m, 1H), 7.29 (d, $J = 8.7$ Hz, 2H), 7.21 (dd, $J = 5.1, 1.8$ Hz, 3H), 7.00 – 6.92 (m, 4H), 5.30 (s, 2H), 5.12 (s, 2H); ^{13}C NMR (151 MHz, CDCl_3) δ 162.75, 160.03, 156.46, 155.51, 147.42, 136.86, 136.57, 134.93, 134.66, 129.82, 128.81, 128.69, 128.29, 128.1, 127.65, 127.53, 127.24, 127.16, 127.06, 120.89, 115.10, 49.11; ESI MS: m/z calc. for $\text{C}_{28}\text{H}_{23}\text{N}_2\text{O}_2^+$: 419.1760, found 419.1779.

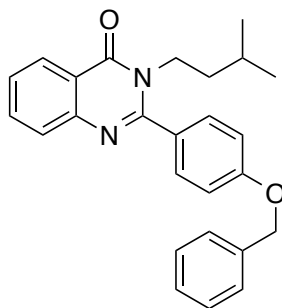


2-(4-(dimethylamino)phenyl)-3-hexylquinazolin-4(3H)-one (3-28): clear, colourless oil (35%); ^1H NMR (600 MHz, Chloroform- d) δ 8.30 (dt, $J = 8.1, 1.0$ Hz, 1H), 7.77 – 7.69

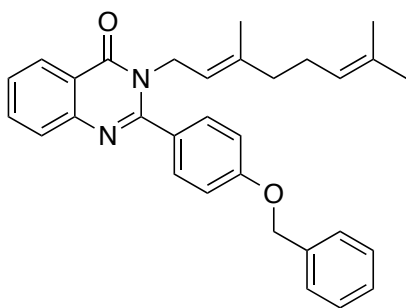
(m, 2H), 7.46 (t, $J = 8.1$ Hz, 1H), 7.44 – 7.39 (m, 2H), 6.80 – 6.75 (m, 2H), 4.11 – 4.05 (m, 2H), 3.04 (s, 6H), 1.63 (t, $J = 7.7$ Hz, 2H), 1.22 – 1.11 (m, 6H), 0.81 (t, $J = 7.1$ Hz, 3H); ^{13}C NMR (151 MHz, CDCl_3) δ 162.76, 157.22, 151.44, 134.25, 129.32, 127.37, 127.32, 126.84, 126.59, 123.21, 120.76, 111.88, 46.30, 40.45, 31.29, 28.74, 26.52, 22.55, 14.11.



2-(4-(dimethylamino)phenyl)-3-hexylquinazolin-4(3H)-one (3-29): pale yellow oil (34%); ^1H NMR (600 MHz, Chloroform-*d*) δ 8.32 (dd, $J = 7.9, 1.3$ Hz, 1H), 7.76 – 7.68 (m, 2H), 7.50 – 7.43 (m, 5H), 7.41 (t, $J = 7.6$ Hz, 2H), 7.37 – 7.33 (m, 1H), 7.11 – 7.07 (m, 2H), 5.15 (s, 2H), 4.04 – 3.96 (m, 2H), 1.60 (t, $J = 7.8$ Hz, 2H), 1.27 (q, $J = 6.6$ Hz, 2H), 1.24 – 1.14 (m, 12H), 0.87 (t, $J = 7.1$ Hz, 3H); ^{13}C NMR (151 MHz, CDCl_3) δ 162.43, 159.91, 156.27, 147.35, 136.56, 134.33, 129.55, 128.79, 128.40, 128.28, 127.53, 127.50, 126.92, 126.87, 120.97, 115.19, 70.26, 46.15, 32.01, 29.59, 29.49, 29.39, 29.05, 28.79, 26.80, 22.80, 14.24; ESI MS: m/z calc. for $\text{C}_{31}\text{H}_{37}\text{N}_2\text{O}_2^+$: 469.2855, found 469.2862.

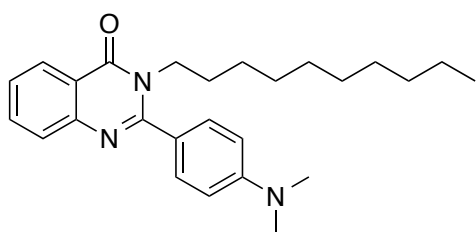


2-(4-(benzyloxy)phenyl)-3-isopentylquinazolin-4(3H)-one (3-30): clear, colourless oil (25%); ^1H NMR (600 MHz, Chloroform-*d*) δ 8.31 (dt, $J = 8.1, 1.1$ Hz, 1H), 7.77 – 7.70 (m, 2H), 7.51 – 7.43 (m, 5H), 7.42 – 7.38 (m, 2H), 7.37 – 7.32 (m, 1H), 7.09 (d, $J = 8.7$ Hz, 2H), 5.16 (s, 2H), 4.02 (dd, $J = 9.9, 6.0$ Hz, 2H), 1.51 – 1.44 (m, 3H), 0.75 (d, $J = 6.2$ Hz, 6H); ^{13}C NMR (151 MHz, CDCl_3) δ 162.37, 159.83, 156.22, 147.33, 136.54, 134.31, 129.52, 128.76, 128.31, 128.22, 127.46, 126.91, 126.80, 122.32, 120.95, 115.19, 70.19, 44.67, 37.54, 26.24, 22.28; ESI MS: m/z calc. for $\text{C}_{26}\text{H}_{27}\text{N}_2\text{O}_2^+$: 399.2073, found 399.2084.

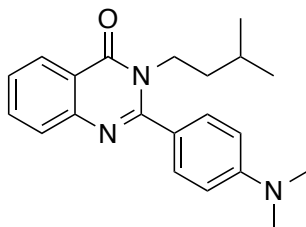


(E)-2-(4-(benzyloxy)phenyl)-3-(3,7-dimethylocta-2,6-dien-1-yl)quinazolin-4(3H)-one (3-31): clear, colourless oil (31%); ^1H NMR (600 MHz, Chloroform-*d*) δ 8.37 – 8.35 (m, 1H), 7.76 (dd, $J = 5.9, 1.5$ Hz, 2H), 7.53 – 7.50 (m, 3H), 7.48 – 7.46 (m, 2H), 7.42 (t, $J = 7.5$ Hz, 2H), 7.37 (t, $J = 7.3$ Hz, 1H), 7.10 – 7.07 (m, 2H), 5.22 (tt, $J = 5.0, 1.3$ Hz, 1H), 5.18 (s, 2H), 5.07 (ddq, $J = 6.9, 4.1, 1.4$ Hz, 1H), 4.66 (d, $J = 6.3$ Hz, 2H), 2.09 – 2.03 (m,

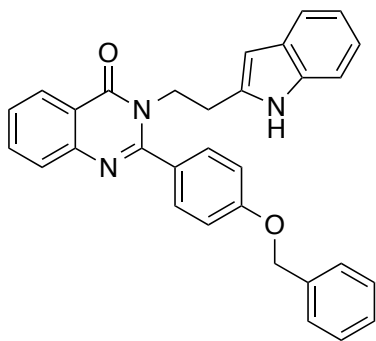
2H), 2.00 – 1.97 (m, 2H), 1.68 (d, $J = 1.4$ Hz, 3H), 1.61 (d, $J = 1.3$ Hz, 3H), 1.35 (d, $J = 1.3$ Hz, 3H); ^{13}C NMR (151 MHz, CDCl_3) δ 162.55, 159.92, 156.49, 147.30, 139.42, 136.57, 134.44, 131.91, 129.82, 128.81, 128.27, 127.50, 127.39, 126.98, 126.91, 123.90, 120.92, 119.48, 115.17, 70.22, 44.95, 39.50, 26.36, 25.81, 24.96, 17.87, 16.29; ESI MS: m/z calc. for $\text{C}_{31}\text{H}_{33}\text{N}_2\text{O}_2^+$: 465.2542, found 465.2526. 27



3-decyl-2-(4-(dimethylamino)phenyl)quinazolin-4(3H)-one (3-32): pale yellow oil (45%); ^1H NMR (600 MHz, Chloroform-*d*) δ 8.33 (dt, $J = 7.9, 1.1$ Hz, 1H), 7.78 – 7.72 (m, 2H), 7.46-7.49 (m, 1H), 7.46 – 7.43 (m, 2H), 6.82 – 6.78 (m, 2H), 4.13 – 4.09 (m, 2H), 3.06 (s, 6H), 1.66 (t, $J = 7.6$ Hz, 2H), 1.29 (q, $J = 6.6$ Hz, 2H), 1.25 – 1.18 (m, 12H), 0.89 (t, $J = 7.1$ Hz, 3H); ^{13}C NMR (151 MHz, CDCl_3) δ 162.75, 157.17, 151.38, 147.48, 134.20, 129.29, 127.34, 126.81, 126.53, 123.04, 120.77, 111.84, 46.28, 40.42, 32.02, 29.62, 29.50, 29.39, 29.10, 28.78, 26.82, 22.80, 14.25; ESI MS: m/z calc. for $\text{C}_{26}\text{H}_{36}\text{N}_3\text{O}^+$: 406.2858, found 406.2852.

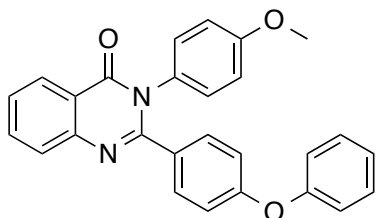


2-(4-(dimethylamino)phenyl)-3-isopentylquinazolin-4(3H)-one (3-33): pale yellow amorphous solid (34%); ^1H NMR (600 MHz, Chloroform-*d*) δ 8.30 (dt, $J = 7.9, 1.1$ Hz, 1H), 7.74 – 7.70 (m, 2H), 7.47 – 7.43 (m, 1H), 7.41 (d, $J = 8.7$ Hz, 2H), 6.77 (d, $J = 8.8$ Hz, 2H), 4.12 – 4.08 (m, 2H), 3.03 (s, 6H), 1.55 – 1.46 (m, 3H), 0.78 (d, $J = 6.4$ Hz, 6H); ^{13}C NMR (151 MHz, CDCl_3) δ 162.78, 157.19, 151.44, 147.52, 134.22, 129.26, 127.33, 126.79, 126.57, 122.99, 120.78, 111.85, 44.91, 40.46, 37.61, 26.33, 22.40, 20.83; ESI MS: m/z calc. for $\text{C}_{21}\text{H}_{26}\text{N}_3\text{O}^+$: 336.2076, found 336.2066.

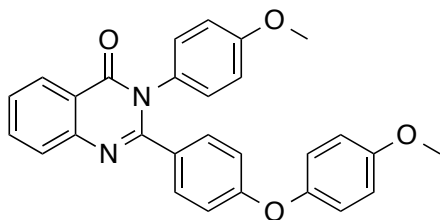


3-(2-(1H-indol-2-yl)ethyl)-2-(4-(benzyloxy)phenyl)quinazolin-4(3H)-one (3-34): brown amorphous solid (24%); ^1H NMR (600 MHz, $\text{DMSO}-d_6$) δ 10.79 (d, $J = 2.4$ Hz, 1H), 8.24 (dd, $J = 8.0, 1.5$ Hz, 1H), 7.85 (ddd, $J = 8.5, 7.1, 1.6$ Hz, 1H), 7.66 (d, $J = 8.1$ Hz, 1H), 7.60 – 7.57 (m, 1H), 7.52 – 7.50 (m, 2H), 7.48 (d, $J = 8.6$ Hz, 2H), 7.43 (dd, $J = 8.3, 6.8$ Hz, 2H), 7.38 – 7.36 (m, 1H), 7.30 (d, $J = 8.1$ Hz, 1H), 7.11 (d, $J = 8.6$ Hz, 2H), 7.02 (t, $J = 7.5$ Hz, 1H), 6.93 – 6.90 (m, 2H), 6.78 (t, $J = 7.4$ Hz, 1H), 5.21 (s, 2H), 4.19 – 4.15 (m, 2H), 2.94 – 2.90 (m, 2H); ^{13}C NMR (151 MHz, DMSO) δ 161.33, 159.10, 155.95, 146.94, 136.78, 136.14, 134.43, 129.66, 128.50, 127.97, 127.93, 127.70, 127.13, 126.82, 126.17, 122.85, 120.97, 120.42, 118.14, 118.07, 117.83, 114.49, 111.35, 110.21, 69.42, 46.22, 23.96; ESI MS: m/z calc. for $\text{C}_{31}\text{H}_{26}\text{N}_3\text{O}_2^+$: 472.2025, found 472.2013. 25

General procedure C for Chan-Lam coupling: Quinazolinone phenol or aniline was prepared from isatoic anhydride, p-anisidine, and 4-hydroxybenzaldehyde using General Procedure B. The resulting phenol (1 eq) was dissolved in freshly distilled DCM (0.1 mM) to which was added crushed molecular sieves (4A), CuOAc₂ (1 eq), TEA (5 eq), and an aryl boronic acid (3 eq). The reaction was stirred under air at room temperature for 48 h. The crude reaction mixture was then concentrated and purified by silica gel chromatography using a 100:0 Hexane:EtOAc → 60:40 Hexane:EtOAc.

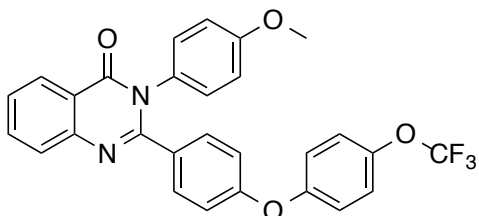


3-(4-methoxyphenyl)-2-(4-phenoxyphenyl)quinazolin-4(3H)-one (3-35): off-white amorphous solid (75% over two steps); ¹H NMR (600 MHz, CDCl₃) δ 8.35 (dt, *J* = 7.9, 1.2 Hz, 1H), 7.84 – 7.78 (m, 2H), 7.52 (ddd, *J* = 8.1, 6.3, 2.0 Hz, 1H), 7.37 – 7.30 (m, 4H), 7.16 – 7.10 (m, 1H), 7.09 – 7.04 (m, 2H), 6.98 – 6.93 (m, 2H), 6.88 – 6.82 (m, 4H), 3.80 (s, 3H); ¹³C NMR (151 MHz, CDCl₃) δ 162.6, 159.4, 158.5, 156.3, 155.3, 134.9, 131.1, 130.4, 130.2, 130.0, 127.7, 127.4, 127.4, 124.1, 121.0, 119.6, 118.0, 114.5, 55.6; ESI MS: *m/z* calc. for C₂₇H₂₀N₂O₃⁺: 421.1547, found 421.1543.

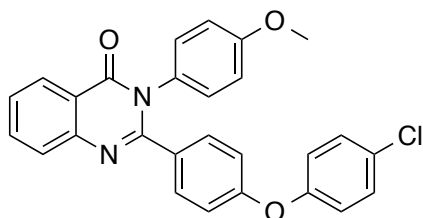


2-(4-(4-methoxyphenoxy)phenyl)-3-(4-methoxyphenyl)quinazolin-4(3H)-one (3-36): off-white amorphous solid (61% over two steps); ¹H NMR (600 MHz, CDCl₃) δ 8.34 (dd, *J* = 7.9, 1.4 Hz, 1H), 7.87 (s, 1H), 7.81 (ddd, *J* = 8.3, 7.1, 1.6 Hz, 1H), 7.53 (ddd, *J* = 8.1,

7.1, 1.2 Hz, 1H), 7.33 – 7.29 (m, 2H), 7.09 – 7.04 (m, 2H), 6.95 – 6.91 (m, 2H), 6.89 – 6.85 (m, 4H), 6.80 – 6.76 (m, 2H), 3.81 (s, 6H); ^{13}C NMR (151 MHz, CDCl_3) δ 162.5, 159.7, 159.4, 156.5, 155.4, 149.2, 147.1, 134.9, 131.1, 130.4, 130.2, 127.4, 127.4, 121.3, 120.9, 116.8, 115.1, 114.5, 55.8, 55.6.

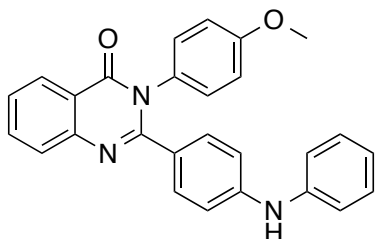


3-(4-methoxyphenyl)-2-(4-(4-(trifluoromethoxy)phenoxy)phenyl)quinazolin-4(3H)-one (3-37): white crystalline solid (80% over two steps); ^1H NMR (600 MHz, CDCl_3) δ 8.38 – 8.33 (m, 1H), 7.86 – 7.78 (m, 2H), 7.54 (ddd, $J = 8.2, 6.7, 1.6$ Hz, 1H), 7.38 – 7.33 (m, 2H), 7.21 – 7.16 (m, 2H), 7.09 – 7.04 (m, 2H), 6.97 – 6.93 (m, 2H), 6.86 (dd, $J = 8.9, 2.6$ Hz, 4H), 3.80 (s, 3H); ^{13}C NMR (151 MHz, CDCl_3) δ 162.6, 159.5, 157.9, 155.1, 154.9, 145.1, 135.0, 132.4, 131.2, 130.3, 130.2, 127.7, 127.5, 127.4, 122.8, 121.0, 120.4 (q, $J = 209$ Hz), 120.3, 118.2, 116.1, 114.5, 55.6.; ESI MS: m/z calc. for $\text{C}_{28}\text{H}_{19}\text{F}_3\text{N}_2\text{O}_4^+$: 505.1370, found 505.1360.



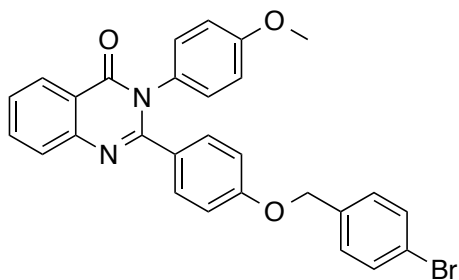
2-(4-(4-chlorophenoxy)phenyl)-3-(4-methoxyphenyl)quinazolin-4(3H)-one (3-38): off-white crystalline solid (62% over two steps); ^1H NMR (600 MHz, CDCl_3) δ 8.38 – 8.33 (m, 1H), 7.86 – 7.79 (m, 2H), 7.53 (ddd, $J = 8.1, 6.8, 1.5$ Hz, 1H), 7.36 – 7.32 (m, 2H), 7.31 – 7.27 (m, 2H), 7.08 – 7.05 (m, 2H), 6.91 – 6.87 (m, 2H), 6.87 – 6.85 (m, 2H), 6.85 – 6.82 (m, 2H), 3.80 (s, 3H); ^{13}C NMR (151 MHz, CDCl_3) δ 162.4, 159.5, 158.2,

155.3, 154.9, 135.0, 131.3, 130.7, 130.2, 130.0, 129.3, 127.6, 127.5, 120.9, 120.8, 118.0, 114.5, 55.6.



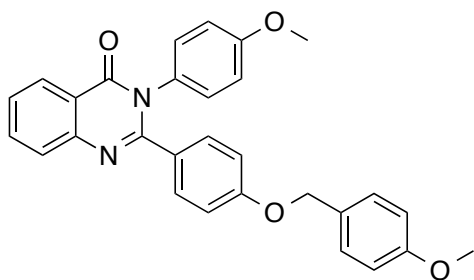
3-(4-methoxyphenyl)-2-(4-(phenylamino)phenyl)quinazolin-4(3H)-one (3-39): pale yellow oil (33% over two steps); ^1H NMR (600 MHz, Acetone- d_6) δ 8.21 (dd, $J = 7.9, 1.5$ Hz, 1H), 7.85 (ddd, $J = 8.5, 7.1, 1.6$ Hz, 1H), 7.78 (d, $J = 8.0$ Hz, 1H), 7.54 (ddd, $J = 8.1, 7.1, 1.3$ Hz, 1H), 7.34 (d, $J = 8.7$ Hz, 2H), 7.28 – 7.25 (m, 3H), 7.16 – 7.12 (m, 2H), 6.95 – 6.91 (m, 4H), 3.80 (s, 3H); ^{13}C NMR (151 MHz, Acetone- d_6) δ 162.8, 160.1, 156.8, 148.5, 145.8, 143.2, 135.2, 132.2, 131.8, 131.5, 130.1, 128.0, 127.6, 127.3, 122.2, 121.8, 119.5, 115.3, 115.0, 114.6, 55.8; ESI MS: m/z calc. for $\text{C}_{27}\text{H}_{21}\text{N}_3\text{O}_2^+$: 420.1707, found 420.1704.

General synthetic procedure D for benzylation: Quinazolinone phenol was prepared from isatoic anhydride, p-anisidine, and 4-hydroxybenzaldehyde using General Procedure B. The resulting phenol (1 eq) was dissolved in dry DMF (0.1 mM) and cooled to 0 °C. NaH (1.1 eq) was added portionwise and the reaction mixture was stirred for 10 minutes. A solution of benzyl bromide (1.1 eq) in DMF (0.5 mM) was added dropwise. The reaction mixture was allowed to warm to room temperature over 1 hour, then quenched by the addition of water. The aqueous was extracted 3 times with dichloromethane. The combined organic phase was dried over sodium sulphate and concentrated. The product was purified by silica gel chromatography using a 100:0 Hexane:EtOAc \rightarrow 60:40 Hexane:EtOAc.



2-(4-((4-bromobenzyl)oxy)phenyl)-3-(4-methoxyphenyl)quinazolin-4(3H)-one (3-40):

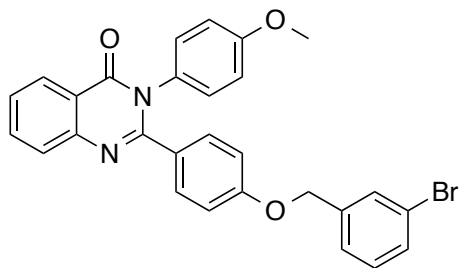
off-white amorphous solid (55% over two steps); ^1H NMR (600 MHz, CDCl_3) δ 8.35 – 8.32 (m, 1H), 7.80 (dd, $J = 6.9, 1.5$ Hz, 2H), 7.52 – 7.48 (m, 3H), 7.32 – 7.29 (m, 2H), 7.25 (d, $J = 1.9$ Hz, 2H), 7.07 – 7.04 (m, 2H), 6.86 – 6.84 (m, 2H), 6.80 – 6.78 (m, 2H), 4.97 (s, 2H), 3.80 (s, 3H); ^{13}C NMR (151 MHz, CDCl_3) δ 162.4, 159.5, 135.5, 135.1, 131.9, 131.2, 130.2, 130.1, 129.7, 129.5, 129.2, 128.7, 127.5, 127.0, 122.2, 122.1, 120.7, 114.5, 114.5, 114.4, 69.4, 55.6; ESI MS: m/z calc. for $\text{C}_{28}\text{H}_{21}\text{BrN}_2\text{O}_3^+$: 513.0808, found 513.0800.



2-(4-((4-methoxybenzyl)oxy)phenyl)-3-(4-methoxyphenyl)quinazolin-4(3H)-one (3-41):

white crystalline solid (69% over two steps); ^1H NMR (600 MHz, CDCl_3) δ 8.33 (dd, $J = 8.0, 1.5$ Hz, 1H), 7.92 (s, 1H), 7.81 (ddd, $J = 8.4, 7.2, 1.6$ Hz, 1H), 7.55 – 7.51 (m, 1H), 7.31 (dd, $J = 8.8, 7.0$ Hz, 4H), 7.07 – 7.05 (m, 2H), 6.91 – 6.89 (m, 2H), 6.87 – 6.84 (m, 2H), 6.83 – 6.80 (m, 2H), 4.95 (s, 2H), 3.82 (s, 3H), 3.80 (s, 3H); ^{13}C NMR (151 MHz, CDCl_3) δ 162.7, 159.7, 159.3, 155.5, 134.8, 131.0, 130.6, 130.1, 129.3, 129.2,

128.5, 128.1, 127.9, 127.5, 127.4, 127.2, 120.8, 114.5, 114.4, 114.1, 69.9, 55.6, 55.4; ESI MS: m/z calc. for $C_{29}H_{24}N_2O_4^+$: 465.1809, found 465.1794.



2-(4-((3-bromobenzyl)oxy)phenyl)-3-(4-methoxyphenyl)quinazolin-4(3H)-one (3-42): off-white amorphous solid (78% over two steps); ^1H NMR (600 MHz, CDCl_3) δ 8.33 (dd, $J = 8.0, 1.5$ Hz, 1H), 7.86 (d, $J = 2.0$ Hz, 1H), 7.80 (ddd, $J = 8.3, 7.1, 1.5$ Hz, 1H), 7.54 (d, $J = 1.8$ Hz, 1H), 7.52 (ddd, $J = 8.2, 7.1, 1.2$ Hz, 1H), 7.45 (dt, $J = 8.1, 1.6$ Hz, 1H), 7.33 – 7.31 (m, 2H), 7.30 – 7.29 (m, 1H), 7.24 (d, $J = 7.8$ Hz, 1H), 7.07 – 7.05 (m, 2H), 6.86 – 6.84 (m, 2H), 6.81 – 6.79 (m, 2H), 4.99 (s, 2H), 3.80 (s, 3H); ^{13}C NMR (151 MHz, CDCl_3) δ 162.5, 159.4, 155.5, 138.8, 134.9, 131.4, 131.3, 131.1, 130.4, 130.3, 130.1, 127.5, 127.4, 127.3, 126.0, 125.9, 125.3, 122.8, 120.8, 115.0, 114.6, 114.5, 69.1, 55.6; ESI MS: m/z calc. for $C_{28}H_{21}BrN_2O_3^+$: 512.0736, found 513.0800.

3.11 References

- (1) Liu, S., Wang, W., Jiang, L., Wan, S., Zhang, L., Yu, R., and Jiang, T. (2015) 2-Pyridinyl-4(3H)-quinazolinone: a scaffold for anti-influenza A virus compounds. *Chem. Biol. Drug. Des.* 86, 1221–1225.
- (2) Corbett, J. W., Ko, S. S., Rodgers, J. D., Gearhart, L. A., Magnus, N. A., Bacheler, L. T., Diamond, S., Jeffrey, S., Klabe, R. M., Cordova, B. C., Garber, S., Logue, K., Trainor, G. L., Anderson, P. S., and Erickson-Viitanen, S. K. (2000) Inhibition of clinically relevant mutant variants of HIV-1 by quinazolinone non-nucleoside reverse transcriptase

inhibitors. *J. Med. Chem.* *43*, 2019–2030.

(3) Peng, L.-P., Nagarajan, S., Rasheed, S., and Zhou, C.-H. (2015) Synthesis and biological evaluation of a new class of quinazolinone azoles as potential antimicrobial agents and their interactions with calf thymus DNA and human serum albumin. *Med. Chem. Commun.* *6*, 222–229.

(4) Lu, W., Baig, I. A., Sun, H.-J., Cui, C.-J., Guo, R., Jung, I.-P., Wang, D., Dong, M., Yoon, M.-Y., and Wang, J.-G. (2015) Synthesis, crystal structure and biological evaluation of substituted quinazolinone benzoates as novel antituberculosis agents targeting acetohydroxyacid synthase. *Eur. J. Med. Chem.* *94*, 298–305.

(5) Zhang, G.-H., Xue, W.-B., An, Y.-F., Yuan, J.-M., Qin, J.-K., Pan, C.-X., and Su, G.-F. (2015) Distinct novel quinazolinone exhibits selective inhibition in MGC-803 cancer cells by dictating mutant p53 function. *Eur. J. Med. Chem.* *95*, 377–387.

(6) Al-Rashood, S. T., Aboldahab, I. A., Nagi, M. N., Abouzeid, L. A., Abdel-Aziz, A. A. M., Abdel-Hamide, S. G., Youssef, K. M., Al-Obaid, A. M., and El-Subbagh, H. I. (2006) Synthesis, dihydrofolate reductase inhibition, antitumor testing, and molecular modeling study of some new 4(3H)-quinazolinone analogs. *Bioorg. Med. Chem.* *14*, 8608–8621.

(7) Cagir, A., Jones, S.H., Gao, R., Eisenhauer B.M., and Hecht, S. M. (2003) Luotonin A. A naturally occurring human DNA topoisomerase I poison. *J. Am. Chem. Soc.* *125*, 13628–13629.

(8) Coatney, G.R., Cooper, W.C., Culwell, W.B., White, W.C., Imboden, C.A. (1950) Trial of febrifugine, an alkaloid obtained from *Dichroa febrifuga* Lour., against the Chesson strain of *Plasmodium vivax*. *J. Natl. Malar. Soc.* *9*, 183–186.

(9) Keller, T. L., Zocco, D., Sundrud, M. S., Hendrick, M., Edenius, M., Yum, J., Kim, Y.-J., Lee, H.-K., Cortese, J. F., Wirth, D. F., Dignam, J. D., Rao, A., Yeo, C.-Y., Mazitschek, R., and Whitman, M. (2012) Halofuginone and other febrifugine derivatives inhibit prolyl-tRNA synthetase. *Nat. Chem. Biol.* *8*, 311–317.

(10) Onambele, L. A., Riepl, H., Fischer, R., Pradel, G., Prokop, A., and Aminake, M. N. (2015) Synthesis and evaluation of the antiplasmodial activity of tryptanthrin derivatives. *Int. J. Parasitol. Drugs Drug Resist.* *5*, 48–57.

- (11) Peng, J., Lin, T., Wang, W., Xin, Z., Zhu, T., Gu, Q., and Li, D. (2013) Antiviral alkaloids produced by the mangrove-derived fungus *Cladosporium* sp. PJX-41. *J. Nat. Prod.* *76*, 1133–1140.
- (12) Pasqualotto, A. C., Thiele, K. O., and Goldani, L. Z. (2010) Novel triazole antifungal drugs: focus on isavuconazole, ravuconazole and albaconazole. *Curr. Opin. Investig. Drugs* *11*, 165–174.
- (13) Lad, L., Luo, L., Carson, J. D., Wood, K. W., Hartman, J. J., Copeland, R. A., and Sakowicz, R. (2008) Mechanism of inhibition of human KSP by ispinesib. *Biochemistry* *47*, 3576–3585.
- (14) Schenkel, L. B., Olivieri, P. R., Boezio, A. A., Deak, H. L., Emkey, R., Graceffa, R. F., Gunaydin, H., Guzman-Perez, A., Lee, J. H., Teffera, Y., Wang, W., Youngblood, B. D., Yu, V. L., Zhang, M., Gavva, N. R., Lehto, S. G., and Geuns-Meyer, S. (2016) Optimization of a novel quinazolinone-based series of Transient Receptor Potential A1 (TRPA1) antagonists demonstrating potent in vivo activity. *J. Med. Chem.* *59*, 2794–2809.
- (15) Niementowski, Von, S. (1895) Synthesen von chinazolinverbindungen. *Adv. Synth. Catal.* *51*, 564–572.
- (16) Alexandre, F.-R., Berecibar, A., and Besson, T. (2002) Microwave-assisted Niementowski reaction: Back to the roots. *Tetrahedron Lett.* *43*, 3911–3913.
- (17) Li, Z., Dong, J., Chen, X., Li, Q., Zhou, Y., and Yin, S.-F. (2015) Metal- and oxidant-free synthesis of quinazolinones from β -ketoesters with o-aminobenzamides via phosphorous acid-catalyzed cyclocondensation and selective C–C bond cleavage. *J. Org. Chem.* *80*, 9392–9400.
- (18) Huang, D., Li, X., Xu, F., Li, L., and Lin, X. (2013) Highly enantioselective synthesis of dihydroquinazolinones catalyzed by SPINOL-phosphoric acids. *ACS Catal.* *3*, 2244–2247.
- (19) Rostamizadeh, S., Amani, A. M., Aryan, R., Ghaieni, H. R., and Shadjou, N. (2008) Synthesis of new 2-aryl substituted 2,3-dihydroquinazoline-4(1H)-ones under solvent-free conditions, using molecular iodine as a mild and efficient catalyst. *Synth. Commun.* *38*,

3567–3576.

- (20) Shaterian, H. R., and Rigi, F. (2015) An efficient synthesis of quinazoline and xanthene derivatives using starch sulfate as a biodegradable solid acid catalyst. *Res. Chem. Intermed.* *41*, 721–738.
- (21) Kim, N. Y., and Cheon, C.-H. (2014) Synthesis of quinazolinones from anthranilamides and aldehydes via metal-free aerobic oxidation in DMSO. *Tetrahedron Lett.* *55*, 2340–2344.
- (22) Shen, G., Zhou, H., Sui, Y., Liu, Q., and Zou, K. (2016) FeCl₃-catalyzed tandem condensation/intramolecular nucleophilic addition/C–C bond cleavage: a concise synthesis of 2-substituted quinazolinones from 2-aminobenzamides and 1,3-diketones in aqueous media. *Tetrahedron Lett.* *57*, 587–590.
- (23) Zhou, J., and Fang, J. (2011) One-pot synthesis of quinazolinones via iridium-catalyzed hydrogen transfers. *J. Org. Chem.* *76*, 7730–7736.
- (24) Zhang, Z., Wang, M., Zhang, C., Zhang, Z., Lu, J., and Wang, F. (2015) The cascade synthesis of quinazolinones and quinazolines using an α -MnO₂ catalyst and tert-butyl hydroperoxide (TBHP) as an oxidant. *Chem. Commun.* *51*, 9205–9207.
- (25) Cheng, R., Guo, T., Zhang-Negrerie, D., Du, Y., and Zhao, K. (2013) One-pot synthesis of quinazolinones from anthranilamides and aldehydes via p-toluenesulfonic acid catalyzed cyclocondensation and phenyliodine diacetate mediated oxidative dehydrogenation. *Synthesis* *45*, 2998–3006.
- (26) Dabiri, M., Salehi, P., Bahramnejad, M., and Alizadeh, M. (2010) A practical and versatile approach toward a one-pot synthesis of 2,3-disubstituted 4(3H)-quinazolinones. *Monatsch Chem.* *141*, 877–881.
- (27) Khosropour, A. R., Mohammadpoor-Baltork, I., and Ghorbankhani, H. (2006) Bi(TFA)₃-[nbp]FeCl₄: a new, efficient and reusable promoter system for the synthesis of 4(3H)-quinazolinone derivatives. *Tetrahedron Lett.* *47*, 3561–3564.
- (28) Xu, L., Jiang, Y., and Ma, D. (2012) Synthesis of 3-Substituted and 2,3-Disubstituted Quinazolinones via Cu-Catalyzed Aryl Amidation. *Org. Lett.* *14*, 1150–1153.
- (29) Li, H., He, L., Neumann, H., Beller, M., and Wu, X.-F. (2014) Cascade synthesis of

- quinazolinones from 2-aminobenzonitriles and aryl bromides via palladium-catalyzed carbonylation reaction. *Green Chem.* *16*, 1336–1343.
- (30) Zheng, Z., and Alper, H. (2008) Palladium-catalyzed cyclocarbonylation of o-iodoanilines with imidoyl chlorides to produce quinazolin-4(3H)-ones. *Org. Lett.* *10*, 829–832.
- (31) Maiden, T. M. M., and Harrity, J. P. A. (2016) Recent developments in transition metal catalysis for quinazolinone synthesis. *Org. Biomol. Chem.* *14*, 8014–8025.
- (32) Jones-Brando, L., Torrey, E. F., and Yolken, R. (2003) Drugs used in the treatment of schizophrenia and bipolar disorder inhibit the replication of *Toxoplasma gondii*. *Schizophr. Res.* *62*, 237–244.
- (33) Hencken, C. P., Jones-Brando, L., Bordón, C., Stohler, R., Mott, B. T., Yolken, R., Posner, G. H., and Woodard, L. E. (2010) Thiazole, oxadiazole, and carboxamide derivatives of artemisinin are highly selective and potent inhibitors of *Toxoplasma gondii*. *J. Med. Chem.* *53*, 3594–3601.
- (34) Chimenti, F., Bizzarri, B., Bolasco, A., Secci, D., Chimenti, P., Carradori, S., Granese, A., Rivanera, D., Frishberg, N., Bordon, C., and Jones-Brando, L. (2009) Synthesis and evaluation of 4-acyl-2-thiazolyhydrazone derivatives for anti-Toxoplasma efficacy in vitro. *J. Med. Chem.* *52*, 4574–4577.
- (35) Gilham, D., Wasiak, S., Tsujikawa, L. M., Halliday, C., Norek, K., Patel, R. G., Kulikowski, E., Johansson, J., Sweeney, M., and Wong, N. C. W. (2016) RVX-208, a BET-inhibitor for treating atherosclerotic cardiovascular disease, raises ApoA-I/HDL and represses pathways that contribute to cardiovascular disease. *Atherosclerosis* *247*, 48–57.
- (36) Bloom, D. C., Giordani, N. V., and Kwiatkowski, D. L. (2010) Epigenetic regulation of latent HSV-1 gene expression. *Biochim. Biophys. Acta* *1799*, 246–256.
- (37) Coleman, H. M., Connor, V., Cheng, Z. S. C., Grey, F., Preston, C. M., and Efstathiou, S. (2008) Histone modifications associated with herpes simplex virus type 1 genomes during quiescence and following ICP0-mediated de-repression. *J. Gen. Virol.* *89*, 68–77.
- (38) Danaher, R. J., Jacob, R. J., Steiner, M. R., Allen, W. R., Hill, J. M., and Miller, C.

- S. (2009) Histone deacetylase inhibitors induce reactivation of herpes simplex virus type 1 in a latency-associated transcript-independent manner in neuronal cells. *J. Neurovirol.* *11*, 306-317.
- (39) Du, T., Zhou, G., and Roizman, B. (2013) Modulation of reactivation of latent herpes simplex virus 1 in ganglionic organ cultures by p300/CBP and STAT3. *Proct. Natl. Acad. Sci.* *110*, E2621–8.
- (40) McClain, L., Zhi, Y., Cheng, H., Ghosh, A., Piazza, P., and Yee, M. B. (2015) Broad-spectrum non-nucleoside inhibitors of human herpesviruses. *Antiviral Res.* *121*, 16-23.
- (41) D'Aiuto, L., Williamson, K., Dimitrion, P., and McNulty, J. (2017) Comparison of three cell-based drug screening platforms for HSV-1 infection. *Antiviral Res* *142*, 136–140.

4 Design and synthesis of quinazolinone alkaloids

4.1 Amaryllidaceae alkaloids have potent bioactivity

The Amaryllidaceae, commonly known as amaryllis, are a family of bulbous flowering plants that produces a variety of alkaloid natural products. Beginning in 1877 with the isolation of lycorine from *N. pseudonarcissus*,¹ over 300 alkaloids have been isolated from the Amaryllidaceae family,² These alkaloids can be classified into different families based on their structure. Phenanthridone Amaryllidaceae alkaloids are differentiated from other Amaryllidaceae alkaloids by their common tricyclic core (Figure 4.1) with an amide- containing B ring and a C ring with several hydroxyl substituents. There are several biologically active molecules in this class.

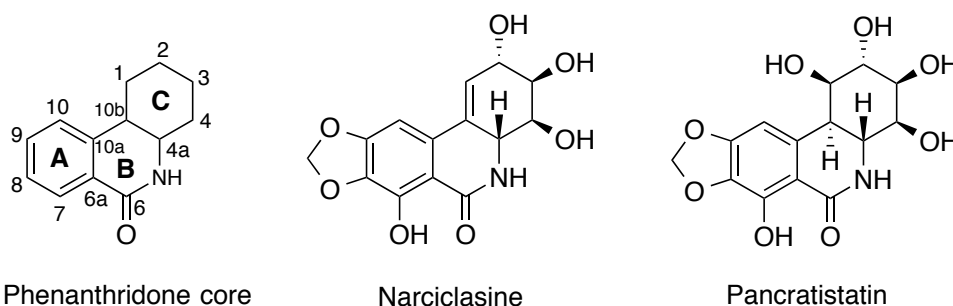


Figure 4.1: Common structure of phenanthridone-type Amaryllidaceae alkaloids. Narciclasine and pancratistatin are members of the phenanthridone alkaloid family that display biological activity.

The most thoroughly studied alkaloids in this family are narciclasine³ and pancratistatin⁴. Both compounds show promising anti-tumour activity in a variety of human cancers. Narciclasine is an inhibitor of protein synthesis, targeting the 60S ribosomal subunit.⁵ Pancratistatin has been shown to selectively induce apoptosis in

cancer cells by targeting cancer cell mitochondria.⁶ A number of closely related analogs also show potent anticancer activity.⁷

Phenanthrindone alkaloids have also been reported to have broad-spectrum antiviral activity. In Japanese encephalitis infected mice, treatment with pancratistatin increased survival rate to 80% from 0% in untreated controls.⁸ Pancratistatin, narciclasine, and related analogs showed significant in vitro inhibitory activity against a panel of flaviviridae and moderate activity against bunyaviridae. SAR analysis of these in vitro assays indicates that oxygenation at the C2, C3, and C4 position is important for antiviral activity, but hydroxyl groups at C1 and C7 can be removed with little loss of function. Some host cell toxicity was observed with this class of alkaloids, though this toxicity was less pronounced in analogs with a cis-fused C-ring than the trans-fused C ring derivatives.

Studies of the antiviral effects of Amaryllidaceae alkaloids outside the phenanthrindone family, particularly lycorine, have also been reported. The activities of such alkaloids against avian influenza virus H5N1,⁹ SARS-associated corona virus,¹⁰ poliovirus,¹¹ and HSV-1¹² are documented in the literature. However, there has been little research into the promising antiviral activity of pancratistatin, narciclasine, and derivatives since the initial report.

In 2015, J. McNulty et al reported the anti-HSV activity of several phenanthrindone alkaloids (Figure 4.2).¹³ The most potent derivative, *trans*-dihydrolycoricidine, reduced viral replication in iPSC neurons more effectively than acyclovir. In addition, *trans*-dihydrolycoricidine prevented reactivation of latent HSV-1

cultures. Few inhibitors of lytic HSV-1 are able to prevent reactivation, so this finding has generated additional interest in the mechanism of action. The McNulty group has also found that phenanthridone alkaloids are potent inhibitors of ZIKV (Figure 4.2).¹⁴ Narciclasine, *trans*-dihydronarciclasine, and pancratistatin had anti-ZIKV activity in nM range. These natural products represent the most potent anti-ZIKV compounds identified in the literature to date. Phenanthridone Amaryllidaceae alkaloids thus represent a promising source of new antiviral lead molecules.

4.2 Phenanthridone quinazolinone hybrids

The promising bioactivity of *trans*-dihydrolycoricidine and other phenanthridone alkaloids calls for further work to further explore the SAR of this scaffold. However, the synthesis of libraries based on the phenanthridone ring system has been limited by the structural complexity of the scaffold. Through *trans*-dihydrolycoricidine is less complex than other phenanthridones, and there a number of synthetic routes to *trans*-dihydrolycoricidine have been reported in the literature, its synthesis is an ongoing challenge. The shortest route to date requires 8 linear steps and, due to the use of a potentially explosive starting reagent, is not easily scalable¹⁵. This makes analog preparation a time- and resource-intensive task.

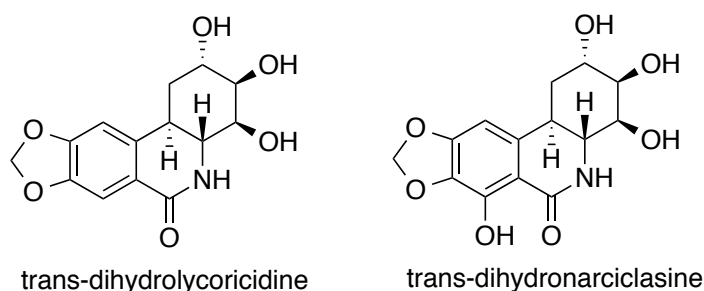


Figure 4.2: Structure of antiviral Amaryllidaceae alkaloids synthesized by the McNulty group

Significant efforts have been made to elucidate the anticancer pharmacophore of alkaloids like pancratistatin, particularly in the Hudlicky group. This work has revealed that A ring substituents are important for activity, and modification of the methylenedioxy group or removal of the 7-OH substitution decrease activity.^{7,16,17} SAR has also been performed on the C ring, revealing that any stereochemical inversion or substitution of the C2, C3, and C4 alcohols is disadvantageous.^{18,19} It has also led to the identification of pancratistatin analogs with lipophilic groups at C1 that are more potent and bioavailable than the natural products.^{20,21,22} It is not known how modification of the B ring may affect anticancer activity. Additionally, the effect that any of these modifications may have on antiviral activity is not well established.

We hypothesize that B-ring aza analogs of trans-dihydrolycoricidine, containing a nitrogen atom at position **10b**, may have antiviral activity similar to the original alkaloids (Figure 4.3). We believe this scaffold may have several advantages over the natural product. Primarily, it should be much easier to prepare these analogs through a convergent route capitalizing on the rapid cyclization of quinazolinones (Figure 4.4). We envisioned that commercially available pentose sugars could be used as a chiral pool starting materials for the synthesis of quinazolinones alkaloid analogs. The strategy is

advantageous because pentose sugars already contain 3 of the 4 stereocentres required for our designed target, thus minimizing the number of asymmetric steps required in our synthesis. We could easily prepare a library of analogs using the convergent route by employing different anthranilamide and pentose substrates.

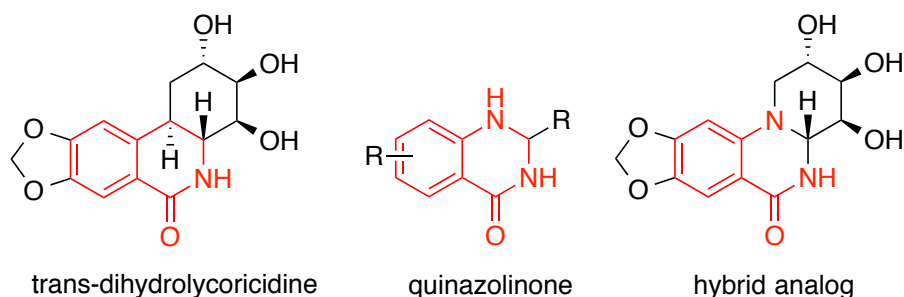


Figure 4.3: Structure of antiviral alkaloid trans-dihydrolycoricidine and a general quinazolinone, with similar core structures highlighted. A hybrid compound containing the quinazolinone core and the A and C-ring functionalization of trans-dihydrolycoricidine is proposed.

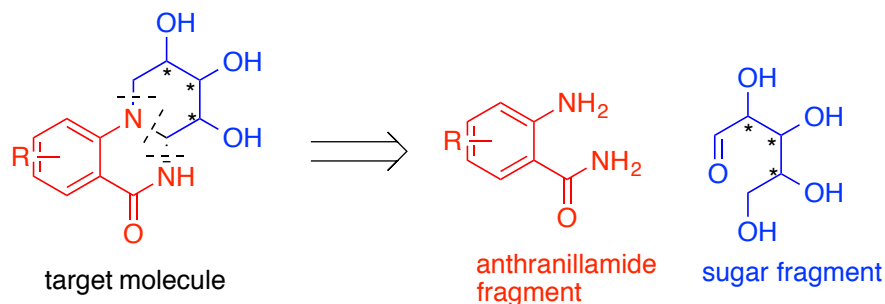


Figure 4.4: Retrosynthetic analysis of target molecule, showing both the pentose sugar and anthranilamide fragments. This convergent route would allow us to prepare a variety of analogs by varying either fragment.

4.3 Synthetic route from D-ribose:

D-ribose can be selectively protected in one step with a methyl glycoside and acetonide using methanol and acetone with an acid catalyst (Figure 4.5). The C5 alcohol

4-1 can then be derivatized in one of several ways to connect the sugar derivative to the anthranillamide component. We initially converted the primary alcohol to iodide **4-2** via an Appel reaction, and attempted to alkylate anthranillamide **4-3**. Even with strong bases (LiHMDS and NaH) and heat, we saw no conversion of starting material, perhaps due to the sterically hindered nature of the sugar iodide. Instead, we oxidized the primary alcohol using Swern conditions to obtain the C5 aldehyde **4-4**. A reductive amination could then be performed with anthranilamide to give **4-5**. After forming one of the key disconnections in our designed retrosynthesis, we could fully deprotect the sugar moiety using mild acid. We were pleased to find that the quinazolinone cyclized immediately upon deprotection, affording **4-6**, which is a C2 epimer of our desired target. **4-6** was obtained as a 9:1 mixture of inseparable diastereomers.

With **4-6** in hand, we envisioned that inversion of the C2 alcohol would provide the desired product. In order to accomplish this inversion, we attempted a selective deprotection of **4-5** to remove the methyl glycoside and afford the 3,4-acetonide protected cyclization product. Our attempts to selectively deprotect the glycoside with LiCl were unsuccessful, producing only unreacted starting material. In the presence of mild acid, only complete deprotection is observed. We therefore decided to amend our synthetic strategy to begin with pentose having the correct stereochemistry.

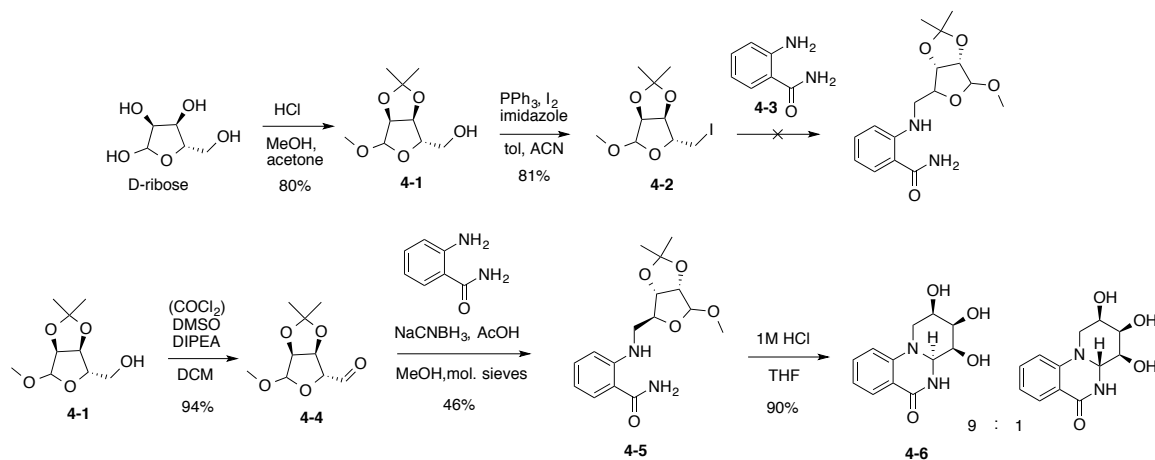


Figure 4.5: Synthesis of quinazolinone alkaloid 4-6 from D-ribose.

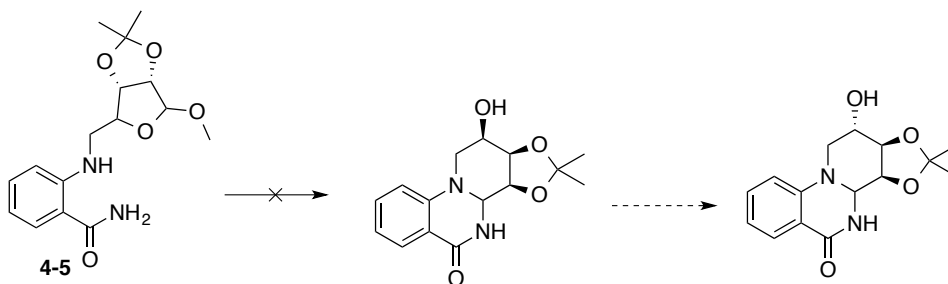


Figure 4.6: Proposed conversion of 4-5 to target molecule through selective deprotection and inversion at C2. Selective deprotection of 5 could not be accomplished, and only product 4-6 was obtained.

4.4 Synthetic route from L-arabinose:

We determined that L-arabinose aligned stereochemically with our desired product if C5 were the central quinazolinone carbon. Due to the anti- geometry of the C2 and C3 alcohols, we were unable to use a similar protection strategy with L-arabinose as we had employed with D-ribose. The initial protection of L-arabinose as the furanoside proved to be difficult, as the pyranoside is thermodynamically favoured. We were able to obtain moderate yields of the methylfuranoside 4-7 by using a cyanuric acid/DMSO system (Figure 4.7). We then differentially protected the remaining alcohols, with a TBS

group on C5 and acetates on C2 and C3 to give **4-8**. The TBS group was then removed with TBAF to afford primary alcohol **4-9**. The primary alcohol was carried on to the aldehyde **4-10** with a Swern oxidation. We anticipated the newly generated aldehyde would cyclize with anthranillamide to form the quinazolinone core. However, stirring **4-10** with anthranillamide and catalytic CSA failed to give the desired product in any significant yield after heating over several days.

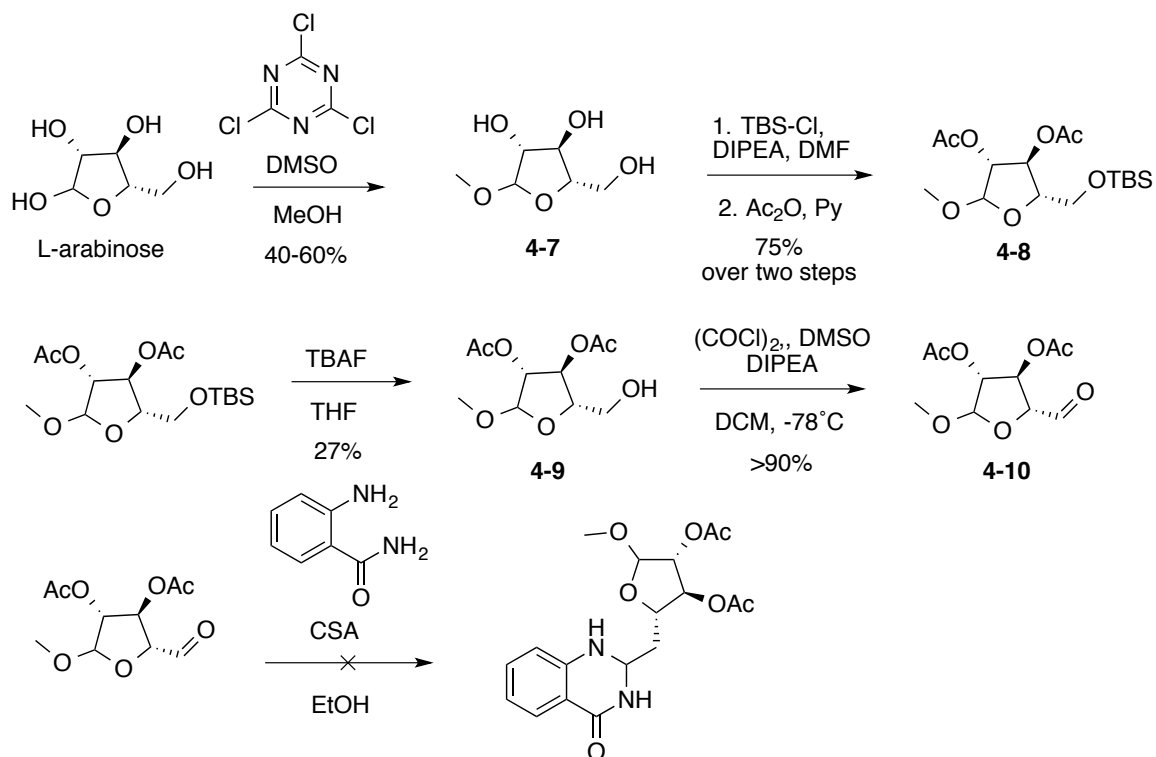


Figure 4.7: Attempts to cyclize aldehyde **4-10**, obtained from L-arabinose over 3 steps, with anthranillamide were unsuccessful.

Instead, we modified our approach to construct the key C-N bond with a reductive amination as the first step of the synthesis. This reductive amination requires forcing conditions, with excess L-arabinose and NaCNBH₃, as well as reflux over several days, but we were able to achieve a good yield of the desired product **4-11** (Figure 4.8). We

then attempted to selectively protect the primary alcohol with TBS-Cl/imidazole or DMT-Cl/DIPEA, but in both cases we observed no reaction with **4-11**. This may be due to hydrogen bonding between the primary alcohol, amine, and amide that renders that alcohol more sterically hindered and less reactive than expected. We found that this alcohol could react with smaller electrophiles, such as Ac₂O or TES-Cl.

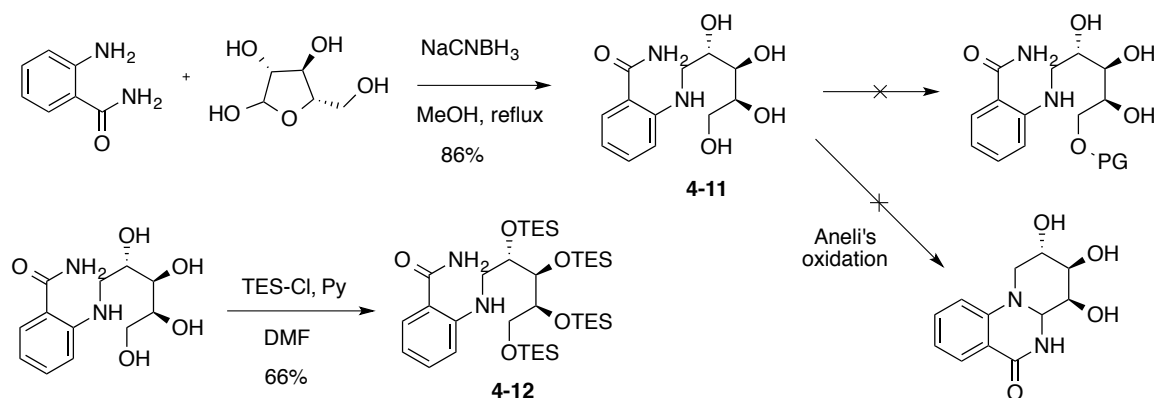


Figure 4.8: L-arabinose and anthranillamide undergo a reductive amination to give **4-11**, which was then completely protected with TES-Cl. Swern oxidation to directly remove the primary TBS and oxidize gave an undesired product.

We envisioned that TES-Cl could be used to protect all four alcohols, yielding **4-12**. The primary TES group could then be removed under Swern conditions to directly afford the aldehyde, which we hoped would cyclize to give the quinazolinone product (Figure 4.9). Instead, we found that the Swern oxidation generated nitrile **4-13**, and a milder cleavage/oxidation step would be required. We also attempted this transformation using CrO₃•Py and PCC as oxidants, but in both cases observed no conversion of starting material. Instead of performing the deprotection and oxidation simultaneously, we attempted to cleave the primary TES group using PPTS, anticipating that we could oxidize the resulting primary alcohol using a mild oxidant like DMP. Unfortunately, we

found that the C2 OTES group is more labile than the primary OTES, and thus the desired primary alcohol could not be produced selectively.

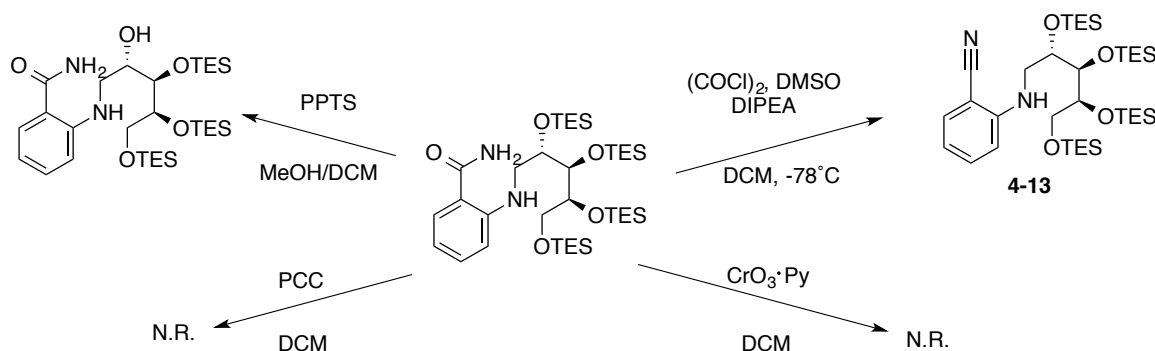


Figure 4.9: Selective deprotection of the primary TES group could not be accomplished either through a direct oxidation or a two-step hydrolysis and oxidation procedure.

Given the difficulties we had encountered with selective deprotection of the primary alcohol, we returned to our initial plan to differentially protect the sugar alcohols. Since protection of the primary alcohol **4-11** was not feasible after reductive amination, we opted to protect this group before performing the reductive amination (Figure 4.10). The C5 hydroxyl of L-arabinose was selectively protected using TBS-Cl in pyridine to give **4-14**. Due to the hydrophilicity of this compound, we opted not to isolate **4-14**, and instead performed the reductive amination directly in the same pot. The reductive amination, which was faster and milder than the reductive amination of the unprotected sugar, afforded us product **4-15**. Our attempts to isolate **4-15** through silica gel chromatography proved unsuccessful, as a small amount of a sugar impurity persistently coeluted and could not be removed. To avoid this problem, we carried forward crude **4-15**, purified only by an aqueous organic workup, and protected the remaining alcohols as acetates using Ac₂O and DIPEA in DCM. This reaction proceeded cleanly to give **4-16** in a 64% yield over 3 steps.

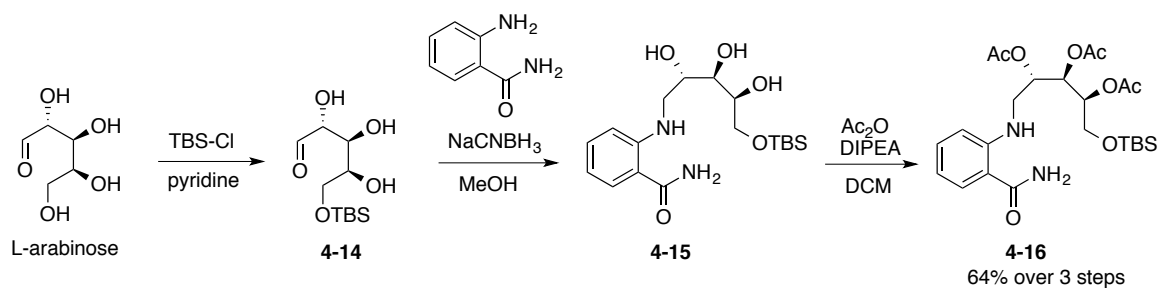


Figure 4.10: L-arabinose is protected at the C5 alcohol with TBS-Cl, then coupled to anthranilamide in a reductive amidation. The resulting product is protected as a triacetate to give **4-16** in 64% yield over 3 steps.

We then attempted a TBAF-mediated deprotection of the TBS group to give primary alcohol **4-17**. While the desired product was obtained from this reaction, we also observed some acyl migration from the three acetate groups resulting in a complex mixture of products. Under acidic conditions, using HF•Py in THF, we observed no acyl transfer in the time periods required for deprotection. With the primary alcohol in hand, tried a number of different conditions to afford our desired aldehyde. Under Parikh-Dohring conditions, no conversion of starting material was observed. Reaction of **4-18** with DMP caused rapid decomposition of the starting material. Oxidation with IBX in DMSO at 60°C was found to cleanly produce the desired product as a 2:1 mixture of separable diastereomers, **4-18** and **4-19**. Hydrolysis of each diastereomer with K₂CO₃ in MeOH afforded the desired triols **4-20** and **4-21**.

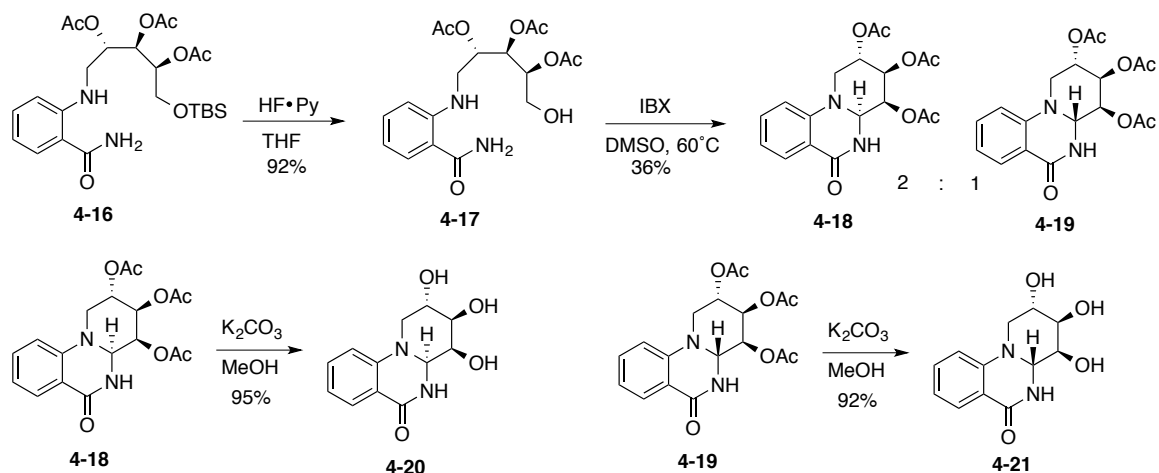


Figure 4.11: Deprotection, oxidation, and ring closure to form quinazolinone core

This synthetic route was repeated with 3,4-methylenedioxyanthranilamide to produce **4-26** and **4-27** as analogs of trans-dihydrolycoricidine (Figure 4.12). These analogs were then tested as described previously for anti-HSV-1 activity.

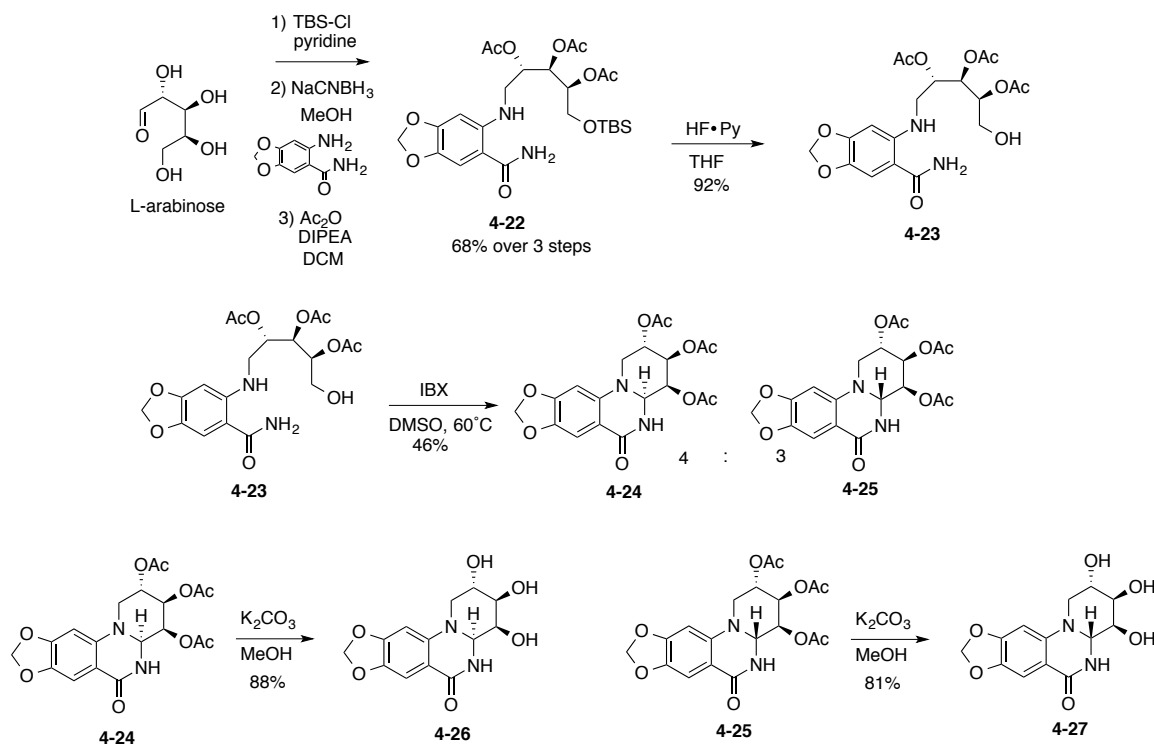


Figure 4.12: Synthesis of 4-26 and 4-27 from L-arabinose and 3,4-methylenedioxyantranilamide

4.5 Biological activity of quinazolinone alkaloids

In an assay measuring inhibition of HSV-1 viral replication in neurons²³, **4-20**, **4-21**, and **4-26** were found to have no activity against HSV-1. After 1 day, treatment with **4-27** qualitatively appeared to inhibit viral replication. However, by day 2, when flow cytometry is performed to quantify viral gene expression, viral replication had reoccurred (Figure 4.13). This may indicate that these quinazolinone analogs are unstable to the assay conditions. No degradation was observed when compounds were dissolved in an aqueous DMSO solution for several weeks, so we hypothesized that the decomposition of these compounds may be biologically mediated. Since these quinazolinone contain a tertiary amine, they may be susceptible to metabolism by the monoamine oxygenases that are produced by neuronal cells.²⁴ To probe this hypothesis, these assays were repeated

using HSV-1 infected Vero cells, a line of monkey kidney cells that do not express monoamine oxygenases. Additionally, a portion of the cells treated with **4-27** were dosed again at 24 h to further eliminate the possibility of degradation. Again, none of the quinazolinone alkaloids showed inhibitory activity toward HSV-1 as was observed with *trans*-dihydrolycoricidine (R430).

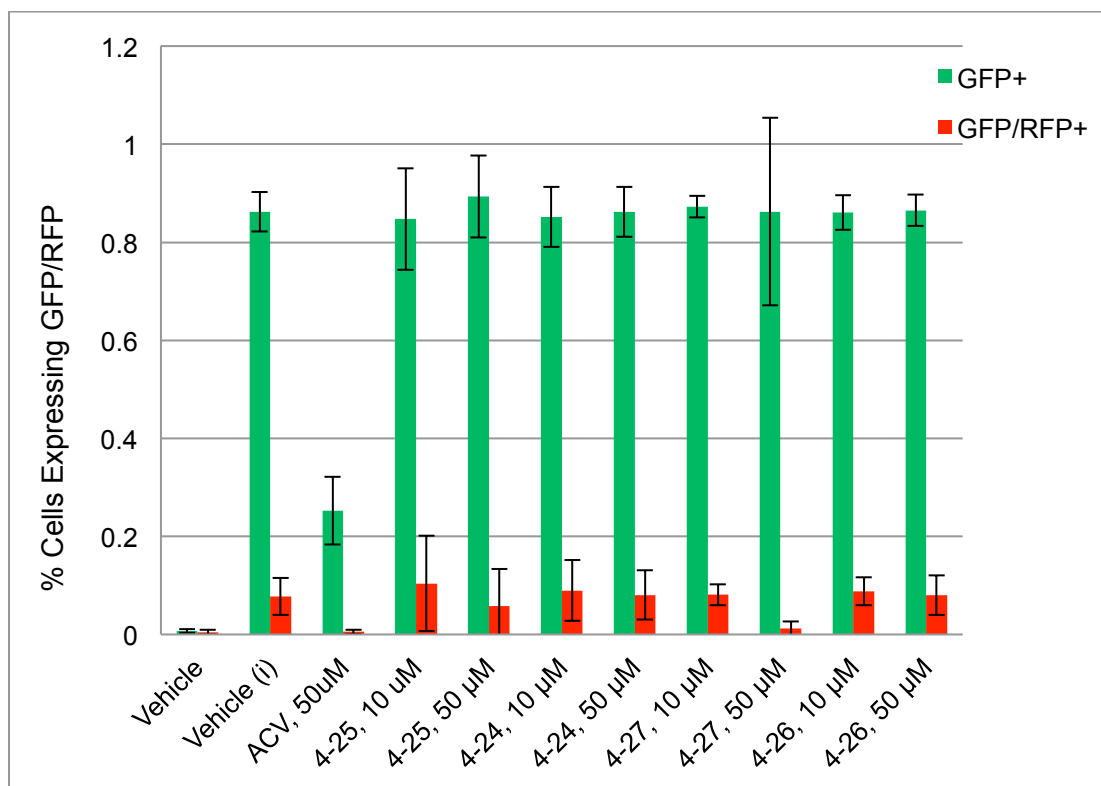


Figure 4.13: Anti-HSV-1 activity of quinazolinone alkaloids in neurons.

quinazolinones,²⁵ while a CACO-2 monolayer assay could be used to assess the potential for active transport.²⁶ Alternatively, the presence of a N atom at the **10b** position may slightly alter the conformation of the C-ring and disrupt the binding of the molecule to the biological target. In this case, charged N atom, such as an HBr salt or N-methylated derivative, at the **10b** position will have a more sp³ character than the tertiary amine and may be a sterically better mimic of *trans*-dihydrolycoricidine.

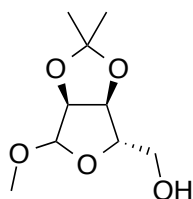
4.6 Conclusion and future work

In conclusion, we have developed a 5-step, convergent route to quinazolinone phenanthrandone hybrid molecules. The use of pentoses as chiral pool reagents allows us to set three stereocentres by choice of starting material, and minimizes the number of asymmetric reactions needed to produce a structurally complex core. This route allows us to easily incorporate a variety of anthranilamide or pentose derivatives in order to probe the pharmacophore involved in antiviral activity of narciclasine-type alkaloids.

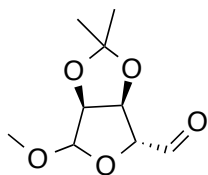
We found that our B-ring modified Amaryllidaceae analogs, containing a nitrogen atom at **10b** to make a quinazolinone core, had no activity against HSV-1. Although there are several reports in the literature describing the pharmacophore of pancratistatin, narciclasine, and related analogs, there are few reports of B-ring modified derivatives. Our work demonstrates that substitution of the **10b** carbon with nitrogen is not tolerated, and the B-ring is thus a key part of the pharmacophore for HSV-1 inhibition. However, the pharmacophore for these molecules does appear to differ for antiviral and anticancer activity. We are also exploring the anticancer and anti-flavivirus activity of these

compounds to elucidate what modifications to the C-ring are tolerated in each of these pharmacophores.

4.7 Experimental

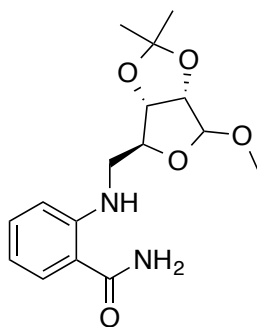


((3aS,4S,6aS)-6-methoxy-2,2-dimethyltetrahydrofuro[3,4-d][1,3]dioxol-4-yl)methanol (4-1): D-ribose (2.0 mmol, 300 mg) was dissolved in a 1:1 mixture of reagent grade methanol and acetone (6.6 mL, 0.3 mM) to which was added 12.1 M HCl (0.20 mmol, 10 μ L, 0.1 eq). The reaction was stirred at room temperature for 2 h. Distilled water (15 mL) was added, and the reaction mixture was extracted with dichloromethane (3 x 15 mL). The combined organic fractions were dried under reduced pressure. The product was obtained as clear, colourless oil in 74% yield and required no further purification; ^1H NMR (600 MHz, Chloroform-*d*) δ 4.85 (s, 1H), 4.69 (d, $J = 5.9$ Hz, 1H), 4.47 (d, $J = 5.9$ Hz, 1H), 4.27 (s, 1H), 3.53 (d, $J = 3.3$ Hz, 1H), 3.50 (d, $J = 3.9$ Hz, 1H), 3.30 (s, 3H), 1.36 (s, 3H), 1.20 (s, 3H); ^{13}C NMR (151 MHz, CDCl_3) δ 111.99, 109.72, 88.06, 85.59, 81.41, 63.76, 55.22, 26.25, 24.62. ESI HRMS calculated for $\text{C}_9\text{H}_{16}\text{O}_5\text{Na}$ $[\text{M}+\text{Na}]^+$: 227.0893, found 227.0895.



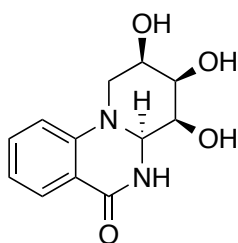
(3aS,4R,6aS)-6-methoxy-2,2-dimethyltetrahydrofuro[3,4-d][1,3]dioxole-4-carbaldehyde (4-4): Oxalyl chloride (0.81 mmol, 69 μ L, 1.1 eq) was dissolved in dry DCM (1.0 mL) and cooled to -78°C . A solution of dimethylsulfoxide (3.67 mmol, 260 μ L, 5.0 eq) in dry DCM (150 μ L) was added. After stirring for 15 minutes, a solution of

2-1 (0.73 mmol, 150 mg, 1.0 eq) in dry DCM (200 μ L, 3.5 mM) was added dropwise. This solution was stirred at -78°C for 30 minutes, then dry DIPEA (3.67 mmol, 640 μ L, 5.0 eq) was added dropwise. The reaction was allowed to warm to room temperature and monitored by TLC. After 2 h, the reaction was quenched by the addition of distilled H_2O and extracted with dichloromethane. The combined organic fractions were dried under reduced pressure to afford the crude product as a yellow oil in 94% yield. The identity of the product was verified by ^1H NMR, however the crude product could not be purified by silica gel chromatography due to significant degradation and was carried forward to be purified after the next reaction.

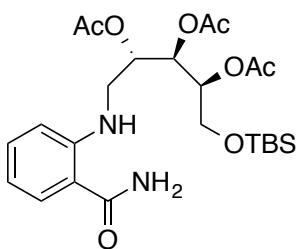


2-((((3aS,4S,6aS)-6-methoxy-2,2-dimethyltetrahydrofuro[3,4-d][1,3]dioxol-4-yl)methyl)amino)benzamide (4-5): Compound 4-4 (113 mg, 0.56 mmols, 1 eq.) was dissolved in dry DCM (5 mL, 0.11 M) to which was added anthranilamide (76 mg, 0.56 mmols, 1 eq.). The reaction mixture was warmed to 30°C before the addition of sodium triacetoxyborohydride (178 mg, 0.84 mmols, 1.5 eq.) and glacial acetic acid (0.05 mL, 0.8 mmols, 1.5 eq.). The reaction was heated at 40°C for 16 h. This mixture was then concentrated under vacuum and directly purified by silica gel chromatography (90:10 hexane:EtOAc \rightarrow 50:50 hexane:EtOAc) to afford **5** as a colourless oil in 80% yield. ^1H NMR (600 MHz, Chloroform-*d*) δ 7.39 (dd, $J = 7.8, 1.5$ Hz, 1H), 7.32 (t, $J = 1.5$ Hz, 1H), 6.72 (d, $J = 8.4$ Hz, 1H), 6.61 (d, $J = 8.0$ Hz, 1H), 5.78 (s, 2H), 5.01 (s, 1H), 4.68 (d, $J = 6.0$ Hz, 1H), 4.64 (d, $J = 5.9$ Hz, 1H), 4.42 (t, $J = 7.6$ Hz, 1H), 3.37 (s, 3H), 3.34 (dd, $J = 13.2, 7.2$ Hz, 1H), 3.29 (dd, $J = 13.1, 7.9$ Hz, 1H), 1.47 (s, 3H), 1.31 (s, 3H); ^{13}C NMR (151 MHz, CDCl_3) δ 172.24, 149.89, 133.71, 128.56, 115.11, 113.65, 112.59, 111.87,

109.73, 85.53, 84.77, 82.79, 55.27, 46.25, 26.57, 25.15. ESI HRMS calculated for $C_{16}H_{22}N_2O_5$ $[M+H]^+$: 322.1529, found 322.1536.

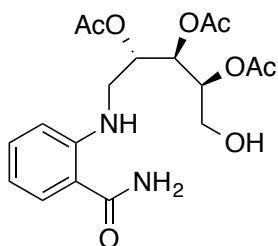


(2R,3R,4S,4aS)-2,3,4-trihydroxy-1,2,3,4,4a,5-hexahydro-6H-pyrido[1,2-a]quinazolin-6-one (4-6): 1H NMR (600 MHz, Methanol- d_4) δ 7.81 (dd, $J = 7.7, 1.7$ Hz, 1H), 7.41 (ddd, $J = 8.7, 7.2, 1.8$ Hz, 1H), 7.03 (d, $J = 8.5$ Hz, 1H), 6.84 (t, $J = 7.5$ Hz, 1H), 4.68 (d, $J = 1.9$ Hz, 1H), 4.15 – 4.09 (m, 2H), 3.92 (dt, $J = 3.3, 1.6$ Hz, 1H), 3.68 – 3.67 (m, 1H), 2.90 (dd, $J = 13.1, 1.4$ Hz, 1H).



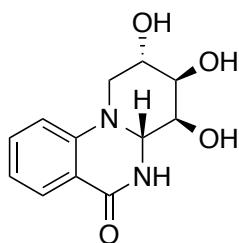
(2S,3R,4S)-1-((tert-butyldimethylsilyl)oxy)-5-((2-carbamoylphenyl)amino)pentane-2,3,4-triyl triacetate (4-16): A round bottom flask was charged with L-arabinose (150 mg, 1.0 mmol, 1 eq) and pyridine (1.20 mL, 15 mmol, 15 eq). To this suspension, *t*-butyldimethylsilylchloride (163 mg, 1.05 mmol, 1.05 eq) was added in portions. This reaction mixture was stirred at room temperature for 2h, then concentrated to a total volume of 0.5 mL to afford protected sugar **4-14**. A solution of anthranilamide (130 mg, 0.95 mmol, 0.95 eq) in dry methanol (1.0 mL) was added to the flask. After 10 minutes, $NaCNBH_3$ (120 mg, 1.91 mmol, 1.9 eq) was added. Upon completion of the reaction as

determined by TLC (typically 5-10 minutes), water was added to quench the reaction mixture. This aqueous solution was extracted with dichloromethane (3 x 15 mL). The combined organic phase was dried over sodium sulphate and concentrated to dryness under reduced pressure to afford the crude product **4-15**, which contained an inseparable sugar impurity. In a round bottom flask, crude **4-15** was dissolved in dry dichloromethane (3.3 mL) to which was added diisopropylethylamine (1.7 mL, 9.9 mmol, 10 eq), acetic anhydride (566 μ L, 6.0 mmol, 6 eq), and N,N-dimethylaminopyridine (6.0 mg, 0.05 mmol, 0.05 eq). This reaction mixture was stirred for 3h at room temperature, then quenched by the addition of water. This aqueous solution was extracted with dichloromethane (3 x 15 mL). The combined organic phase was dried over sodium sulphate and concentrated to dryness under reduced pressure. This material was then purified by chromatography (80:20 hexane:EtOAc \rightarrow 30:70 hexane:EtOAc) to afford **4-16** as a yellow oil in 64% yield over three steps. ^1H NMR (600 MHz, Chloroform-*d*) δ 7.44 (dd, $J = 7.9, 1.5$ Hz, 1H), 7.36 (ddd, $J = 8.6, 7.2, 1.6$ Hz, 1H), 6.93 (d, $J = 8.4$ Hz, 1H), 6.70 (t, $J = 7.5$ Hz, 1H), 5.43 (dd, $J = 8.4, 2.4$ Hz, 1H), 5.38 (ddd, $J = 8.1, 5.8, 2.4$ Hz, 1H), 5.07 (ddd, $J = 8.3, 5.0, 3.2$ Hz, 1H), 3.73 (dd, $J = 11.5, 3.2$ Hz, 1H), 3.66 (dd, $J = 11.5, 5.0$ Hz, 1H), 3.39 – 3.31 (m, 2H), 2.13 (s, 3H), 2.09 (s, 3H), 2.01 (s, 3H), 0.85 (s, 9H), 0.01 (s, 3H), -0.00 (s, 3H); ^{13}C NMR (151 MHz, CDCl_3) δ 171.54, 170.75, 170.16, 170.02, 134.70, 133.81, 128.56, 116.96, 113.51, 108.00, 71.01, 69.66, 68.76, 61.82, 60.55, 44.35, 25.85, 21.10, 20.96, 20.89, 18.33, -5.42. ESI HRMS calculated for $\text{C}_{24}\text{H}_{38}\text{N}_2\text{O}_8\text{Si}$ $[\text{M}+\text{H}]^+$: 511.2470, found 511.2470.

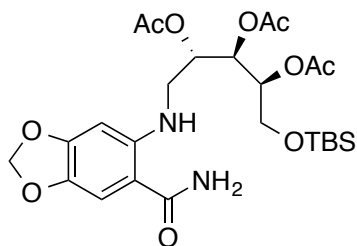


(2S,3R,4S)-1-((2-carbamoylphenyl)amino)-5-hydroxypentane-2,3,4-triyl triacetate (4-17): **4-16** (107 mg, 0.20 mmol, 1.0 eq) was dissolved in dry THF (3.2 mL) to which

12.7, 10.6 Hz, 1H); ^{13}C NMR (151 MHz, MeOD) δ 166.57, 150.30, 135.46, 128.99, 119.25, 117.31, 112.64, 75.47, 73.27, 71.57, 66.80, 49.85.

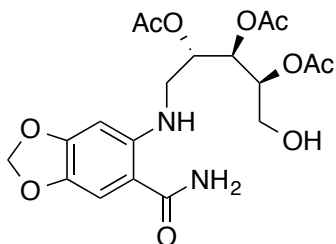


(2S,3R,4S,4aR)-2,3,4-trihydroxy-1,2,3,4,4a,5-hexahydro-6H-pyrido[1,2-a]quinazolin-6-one (4-21): **4-19** (3.5 mg, 0.01 mmol, 1.0 eq) and K_2CO_3 (0.6 mg, 0.005 mmol, 0.5 eq) were dissolved in 3:1 mixture of MeOH:water (100 μL). After 30 minutes, this mixture was purified directly by silica gel chromatography (100:0 DCM:MeOH \rightarrow 80:20 DCM:MeOH) to afford **4-21** as a white, amorphous solid in 92% yield. ^1H NMR (600 MHz, Methanol- d_4) δ 7.81 (dd, $J = 7.7, 1.7$ Hz, 1H), 7.43 (ddd, $J = 8.8, 7.2, 1.7$ Hz, 1H), 6.98 (d, $J = 8.4$ Hz, 1H), 6.89 – 6.85 (m, 1H), 4.59 (d, $J = 9.0$ Hz, 1H), 4.02 – 3.98 (m, 2H), 3.95 (t, $J = 3.5$ Hz, 1H), 3.70 (dd, $J = 13.0, 2.4$ Hz, 1H), 3.13 (dd, $J = 13.0, 2.3$ Hz, 1H); ^{13}C NMR (151 MHz, MeOD) δ 166.49, 151.39, 135.48, 129.12, 119.89, 117.76, 113.87, 71.61, 70.29, 69.77, 68.93, 46.82.

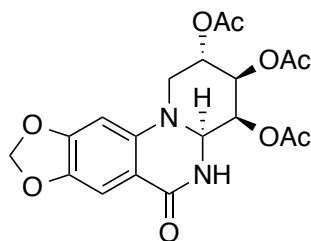


(2S,3R,4S)-1-((tert-butyldimethylsilyloxy)-5-((6-carbamoylbenzo[d][1,3]dioxol-5-yl)amino)pentane-2,3,4-triyl triacetate (4-22): A round bottom flask was charged with L-arabinose (50 mg, 0.35 mmol, 1 eq) and pyridine (400 μL , 15 mmol, 15 eq). To this

suspension, *t*-butyldimethylsilylchloride (54 mg, 0.36 mmol, 1.05 eq) was added in portions. This reaction mixture was stirred at room temperature for 2h, then concentrated to a total volume of 0.5 mL. A solution of 3,4-methylenedioxyanthranilamide (60 mg, 0.33 mmol, 0.95 eq) in dry methanol (320 μ L) was added to the flask. After 10 minutes, NaCNBH₃ (42 mg, 0.66 mmol, 1.9 eq) was added. Upon completion of the reaction as determined by TLC (typically 2-5 minutes), water was added to quench the reaction mixture. This aqueous solution was extracted with dichloromethane (3 x 5 mL). The combined organic phase was dried over sodium sulphate and concentrated to dryness under reduced pressure. This mixture was dissolved in dry dichloromethane (1.0 mL) to which was added diisopropylethylamine (575 μ L, 3.3 mmol, 10 eq), acetic anhydride (187 μ L, 1.98 mmol, 6 eq), and *N,N*-dimethylaminopyridine (2.0 mg, 0.016 mmol, 0.05 eq). This reaction mixture was stirred for 3h at room temperature, then quenched by the addition of water. This aqueous solution was extracted with dichloromethane (3 x 15 mL). The combined organic phase was dried over sodium sulphate and concentrated to dryness under reduced pressure. This material was then purified by chromatography (80:20 hexane:EtOAc \rightarrow 30:70 hexane:EtOAc) to afford **4-22** as a yellow oil in 68% yield over three steps. ¹H NMR (600 MHz, Chloroform-*d*) δ 6.85 (s, 1H), 6.42 (s, 1H), 5.90 (s, 2H), 5.58 (s, 2H), 5.42 (dd, *J* = 8.4, 2.4 Hz, 1H), 5.33 (ddd, *J* = 7.7, 5.5, 2.4 Hz, 1H), 5.07 (ddd, *J* = 8.4, 5.0, 3.3 Hz, 1H), 3.73 (dd, *J* = 11.5, 3.2 Hz, 1H), 3.66 (dd, *J* = 11.4, 5.0 Hz, 1H), 3.33 (dd, *J* = 15.4, 5.9 Hz, 1H), 3.25 (dd, *J* = 14.5, 7.2 Hz, 1H), 2.13 (s, 3H), 2.08 (s, 3H), 2.02 (s, 3H), 0.86 (s, 9H), 0.02 (s, 3H), 0.01 (s, 3H); ¹³C NMR (151 MHz, CDCl₃) δ 171.44, 170.59, 170.15, 169.99, 152.60, 147.91, 138.51, 107.12, 105.24, 101.43, 93.95, 71.08, 69.70, 68.89, 61.80, 44.26, 25.86, 21.13, 20.92, 20.89, 18.33, -5.41. ESI HRMS calculated for C₂₅H₃₈N₂O₁₀Si [M+H]⁺: 555.2368, found 555.2366.

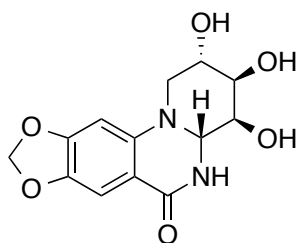


(2S,3R,4S)-1-((6-carbamoylbenzo[d][1,3]dioxol-5-yl)amino)-5-hydroxypentane-2,3,4-triyl triacetate (4-23): 4-22 (95 mg, 0.17 mmol, 1.0 eq) was dissolved in dry THF (2.7 mL) to which was added HF•pyridine (233 μ L). This reaction mixture was stirred for 20-30 minutes at room temperature and closely monitored by TLC to avoid rearrangement of acetate protecting groups. When the reaction was complete (typically 15-25 minutes), it was quenched by the addition of solid NaHCO₃. After 15 minutes, water and dichloromethane were added to form an aqueous-organic partition. The aqueous was extracted exhaustively with dichloromethane, then the combined organic phases were dried with sodium sulphate and concentrated to dryness. This afforded 4-23 as a pale yellow oil in 95% yield. No further purification was performed.



(2S,3R,4S,4aS)-6-oxo-2,3,4,4a,5,6-hexahydro-1H-[1,3]dioxolo[4,5-g]pyrido[1,2-a]quinazoline-2,3,4-triyl triacetate (4-24): 2-iodoxybenzoic acid (54 mg, 0.20 mmol, 1.2 eq, prepared according to *J. Org. Chem.*, 1999, 64 (12), pp 4537–4538) was dissolved in reagent grade DMSO (500 μ L) and heated to 60 °C for 30 minutes. A solution of 4-23 (72 mg, 0.16 mmol, 1.0 eq) in DMSO (200 μ L) was then added. This reaction mixture was stirred for 15 minutes at 60 °C, then purified directly by silica gel chromatography (100:0 Et₂O:EtOAc \rightarrow 90:10 Et₂O:EtOAc) to afford 4-24 and 4-25 as a 4:3 mixture of diastereomers in 45% yield. 4-24 was obtained as a clear, colourless oil. ¹H NMR (600 MHz, Chloroform-*d*) δ 7.38 (s, 1H), 6.48 (s, 1H), 6.20 (s, 1H), 5.97 (d, *J* = 1.9 Hz, 2H),

After 30 minutes, this mixture was purified directly by silica gel chromatography (100:0 DCM:MeOH \rightarrow 80:20 DCM:MeOH) to afford **4-26** as a white, amorphous solid in 88% yield; ^1H NMR (600 MHz, Methanol- d_4) δ 7.20 (s, 1H), 6.55 (s, 1H), 5.94 (d, J = 1.2 Hz, 2H), 4.55 (d, J = 1.9 Hz, 1H), 3.95 – 3.91 (m, 2H), 3.82 (dd, J = 12.4, 5.1 Hz, 1H), 3.43 – 3.41 (m, 1H), 2.49 (dd, J = 12.4, 10.4 Hz, 1H); ^{13}C NMR (151 MHz, MeOD) δ 154.65, 148.18, 142.19, 129.60, 128.88, 107.69, 102.96, 95.32, 75.14, 72.39, 71.74, 67.08, 50.65. ESI HRMS calculated for $\text{C}_{13}\text{H}_{14}\text{N}_2\text{O}_6$ $[\text{M}+\text{H}]^+$: 295.0925, found 295.0917.



(2S,3R,4S,4aR)-2,3,4-trihydroxy-1,2,3,4,4a,5-hexahydro-6H-[1,3]dioxolo[4,5-g]pyrido[1,2-a]quinazolin-6-one (4-27): **4-25** (4.7 mg, 0.011 mmol, 1.0 eq) and K_2CO_3 (0.8 mg, 0.006 mmol, 0.5 eq) were dissolved in 3:1 mixture of MeOH:water (130 μL). After 30 minutes, this mixture was purified directly by silica gel chromatography (100:0 DCM:MeOH \rightarrow 80:20 DCM:MeOH) to afford **4-27** as a white, amorphous solid in 81% yield. ^1H NMR (600 MHz, Methanol- d_4) δ 7.24 (s, 1H), 6.63 (s, 1H), 5.97 (s, 2H), 4.53 (d, J = 8.8 Hz, 1H), 4.03 – 3.99 (m, 2H), 3.94 (t, J = 3.6 Hz, 1H), 3.58 (dd, J = 12.9, 2.6 Hz, 1H), 3.13 (dd, J = 12.9, 2.3 Hz, 1H); ^{13}C NMR (151 MHz, CDCl_3) δ 172.42, 161.63, 156.86, 141.98, 115.76, 110.87, 104.49, 79.50, 77.63, 77.21, 55.91, 49.53. ESI HRMS calculated for $\text{C}_{13}\text{H}_{14}\text{N}_2\text{O}_6$ $[\text{M}+\text{H}]^+$: 295.0925, found 295.0917.

4.8 References

- (1) Gerrard, A. W. (1877) The proximate principles of the *Narcissus pseudonarcissus*. *Pharm. J.* 8, 214–215.
- (2) Jin, D. Z., and Xu, X.-H. (2013) Amaryllidaceae alkaloids, in *Natural Products*, pp

479–522. Springer Berlin Heidelberg, Berlin, Heidelberg.

- (3) Piozzi, F., Fuganti, C., Mondelli, R., and Ceriotti, G. (1968) Narciclasine and narciprimine. *Tetrahedron* 24, 1119–1131.
- (4) Pettit, G. R., Gaddamidi, V., Cragg, G. M., Herald, D. L., and Sagawa, Y. (1984) Isolation and structure of pancratistatin. *Chem. Commun.* 24, 1693–1694.
- (5) Fürst, R. (2016) Narciclasine – An amaryllidaceae alkaloid with potent antitumor and anti-inflammatory properties. *Planta Medica* 82, 1389–1394.
- (6) Griffin, C., Karnik, A., McNulty, J., and Pandey, S. (2011) Pancratistatin selectively targets cancer cell mitochondria and reduces growth of human colon tumor xenografts. *Mol. Cancer. Ther.* 10, 57–68.
- (7) Pettit, G. R., Pettit, G. R., III, and Backhaus, R. A. (1993) Antineoplastic agents, 256. Cell growth inhibitory isocarbostryls from *Hymenocallis*. *J. Nat. Prod.* 56, 1682–1687.
- (8) Gabrielsen, B., Monath, T. P., Huggins, J. W., Kefauver, D. F., Pettit, G. R., Groszek, G., Hollingshead, M., Kirsi, J. J., Shannon, W. M., Schubert, E. M., DaRe, J., Ugarkar, B., Ussery, M. A., and Phelan, M. J. (1992) Antiviral (RNA) activity of selected Amaryllidaceae isoquinoline constituents and synthesis of related substances. *J. Nat. Prod.* 55, 1569–1581.
- (9) He, J., Qi, W. B., Wang, L., Tian, J., Jiao, P. R., Liu, G. Q., Ye, W. C., and Liao, M. (2013) Amaryllidaceae alkaloids inhibit nuclear-to-cytoplasmic export of ribonucleoprotein (RNP) complex of highly pathogenic avian influenza virus H5N1. *Influenza Other Respir. Viruses* 7, 922–931.
- (10) Li, S., Chen, C., Zhang, H., Guo, H., Wang, H., Wang, L., Zhang, X., Hua, S., Yu, J., and Xiao, P. (2005) Identification of natural compounds with antiviral activities against SARS-associated coronavirus. *Antiviral Res.* 67, 18–23.
- (11) Hwang, Y., Chu, J., Yang, P., Chen, W., and Yates, M. (2008) Rapid identification of inhibitors that interfere with poliovirus replication using a cell-based assay. *Antiviral Res.* 77, 232–236.
- (12) Renard-Nozaki, J., Kim, T., Imakura, Y., Kihara, M., and Kobayashi, S. (1989) Effect of alkaloids isolated from Amaryllidaceae on Herpes simplex virus. *Res. Virol.*

140, 115–128.

- (13) McNulty, J., D'Aiuto, L., Zhi, Y., McClain, L., Zepeda-Velázquez, C., Ler, S., Jenkins, H. A., Yee, M. B., Piazza, P., Yolken, R. H., Kinchington, P. R., and Nimgaonkar, V. L. (2016) iPSC neuronal assay identifies Amaryllidaceae pharmacophore with multiple effects against herpesvirus infections. *ACS Med. Chem. Lett.* *7*, 46–50.
- (14) Revu, O., Zepeda-Velázquez, C., Nielsen, A. J., McNulty, J., Yolken, R. H., and Jones-Brando, L. (2016) Total synthesis of the natural product (+)-trans-duhydronarciclasine via an asymmetric organocatalytic [3+3]-cycloaddition and discovery of its potent anti-Zika virus (ZIKV) activity. *ChemistrySelect* *1*, 5895–5899.
- (15) McNulty, J., and Velázquez, C. Z. (2014) Enantioselective organocatalytic Michael/aldol sequence: Anticancer natural product (+)-trans-dihydrolycoricidine. *Angew. Chem. Int. Ed.* *53*, 8450–8454.
- (16) Hillebrenner, H. L., Adams, D. R., and Hudlicky, T. (2004) Synthesis and biological activity of some structural modifications of pancratistatin. *Bioorg. Med. Chem. Lett.* *14*, 2911–2915.
- (17) Nieto-García, O., and Alonso, R. (2013) Synthesis and cytotoxicity of (+/-)-7, 9-dideoxy-pancratistatin analogues. *Org. Biomol. Chem.* *11*, 515–522.
- (18) McNulty, J., Larichev, V., and Pandey, S. (2005) A synthesis of 3-deoxydihydrolycoricidine: refinement of a structurally minimum pancratistatin pharmacophore. *Bioorg. Med. Chem. Lett.* *15*, 5315–5318.
- (19) Pettit, G. R., Tan, R., Bao, G.-H., Melody, N., Doubek, D. L., Gao, S., Chapuis, J.-C., and Williams, L. (2012) Antineoplastic agents. 587. Isolation and structure of 3-epipancratistatin from *Narcissus* cv. ice follies. *J. Nat. Prod.* *75*, 771–773.
- (20) Vshyvenko, S., Scattolon, J., and Hudlicky, T. (2011) Synthesis of C-1 homologues of pancratistatin and their preliminary biological evaluation. *Bioorg. Med. Chem. Lett.* *21*, 4750–4752.
- (21) Vshyvenko, S., Scattolon, J., Hudlicky, T., Romero, A. E., Kornienko, A., Ma, D., Tuffley, I., and Pandey, S. (2012) Unnatural C-1 homologues of pancratistatin — Synthesis and promising biological activities. *Can. J. Chem.* *90*, 932–943.

- (22) Ma, D., Pignanelli, C., Tarade, D., Gilbert, T., and Noel, M. (2017) Cancer cell mitochondria targeting by pancratistatin analogs is dependent on functional complex II and III. *Sci. Rep.* 7, 42957.
- (23) D'Aiuto, L., Williamson, K., Dimitrion, P., and McNulty, J. (2017) Comparison of three cell-based drug screening platforms for HSV-1 infection. *Antiviral Res.* 142, 136–140.
- (24) Holschneider, D. P., and Shih, J. C. (2000) Monoamine oxidase: basic and clinical perspectives, in *Neuropsychopharmacology: The Fourth Generation of Progress*. Raven Press, New York.
- (25) Ottaviani, G., Martel, S., and Carrupt, P. A. (2006) Parallel artificial membrane permeability assay: a new membrane for the fast prediction of passive human skin permeability. *J. Med. Chem.* 49, 3948–3954.
- (26) Hubatsch, I., Ragnarsson, E., and Artursson, P. (2007) Determination of drug permeability and prediction of drug absorption in Caco-2 monolayers. *Nat. Protoc.* 2, 2111–2119.

5 Isolation of natural products from *Xylaria polymorpha*

5.1 Natural products are a rich source of antimicrobial drug leads

Even before the development of modern synthesis and drug discovery processes, natural products have been a valuable source of antimicrobials. The majority of newly approved drugs between 1981 and 2014 were natural products, natural-produced derived, or synthetic derivatives of a natural product pharmacophore.¹ For antimicrobials, just 33% of newly approved drugs were of purely synthetic origins. These natural product derived drugs often represent major advances in medicine because they have novel mechanisms of actions and complex structures not typically included in the chemical space of combinatorial chemistry. This is the case with antiparasitic artemisinins, which are derived from *Artemisia annua* sesquiterpene lactones with an uncommon endoperoxide bridge.² This endoperoxide, when activated by heme, reacts covalently with a variety of parasite proteins, inducing cell death through a novel mechanism³. Oseltamivir, a semi-synthetic antiviral produced from shikimic acid, was one of the first approved neuraminidase inhibitors and represents a major advance in the treatment of influenza.⁴ Daptomycin is a cyclic lipopeptide first isolated from *Streptomyces roseosporus* and approved for the treatment of gram-positive infections⁵. It represents the first antibiotic in its class, and its ability to insert into cell walls, aggregate, and depolarize membranes is a novel mechanism of action in the fight against Gram-positive bacteria.⁶

The renewed interest in natural products as a source of leads for drug discovery may be related to the increased structural complexity of natural products compared to combinatorial compound libraries.⁷ High-throughput synthesis can be used to prepare

very large compound libraries, but the molecules in these libraries do not cover large areas of chemical space. Compared to both natural products and approved drugs, combinatorial chemistry libraries tend to be more lipophilic, less oxygen-rich, and more planar, containing both more aromatic rings and fewer chiral centres.⁸ Despite the enthusiasm for high-throughput techniques in recent decades, few drugs have emerged from these combinatorial libraries and screens.^{1,7} The limitations of high-throughput combinatorial methods have prompted a return to exploring natural products in drug discovery.

Based on the past success of natural product derived drugs, as well as their increased structural diversity compared to conventional compound libraries, natural products may represent a valuable source for drug discovery. In addition to the identification of new natural products as novel drug leads, identifying the novel mechanism of action of biologically active natural products may allow for the identification of new targets for drug development. The source of such natural products may serve as a guide to determine their activity and mechanism of action.

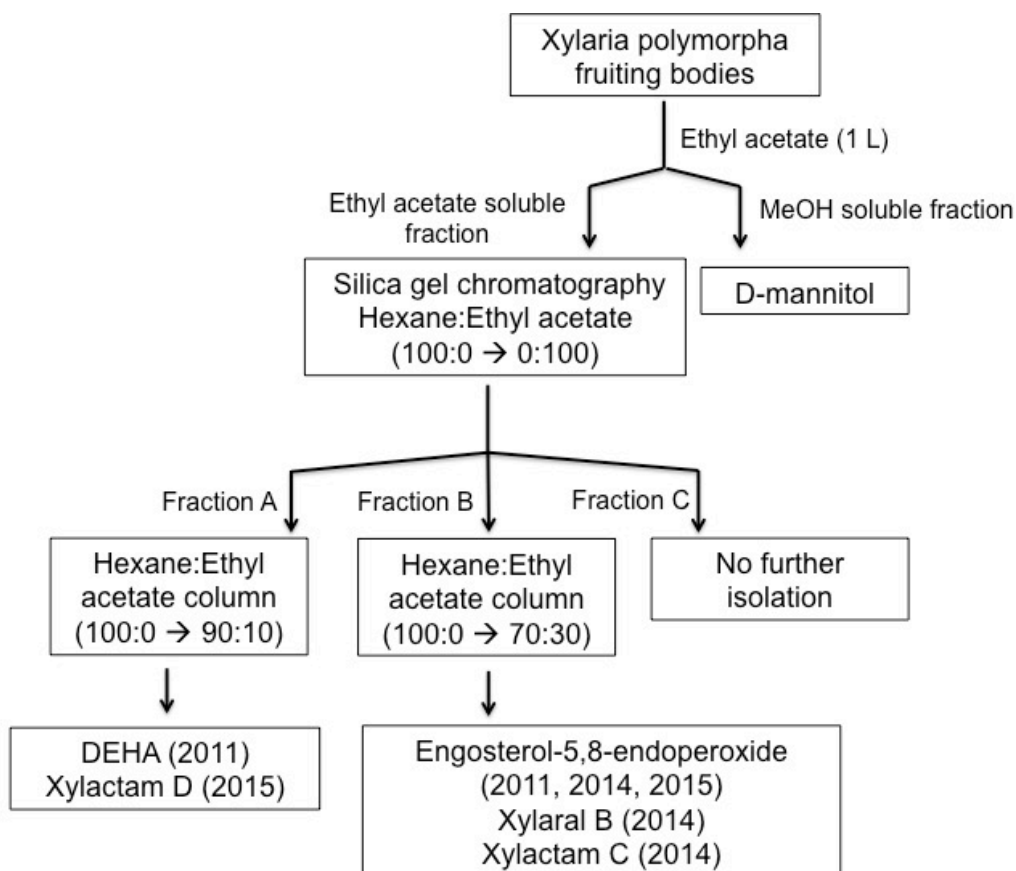
5.2 Isolation of novel natural products from *Xylaria polymorpha*

Xylaria polymorpha is a member of family Xylaraceae in the genus Ascomyces. This saprotrophic fungus is the most common member of the *Xylaria* genus, and is commonly found on decaying wood in North America forests.⁹ *Xylaria polymorpha* is colloquially known as Dead Man's Fingers due to the appearance of the fruiting bodies, which are black or brown clusters that protrude from dead wood on the lower stem or root bark.¹⁰

Diverse bioactive natural products have been isolated from *Xylaria polymorpha* and other *xylaria* species. This includes cytochalasins, a group of cytotoxic alkaloids that are produced by different *Xylaria* species.¹¹ Antifungal metabolites, including xylarinic acids from *X. polymorpha*, and multiplolide lactones from *X. multiplex*, have also been reported. A variety of terpene metabolites are produced by *Xylaria* species,¹² particularly sesquiterpenes such as xylcarpins,¹³ xylaranols,¹⁴ erimophilanes,¹⁵ and xylaguaianols A–D.¹⁶ *Xylaria* species also produce xyloketals, novel phenolic ketals with acetylcholinesterase activity,¹⁷ as well as mellein and pthalide derivatives.¹⁸ Polyketide derived natural products include the antibacterial xylariolides,¹⁹ xylarenones²⁰, xylaral,²¹ and xylactams A and B.^{22,23} This selection shows the diversity of *Xylaria* natural products in both structure and bioactivity. More comprehensive reviews of secondary metabolites produced by *Xylaria sp.* are available in the literature.^{24,25} Most reports of *Xylaria* metabolites have been isolated from *Xylaria sp.* growing on tropical plants. We therefore became interested in isolating natural products from *Xylaria polymorpha* growing in a southern Canadian climate.

5.3 *X. polymorpha* collection and extraction

Xylaria fruiting bodies obtained from a forested area in St. Catharine's, Ontario in May 2011, 2014, and 2015 were soaked separately in ethyl acetate for seven days (Figure 5.1). The resulting solution was filtered to remove solid fungus and evaporated under reduced pressure. The ethyl acetate extracts were then redissolved in methanol. The methanol-soluble fraction was removed and concentrated under reduced pressure. The remaining methanol-insoluble fractions were chromatographed using silica gel chromatography with a gradient of Hexane:EtOAc (100:0 Hexane:EtOAc \rightarrow 0:100 Hexane:EtOAc) to yield fractions A, B, and C, of increasing polarity. The most non-polar fraction A was further chromatographed using a silica gel column with a gradient elution (100:0 Hexane:EtOAc \rightarrow 90:10 Hexane:EtOAc) to afford di(2-ethylhexyl)adipate (DEHA) **5-2** (2011) and xylactam D **5-5** (2015). The fractions of intermediate polarity was further purified using silica column chromatography with a gradient elution (100:0 Hexane:EtOAc \rightarrow 70:30 Hexane:EtOAc) to afford ergosterol-5,8-endoperoxide **5-1** (2011, 2014, 2015), xylaral B **5-3** (2014), and xylactam C **5-4** (2014).

Figure 5.1: Isolation tree-diagram from *Xylaria polymorpha* fruiting bodies

5.4 Isolation of ergosterol-5,8-endoperoxide

Compound **5-1** was obtained as a white crystalline solid. ^1H NMR showed four olefinic protons at δ 6.51, 6.24, 5.22, and 5.14. ^{13}C and qDEPT experiments showed corresponding carbon signals at δ 130.8, 132.3, 135.2, 135.2. These experiments taken together indicate the presence of two disubstituted alkenes. A single highly coupled proton (δ 3.97), and six methyl groups (δ 0.83, 0.83, 0.84, 0.88, 0.91 and 1.0) were also present in the ^1H NMR spectrum. The ^{13}C and qDEPT experiments indicated that 28 distinct carbon environments are present. This structural data suggests a terpenoid

structure, and we found the spectrum to be in good agreement for the literature data for ergosterol-5,8-endoperoxide (Figure 5.2). X-ray crystallography performed on compound **5-1** further confirmed the structure to be that of ergosterol-5,8-endoperoxide. Although ergosterol has previously been identified as a metabolite present in *X. polymorpha*,¹² ergosterol-5,8-endoperoxide has not been previously isolated from *Xylaria* species. Ergosterol-5,8-endoperoxide was first isolated by from, and since then has been found in several other fungal species. Despite some speculation that ergosterol-5,8-endoperoxide is merely an artefact of photooxidation of ergosterol during isolation,²⁶ radiolabelling studies have been used to identify a peroxidase that catalyses this oxidation and to differentiate the photomediated and enzyme catalyzed pathways towards ergosterol-5,8-endoperoxide.²⁷ No ergosterol was detected in this sample of *X. polymorpha*, but the relative expression of ergosterol and ergosterol endoperoxide may be controlled by

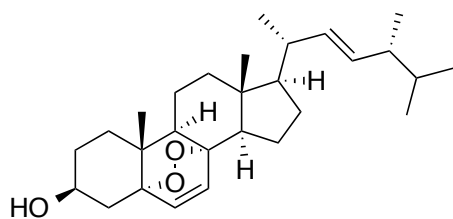


Figure 5.2: Structure of ergosterol-5,8-endoperoxide. Spectral data for **5-1** is identical to the literature data for ergosterol-5,8-endoperoxide.

ergosterol-5,8-endoperoxide

environmental conditions and the developmental stage of the fungus.

Ergosterol-5,8-endoperoxide has significant anti-tumour activity in a variety of human cell lines. Ergosterol-5,8-endoperoxide has been shown to induce apoptosis in HL60 human leukemia cells,²⁸ inhibit Jak/Stat3 signalling in multiple myeloma U266 cells,²⁹ and act as a DNA topoisomerase inhibitor in human colon tumour COLO-205

cells.³⁰ Ergosterol-5,8-endoperoxide has also been found to have anti-plasmodial³¹ anti-mycobacterial,³² and anti-leishmanial³³ activity. Based on these results, as well as the common endoperoxide functionality with antiparasitic natural product artemisinins, we hypothesized that ergosterol-5,8-endoperoxide may also have anti-*Toxoplasma* activity.

Ergosterol-5,8-endoperoxide was tested according to the previously described *T. gondii* 5-day growth assay. We found that this natural product inhibits the growth of *T. gondii* with an IC₅₀ of 18 μM. This compound also showed some toxicity to the host HFF cells, with a TD₅₀ of 57 μM. However, even this moderate activity is interesting given that ergosterol-5,8-endoperoxide contains the same peroxide motif associated with the antiparasitic activity of artemisinins.³⁴ This suggests that analogs of ergosterol and related steroids bearing the same endoperoxide functionality may show significant activity against *T. gondii* and related parasites.

5.5 Isolation of di(2-ethylhexyl) adipate and structural reassignment of microdiplactone

We isolated compound **5-2** as a colourless oil. In addition to several peaks below δ 1.5 consistent with a saturated carbon fragment, the ¹H NMR spectrum in CDCl₃ showed a distinctive doublet of quartets at δ 3.98, suggesting an oxymethylene group. The ¹H NMR spectrum also showed two proton signals at δ 1.60 and 2.26 that integrate to 2H and correlate only to each other in the COSY spectrum. This A₂B₂ system suggests two adjacent methylenes that are isolated from the rest of the structure. A heptet signal at δ 1.56 integrating to 1H is indicative of a branching alkyl chain. COSY experiments show this proton couples to signals at δ 3.98, 1.34, and 1.28. ¹³C NMR showed 11 distinct carbon environments, and qDEPT experiments further revealed 3 methyl or methane

signals and 8 signals corresponding to methylene and quaternary carbons. ^{13}C signals at δ 173.3 and 67.0 that suggested the presence of a lactone functionality. We searched the literature to see if this natural product had been previously reported, and we found that our spectral data matched almost perfectly with the spectral data associated with microdiplactone (Figure 5.3), a lactone first isolated from *Microdiplodia sp.* in 2011.³⁵ Despite the good agreement of our ^1H and ^{13}C NMR spectra with the data reported for microdiplactone, we found that the 2D NMR data (COSY, HSQC, and HMBC) data were not consistent with the proposed structure. COSY experiments indicate the heptet signal at δ 1.56 couples to signals at δ 3.98, 1.34, and 1.28. Furthermore, those signals at δ 1.34 and 1.28 both correlate to terminal methyl groups with signals at δ 0.88. We believe this is suggestive of a 2-ethylhexyl moiety rather than the two propyl groups in the proposed structure of microdiplactone. We continued to examine the literature for a structure consistent with our spectral data, and found that data was in good agreement with that of di(2-ethylhexyl) adipate (DEHA) (Figure 5.7), a plasticizer used to improve malleability of PVC plastics.³⁶

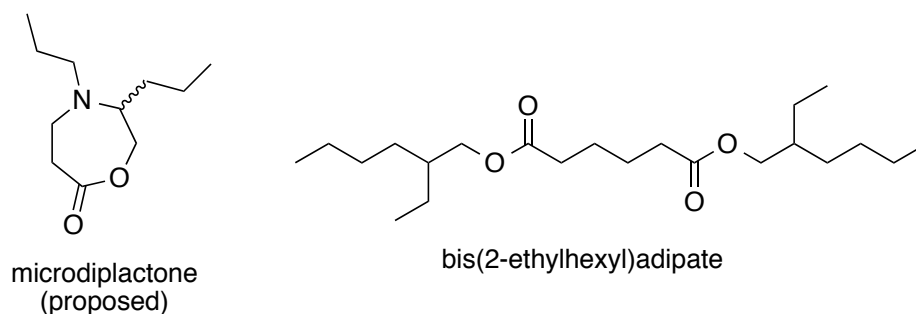


Figure 5.3: Proposed structure of microdiplactone. We propose the revised structure, di(2-ethylhexyl) adipate.

We initially suspected that di(2-ethylhexyl) adipate may be a contaminant introduced during isolation. To identify the source of this contamination, we repeated our *X. polymorpha* extraction conditions with several common lab plastics (pipette bulbs, plastic syringes, parafilm, micropipette tips, plastic vial lids, plastic wrap) to determine if di(2-ethylhexyl) adipate could be isolated. Crude ^1H NMR spectra showed no evidence of di(2-ethylhexyl) adipate in any of the plastic material analyzed. This led us to consider the possibility that di(2-ethylhexyl) adipate could be an environmental contaminant. DEHA has been detected in both water and soil in Canada,^{37,38} and is a known contamination in food and personal care products.³⁹ DEHA in soil or water samples could be absorbed by *X. polymorpha* and thus be present in extracts of the fruiting bodies.

It is also possible that DEHA is a genuine natural product biosynthesized by *X. polymorpha*. Di(2-ethylhexyl) phthalate, a related plasticizer, has been isolated from various natural product sources.⁴⁰⁻⁴³ Despite some speculation the DEHP detection was due to environmental contamination, DEHP found in marine algae showed ^{14}C levels consistent with a biosynthetic origin rather than production from a petrochemical source.⁴² A recent report also showed that $\text{NaH}^{13}\text{CO}_3$ was incorporated into phthalates produced by freshwater algae, providing further support for the idea of biosynthetic plasticizers.

The unclear origin of DEHA in *X. polymorpha* calls for further research into its presence in the fungus. DEHA was only detected in the sample from 2011, indicating its presence may be due to environmental contamination or growth conditions that were specific to that year. Future work may involve determining the abundance of ^{14}C in *X.*

polymorpha derived DEHA, where no detection of ^{14}C would indicate that the source is environmental contamination. Additionally, a ^{13}C labeled precursor could be fed to *X. polymorpha* grown in house to see if resulting DEHA shows ^{13}C incorporation.

5.6 Isolation of New Xylarals and Xylactams

Compounds **5-2**, **5-4**, and **5-5** were obtained in very low abundance from the most non-polar fraction (**5-5**) and the fraction of medium polarity (**5-3** and **5-4**). Each compound was an amorphous white solid, and ^1H and ^{13}C NMR indicated that these compounds have significant structural similarity and may belong to the same class.

5-3, **5-4**, and **5-5** all have one or more low field singlets above δ 9 ppm which we suspected may be carboxylic acid or phenol signals. Additionally, several olefinic protons between δ 6.0 and 7.1 ppm indicate the presence of one or more olefins. We reviewed the literature for natural products with similar structures and identified similarities to the spectra xylaral and xylactams A and B (Figure 5.4).

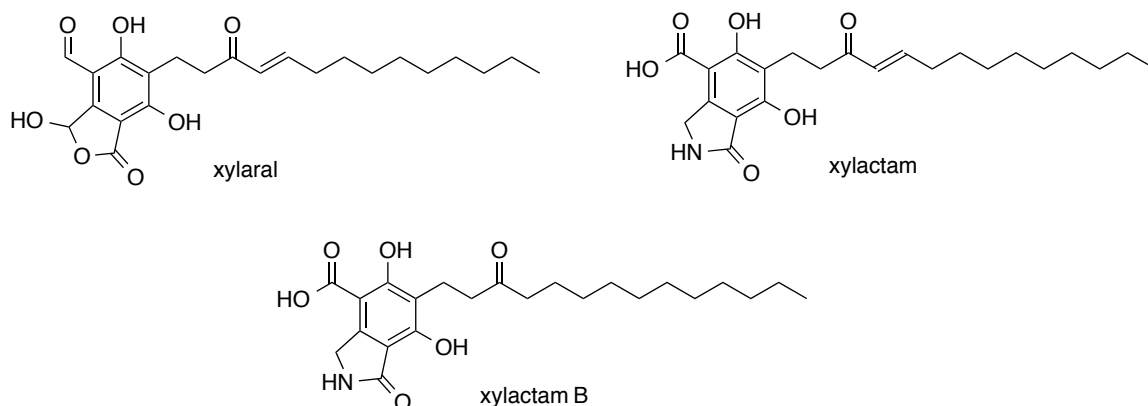


Figure 5.4: Structures of *Xylaria* polyketide natural products, xylaral, xylactam, and xylactam B.

5.6.1 Xylaral B

The ^1H NMR spectrum of **5-3** showed sharp, low field singlets at δ 12.34, 10.02, and 9.24 ppm, suggesting the structure contains an aldehyde and two acids or phenols. In addition, there are two olefinic protons at δ 6.14 and 6.92 that strongly correlate to one another in the COSY spectrum. The J constant for this coupling is 15.8 Hz, which is indicative of a disubstituted E alkene in the natural product. We also identified an A_2B_2 system in proton signals at δ 2.99 and 2.92 that integrate to 2H and couple only to each other. The ^1H NMR spectrum also shows a number of peaks between 1-2 ppm that suggest the presence of a saturated lipophilic chain. From the ^{13}C NMR, we can discern that three carbonyl groups are present based on signals at δ 187.0, 191.1, and 200.9. The region between δ 100 and 170 contains eight carbon signals. In consideration of the ^1H NMR spectra, we believe this is suggestive of an olefin and a fully substituted benzyl group. The ^{13}C NMR spectra also shows 12 carbon signals in the aliphatic region, which is consistent with a saturated carbon chain in the natural product. An HSQC experiment was used to determine that a singlet integrating to 2H that appears at δ 6.51 in the ^1H spectrum correlates to a carbon signal at δ 102. Due to the low field signals for these protons, we believe this carbon is adjacent to the lactone functionality and another heteroatom. HMBC further showed this carbon signal to be close in space to a methoxy group at δ 3.71.

Based on NMR data for xylaral, which also contains a fully substituted aromatic ring, a 5-membered lactone/lactam, an alkene adjacent to a ketone, and a saturated carbon chain, we believe **5-3** is a xylaral derivative.²¹ **5-3** contains a methoxy group not found in the structure of xylaral. HSQC and HMBC confirmed this group is connected to the

lactone located on the lactone ring. We therefore propose that our isolated natural product is 3-OMe xylaral, or xylaral B (Figure 5.5).

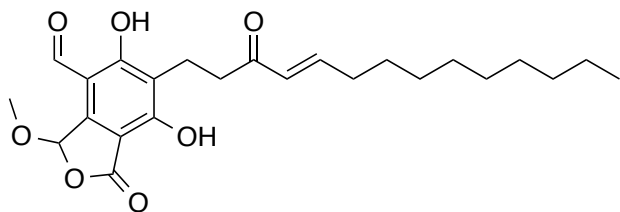


Figure 5.5: Proposed structure of **5-3**, xylactam B.

5.6.2 Xylactam C

Based on the spectral similarity between **5-3** and **5-4**, we believed the structures were closely related. The ^1H NMR of compound **5-4** also showed two sharp, low field singlets at δ 13.8, 10.1, suggesting that there are two phenols in the unknown natural product. Several overlapping peaks between δ 1-2 indicate that **5-4** also contains a saturated carbon chain. We also observed proton signals at δ 2.99 and 3.14 in a similar A_2B_2 system previously described for xylaral B. Four olefinic proton signals are present in the ^1H NMR spectrum at δ 6.14, 6.27, 7.01, and 7.27. ^{13}C NMR shows 10 protons in the aromatic and olefinic region, which consistent with **5-4** containing a fully substituted phenyl ring and two alkenes. COSY experiments allowed us to trace connectivity from the signal at δ 6.14, adjacent to the ketone, through to the signal δ 6.27 that also couples to δ 2.25, thus connecting to the rest of the saturated carbon chain, the signals for which are seen between δ 1-2. The coupling constants between the olefinic protons are between 14.5-16 Hz. This spectrum is consistent with three alkenes conjugated to a carbonyl.

The ^{13}C NMR spectrum contains peaks at δ 170.3, 173.5, and 204.1, suggesting the structure contains a ketone (δ 204.1) and two acid or amide carbonyls, and a peak at δ

102.8 consistent with a lactone or lactam. Together with the broad singlet at δ 6.58 (1H) and the sharp singlet at δ 4.49 (2H) in the ^1H NMR spectrum, this spectral data suggests a lactam functionality as seen previously in the structure of xylactams A and B. We have thus called **5-4** xylactam C, a new member of the xylactam with a different ‘tail’ moiety (Figure 5.6). This structure is consistent with the molecular formula $\text{C}_{23}\text{H}_{29}\text{NO}_6$, as indicated by the mass spectrometry data.

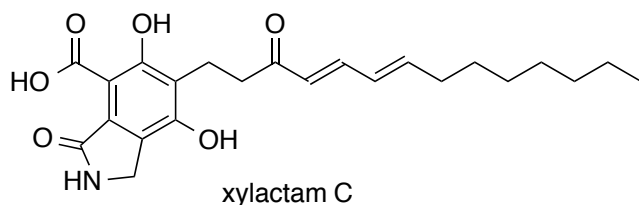


Figure 5.6: Proposed structure of **5-4**, xylactam C

5.6.3 Xylactam D

Spectral data for compound **5-5** indicates significant structural similarity to **5-4**, suggesting it is also a member of the xylactam family. Key differences in the spectral data between xylactams allow us to determine the structure of compound **5-5**. The ^1H NMR for **5-5** contains four olefinic protons at δ 6.10, 6.17, 6.27, and 7.27, with coupling constants between 15-16 Hz. COSY experiments show that correlations can be followed from δ 6.10 to δ 7.27 to δ 6.17 to δ 6.27. The proton signal at δ 6.27 also couples to δ 2.18, which in turn correlates to the overlapping signals at δ 1-2, indicating the conjugated alkenes connect directly to the alkyl tail.

Compound **5-5** has several ^1H signals not visible in the ^1H NMR for xylactams A, B, or C. A new triplet signal at δ 3.66 (2H) correlates to a signal at δ 1.59 (3H), which also couples to a doublet at δ 0.97 (6H). These signals are characteristic of an isopentyl

group. The connectivity of the isopentyl group to the rest of the molecule cannot be traced by COSY, HSQC, or HMBC spectra, indicating that it is likely connected through a heteroatom. The downshifting of the triplet signal at δ 3.66 is further evidence that this isopropyl moiety is connected to a N- or O- atom. Based on the absence of the characteristic amide N-H peak seen in the spectrum of xylactams A, B, and C between δ 6.5-6.8, the isopentyl group is located on the amide N-atom (Figure 5.7). This structure is consistent with the molecular formula $C_{28}H_{39}NO_6$, as indicated by the mass spectrometry data. Biosynthetically, this isopentyl group may arise from a fungal hydrogenase promoted reduction of an isopentenyl or dimethylallyl group. These groups are installed by isopentenyl or dimethylallyl pyrophosphate, suggesting this structure is a meroterpene, containing both polyketide and terpenoid functionality.

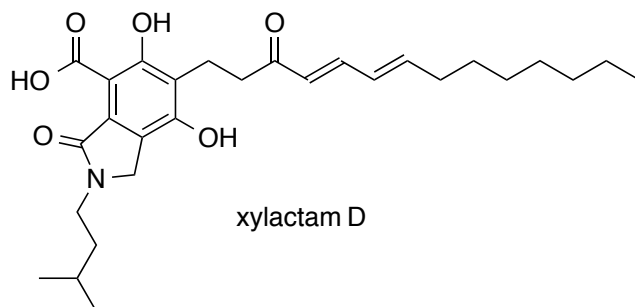


Figure 5.7: Structure of **5-5**, xylactam D.

5.7 Conclusion and future work

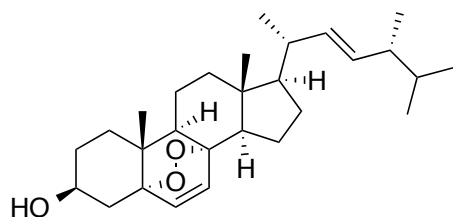
In conclusion, we have identified interesting natural products in *Xylaria polymorpha* fruiting bodies. Despite the diverse structure and bioactivity of natural products from *Xylaria sp.*, the literature contains few reports of natural products from the fruiting bodies of Canadian *X. polymorpha*. We isolated five interesting natural products,

including 3 novel polyketide derivatives, xylaral B, xylactam C, and xylactam D. We also reassigned the structure of microdplactone to di(2-ethylhexyl) adipate. This molecule may be an environmental contaminant or a true natural product. We also report for the first time the activity of ergosterol-5,8-endoperoxide against the parasite *T. gondii*. No reports of the biological activity of xylaral, xylactam A, or xylactam B exist in the literature, but we hypothesize these compounds may be produced for as part of a fungal-plant and/or microbial arms race and may thus have antimicrobial or herbicidal properties. Related fungal endophytes are known to produce polyketides that inhibit plant growth through inhibition of phenylalanine ammonia lyase (PAL),⁴⁴ closing down protective flavonoid/stilbene secondary metabolic defenses in the plant. The biological activities, including antimicrobial and herbicidal activity of these novel xylaral and xylactams will be investigated in the near future when access to larger quantities becomes available.

5.8 Experimental

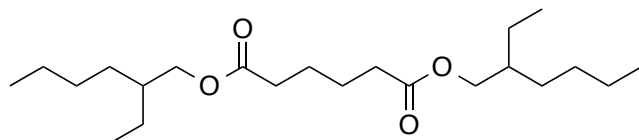
14.5 g (2014) or 11.3 g (2015) of dried *Xylaria polymorpha* fruiting bodies collected in St. Catharines, Ontario were extracted in 1.0 L of reagent grade EtOAc. After soaking for 7 days, the extract was decanted and dried under reduced pressure. 100 mL of MeOH was then added and the MeOH-soluble portion was decanted and dried under reduced pressure. The MeOH-insoluble fraction was dissolved in DCM and purified by silica gel chromatography (100% hexane → 100% EtOAc gradient). Fractions of similar polarity were combined to produce fractions A, B, and C of increasing polarity. Fraction

A was further purified by silica gel chromatography (100:0 hexane:EtOAc \rightarrow 90:10 hexane:EtOAc gradient). Fraction B was further purified by silica gel chromatography (100:0 hexane:EtOAc \rightarrow 70:30 hexane:EtOAc gradient). Natural products obtained were characterized using ^1H NMR, ^{13}C NMR, and HRMS.



ergosterol-5,8-endoperoxide

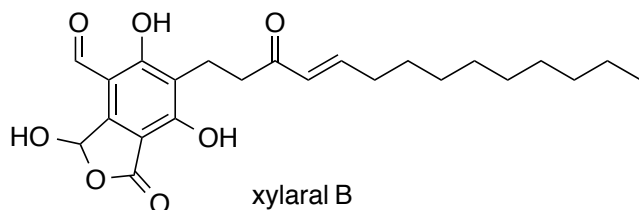
Ergosterol-5,8-endoperoxide (5-1): white crystalline solid (4.8 mg); ^1H NMR (600 MHz, Chloroform-*d*) δ 6.50 (d, $J = 8.5$ Hz, 1H), 6.24 (d, $J = 8.5$ Hz, 1H), 5.22 (dd, $J = 15.2, 7.6$ Hz, 1H), 5.14 (dd, $J = 15.3, 8.3$ Hz, 1H), 3.97 (td, $J = 11.4, 5.5$ Hz, 1H), 2.11 (ddd, $J = 13.7, 5.0, 2.0$ Hz, 1H), 2.05 – 1.66 (m, 10H), 1.52 – 1.32 (m, 9H), 1.25 (s, 3H), 1.23 (dd, $J = 10.3, 7.9$ Hz, 3H), 1.00 (d, $J = 6.6$ Hz, 3H), 0.91 (d, $J = 6.8$ Hz, 3H), 0.88 (s, 3H), 0.83 (d, $J = 6.8$ Hz, 3H), 0.82 (t, $J = 3.6$ Hz, 3H), 0.80 – 0.76 (m, 1H); ^{13}C NMR (151 MHz, CDCl_3) δ 135.56, 135.35, 132.46, 130.90, 82.30, 79.57, 77.37, 77.16, 76.95, 66.63, 56.36, 51.84, 51.25, 44.72, 42.93, 39.88, 39.50, 37.10, 34.85, 33.22, 30.29, 29.87, 28.80, 23.56, 21.04, 20.79, 20.10, 19.80, 18.33, 17.71, 13.03.



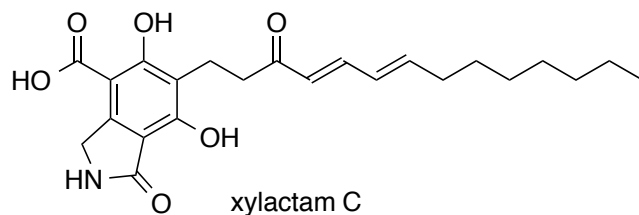
di(2-ethylhexyl)adipate

DEHA (5-2): ^1H NMR (600 MHz, Chloroform-*d*): clear, colourless oil (1.0 mg); δ 3.98 (dq, $J = 10.9, 5.6$ Hz, 2H), 2.40 – 2.24 (m, 2H), 1.74 – 1.61 (m, 2H), 1.55 (h, $J = 6.1$ Hz,

1H), 1.42 – 1.18 (m, 9H), 0.89 (td, $J = 7.1, 3.3$ Hz, 6H); ^{13}C NMR (151 MHz, CDCl_3) δ 172.49, 76.21, 76.00, 75.78, 65.78, 37.73, 32.99, 29.40, 27.91, 23.47, 22.78, 21.95, 13.02, 9.96.

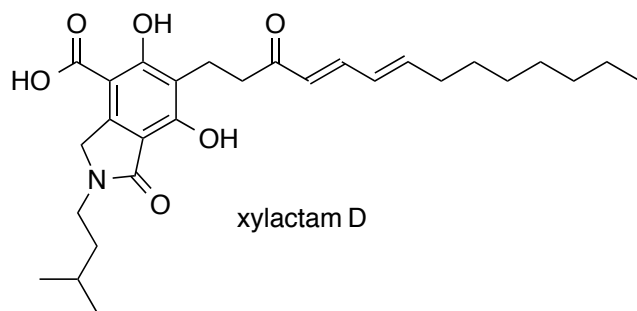


Xylaral B (5-3): ^1H NMR (600 MHz, Chloroform-*d*) δ white amorphous solid (1.2 mg); 12.34 (s, 1H), 10.02 (s, 1H), 9.24 (s, 1H), 6.94 (dt, $J = 15.9, 7.0$ Hz, 2H), 6.51 (s, 1H), 6.14 (dt, $J = 15.7, 1.5$ Hz, 1H), 3.71 (s, 3H), 2.99 (d, $J = 6.3$ Hz, 2H), 2.92 (t, $J = 6.8$ Hz, 2H), 2.26 – 2.22 (m, 2H), 1.50 – 1.44 (m, 4H), 1.30 (d, $J = 17.1$ Hz, 20H), 0.90 (m, 5H); ^{13}C NMR (151 MHz, CDCl_3) δ 200.86, 191.11, 187.03, 167.98, 167.58, 160.11, 149.35, 129.56, 127.57, 127.28, 101.84, 77.21, 77.00, 76.79, 59.86, 57.12, 38.32, 32.59, 31.85, 29.70, 29.46, 28.02, 22.66, 19.81, 16.51, 14.10.



Xylactam C (5-4): δ off-white amorphous solid (0.8 mg); ^1H NMR (600 MHz, Chloroform-*d*) 13.81 (d, $J = 1.0$ Hz, 1H), 10.13 (s, 1H), 7.27 (s, 1H), 7.02 (dt, $J = 15.9, 6.9$ Hz, 1H), 6.58 (s, 1H), 6.27 (dt, $J = 14.4, 6.9$ Hz, 1H), 6.14 (dt, $J = 15.9, 1.6$ Hz, 1H), 4.49 (s, 2H), 3.17 – 3.11 (m, 2H), 3.02 – 2.96 (m, 2H), 2.21 (dt, $J = 20.8, 7.3$ Hz, 3H), 1.43 (q, $J = 7.0, 6.4$ Hz, 3H), 1.27 (d, $J = 16.3$ Hz, 13H), 0.87 (t, $J = 7.0$ Hz, 3H); ^{13}C NMR (151 MHz, CDCl_3) δ 204.09, 173.49, 172.49, 164.85, 155.04, 151.49, 148.74,

146.25, 129.09, 128.48, 128.23, 126.27, 102.59, 77.21, 77.00, 76.79, 44.55, 39.61, 39.36, 33.27, 31.74, 29.43, 29.34, 29.26, 29.18, 29.12, 29.05, 28.54, 22.61, 16.99, 16.89, 14.07. ESI HRMS calculated for $C_{23}H_{30}NO_6$ $[M+H]^+$: 416.2073, found 416.2075.



Xylactam D (5-5): 1H NMR (600 MHz, Chloroform-*d*) δ off white amorphous solid (1.6 mg); 13.81 (s, 1H), 10.04 (s, 1H), 7.32 – 7.25 (m, 12H), 7.26 – 7.19 (m, 10H), 6.27 (dt, J = 14.3, 7.0 Hz, 1H), 6.17 (dd, J = 15.1, 10.7 Hz, 1H), 6.10 (d, J = 15.5 Hz, 1H), 4.41 (d, J = 4.3 Hz, 2H), 3.66 (t, J = 7.2 Hz, 2H), 3.16 – 3.11 (m, 2H), 2.98 (dd, J = 6.7, 4.3 Hz, 2H), 2.22 – 2.15 (m, 2H), 1.62 – 1.52 (m, 21H), 1.42 (dd, J = 13.2, 6.1 Hz, 3H), 1.26 (d, J = 7.6 Hz, 19H), 0.97 (d, J = 6.1 Hz, 6H), 0.88 (td, J = 7.0, 3.9 Hz, 6H); ^{13}C NMR (151 MHz, $CDCl_3$) δ 204.14, 172.74, 170.27, 164.63, 154.75, 148.64, 146.17, 129.41, 128.50, 126.34, 122.94, 120.10, 102.60, 77.21, 77.00, 76.79, 48.91, 41.86, 39.64, 36.94, 33.27, 31.74, 29.70, 29.12, 29.05, 28.55, 25.76, 22.61, 22.37, 16.90, 14.07. ESI HRMS calculated for $C_{28}H_{40}NO_6$ $[M+H]^+$: 486.2856, found 486.2854.

5.9 References

- (1) Newman, D. J., and Cragg, G. M. (2016) Natural products as sources of new drugs from 1981 to 2014. *J. Nat. Prod.* 79, 629–661.
- (2) Klayman, D. L. (1985) Qinghaosu (Artemisinin): an antimalarial drug from China. *Science* 228, 1049–1056.
- (3) Wang, J., Zhang, C.-J., Chia, W. N., Loh, C. C. Y., Li, Z., Lee, Y. M., He, Y., Yuan,

- L.-X., Lim, T. K., Liu, M., Liew, C. X., Lee, Y. Q., Zhang, J., Lu, N., Lim, C. T., Hua, Z.-C., Bin Liu, Shen, H.-M., Tan, K. S. W., and Lin, Q. (2015) Haem-activated promiscuous targeting of artemisinin in *Plasmodium falciparum*. *Nat. Commun.* *6*, 10111.
- (4) Magano, J. (2009) Synthetic approaches to the neuraminidase inhibitors Zanamivir (Relenza) and Oseltamivir phosphate (Tamiflu) for the treatment of influenza. *Chem. Rev.* *109*, 4398–4438.
- (5) Tally, F. P., and DeBruin, M. F. (2000) Development of daptomycin for Gram-positive infections. *J. Antimicrob. Chemother.* *46*, 523–526.
- (6) Canepari, P., Boaretti, M., Lleo, M. M., and Satta, G. (1990) Lipoteichoic acid as a new target for activity of antibiotics: mode of action of daptomycin (LY146032). *Antimicrob. Agents Chemother.* *34*, 1220–1226.
- (7) Macarron, R., Banks, M. N., Bojanic, D., Burns, D. J., Cirovic, D. A., Garyantes, T., Green, D. V. S., Hertzberg, R. P., Janzen, W. P., Paslay, J. W., Schopfer, U., and Sittampalam, G. S. (2011) Impact of high-throughput screening in biomedical research. *Nat. Rev. Drug. Discov.* *10*, 188–195.
- (8) Ortholand, J.-Y., and Ganesan, A. (2004) Natural products and combinatorial chemistry: back to the future. *Curr. Opin. Chem. Biol.* *8*, 271–280.
- (9) Rogers, J. D., and Callan, B. E. (1986) *Xylaria polymorpha* and its allies in continental United States. *Mycologia* *78*, 391–400.
- (10) Bessette, A., Bessette, A. R., and Fischer, D. W. (1997) Mushrooms of northeastern North America. Syracuse University Press.
- (11) Dagne, E., Gunatilaka, A. A. L., Asmellash, S., Abate, D., Kingston, D. G. I., Hofmann, G. A., and Johnson, R. K. (1994) Two new cytotoxic cytochalasins from *Xylaria obovata*. *Tetrahedron* *50*, 5615–5620.
- (12) Jang, Y.-W., Lee, I.-K., Kim, Y.-S., Seok, S.-J., Yu, S. H., and Yun, B.-S. (2009) Chemical constituents of the fruiting body of *Xylaria polymorpha*. *Mycobiology* *37*, 207–210.
- (13) Yin, X., Feng, T., Li, Z.-H., Su, J., Li, Y., Tan, N.-H., and Liu, J.-K. (2011) Chemical investigation on the cultures of the fungus *Xylaria carpophila*. *Nat. Prod.*

Bioprospect. 1, 75–80.

(14) Li, Y. Y., Hu, Z. Y., Lu, C. H., and Shen, Y. M. (2010) Four new terpenoids from *Xylaria* sp. 101. *Helv. Chim. Acta 93*, 796–802.

(15) Isaka, M., Chinthanom, P., Boonruangprapa, T., Rungjindamai, N., and Pinruan, U. (2010) Eremophilane-type sesquiterpenes from the fungus *Xylaria* sp. BCC 21097. *J. Nat. Prod. 73*, 683–687.

(16) Wei, H., Xu, Y.-M., Espinosa-Artiles, P., Liu, M. X., Luo, J.-G., U'Ren, J. M., Elizabeth Arnold, A., and Leslie Gunatilaka, A. A. (2015) Sesquiterpenes and other constituents of *Xylaria* sp. NC1214, a fungal endophyte of the moss *Hypnum* sp. *Phytochemistry 118*, 102–108.

(17) Lin, Y., Wu, X., Feng, S., Jiang, G., Luo, J., Zhou, S., Vrijmoed, L. L. P., Jones, E. B. G., Krohn, K., Steingröver, K., and Zsila, F. (2001) Five unique compounds: Xyloketal from mangrove fungus *Xylaria* sp. from the south china sea coast. *J. Org. Chem. 66*, 6252–6256.

(18) Zheng, N., Yao, F., Liang, X., Liu, Q., Xu, W., Liang, Y., Liu, X., Li, J., and Yang, R. (2017) A new phthalide from the endophytic fungus *Xylaria* sp. GDG-102. *Nat. Prod. Res. 6*, 1–6.

(19) Hu, Z. Y., Li, Y. Y., Lu, C. H., Lin, T., and Hu, P. (2010) Seven novel linear polyketides from *Xylaria* sp. NCY2. *Helv. Chim. Acta 93*, 925–933.

(20) de Oliveira, C. M., Silva, G. H., Regasini, L. O., Otávio Flausino, J., López, S. N., Abissi, B. M., de Souza Berlinck, R. G., Sette, L. D., Bonugli-Santos, R. C., Rodrigues, A., da Silva Bolzani, V., and Araujo, A. R. (2011) Xylarenones C–E from an endophytic fungus isolated from *Alibertia macrophylla*. *J. Nat. Prod. 74*, 1353–1357.

(21) Gunawan, S., Steffan, B., and Steglich, W. (1990) Xylaral, ein hydroxyphthalid-derivat aus fruchtkörpern von *Xylaria polymorpha* (Ascomycetes). *Eur. J. Org. Chem. 1990*, 825–827.

(22) Wang, X.N., Tan, R.X., and Liu, J.K. (2010) Xylactam, a new nitrogen-containing compound from the fruiting bodies of ascomycete *Xylaria euglossa*. *J. Antibiot. 58*, 268–270.

- (23) Piyasena, N. P. K. G., Schöffler, A., and Laatsch, H. (2015) Xylactam B, A New Isobenzofuranone from an Endophytic *Xylaria* sp. *Nat. Prod. Commun.* 10, 1715–1717.
- (24) Song, F., Wu, S. H., Zhai, Y. Z., Xuan, Q. C., and Wang, T. (2014) Secondary metabolites from the genus *Xylaria* and their bioactivities. *Chem. Biodivers.* 11, 673–694.
- (25) Macías-Rubalcava, M. L., and Sánchez-Fernández, R. E. (2016) Secondary metabolites of endophytic *Xylaria* species with potential applications in medicine and agriculture. *World. J. Microbiol. Technol.* 33, 15.
- (26) Adam, H. K., Campbell, I. M., and McCorkindale, N. J. (1967) Ergosterol peroxide: a fungal artifact. *Nature* 216, 397–397.
- (27) Bates, M. L., Reid, W. W., and White, J. D. (1976) Duality of pathways in the oxidation of ergosterol to its peroxide in vivo. *J. Chem. Soc. Chem. Commun.* 44–15.
- (28) Takei, T., Yoshida, M., Ohnishi-Kameyama, M., and Kobori, M. (2014) Ergosterol peroxide, an apoptosis-inducing component isolated from *Sarcodon aspratus* (Berk.) S. Ito. *Biosci. Biotechnol. Biochem.* 69, 212–215.
- (29) Rhee, Y.-H., Jeong, S.-J., Lee, H.-J., Lee, H.-J., Lee, H. J., Koh, W., Jung, J. H., Kim, S.-H., and Sung-Hoon, K. (2012) Inhibition of STAT3 signaling and induction of SHP1 mediate antiangiogenic and antitumor activities of ergosterol peroxide in U266 multiple myeloma cells. *BMC Cancer* 2012 12:1 12, 28.
- (30) Kuo, L.-M. Y., Chen, K.-Y., Hwang, S.-Y., Chen, J.-L., Liu, Y.-Y., Liaw, C.-C., Ye, P.-H., Chou, C.-J., Shen, C.-C., and Kuo, Y.-H. (2005) DNA topoisomerase I inhibitor, ergosterol peroxide from *Penicillium oxalicum*. *Planta Medica* 71, 77–79.
- (31) Kimani A M Kuria, Hezekiah Chepkwony, Cindy Govaerts, Eugene Roets, Roger Busson, Peter de Witte, Istvan Zupko, Georges Hoornaert, Ludo Quiryneen, Louis Maes, Leen Janssens, Jos Hoogmartens, A., Gert Laekeman. (2002) The antiplasmodial activity of isolates from *Ajuga remota*. *J. Nat. Prod.* 65, 789–793.
- (32) Cantrell, C. L., Rajab, M. S., Franzblau, S. G., Fronczek, F. R., and Fischer, N. H. (1999) Antimycobacterial Ergosterol-5,8-endoperoxide from *Ajuga remota*. *Planta Medica* 65, 732–734.
- (33) Correa, E., Cardona, D., Quiñones, W., Torres, F., Franco, A. E., Vélez, I. D.,

- Robledo, S., and Echeverri, F. (2006) Leishmanicidal activity of *Pycnoporus sanguineus*. *Phytother. Res.* 20, 497–499.
- (34) Kaiser, M., Wittlin, S., Nehrbass-Stuedli, A., Dong, Y., Wang, X., Hemphill, A., Matile, H., Brun, R., and Vennerstrom, J. L. (2007) Peroxide bond-dependent antiplasmodial specificity of artemisinin and OZ277 (RBx11160). *Antimicrob. Agents Chemother.* 51, 2991–2993.
- (35) Siddiqui, I. N., Zahoor, A., Hussain, H., Ahmed, I., Ahmad, V. U., Padula, D., Draeger, S., Schulz, B., Meier, K., Steinert, M., Kurtán, T., Flörke, U., Pescitelli, G., and Krohn, K. (2011) Diversonol and blennolide derivatives from the endophytic fungus *Microdiplodia* sp.: Absolute configuration of diversonol. *J. Nat. Prod.* 74, 365–373.
- (36) Cao, X.-L., Zhao, W., Churchill, R., and Hilts, C. (2014) Occurrence of di-(2-ethylhexyl)adipate and phthalate plasticizers in samples of meat, fish, and cheese and their packaging films. *J. Food. Prot.* 77, 610–620.
- (37) Horn, O., Nalli, S., Cooper, D., and Nicell, J. (2004) Plasticizer metabolites in the environment. *Water Res.* 38, 3693–3698.
- (38) Beauchesne, I., Barnabé, S., and Cooper, D. G. (2008) Plasticizers and related toxic degradation products in wastewater sludges. *Water Sci. Technol.* 57, 367–374.
- (39) Zhou, S. N., Moody, R. P., Aikawa, B., Yip, A., Wang, B., and Zhu, J. (2013) In vitro dermal absorption of Di(2-ethylhexyl)adipate (DEHA) in a roll-on deodorant using human skin. *J. Toxicol. Environ. Health* 76, 157–166.
- (40) Giust, J. A., Seipelt, C. T., Anderson, B. K., Deis, D. A., and Hinders, J. D. (1990) Determination of bis(2-ethylhexyl) phthalate in cow's milk and infant formula by high-performance liquid chromatography. *J. Agric. Food Chem.* 38, 415–418.
- (41) Al-Bari, M. A. A., Bhuiyan, M. S. A., Flores, M. E., Petrosyan, P., García-Varela, M., and Islam, M. A. U. (2005) *Streptomyces bangladeshensis* sp. nov., isolated from soil, which produces bis-(2-ethylhexyl)phthalate. *Int. J. Syst. Evol. Microbiol.* 55, 1973–1977.
- (42) Namikoshi, M., Fujiwara, T., Nishikawa, T., and Ukai, K. (2006) Natural abundance 14c content of Dibutyl Phthalate (DBP) from three marine algae. (2006) *Marine Drugs* 4,

290–297.

(43) Babu, B., and Wu, J. T. (2010) Production of phthalate esters by nuisance freshwater algae and cyanobacteria. *Sci. Total Environ.* 418, 4969–4975.

(44) Fürstner, A., Radkowski, K., Wirtz, C., Goddard, R., Lehmann, C. W., and Mynott, R. (2002) Total syntheses of the phytotoxic lactones herbarumin I and II and a synthesis-based solution of the pinolidoxin puzzle. *J. Am. Chem. Soc.* 124, 7061–7069.

6 Natural products from *Ficus benjamina* latex

6.1 Natural products for plant defense

Plants represent a rich source of natural products, and many interesting bioactive metabolites are produced to defend against predators or microbes. Bioactive natural products produced for self-defence can have utility in drug discovery and agriculture. One such example of this process is cardiac glycosides, such as digoxin, which are steroid derivatives produced by *Digitalis* and *Nerium* species (Figure 6.1).¹ Cardiac glycosides are potent inhibitors of Na⁺/K⁺-ATPase, and are thus toxic to herbivores that consume these plants.¹ Because of their extremely potent bioactivity, cardiac glycosides have also found use in treatment of heart disease.² Similarly, nicotine produced by *Nicotiana glauca*, has been shown to reduce plant consumption by insects (Figure 5.1).³ Nicotine is a nicotinic acetylcholine receptor antagonist that is toxic to most herbivores, and thus was one of the first pesticides used in agriculture.⁴

In addition to discouraging consumption by herbivores, plants may also produce natural products to protect against infection by pathogenic organisms. α -Tomatine is a constitutively produced steroidal glycoalkaloid with antifungal activity (Figure 5.1).⁵ Although some fungi have developed enzymes for detoxification of α -tomatine, the presence of α -tomatine limits the pathogens to which tomatoes are susceptible. Similarly, *Arabidopsis thaliana* constitutively produces the indole alkaloid camalexin with antifungal and antibacterial activity (Figure 6.1).⁶ Resveratrol and δ -viniferin are produced by *Vitis vinifera* in response to fungal infection (Figure 5.1).⁷ These

phytochemicals and other plant defense metabolites represent a rich source of natural products that may be valuable to human health and agriculture.

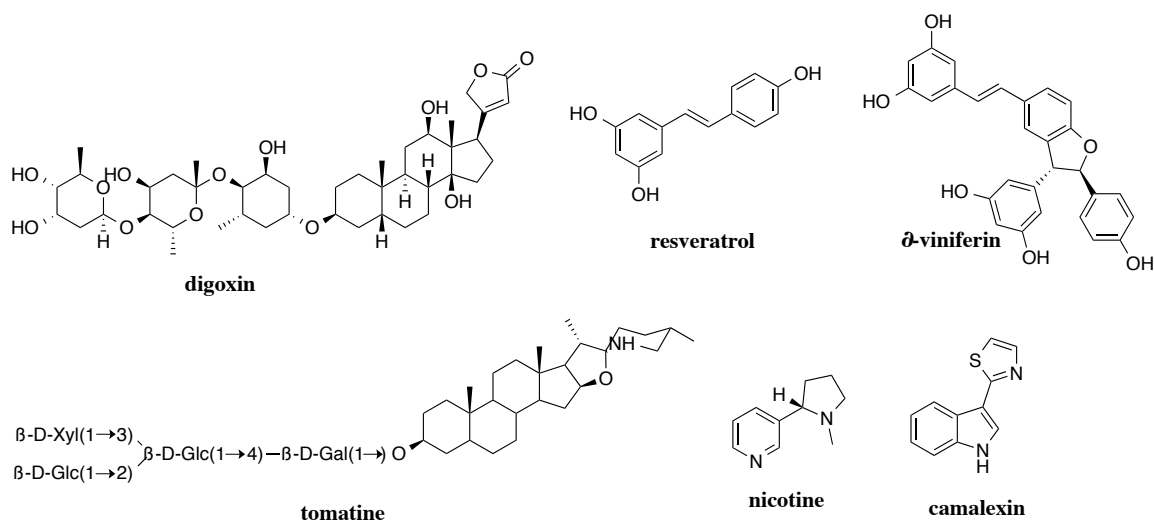


Figure 6.1: Natural products involved in plant defence. These natural products have applications in human medicine and agriculture.

6.2 Isolation of candicine from *F. benjamina*

We became interested in the plant defense mechanisms of *Ficus benjamina*, and made an interesting discovery about the natural products contained in plant latex. A manuscript describing these findings is under preparation for submission to the Journal of Natural Products. C. Brown performed isolations and synthesis. J. McNulty grew the *F. benjamina* sample and obtained latex. L. Brando, V. Nimgaonkar, L. D’Aiuto, M. Pritchard assayed candicine for antiviral activity. C. Brown and J. McNulty prepared the manuscript.

6.2.1 Discovery of candicine as the major induced latex constituent in *Ficus benjamina* (Moraceae) and its potent, selective antiviral activity

Plants of the Moraceae family are numerous, with well over 1100 named species,¹ most of which belong to the *Ficus* (>750 species) genera.² They are widely distributed geographically from tropical to temperate climates. The Moraceae family includes common species such as the mulberry and fig tree, as well as many tropical species of tree, shrub and vine, several of which are commonly grown indoors as decorative house plants. The Moraceae family are characterized by a laticiferic synapomorphy involving the production of a milky latex from various portions of the plant. They demonstrate a fascinating plant-insect evolutionary history,³ with individual species distinguished through a divergent obligate mutualism, involving the pollination of each species with individual fig wasps.⁴⁻⁵ We became interested in investigating the secondary metabolic content from the common houseplant *Ficus benjamina*, based on these interesting and specific plant-insect interactions and observations that the plant might be producing defensive metabolites.⁶⁻⁷ For example, a recent study reported the occurrence of 28 alkaloids in the leaves and bark of *F. benjamina*.⁶ These metabolites are of incredible structural diversity given their occurrence in a single source and included indole, indolizidine, quinoline, isoquinoline, steroidal, pyridyl, carbazole, acridine and tropane alkaloids. A few specific examples of these structural types is collected in Figure 6.2, highlighting the potential value of this plant as a resource for developing new lead compounds. Another recent investigation reported on the antibacterial and antifungal activity of crude extracts from the leaves, stem and root of *F. benjamina*, as well as the

identification of substituted cinnamic acid derivatives (*p*-coumaric, ferulic and syringic acids).⁷ The isolation of antiviral flavone-glycosides from the leaves,⁸ and latex coagulation from the plant has been described.⁹ The crude ethanol extract of bark, leaf and fruit from *F. benjamina* was shown to have anti-infective activity to herpes viruses (HSV-1, HSV-2, VZV).¹⁰ Surprisingly, the secondary metabolic content of the latex produced by *F. benjamina* has not been reported to date. Given the noted plant-insect interactions and potential production of valuable antiviral¹⁰⁻¹³ and other antimicrobial lead compounds described above, we now report the investigation of the production and surprising composition of the latex from this plant.

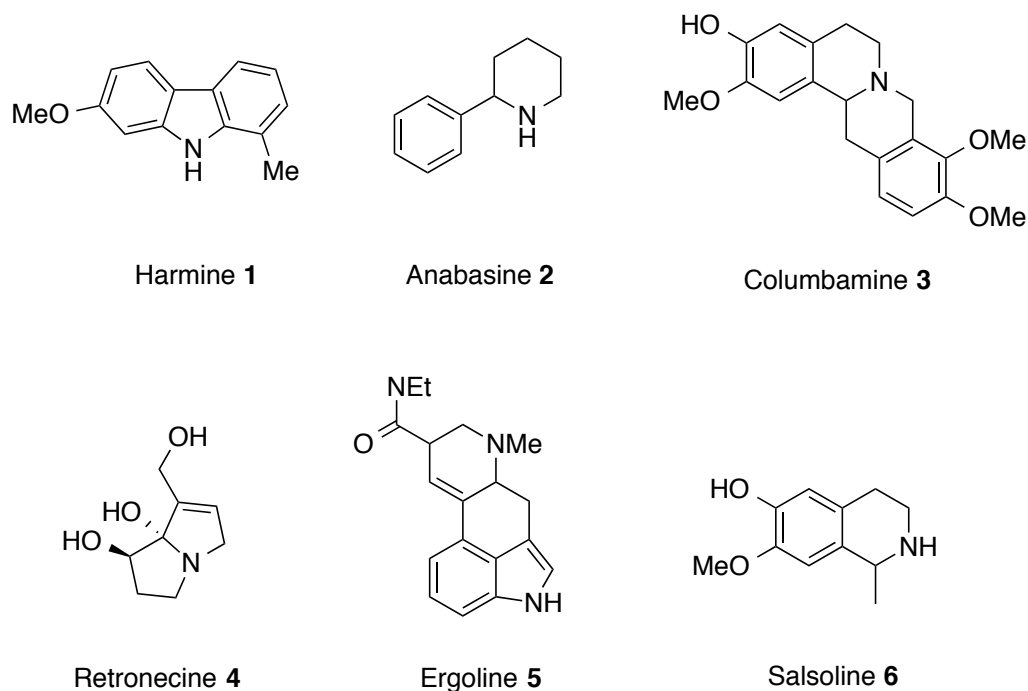


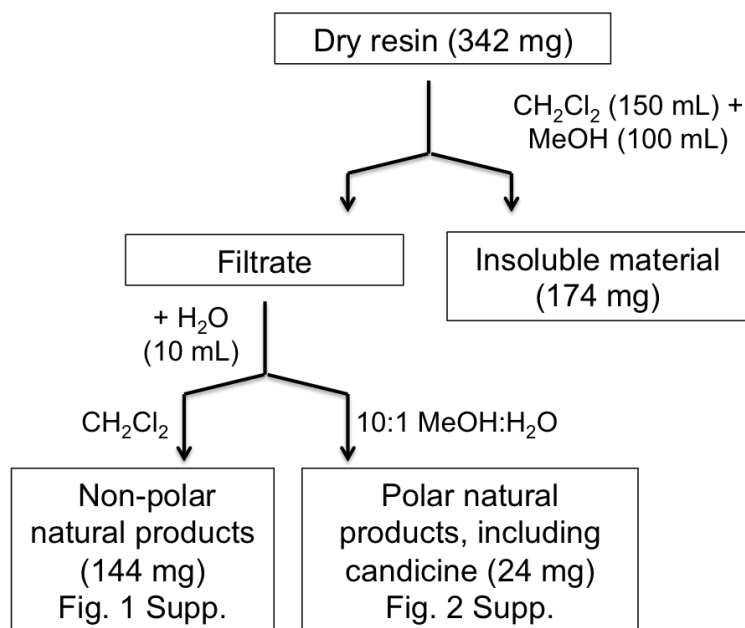
Figure 6.2: A selection of known alkaloids identified from *Ficus benjamina*.

We made the observations that the plant exudes a copious milky-white latex upon leaf pruning from the leaf node, or upon leaf cutting from exposed leaf veins. This

observation, characteristic of laticiferic plants, indicated the possibility that defensive insecticidal and/or antimicrobial compounds might be produced. In each case the latex is exuded under some pressure, rapidly coating the freshly exposed surfaces. The latex air dries to a hard, slightly amber colored glassy-resin within 24 hours (Figure 6.3). Dried latex was removed and extracted with a 3:2/v:v mixture of methanol and dichloromethane at room temperature for 4 hours and then filtered to remove an insoluble material (51%). Deionized water was added to the filtrate to separate the dichloromethane and aqueous methanol phases as shown in Scheme 6.1. The separate phases were dried and the crude material analyzed by ^1H and ^{13}C NMR spectroscopy. The non-polar dichloromethane extract (42% by weight) was shown to consist of a mixture of saturated and unsaturated fatty acid glycerides and not further pursued (see experimental). In contrast, the methanolic extract (7% by weight) consisted of *primarily a single secondary metabolite* (SI, Fig. 2). The ^1H and ^{13}C NMR of this compound were consistent with the known natural product candicine, or *N,N,N*-trimethyltyramine, a phenethylamine alkaloid, Figure 6.4.¹⁴



Figure 6.3: Latex obtained from *F. benjamina* leaf (l) and leaf node (r).



Scheme 6.1: Isolation tree-diagram from the air-dried latex of *Ficus benjamina*.

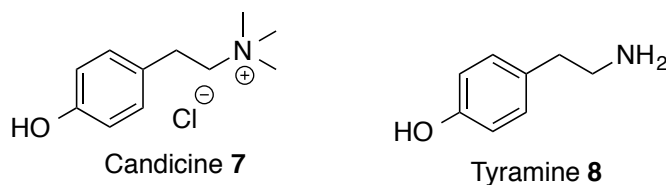
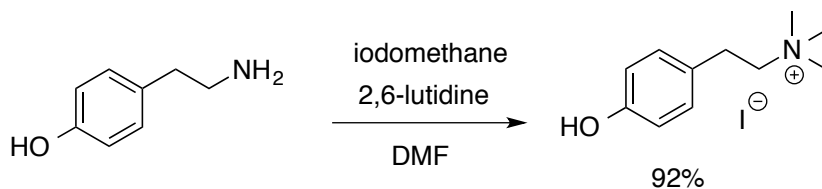


Figure 6.4: Structure of candicine and related phenethylamine tyramine

In order to confirm this structure assignment, candicine was synthetically prepared through exhaustive methylation of tyramine (Scheme 6.2) Using classical literature procedures for exhaustive methylation (iodomethane, K_2CO_3 in MeOH), the candicine salt could not be easily separated from excess of other salts. Employing the hydrophobic base 2,6-lutidine in DMF allowed easy purification by extraction of candicine selectively into the aqueous phase.¹⁵ The aqueous solution was evaporated to obtain a pale yellow solid which was washed with dry acetone to afford candicine iodide as a white solid. The

^1H and ^{13}C spectrum obtained confirmed the structure of candicine obtained from *F. benjamina*.



Scheme 6.2: Synthesis of candicine iodide from tyramine using iodomethane with 2,6-lutidine in DMF.

Of the many reports detailing isolation of secondary metabolites from *F. benjamina*,⁶⁻¹⁰ no mention of the occurrence of candicine has been noted, however, no prior study has investigated the contents of the laticiferous resin. Natural candicine has previously been isolated from several plants including cacti,^{14,16} barley (maltoxin),¹⁷ satinwood,¹⁸ and recently several species of the citrus genus.¹⁹ Candicine has also been identified in the skin secretions of South American frogs of the genus *Leptodactylus*,^{20,21} and *Phyllomedusa* that have shown potent insecticidal activity (larvicidal and adulticidal) to the mosquitoes *Anopheles darlingi* and *Aedes aegypti*, important vectors in the transmission of Dengue and Zika viruses.²¹ Other studies have documented the nicotine-like activity of candicine, again in accord with insecticidal activity.²²

As the polar leaf extract of *F. Benjamina* has been associated with antiviral activity to Herpesviruses,¹⁰ we decided to fully investigate the antiviral potential of pure, synthetic candicine iodide. While no activity was detected against HSV-1, candicine proved to have potent antiviral activity against murine cytomegalovirus (CMV), a virus in the *Herpesviridae* family.²³ Candicine iodide was found to significantly inhibit replication of murine CMV exhibiting an EC₅₀ of 220 nM in a quantitative PCR based assay. This

effect was not a result of host cell toxicity, as no toxicity was observed at the highest concentration (>150 μM) investigated using a CellTiter-Glo assay, resulting in a very high selectivity index (>682). The antiviral activity of candicine has previously not been reported in the literature and adds further to our understanding of the defensive role of candicine. We also investigated the potential activity against Zika virus (ZIKV), an RNA flavivirus (Family Flaviviridae, Genus Arbovirus Group) employing our recently reported assay,¹² in which candicine was determined to be inactive, showed no antiviral activity at the highest concentration of 320 μM .

In addition to the very selective, potent anti-CMV activity demonstrated by candicine, the insecticidal activity of extracts containing candicine²¹ against the prominent viral vectors *Aedes aegypti* and *Anopheles darlingi* suggests *F. benjamina* may have utility as a natural, non-neonicotinoid pesticide, replacing or reducing the use of synthetic neonicotinoids.²⁴⁻²⁶ It is interesting to note that *F. benjamina* and related *Ficus* *sp.* are native or can be naturalized in the same tropical regions where mosquito-borne viruses are highly prevalent. Neonicotinoid insecticide use is now clearly associated with population changes, including extinction rates, of natural insect pollinators,²⁵ stimulating the search for natural, non-neonicotinoid based insecticides from biomass materials.²⁶

In conclusion, *F. benjamina* laticiferous resin has been shown to contain significant quantities of the phenethylamine alkaloid candicine. This report is the first evidence of candicine production in *Ficus* species. We report for the first time the antiviral activity of this compound as a potent and highly selective inhibitor of murine CMV. The potent bioactivity of this molecule suggests it may be involved in plant

defense through several mechanisms, including antiviral and insecticidal activity, possibly related to its known nicotine-like activity.²² The diverse biological effects of candicine demonstrate the utility of studying natural products produced by plants under conditions mimicking predation and pathogenic pressure. Further investigations into the antiviral activity of candicine and other extracts from this and related species, including insecticidal activity is under active investigation.

References:

- (1) Datwyler, S. L.; Weiblen, G. D., *Am. J. Botany*, **2004**, *91*, 767-777.
- (2) For botanical classification see: An update of the angiosperm phylogeny group classification for the orders and families of flowering plants, APG II. *Bot. J. Linn. Soc.*, **2003**, *141*, 399-436.
- (3) Zerega, N. J. C.; Clement, W. L.; Datwyler, S. L.; Weiblen, G. D., *Molec. Phylogen. Evoln.* **2005**, *37*, 402-416.
- (4) Lopez-Vaamonde, C.; Wikstrom, N.; Kjer, K. M.; Weiblen, G. D.; Rasplus, J. Y.; Machado, C. A.; Cook, J. M., *Molec. Phylogen. Evoln.* **2009**, *52*, 715-726.
- (5) Cook, J. M.; Rasplus, J. Y., *Trends Ecol. Evoln.*, **2003**, *18*, 241-248.
- (6) Novelli, S.; Lorena, C.; Antonella, C., *Am. J. Plant Sci.*, **2014**, *5*, 4029-4039.
- (7) Imran, M.; Rasool, N.; Rizwan, K.; Zubair, M.; Riaz, M.; Zia-Ul-Haq, M.; Rana, U. A.; Nafady, A.; Jaafar, H. Z. E., *Chem. Cent. J.*, **2014**, *8*, 12.
- (8) Yarmolinsky, L.; Huleihel, M.; Zaccai, M.; Ben-Shabat, S., *Fitoterapia*. **2012**, *83*, 362–367.
- (9) Bauer, G. *et al.*, *PLoS ONE*. **2014**, *9*, e113336.
- (10) Yarmolinski, L.; Zaccai, M.; Ben-Shabat, S.; Mills, D.; Huleihel, M., *New Biotech.*, **2009**, *26*, 307-313.
- (11) D’Aiuto, L.; Zhi, Y.; McClain, L.; McNulty, J.; Brown, C. E.; Nielsen, A. J.; Yee, M. B.; Piazza, P.; Yolken, R. H.; Kinchington, P. R.; Nimgaonkar, V. L., *Antiviral Res.*, **2017**, *142*, 136-140.

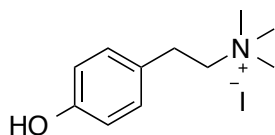
- (12) Revu, O.; Zepeda-Velazquez, C.; Nielsen, A. J.; McNulty, J.; Yolken, R. H.; Jones-Brando, L., *ChemistrySelect*, **2016**, *1*, 5895-5899.
- (13) McNulty, J.; D'Aiuto, L.; Zhi, Y.; McClain, L.; Zepeda-Velázquez, C.; Ler, S.; Jenkins, H. A.; Yee, M. B.; Piazza, P.; Yolken, R. H.; Kinchington, P. R.; Nimgaonkar, V. L., *ACS Med. Chem. Lett.*, **2016**, *7*, 46-50.
- (14) Shabana, M.; Gonaïd, M.; Salama, M. M.; Abdel-Sattar, E., *Nat. Prod. Res.*, **2006**, *20*, 710–714.
- (15) Sommer, H. Z.; Jackson, L. L., *J. Org. Chem.* **1970**, *35*, 1558-1562.
- (16) Meyer B. N.; Helfrich, J. S.; Nichols, D. E.; McLaughlin, J. L.; Davis, D. V.; Cooks, R. G., *J. Nat. Prod.*, **1983**, *46*, 688–693.
- (17) Urakawa, N. Hirabe, Y.; Okubu, Y., *Jpn J Pharmacol.* **1961**, *11*, 4–10.
- (18) Tomko, J.; Awad, A. T.; Beal, J. L.; Doskotch, R. W., *J. Pharm. Sci.*, **1968**, *57*, 329-330.
- (19) Servillo, L.; Giovane, A.; D'Onofrio, N.; Casale, R.; Cautela, D.; Ferrari, G.; Balestrieri, M. L.; Castaldo, D., *J. Agric. Food Chem.* **2014**, *62*, 2679-2684.
- (20) Erspamer, V.; Roseghini, M.; Cei, J. M., *Biochem. Pharmacol.*, **1964**, *13*, 1083–1093.
- (21) Trindade, F. T. T.; Soares, A. A.; de Moura, A. A.; Rego, T. B.; Soares, A. M.; Stabeli, R. G.; Calderon, L. A.; Silva, A. A., *J. Venom. Anim. Tox. Tropic. Dis.*, **2014**, *20*, 28.
- (22) Reti, L. in *The Alkaloids, Chemistry and Physiology*, (Manske, R. H. F.; Holmes, H. L. Eds), **1953**, *3*, 313-338.
- (23) Tang, Q.; Maul, G. G., *J. Virol.* **2006**, *80*, 7510–7521.
- (24) Midega, C. A. O.; Bruce, T. J. A.; Pickett, J. A.; Khan, Z. R., *Ecol Entomol.* **2015**, *40*, 70–81.
- (25) Woodcock, B. A.; Isaac, N. J. B.; Bullock, J. M.; Roy, D. B.; Garthwaite, D. G.; Crowe, A.; Pywell, R. F., *Nat. Commun.*, **2016**, *7*:12459.

(26) Booker, C. J.; Bedmutha, R.; Vogel, T.; Gloor, A.; Xu, R.; Ferrante, L.; Yeung, K. K-C.; Scott, I. M.; Conn, K. L.; Berruti, F.; Briens, C., *Ind. Eng. Chem. Res.*, **2010**, *49*, 10074-10079.

6.3 Experimental

Samples of the laticiferous resin of *F. benjamina* were induced through leaf-pruning causing immediate production of the latex. Approximately 24 hours later, samples of the air-dried latex (342 mg) were collected at the leaf nodes and were suspended in a dichloromethane (150 mL) and MeOH (100 mL) solution at room temperature and stirred for 4 hours. The suspension was then filtered to remove insoluble resin. Deionized water (10 mL) was added to the filtrate to separate the dichloromethane and aqueous-MeOH phases which were partitioned and separately dried. Upon solvent removal, 144 mg (42%) of solid was obtained from the dichloromethane extract and 24 mg (7%) from the methanolic extract. ^1H and ^{13}C NMR (Bruker, 600 MHz) was used to analyze the crude material. The methanolic extract contains one major compound, identified as candicine. ^1H NMR (600 MHz, Methanol- d_4) δ 7.16 – 7.12 (m, 2H), 6.78 – 6.74 (m, 2H), 3.53 – 3.49 (m, 2H), 3.20 (s, 9H), 3.05 – 3.01 (m, 2H); ^{13}C NMR (151 MHz, MeOD) δ 157.8, 131.1, 127.3, 116.7, 68.8, 53.6, 29.5.

2. Synthesis of 2-(4'-hydroxyphenyl)ethyl *N,N,N*-trimethylammonium iodide (candicine):



Tyramine (100 mg, 0.73 mmol) was dissolved in 0.5 mL of dry DMF under N₂ to which was added lutidine (253 μL, 2.19 mmol, 3 eq). Iodomethane (318 μL, 5.10 mmol, 7 eq) was then added dropwise. After 2 hours, H₂O was added and the mixture was extracted with DCM three times. The aqueous solution was evaporated under N₂ to obtain a pale yellow solid. This material was washed three times with acetone to afford candicine iodide as a white amorphous powder in 92% yield.

¹H NMR (600 MHz, Methanol-*d*₄) δ 7.18 – 7.14 (m, 2H), 6.78 – 6.74 (m, 2H), 3.57 – 3.50 (m, 2H), 3.22 (s, 9H), 3.06 – 3.01 (m, 2H); ¹³C NMR (151 MHz, MeOD) δ 157.8, 131.1, 127.3, 116.7, 68.8, 53.8, 29.5.

6.4 References

- (1) Agrawal, A. A., Petschenka, G., Bingham, R. A., Weber, M. G., and Rasmann, S. (2012) Toxic cardenolides: chemical ecology and coevolution of specialized plant–herbivore interactions. *New Phytologist* 194, 28–45.
- (2) The Digitalis Investigation Group. (2009) The effect of digoxin on mortality and morbidity in patients with heart failure. *N. Engl. J. Med.* 336, 525–533.
- (3) Steppuhn, A., Gase, K., Krock, B., Halitschke, R., and Baldwin, I. T. (2004) Nicotine's defensive function in nature. *PLoS Biol.* 2, E217.
- (4) Ujváry, I. (1999) Nicotine and other insecticidal alkaloids, in *Nicotinoid insecticides and the nicotinic acetylcholine receptor*, pp 29–69. Springer Japan, Tokyo.
- (5) Morrissey, J. P., and Osbourn, A. E. (1999) Fungal resistance to plant antibiotics as a mechanism of pathogenesis. *Microbiol. Mol. Biol. Rev.* 63, 708–724.
- (6) Glawischnig, E. (2007) Camalexin. *Phytochemistry* 68, 401–406.
- (7) Timperio, A. M., D'Alessandro, A., Fagioni, M., Magro, P., and Zolla, L. (2012) Production of the phytoalexins trans-resveratrol and delta-viniferin in two economy-

relevant grape cultivars upon infection with *Botrytis cinerea* in field conditions. *Plant Physiol. Biochem.* 50, 65–71.

7 Conclusion and future directions

Through heterocyclic chemistry and the isolation of new natural products, we have identified several novel bioactive small molecules with antiparasitic and antiviral activity. Among the most potent derivatives are 3-diarylether quinolines with 5 μM activity against *T. gondii*. To prepare these compounds, we developed a novel TFA-catalysed Povarov reaction using enol ethers as carbonyl surrogates. This multicomponent cyclization allows access to 2,3-disubstituted quinolines under mild and very rapid conditions. The enol ether synthon may also be an interesting substrate in other cycloadditions.

Our efforts to explore other multicomponent cyclizations led us to prepare a library of quinazolinones and dihydroquinazolinones from commercially available carbonyls, amines, and isatoic anhydride. The selectivity of this reaction for the quinazolinone or dihydroquinazolinone product can be controlled by temperature and solvent choice. The quinazolinones we prepared had exciting activity against both *T. gondii* and HSV-1. SAR analysis of our first generation library allowed us to design second generation libraries targeted towards either antiparasitic or antiviral activity. From these second generation libraries, we were able to differentiate the anti-*Toxoplasma* pharmacophore, defined by an electron-rich aryl substituent at C2 and a bulky alkyl substituent at N3, from the anti-HSV-1 pharmacophore, defined by a benzyloxybenzyl substituent at C2 and an aryl substituent at N3.

We also sought to probe the B-ring pharmacophore of antiviral Amaryllidaceae alkaloids by designing and synthesizing hybrid compounds containing a

dihydroquinazolinone core. Unlike the natural products, these hybrid analogs can be prepared in 5 steps from commercially available starting materials using pentose sugars as a chiral pool reagent. However, these compounds were found to have no HSV-1 activity, indicating that substitution of a nitrogen atom for a carbon at position **10b** is not tolerated in the antiviral pharmacophore. As no SAR of the B-ring has yet been reported in the anticancer pharmacophore, we are currently exploring the anti-tumour activity of these analogs.

We have also discovered interesting small molecules and bioactivity through natural product isolation. We isolated the phenethylamine alkaloid candicine as a major component of *F. benjamina* latex in 7-13% yield. We report for the first time the potent and selective activity of this compound against murine CMV. Due to the neurotoxic, insecticidal, and anti-infective activity of this compound, we believe it is produced defensively by the plant.

From the Canadian strain of *Xylaria polymorpha* fungus, we identified several interesting natural products. Ergosterol-5,8-endoperoxide was determined to have moderate activity against *T. gondii*, and may have a similar mechanism of action to endoperoxide-containing artemisinin. We isolated microdiplactone and revised its structure to di(2-ethylhexyl) adipate, which may be biosynthesized or present through environmental contamination. Finally, we isolated three novel polyketides xylaral B, xylactam C, and xylactam D and assigned their structures based on NMR and MS experiments. We are exploring the anti-infective activity of these natural products and hope to determine their biological activity.

In conclusion, we have developed new chemistry and found new natural products in the search for anti-infective small molecules. We have also identified several heterocyclic small molecules and natural products with potent anti-*Toxoplasma* and anti-HSV-1 activity. By identifying the targets of these molecules using a pulldown assay with either fluorescence or affinity probes, we may identify new mechanisms of action that can be targeted for further drug development.

Appendix 1 – NMR Spectroscopy Data

